UNIVERSIDADE ESTADUAL DE CAMPINAS
INSTITUTO DE BIOLOGIA

VALÉRIA YUKARI ABE

"ANÁLISE FUNCIONAL DE EFETORES 'TAL' DE *Xanthomonas citri* E *Xanthomonas aurantifolii* PATOTIPO 'C' E ESTUDO DA ATIVAÇÃO DE SEUS GENES ALVOS NA PLANTA HOSPEDEIRA"

"FUNCTIONAL ANALYSIS OF TAL EFFECTORS FROM *Xanthomonas citri* AND *Xanthomonas aurantifolii* PATHOTYPE 'C' AND GENE TARGET ACTIVATION IN HOST PLANTS"

CAMPINAS
2016

VALÉRIA YUKARI ABE

"ANÁLISE FUNCIONAL DE EFETORES 'TAL' DE *Xanthomonas citri* E *Xanthomonas aurantifolii* PATOTIPO 'C' E ESTUDO DA ATIVAÇÃO DE SEUS GENES ALVOS NA PLANTA HOSPEDEIRA"

"FUNCTIONAL ANALYSIS OF TAL EFFECTORS FROM *Xanthomonas citri* AND *Xanthomonas aurantifolii* PATHOTYPE 'C' AND GENE TARGET ACTIVATION IN HOST PLANTS"

Tese apresentada ao Instituto de Biologia da Universidade Estadual de Campinas como parte dos requisitos exigidos para a obtenção do título de Doutora em Genética e Biologia Molecular, na área de Genética Vegetal e Melhoramento

Thesis presented to the Institute of Biology of the University of Campinas in partial fulfillment of the requirements for the degree of Doctor in Genetic and Molecular Biology, in the area of Genetics and Plant Breeding

ESTE ARQUIVO DIGITAL CORRESPONDE À VERSÃO FINAL DA TESE DEFENDIDA PELA ALUNA VALÉRIA YUKARI ABE E ORIENTADA PELO DR. CELSO EDUARDO BENEDETTI.

Orientador: CELSO EDUARDO BENEDETTI

CAMPINAS

2016

Agência(s) de fomento e nº(s) de processo(s): FAPESP, 2011/19988-0

Ficha catalográfica
Universidade Estadual de Campinas
Biblioteca do Instituto de Biologia
Mara Janaina de Oliveira - CRB 8/6972

Ab33a

Abe, Valeria Yukari, 1985-
Analise funcional de efetores 'TAL' de *Xanthomonas citri* e *Xanthomonas aurantifolii* patotipo 'C' e estudo da ativação de seus genes alvos na planta hospedeira / Valeria Yukari Abe. – Campinas, SP : [s.n.], 2016.

Orientador: Celso Eduardo Benedetti.
Tese (doutorado) – Universidade Estadual de Campinas, Instituto de Biologia.

1. Cancro citrico. 2. *Xanthomonas citri* subsp. *citri*. 3. Proteina PthA. I. Benedetti, Celso Eduardo. II. Universidade Estadual de Campinas. Instituto de Biologia. III. Titulo.

Informações para Biblioteca Digital

Titulo em outro idioma: Functional analysis of TAL effectors from *Xanthomonas citri* and *Xanthomonas aurantifolii* pathotype 'C' and gene target activation in host plants
Palavras-chave em inglês:
Citrus canker
Xanthomonas citri subsp. *citri*
PthA protein
Área de concentração: Genética Vegetal e Melhoramento
Titulação: Doutora em Genética e Biologia Molecular
Banca examinadora:
Celso Eduardo Benedetti [Orientador]
Cleverson Carlos Matiolli
Andrea Balan
Francisco de Assis Alves Mourão Filho
Henrique Ferreira
Data de defesa: 29-03-2016
Programa de Pós-Graduação: Genética e Biologia Molecular

Campinas, 29 de Março de 2016.

COMISSÃO EXAMINADORA

Prof. Dr. Celso Eduardo Benedetti

Dr. Cleverson Carlos Matiolli

Profa. Dra. Andrea Balan

Prof. Dr. Francisco de Assis Alves Mourão Filho

Prof. Dr. Henrique Ferreira

Os membros da Comissão Examinadora acima assinaram a Ata de Defesa, que se encontra no processo de vida acadêmica do aluno.

AGRADECIMENTOS

Eu quero agradecer primeiramente meus pais, pelo esforço e dedicação durante toda a minha vida e por terem me dado a base para me tornar quem sou hoje.

Aos meus irmãos Masami, Sayuri e Massaru, pelo carinho e amizade, e por ter sempre com quem contar.

Ao meu namorado e melhor amigo Bruno, pelo amor e companheirismo, me apoiando incondicionalmente em todos os momentos e me fortalecendo nas horas mais difíceis.

Um obrigado especial ao meu orientador Celso, pela atenção e disponibilidade, pelos ensinamentos valiosos e discussões construtivas, por ter me ajudado nas incontáveis infiltrações bacterianas e além de tudo, por ser essa pessoa exemplar que admiro muito.

Aos meus queridos amigos do laboratório Caio, Dri, Hugo, Mari, Bruna, Paula, Jaque, Nayara, Jackeline e Cris. Obrigada pela amizade, por aquela "forcinha" sempre que precisei, pelos divertidos almoços e por tornarem o meu dia a dia sempre mais agradável.

Às minhas amigas Ângela e Amanda, pelo carinho e pelos ótimos momentos de descontração.

Aos meus irmãos de coração, Paula, Kelly, Shira, Yuriko e Roberta, sempre torcendo por mim e compartilhando momentos incríveis.

À todos meus amigos que participaram de alguma forma para que eu chegasse até aqui.

Ao Dr. Maxuel, por ter cedido os vetores pNPTS138, pMR20 e pUFR047 utilizados neste trabalho.

Ao Dr. Dean Gabriel, por ter cedido o mutante B21.2 também utilizado neste trabalho.

À Ismaela, por ter feito a figura de ação dos efetores TAL, mostrando a translocação do PthA para o interior da célula hospedeira.

Às pesquisadoras Dra. Alessandra Alves e Dra. Melissa Fessel, pela importante contribuição na minha pré-banca.

Aos membros titulares da minha banca, Dra. Andrea Balan, Dr. Cleverson Carlos Matiolli, Dr. Henrique Ferreira, Dr. Francisco de Assis Alves Mourão Filho pelas importantes considerações feitas para o aprimoramento da tese. E aos demais membros, Dra. Anete Pereira de Souza, Dr. Ivan de Godoy Maia e Dr. Paulo Arruda, pela disponibilidade.

À FAPESP pela bolsa concedida.

Ao CNPEM/LNBio, pela infraestrutura e por permitir a execução do meu projeto e ao CTBE por permitir o uso de alguns equipamentos.

À UNICAMP e ao programa de pós-graduação em Genética e Biologia Molecular, pela oportunidade de estudo.

RESUMO

O cancro cítrico, causado pelas bactérias *Xanthomonas citri* e *Xanthomonas aurantifolii*, é uma doença de grande importância para o Brasil. Enquanto *X. citri* causa cancro em todas variedades comerciais de citros, *X. aurantifolii* patotipo C afeta apenas o limão Galego, desencadeando uma resposta de defesa em laranja doce. A maioria das espécies de *Xanthomonas* translocam proteínas efetoras para o citoplasma da célula hospedeira durante a infecção para suprimir defesas da planta e favorecer o crescimento bacteriano. *X. citri* e *X. aurantifolii* C utilizam proteínas efetoras tipo TAL (‘*transcription activator-like’*), pertencentes a família PthA, para ativar a transcrição de genes de suscetibilidade (*S*) em citros. O isolado 306 de *X. citri* codifica quatro variantes da proteína PthA, porém, apenas a proteína PthA4 foi demonstrada atuando como fator de patogenicidade em citros. Por outro lado, o isolado ICMP 8435 de *X. aurantifolii* C codifica duas variantes de PthC, que poderiam atuar como proteínas de avirulência (Avr) na laranja doce. Neste trabalho, avaliou-se a contribuição de cada PthA no desenvolvimento do cancro cítrico e no crescimento bacteriano na planta e o possível papel dos efetores PthCs como proteínas Avr em laranja doce. Além disso, avaliou-se a expressão de alvos diretos de ativação desses efetores em citros, visando identificar prováveis genes *S* associados ao desenvolvimento do cancro cítrico. Para tanto, foram obtidos mutantes de deleção para os genes *pthAs* os quais foram complementados com os genes *pthCs* e usados para desafiar as variedades comerciais de citros para avaliação dos sintomas do cancro e análise de expressão gênica. Verificou-se que PthA4 é essencial para a indução do cancro cítrico em todas as variedades de citros testadas; entretanto, PthA1 e PthA3 desempenham papel aditivo no desenvolvimento dos sintomas do cancro, atuando de forma hospedeiro-dependente. A deleção de dois ou mais genes *pthA*s reduziu o crescimento bacteriano *in planta* mais pronunciadamente do que deleções num único gene, sugerindo um papel aditivo dos PthAs na patogenicidade e crescimento bacteriano. Além disso, foi observado que PthC1 não atua como uma proteína Avr em laranja doce. Verificou-se ainda que a contribuição dos PthAs 1 e 3 na formação do cancro em laranja ‘Pêra’ não se correlaciona com a ativação de *LOB1* (*LATERAL ORGAN BOUNDARIES* 1), único gene *S* associado ao cancro cítrico conhecido até o momento, mas sim com a indução de outros alvos de PthAs, incluindo *LOB2* e *DIOX* (dioxigenase de citros). *LOB1*, *LOB2* e *DIOX* apresentaram expressão diferencial e dependente de PthAs entre laranja Pêra e limão Tahiti. Tal expressão diferencial parece estar relacionada a polimorfismos encontrados nos sítios de ligação dos PthAs nas regiões promotoras desses genes. Foram observadas evidências de que somente a ativação de *LOB1* não é suficiente para a formação do

cancro, e que o gene *DIOX* atua como gene *S* em laranja 'Pêra', mas não em limão Tahiti, sugerindo que a ativação de múltiplos genes *S* em citros são necessários para a completa formação do cancro.

ABSTRACT

Citrus canker, caused by *Xanthomonas citri* and *Xanthomonas aurantifolii*, is a serious disease that affects most commercial citrus plantations in Brazil. While *X. citri* causes canker in all commercial citrus varieties, *X. aurantifolii* pathotype C causes disease only in 'Mexican' lime, triggering defense responses in sweet orange. *Xanthomonas* spp. usually translocate effector proteins into the host cell cytoplasm during the infection to suppress plant defenses and enhance bacterial growth. *X. citri* and *X. aurantifolii* C employ transcription activator-like (TAL) effectors of the PthA family to activate host disease susceptibility (*S*) genes. The *X. citri* strain 306 encodes four variants of PthA proteins, but only PthA4 was shown to act as pathogenic factor on citrus. On the other hand, the *X. aurantifolii* C strain ICMP 8435 encodes two variants of PthCs that could act as avirulence proteins (Avr) in sweet orange. This work aimed to assess the contribution of each PthA in citrus canker development and bacterial growth *in planta*; and verify the possible role of PthCs as Avr proteins in sweet orange. In addition, the expression of direct targets of these effectors in citrus were evaluated to identify candidate *S* genes associated with canker development. Thus, deletion mutants for the *pthA*s genes were obtained, which were complemented with *pthC*s genes. These mutants were used to challenge various commercial citrus varieties for canker symptoms evaluation and gene expression analysis. It was found that PthA4 was essential for citrus canker induction in all citrus varieties tested; however, PthA1 and PthA3 played an additive role in canker development induced by PthA4, acting in a host-dependent manner. Deletions in two or more *pthA* genes reduced bacterial growth *in planta* more pronouncedly than single deletions, suggesting an additive role of PthAs in pathogenicity. Furthermore, it was observed that PthC1 does not act as an Avr protein in sweet orange plants. Additionally, the contribution of PthAs 1 and 3 in canker formation in 'Pera' plants did not correlate with the activation of the canker *S* gene *LOB1* (*LATERAL ORGAN BOUNDARIES* 1), the only citrus canker *S* gene known to date, but with the induction of other PthA targets, including *LOB2* and citrus dioxygenase (*DIOX*). *LOB1*, *LOB2* and *DIOX* showed differential PthA-dependent expression between 'Pera' and 'Tahiti' plants that appears to be associated with nucleotide polymorphisms found at or near PthA-binding sites. The data shown here also indicates that *LOB1* activation alone is not sufficient to elicit cankers on citrus, and that *DIOX* acts as a canker S gene in 'Pera' but not 'Tahiti' plants, suggesting that activation of multiple *S* genes, such as *LOB1* and *DIOX*, is necessary for full canker development.

SUMÁRIO

1. INTRODUÇÃO

1.1 A citricultura brasileira e o cancro cítrico

As plantas de citros (*Citrus* spp.) pertencem à família Rutaceae e são originárias das regiões sul e sudeste da Ásia. Devido às suas características, as plantas de citros foram selecionadas e cultivadas em várias outras regiões do mundo, sendo introduzidas no Brasil na época da colonização. No Brasil, os citros conseguiram se adaptar, expandindo-se por todo o território nacional. Hoje, o setor citrícola brasileiro é altamente organizado e competitivo, possuindo grande destaque no agronegócio (Neves, 2010).

Atualmente, o Brasil é o maior produtor e exportador mundial de suco de laranja, com uma produção estimada de laranja superior a 11,3 milhões de toneladas na safra 2015/2016, sendo aproximadamente 8,9 milhões de toneladas destinadas a produção de suco (CitrusBR, 2016; Ministério da Agricultura, 2016). Somente no ano de 2015, o Brasil exportou mais de 1 milhão de toneladas de suco de laranja concentrado equivalente, rendendo mais de US$1,7 bilhão (CitrusBr, 2016).

Apesar de haver projeções para um aumento de 0,89% na taxa anual de produção de laranja (Ministério da Agricultura, 2016), o setor tem enfrentado grandes dificuldades. Como exemplo, temos a forte oscilação dos preços internacionais do suco de laranja, a introdução e preferência por novas bebidas que passam a ganhar maior participação no mercado, o aumento nos custos de produção que incluem gastos com fertilizantes, irrigação, mão de obra, além de diversos fatores de ordem fitossanitária. Neste último, podemos destacar o cancro cítrico, o "greening" ou "huanglongbing" (HLB), a clorose variegada dos citros (CVC), a morte súbita dos citros (MSC), entre outros (CitrusBR, 2016).

O cancro cítrico, provavelmente oriundo dos mesmos centros de origem dos citros, é uma das doenças economicamente mais importantes, pois ocorre de forma endêmica em todos os países produtores e afeta todas as espécies e variedades comerciais importantes de citros. O cancro cítrico foi detectado pela primeira vez no Brasil em 1957, nos estados de São Paulo e Paraná. Desde então vem acarretando muitos gastos e perdas, principalmente nos estados do Paraná, São Paulo e no Triângulo Mineiro (cinturão citrícola), onde se concentra a maior parte da produção nacional de citros (Amaral, 2003; Behlau & Belasque Jr., 2014; CitrusBR, 2016).

O cancro cítrico é uma doença causada por dois grupos de linhagens de fitobactérias filogeneticamente distintos do gênero *Xanthomonas*: *Xanthomonas citri* (também conhecido como *X. citri* subsp. *citri*) e *Xanthomonas aurantifolii* (ou *X. fuscans* subs. *aurantifolii*) patotipos 'B' e 'C'. *X. citri* é responsável pela doença do grupo Asiático, ou cancrose A. Este é considerado o grupo mais agressivo, com uma ampla gama de hospedeiros, atacando a maioria

das espécies de citros, incluindo laranja doce (*Citrus sinensis*), Grapefruit ou Pomelo (*Citrus paradisi*) e limão verdadeiro (*Citrus limon*) (Leite *et al.*, 1994; Shubert *et al.*, 2003). Outros dois grupos mais novos, conhecidos como A* (Verniere *et al.*, 1998) e A^w (Sun *et al.*, 2004) são restritos ao sudeste da Ásia e Flórida, respectivamente. A* é limitado à infecção do limão Galego (ou lima ácida, *Citrus aurantifolia*) e A^w causa cancro somente no limão Galego e em Alemow (*Citrus macrophylla*). A bactéria *X. aurantifolii* possui uma estreita gama de hospedeiros, pertencente ao grupo da América do Sul, responsável pela cancrose B que é restrita à Argentina, Paraguai e Uruguai, e a cancrose C, presente exclusivamente no Brasil e que se restringe à infecção do limão Galego (Amaral, 2003; Shubert *et al.*, 2003; Cernadas *et al.*, 2008).

Os sintomas causados por *X. citri* e *X. aurantifolii* são os mesmos e são caracterizados pela formação de lesões circulares e erupções com o aspecto de "watersoaking" (lise da célula do hospedeiro liberando água e nutrientes para o apoplasto), formando pústulas inicialmente brancas ou amareladas, evoluindo para um câncer de coloração castanho claro ou marrom (Brunings & Gabriel, 2003). Estes sintomas podem ser observados tanto em folhas, como frutos e ramos (Figura 1) (Shubert *et al.*, 2003). Em condições severas, esta doença causa desfolha e queda prematura dos frutos. O cancro em si, principal manifestação da doença, é atribuído à indução de hipertrofia (aumento no tamanho celular) e hiperplasia (divisão celular excessiva) que eventualmente leva à ruptura da epiderme e seu surgimento em forma de erupção, favorecendo a disseminação do patógeno (Amaral, 2003; Brunings & Gabriel, 2003). Esta disseminação pode ocorrer através da água de chuva, uso de equipamentos de trabalho contaminados, ou ainda a longas distâncias pelo transporte de mudas contaminadas. A penetração no hospedeiro ocorre via estômatos ou ferimentos, sendo que a infecção pode ainda ser facilitada na presença de insetos herbívoros, como a larva minadora do citros (*Phyllocnistis citrella*), que forma galerias nas folhas, servindo como porta de entrada para a bactéria (Prates *et al.*, 1996; Brunings & Gabriel, 2003; Schubert & Sun, 2003; Belasque Jr. *et al.*, 2005).

Figura 1. Sintomas do cancro cítrico em folhas, frutos e ramos. É possível observar halos cloróticos no local da lesão evoluindo para um câncer de coloração marrom com grande proliferação celular (Behlau & Belasque Jr., 2014).

Considerado uma praga quarentenária A2 pelo Ministério da Agricultura, Pecuária e Abastecimento (MAPA), as medidas de combate ao cancro cítrico incluem a erradicação de plantas contaminadas e pulverização com cobre das plantas presentes em um raio de 30 m. Além disso, vistorias periódicas são necessárias para a manutenção de um pomar saudável (Behlau & Belasque Jr., 2014). Não existe um método curativo para a doença, e para o seu controle são adotadas medidas preventivas como o uso de mudas sadias, vindas de viveiros certificados, uso de quebra-ventos, uso de ferramentas, máquinas e implementos limpos e desinfestados e controle da larva minadora do citros (Amaral, 2003; Koller, 2006; Behlau *et al.*, 2007, Behlau & Belasque Jr., 2014).

Muitas destas medidas de controle são onerosas para o citricultor, de forma que um método de controle desejável e que não acrescentaria maiores custos ao produtor seria a adoção de variedades resistentes à bactéria. No entanto, não foi constatado resistência total à *X. citri* nas variedades comerciais de citros (Brunings & Gabriel, 2003). Por outro lado, o avanço da

biotecnologia tem permitido o estudo de diversos mecanismos de virulência e resistência, assim como um maior esclarecimento das interações planta-patógeno, a fim de obter plantas de citros resistentes ao cancro cítrico (de Oliveira *et al.*, 2013; Pitino *et al.*, 2015).

1.2 Interação planta–patógeno: o ataque dos fitopatógenos e os mecanismos de defesa da planta

Os fitopatógenos utilizam diferentes estratégias como secreção de proteínas e outras moléculas para dentro das células dos seus respectivos hospedeiros modulando o sistema de defesa da planta e permitindo o estabelecimento da colonização parasítica (Abramovitch *et al*., 2006; Birch *et al*., 2006; Block *et al*., 2008). Em contrapartida, em resposta à infecção, as plantas desenvolveram, ao longo do processo evolutivo, sistemas complexos de defesa. As plantas, diferentemente dos animais, não possuem um sistema imune adaptativo, mas sim um sistema imune inato que depende da autonomia de cada célula para ter sucesso contra infecções de fitopatógenos (Dangl & Jones, 2001; Jones & Dangl, 2006; Dodds & Rathjen, 2010).

Durante uma interação planta-patógeno, a planta normalmente pode reagir utilizando duas linhas de defesa (Figura 2). A primeira corresponde ao reconhecimento de padrões moleculares conservados associados a patógenos ('*pathogen-associated molecular patterns*' ou PAMPs) por proteínas receptoras localizadas na membrana plasmática ('*pattern recognition receptors*' ou PRRs) (Jones & Dangl, 2006; Dodds & Rathjen, 2010). Os PAMPs (ou MAMPs '*microbe-associated molecular pattern'*) são tipicamente componentes microbianos essenciais, que normalmente possuem funções estruturais ou enzimáticas fundamentais para o desenvolvimento do patógeno, como quitina, principal componente estrutural de parede celular de fungos (De Wit *et al.*, 2009; Stergiopoulos & De Wit, 2009), e a flagelina, uma subunidade protéica que compõe o filamento flagelar, elemento importante na virulência de fitobactérias (Zipfel & Felix, 2005).

Quando os PAMPs são reconhecidos por PRRs é disparada uma resposta de defesa basal conhecida como imunidade desencadeada por PAMPs ('*PAMP-triggered immunity*' ou PTI) que normalmente leva à morte celular programada, sinalização por hormônios, reforço de parede celular através da deposição de calose, produção de espécies reativas de oxigênio, ativação da cascata de sinalização por proteínas MAPK ('*mitogen-activated protein kinase'*) e a expressão de genes de defesa (Abramovitch & Martin, 2004).

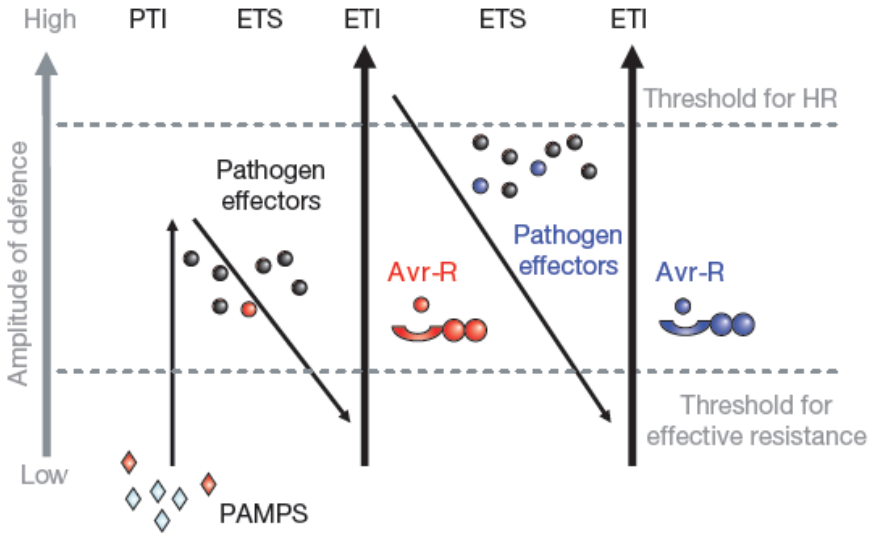

Figura 2. Modelo "zigzag" ilustrando o sistema imune vegetal com duas linhas de defesa. A primeira linha de defesa corresponde a imunidade desencadeada por PAMPs (PTI). Patógenos capazes de suplantar a PTI translocam proteínas efetoras para o interior da célula do hospedeiro gerando uma suscetibilidade desencadeada por efetores (ETS). Em contrapartida, em uma segunda linha de defesa, plantas que possuem o gene *R* são capazes de reconhecer a proteína efetora ou Avr gerando uma imunidade desencadeada por efetores (ETI) (Jones & Dangl, 2006).

Patógenos capazes de suplantar a defesa basal das plantas, em geral, o fazem via translocação de proteínas efetoras para o interior da célula do hospedeiro. Estas proteínas efetoras normalmente são caracterizadas como fatores de virulência que alteram a estrutura e função das células hospedeiras promovendo a infecção, além de melhorar o potencial de colonização do tecido celular, sobrevivência e reprodução dos patógenos (Torto *et al.*, 2003; Kamoun, 2009; Yin & Hulbert, 2010; Oliva *et al.*, 2010). Assim, a ação destas proteínas efetoras pode resultar em uma suscetibilidade desencadeada por efetores ('*effector-triggered susceptibility*' ou ETS). Em contrapartida, numa segunda linha de defesa que normalmente ocorre no interior da célula, as plantas reconhecem direta ou indiretamente as proteínas efetoras dos patógenos através de proteínas codificadas por genes *R*, também conhecidas como proteínas NB-LRR devido à presença dos domínios de ligação a nucleotídeo ('*nucleotide binding*' ou NB) e dos domínios ricos em leucina ('*leucine rich repeat*' ou LRR) (Jones & Dangl, 2006). Esse reconhecimento específico de proteínas efetoras por proteínas NB-LRR resulta na imunidade desencadeada pelo efetor ('*effector-triggered immunity*' ou ETI), um tipo de defesa que dispara morte celular programada ou reação de hipersensibilidade tipo HR ('*Hypersensitive Response*') ao redor da infecção (De Wit, 2007; Jones & Dangl, 2006; Dodds & Rathjen, 2010).

Dessa forma, alguns efetores induzem resposta de defesa em plantas resistentes contendo os genes *R* correspondentes e, neste caso, as proteínas efetoras são denominadas "proteínas Avr". Esses mecanismos levam, portanto, a uma co-evolução entre patógeno e hospedeiro, onde os patógenos respondem com mutação, perda de efetores ou desenvolvimento de novos efetores que podem suprimir ETI, enquanto as plantas acabam gerando proteínas R com novas especificidades e que passam a reconhecer novos efetores (Stergiopoulos & De Wit, 2009; Dodds & Rathjen, 2010).

1.3 Proteínas efetoras tipo TAL de *Xanthomonas*

O gênero *Xanthomonas* abrange 27 espécies de fitobactérias que podem causar doença em aproximadamente 400 plantas hospedeiras, incluindo várias culturas de importância econômica, como o arroz, pimentão, tomate, entre outras, destacando aqui os citros (Ryan *et al.*, 2011). Além disso, bactérias do gênero *Xanthomonas* possuem seis tipos de sistemas secretórios (de I a VI) (Büttner & Bonas, 2009) dentre os quais focaremos no sistema de secreção do tipo III ('***t**ype III **s**ecretion **s**ystem*' ou T3SS). O T3SS (Figura 3) consiste em um especializado sistema de secreção que realiza o transporte de moléculas ou proteínas efetoras diretamente para o citoplasma da planta hospedeira, através do seu aparato semelhante a uma agulha que atravessa a membrana interna e externa da célula bacteriana (Kubori *et al.*, 2000; Büttner & He, 2009). Os genes que codificam as proteínas do T3SS, denominados de *hrp* ('*hypersensitive response and pathogenicity*'), são necessários para a patogenicidade e indução das reações de hipersensibilidade no hospedeiro e não-hospedeiro, respectivamente (Szurek *et al.*, 2002; Abramovitch & Martin, 2004; Bittel & Robatzek, 2007; Kay & Bonas, 2009; Büttner & Bonas, 2010).

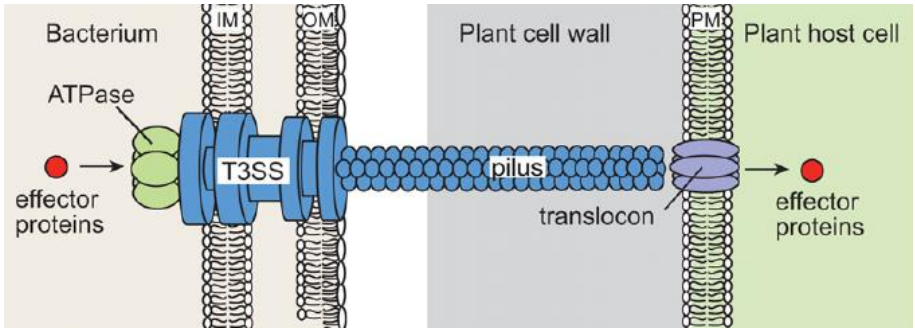

Figura 3. Esquema do sistema de secreção tipo III (T3SS) presentes em bactérias do gênero *Xanthomonas*. Este sistema possibilita a translocação de proteínas efetoras da bactéria, atravessando as membranas interna (IM) e externa (OM), para o interior da célula hospedeira, atravessando a parede celular e a membrana plasmática (PM) atingindo o citoplasma da célula da planta (Büttner & He, 2009).

O T3SS de *Xanthomonas* é capaz de translocar um coquetel de proteínas efetoras para dentro da célula da planta. Entretanto, o tipo de proteínas efetoras mais bem caracterizadas de *Xanthomonas* são aquelas denominadas efetores TAL ('*transcription activator-like*'). Estas proteínas são translocadas para o interior da célula vegetal através do T3SS e depois direcionadas para o núcleo, onde são capazes de modular a transcrição gênica (Figura 4) (Kay *et al.*, 2007; Römer *et al.*, 2007).

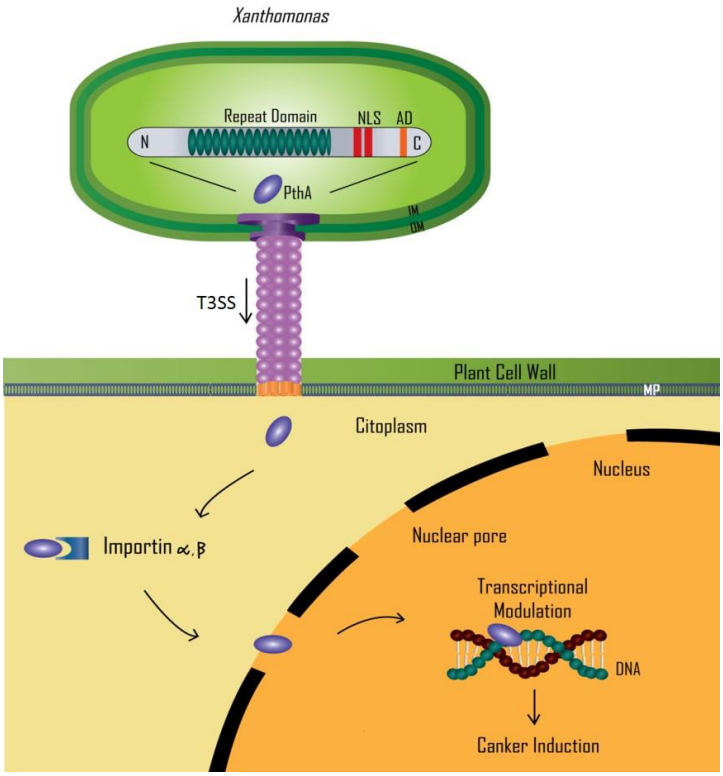

Figura 4. Transporte da proteína efetora (PthA) para dentro da célula hospedeira. A proteína efetora é translocada da bactéria *Xanthomonas* para o citoplasma da planta pelo sistema de secreção do tipo III (T3SS). Uma vez dentro da célula da planta, a proteína efetora é direcionada para o núcleo com o auxílio de outras proteínas do hospedeiro (α e β importina), onde pode se ligar ao DNA sendo capaz de modular a transcrição gênica, gerando o cancro.

Os efetores TAL possuem em comum a porção N-terminal, necessária para a translocação pelo T3SS e a porção C-terminal, onde se encontra o sinal de localização nuclear e o domínio de ativação (Figura 5). Os efetores TAL ainda apresentam um domínio central de ligação ao DNA que confere à bactéria especificidade à hospedeira. Trata-se de uma região composta por motivos de 34 aminoácidos que se repetem em *tandem*, onde cada um dos motivos apresenta resíduos variáveis ('*repeat-variable diresidue*' ou RVD) nas posições 12 e 13 de cada repetição (Figura 5). Estes se ligam preferencialmente a uma base no DNA e o número e a

organização das repetições determinam a sequência de DNA alvo que será reconhecida por um dado efetor. Assim, é possível predizer quais serão os genes alvos de ligação dos efetores TAL conhecendo-se suas sequências de RVDs (Boch *et al.*, 2009; Moscou & Bogdanove, 2009; Boch & Bonas, 2010; Bogdanove & Voytas, 2011).

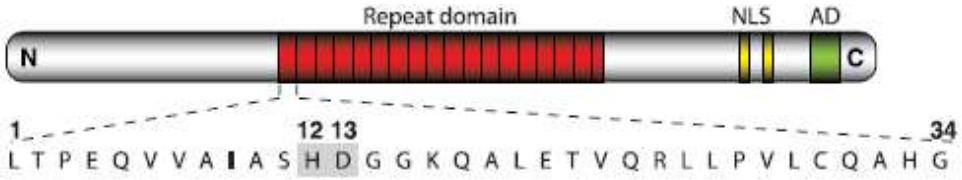

Figura 5. Organização dos efetores TAL. Em vermelho está representado o domínio de repetição composto por 34 motivos de aminoácidos, destacando os aminoácidos 12 e 13 que são resíduos variáveis. Em amarelo é ilustrado o sinal de localização nuclear (NLS) e em verde o domínio de ativação (AD). N e C correspondem à porção N-terminal e C-terminal, respectivamente (Boch *et al.*, 2009).

As proteínas efetoras do tipo TAL pertencem à família AvrBs3/PthA e funcionam como fatores de transcrição na célula da planta. A proteína efetora AvrBs3 de *Xanthomonas vesicatoria*, bactéria responsável pela mancha bacteriana nas culturas de pimentão e tomate, é o efetor TAL mais bem caracterizado (Bonas *et al.*, 1989). Uma vez no núcleo das células hospedeiras, AvrBs3 induz a expressão do gene *upa20*, um regulador majoritário de hipertrofia das células do mesófilo. O gene *upa20* codifica um fator de transcrição que regula o processo de hipertrofia celular e como resultado, há a ruptura da epiderme da folha e a dispersão da bactéria. Por outro lado, em genótipos resistentes à *X. vesicatoria*, AvrBs3 funciona como uma proteína Avr, não por ela ser reconhecida por um gene *R*, mas por transativar diretamente o gene *Bs3* que confere resistência a essa bactéria (Kay *et al.*, 2007; Römer *et al.*, 2007).

A proteína efetora PthA de *X. citri*, que é cerca de 97% idêntica à AvrBs3, foi uma das primeiras proteínas "avr" para a qual se demonstrou uma função no desenvolvimento dos sintomas do cancro cítrico. O gene *pthA* quando transferido para outras *Xanthomonas* não-patogênicas a citros, confere patogenicidade a essas bactérias em citros (Swarup *et al*., 1991). Além disso, a expressão transitória de PthA em folhas de laranja leva à formação de micro-pústulas mostrando que PthA é suficiente para promover hipertrofia celular em folhas de citros (Duan *et al*., 1999; Brunings & Gabriel, 2003; Al-Saadi *et al.*, 2007).

Os isolados de *X. citri* 306 e 3212 contêm quatro variantes da proteína PthA (PthA 1 a 4), as quais diferem entre si basicamente pelo número de repetições do domínio central e pelos RVDs dentro das regiões de repetição. Dessa forma, PthA4 possui 17,5 repetições de 34

aminoácidos, PthA1 possui 16,5, PthA2 e PthA3 tem 15,5 repetições (da Silva *et al.*, 2002; Brunings & Gabriel, 2003). A proteína PthA4 é considerada o homólogo funcional de AvrBs3, pois é a variante essencial para causar hipertrofia e hiperplasia nas células hospedeiras de citros (variedades Valência e Duncan 'grapefruit') (da Silva *et al.*, 2002; Al-Saadi *et al.*, 2007; Yan & Wang, 2012; Hu *et al.*, 2014). Considerando que ao longo da evolução *X. citri* manteve as quatro variantes da proteína PthA, e que o número e a ordem de RVDs de um dado efetor TAL determina sua sequência alvo, podemos inferir que mesmo as proteínas com 16,5 ou 15,5 repetições podem estar contribuindo no desenvolvimento do cancro, ativando a expressão de diferentes alvos, ou ainda contribuindo aditivamente na ativação de genes alvos em comum na planta hospedeira; porém a maneira como essas proteínas ativam a transcrição na célula hospedeira ainda permanece desconhecida.

A bactéria *X. aurantifolii* C, estirpe ICMP 8435, possui duas variantes do efetor TAL PthC, onde PthC1 possui 17,5 repetições do domínio central e PthC2 possui 14,5 repetições (Cernadas *et al.*, 2008). Apesar dos efetores TAL normalmente desempenharem um papel fundamental no desenvolvimento de doença, atuando como fatores determinantes para a patogenicidade, algumas variantes de PthA parecem atuar como fatores de avirulência em certas variedades de citros (Shiotani *et al.*, 2007; Chiesa *et al.*, 2013).

Uma análise do perfil transcricional em resposta à infecção por *X. citri* e *X. aurantifolii* C em laranja doce indicaram que enquanto *X. citri* ativa genes relacionados a divisão celular, remodelamento de parede e síntese de auxina e giberelina, que são necessárias para o desenvolvimento do cancro, *X. aurantifolii* C transativa inibidores de endoglucanases e biossíntese de fenilpropanóides, envolvidos na defesa basal (Cernadas *et al.*, 2008). Sendo assim, o fato de *X. aurantifolii* causar cancro em limão Galego, mas desencadear resposta de defesa em laranja doce, somado ao fato de que esta bactéria transativa genes relacionados a resposta de defesa em laranja doce, sugere que PthC possa estar atuando como gene *avr*, ou ativando genes que conferem resistência a *X. aurantifolii* C em laranja doce.

Apesar de vários efetores de *Xanthomonas* serem conhecidos, o número de alvos dessas proteínas efetoras identificados na planta hospedeira ainda é reduzido. Uma abordagem para a identificação de novos alvos pode ter início no uso de algorítmos computacionais para predizer possíveis alvos de efetores TAL (Grau *et al.*, 2013; Richter *et al.*, 2014; Pereira *et al.*, 2014). Estudos prévios realizados em nosso laboratório, utilizando técnicas de expressão transitória de genes em epicótilos de laranja, identificaram vários genes de *C. sinensis* como potenciais alvos de efetores de *X. citri* e *X. aurantifolii* C (Pereira *et al.*, 2014). Porém, até o momento, o único gene de suscetibilidade, relacionado ao cancro cítrico, que se tem

conhecimento é o gene *LOB1* (*LATERAL ORGAN BOUNDARIES 1*) (Hu *et al.*, 2014; Li *et al.*, 2014; Pereira *et al.*, 2014). A expressão do gene *LOB1* de citros está associada à expressão de genes ligados à expansão celular. Foi verificado que a proteína PthA4 se liga especificamente na região promotora de *LOB1* aumentando a sua expressão, e que essa expressão dependente de PthA está relacionada com o desenvolvimento de cancro (Hu *et al.*, 2014). Entretanto, além do gene *LOB1*, vários outros genes relacionados com divisão celular, remodelamento de parede e biossítese de auxina e giberelina, como os genes *LOB2*, *LOB3* e *DIOX* (dioxigenase) foram identificados como potenciais alvos diretos de PthAs (Pereira *et al.*, 2014), mas a função desses genes no desenvolvimento do cancro cítrico ainda requer novos estudos.

2. JUSTIFICATIVAS E OBJETIVOS

Considerando a importância da citricultura para a economia brasileira e os problemas fitossanitários acarretados pelo cancro cítrico, o objetivo deste trabalho foi elucidar a função dos efetores TAL de *X. citri* e *X. aurantifolii* patotipo C como fatores de patogenicidade/avirulência em diferentes plantas hospedeiras de citros. Portanto, objetivou-se avaliar a contribuição de cada um dos efetores TAL (PthAs e PthCs) na indução e desenvolvimento do cancro cítrico, ou no possível desencadeamento de resposta de defesa em determinadas hospedeiras e ainda avaliar a expressão de potenciais alvos diretos desses efetores em citros, visando identificar prováveis genes de suscetibilidade ao cancro cítrico.

3. MATERIAL E MÉTODOS

3.1 Geração de mutantes de deleção de PthAs

3.1.1 Construção do cassete de deleção e clonagem em vetor suicida

Para a construção dos cassetes de deleção dos genes *pthA*s, foram desenhados oligonucleotídeos específicos que anelam nas regiões flanqueadoras dos genes *pthA*s (Tabela 1). Desta forma, as sequências dos genes de interesse foram obtidas utilizando-se os oligonucleotídeos F1/R1 e F2/R2 de cada gene (Tabela 1), através da amplificação por PCR do DNA genômico de *X. citri* estirpe 306.

Tabela 1. Oligonucleotídeos utilizados na construção do cassete de deleção. Cada oligonucleotídeo possui um sítio de restrição (sublinhados) para a realização da digestão e posterior ligação no vetor suicida. PthA-R1 (*NdeI*) e PthA-F2 (*NdeI*) são comuns a todos os PthAs. As enzimas de restrição utilizadas estão entre parênteses.

Gene	Oligonucleotídeo
pthA1	F1(*HindIII*) 5´-AAGCTTATGGCAAGGCCGAAGGGAACCTACCCGCG-3’
pthA1-4	R1(*Nde1*) 5’-GAATGGGATCCATATGGCATACCTCTTTACATGGTCGCC-3’
pthA1-4	F2(*Nde1*) 5’-GCTCGCATGGCATATGGAGCTATTGCCTCAGTGAGGC-3’
pthA1	R2(*EcoR1*) 5’-TTGAATTCCTGCGCCACTACGCCTATTCCATCGTGAAC -3’
pthA2	F1(*HindIII*) 5’-AAGCTTCCTCCGTGGAGACGGCGTGTTCTGCCCGCC-3’
pthA2	R2(*EcoR1*) 5’-GAATTCCGCGCGTATCCACGCGCGAACAGAACCC-3’
pthA3	F1(*HindIII*) 5’-AAGCTTGTGATTCCAGCCAAAGCCCTTCACGTTGCG-3’
pthA3	R2(*EcoR1*) 5’-GAATTCCCGGCACTGCATCCTCTTTGAGCACCTGCG-3’
pthA4	F1(*HindIII*) 5’-AAGCTTGCGGGAGTCCCTGCGGCACGATGGATCAAG-3’
pthA4	R2(*EcoR1*) 5’-GAATTCCAGTTGAGCGCGCTCGGCCTGGTCGTGAAC-3’

A bactéria *X. citri* foi estriada em meio LB ágar sem sal, ou LBON ágar (1% de bacto triptona, 0,5% de extrato de levedura e 1,5% de ágar) + ampicilina 100 µg/mL e mantida em estufa a 28ºC por 48 h. Uma colônia isolada foi retirada, misturada em 50 µL de água milli-Q e aquecida a 95ºC por 5 min, obtendo assim o DNA genômico de *X. citri*. Na amplificação por PCR foram utilizadas as seguintes condições: 2,5 mM de cada dNTP, 1,5 mM de $MgCl_2$, 5 µM de cada iniciador, 4 µL do DNA e 2 U de *Taq* DNA polimerase *high fidelity* para um

volume final de 40 µL. As condições do ciclo utilizado foram: 1 ciclo de 94ºC por 4 min, seguido de trinta e cinco ciclos de 30 s de desnaturação a 94ºC, 30 s de anelamento a 58ºC e 1 min e 20 s de extensão a 72ºC. As regiões flanqueadoras amplificadas, tanto *upstream* quanto *downstream* aos genes *pthA*s, contêm cerca de 1000 pb (Figura 6).

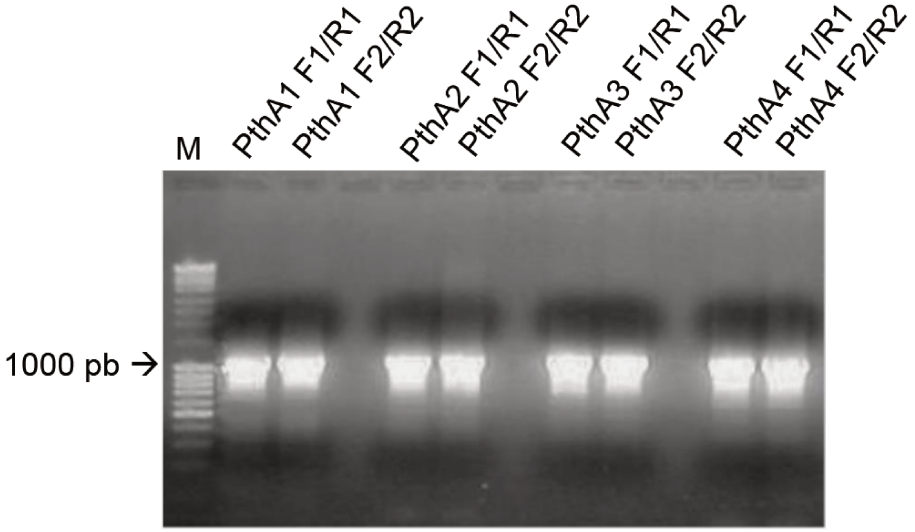

Figura 6. Resultado da amplificação por PCR do DNA genômico de *X. citri* resolvido em gel de agarose 1%. A figura revela a amplificação dos incertos flanqueadores de *pthA*, sendo utilizado um par de primers distinto para cada reação. A seta indica a banda majoritária de aproximadamente 1000 pb e "M" o marcador molecular.

Os fragmentos de PCR com aproximadamente 1000 pb foram excisados do gel de agarose 1% e purificados utilizando o kit *Gel Extraction Kit* (Qiagen) de acordo com o protocolo do fabricante. O produto de PCR purificado foi ligado ao vetor pGEM-T-Easy e a ligação transformada em células competentes de *Escherichia coli* DH5α por choque térmico. Estas células foram mantidas a 37ºC, 200 rpm por 1 h e plaqueadas em meio LB ágar (1% de bacto triptona, 0,5% de extrato de levedura, 1% de cloreto de sódio e 1,5% de ágar, pH 7,5) seletivo com ampicilina 100 µg/mL + IPTG + X-Gal e posteriormente incubadas em estufa a 37°C por 16 h. A seleção dos transformantes foi feita por meio de PCR de colônias brancas utilizando os primers F1/R1 e F2/R2 de cada *pthA*. Em seguida, a cultura foi crescida em meio líquido LB + ampicilina 100 µg/mL por 16 h e a extração plasmidial efetuada através do kit *Spin Miniprep Kit* (Qiagen), seguindo as instruções do fabricante. As sequências dos fragmentos de 1000 pb foram confirmadas por sequenciamento do DNA plasmidial utilizando-se os primers T7 e SP6, que se anelam no vetor pGEM-T-Easy. Os fragmentos amplificados com os oligonucleotídeos F1/R1 foram digeridos com as enzimas de restrição *HindIII* e *NdeI*,

e os fragmentos amplificados com F2/R2, digeridos com *NdeI* e *EcoRI*. O vetor suicida pNPTS138 (Jacobs *et al.*, 1999; Andrade, 2011; Andrade *et al.*, 2014) (Figura 7), que confere resistência à canamicina e sensibilidade à sacarose, foi digerido com *HindIII* e *EcoRI* para a realização de uma ligação tripla. Efetuou-se a ligação tripla unindo-se os fragmentos amplificados de 1000 pb purificados e digeridos (F1/R1 e F2/R2) ao vetor suicida digerido, a fim de se obter os fragmentos de aproximadamente 2000 pb clonados neste vetor (Figura 7). Nesta etapa foi utilizado a enzima T4 DNA ligase sob incubação no banho a 16ºC por 16 h. Em seguida, a ligação tripla foi usada para transformar células de *E. coli* DH5α quimiocompetentes, que posteriormente foram plaqueadas em meio LB ágar contendo canamicina 100 µg/ml para seleção dos transformantes. A confirmação das clonagens no vetor suicida foi feita através de PCR e sequenciamento dos plasmídeos utilizando-se os primers F1 e R2 de cada gene (Figura 8).

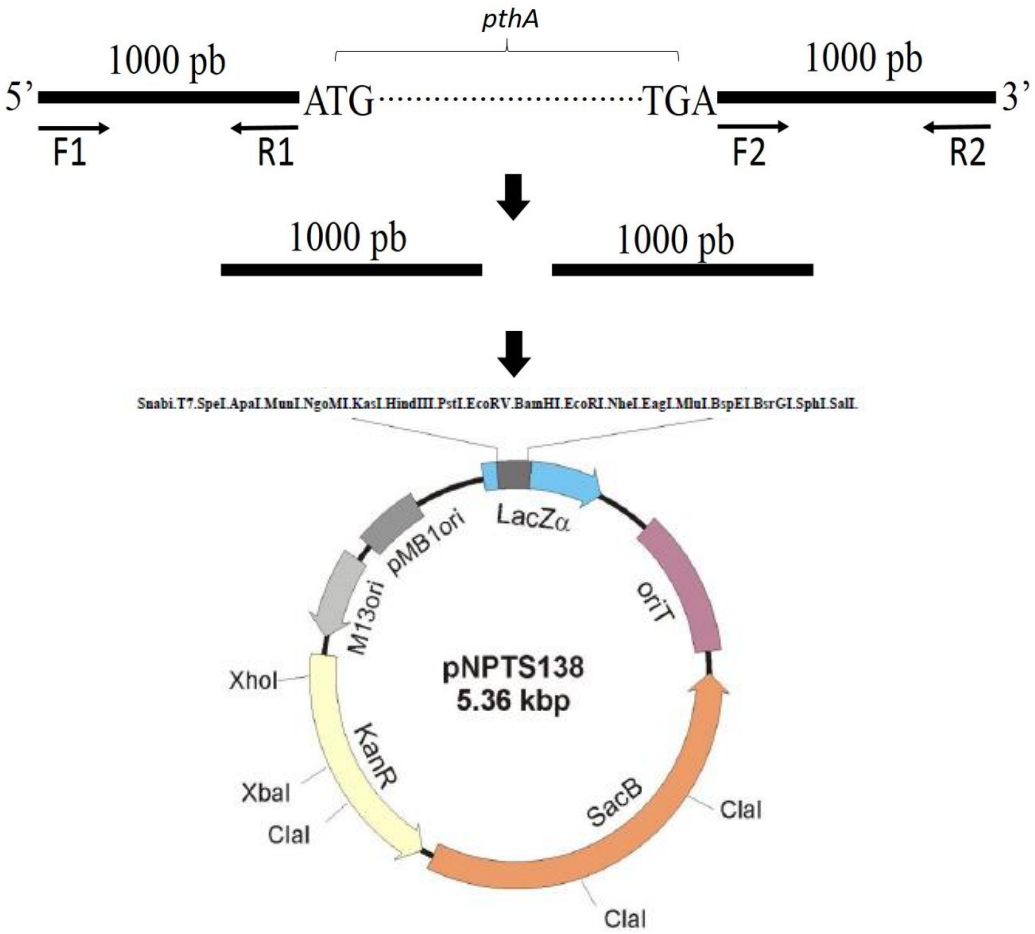

Figura 7. Representação esquemática da estratégia de clonagem das regiões de 1000 pb *upstream* e *downstream* dos *pthAs* no vetor pNPTS138. Os fragmentos de 1000 pb foram obtidos por PCR utilizando os primers F1/R1 e F2/R2. Estes fragmentos, totalizando 2000 pb foram clonados no vetor suicida pNPTS138. As regiões ATG e TGA representam os códons de início e parada, respectivamente, dos genes *pthAs* (adaptação de Andrade, 2011).

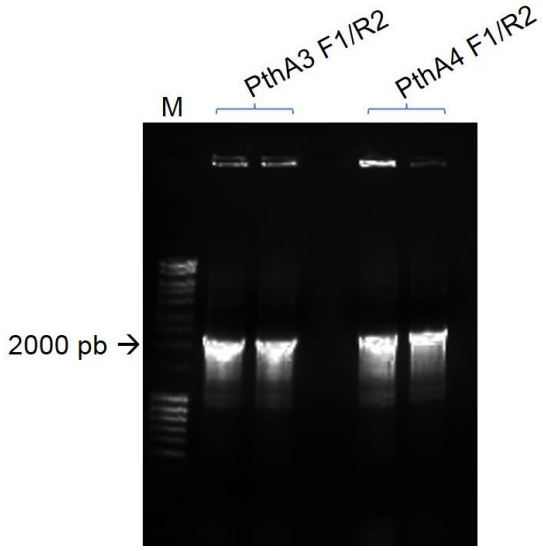

Figura 8. Confirmação da obtenção do cassete de deleção por PCR resolvida em gel de agarose 1%. Nesta figura estão ilustradas somente a amplificação do cassete de deleção dos genes *pthA3* e *pthA4*, onde foram utilizados os primers F1 e R2 de cada gene *pthA* correspondente. A seta indica bandas com aproximadamente 2000 pb e "M" corresponde ao marcador molecular.

3.1.2 Preparo de células eletrocompetentes e transformação por eletroporação de *X. citri*

Para o preparo das células eletrocompetentes, células de *X. citri* estirpe 306 foram crescidas em 200 mL de meio LBON, a 28ºC, 200 rpm, até atingir uma OD_{600} de 0,5 a 0,6. As células foram mantidas no gelo por 10 min e então centrifugadas a 4000g por 10 min, a 4ºC. Posteriormente as células foram lavadas duas vezes com água milli-Q gelada, e submetidas a mais duas lavagens com glicerol 10%. Após as lavagens, as células foram ressuspendidas em 1 mL de glicerol 10% e aliquotados 60 µL em tubos *eppendorf* para o armazenamento a -80ºC.

No procedimento de eletroporação foram misturados de 100 a 200 ng do DNA plasmidial (pNPTS138 contendo os fragmentos *upstream* e *downstream* de cada *pthA*) com os 60 µL de célula competente. Em seguida aliquotamos essas células em cubetas de eletroporação de 2 mm, mantendo sempre as células no gelo. A eletroporação foi realizada utilizando o equipamento *Gene Pulser Xcell* da Bio-Rad, sob as seguintes condições: aplicação de pulso na voltagem de 3,0 KV a 25µF, 200Ω. Imediatamente após a eletroporação, foram adicionados 1 ml de meio líquido LBON, permanecendo as células incubadas por 4 h no shaker a 28ºC, 200 rpm, para a recuperação das células transformantes. Após este período, plaqueamos as células em meio LBON ágar seletivo contendo ampicilina 100 µg/ml e canamicina 100 µg/ml e mantivemos em estufa a 28ºC por 48 h (Oshiro *et al.*, 2006; Andrade, 2011).

3.1.3 Seleção e confirmação de mutantes de deleção de *pthA*s obtidos através de recombinação homóloga

As células transformantes que cresceram em meio contendo ampicilina 100 µg/ml e canamicina 100 µg/ml foram selecionadas e repicadas sucessivamente em dois meios seletivos: LBON + ampicilina 100 µg/ml + canamicina 100 µg/ml e LBON + ampicilina 100 µg/ml + canamicina 100 µg/ml + 5% de sacarose. Este corresponde ao primeiro evento de recombinação homóloga, onde o plasmídeo pNPTS138 é inserido no genoma de *X. citri*. Como o vetor suicida pNPTS138 expressa o gene *SacB*, que confere sensibilidade a sacarose, somente foram selecionadas as colônias que cresceram em LBON + ampicilina 100 µg/ml + canamicina 100 µg/ml e não cresceram em LBON + ampicilina 100 µg/ml + canamicina 100 µg/ml + 5% de sacarose. Essas colônias selecionadas foram crescidas em meio LBON contendo ampicilina 100 µg/ml, a 28ºC, 200 rpm, por 20 h. Nesta etapa espera-se que ocorra o segundo evento de recombinação homóloga e saída do vetor suicida contendo a região do gene de interesse que foi recombinado. Foi feita uma diluição de 10^{-3}, 10^{-4} e 10^{-5} das células crescidas e plaqueamento em meio LBON + ampicilina 100 µg/ml + 5% de sacarose. As placas foram mantidas em estufa a 28ºC por 48 h. As colônias que cresceram neste meio foram repicadas sucessivamente em dois meios seletivos: LBON + ampicilina 100 µg/ml + 5% de sacarose e LBON + ampicilina 100 µg/ml + canamicina 100 µg/ml + 5% de sacarose (Figura 9). As células que cresceram somente no meio LBON + ampicilina 100 µg/ml + 5% de sacarose foram selecionadas, pois, provavelmente são células que sofreram duplo evento de recombinação e perderam o vetor pNPTS138 (Oshiro *et al.*, 2006; Andrade, 2011). Para a confirmação da deleção do gene de interesse foram feitas reações de PCR utilizando-se os oligonucleotídeos que flanqueiam o gene deletado (F1 e R2) (Figuras 10 e 11). No total foram confirmadas a obtenção de 7 mutantes de deleção de *pthA*s, sendo três mutantes simples (Δ1, Δ3 e Δ4), três mutantes duplos (Δ1-3, Δ1-4 e Δ3-4) e um mutante triplo (Δ1-3-4) (Figura 11). Reações de PCR controle também foram efetuados para a confirmação dos mutantes, sendo utilizado os primers PthAN2/R2 e PthAN2/PthAC (Figuras 10 e 12) (Tabela 2). Além disso, foi efetuado o sequenciamento dos mutantes de deleção amplificando as regiões que flanqueiam os genes deletados, utilizando o primer seqPthANF (Tabela 2) (Figuras 10 e 13).

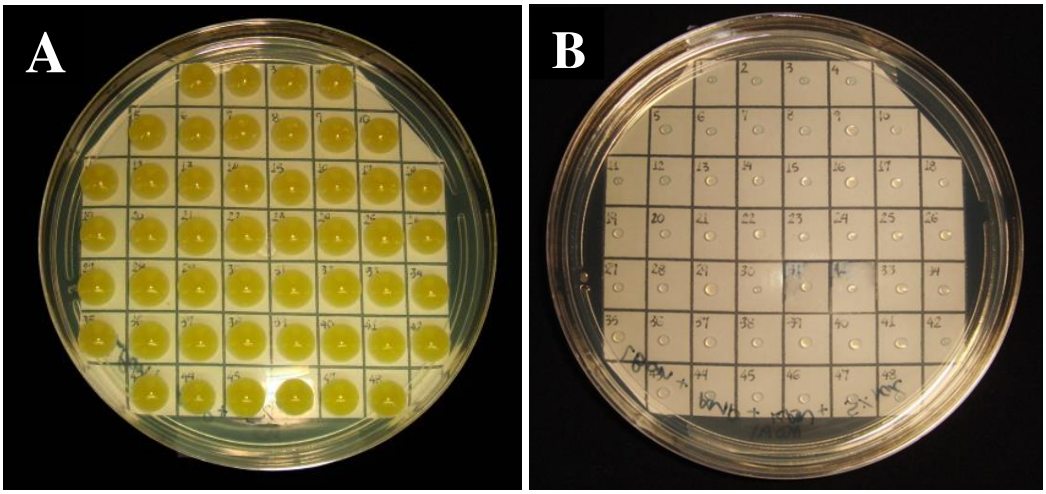

Figura 9. Seleção de colônias bacterianas nas etapas do processo de recombinação homóloga. As figuras **A** e **B** representam a seleção de colônias na última etapa do evento de recombinação. Na figura **A** o meio seletivo corresponde a LBON + ampicilina + 5% de sacarose e na figura **B** LBON + ampicilina + canamicina + 5% de sacarose. As colônias foram repicadas simultaneamente nos dois meios, de forma que cada quadrado, posicionado no mesmo local de cada placa, corresponde a mesma colônia bacteriana. As bactérias que sofreram o segundo evento de recombinação homóloga devem crescer no meio contendo LBON + ampicilina + 5% de sacarose e não crescer no meio LBON + ampicilina + canamicina + 5% de sacarose. Neste exemplo, todas as colônias são potenciais colônias com deleção no gene *pthA*, pois todas cresceram no meio A e não cresceram no meio B.

Os mutantes de deleção dupla (Δ1-3, Δ1-4 e Δ3-4) e tripla (Δ1-3-4) foram gerados utilizando os mutantes simples em etapas sucessivas de deleção de *pthA*, de forma que em uma etapa foi nocauteado o gene *pthA1*, na outra etapa o gene *pthA3* e assim por diante.

Apesar de grandes esforços, infelizmente não foi possível obter o mutante de deleção do gene *pthA2*, o que sugere que esta proteína possa ter outro papel na célula bacteriana ou que a região adjacente ao gene selecionado para o evento de recombinação possa conter algum gene importante para a sobrevivência da bactéria.

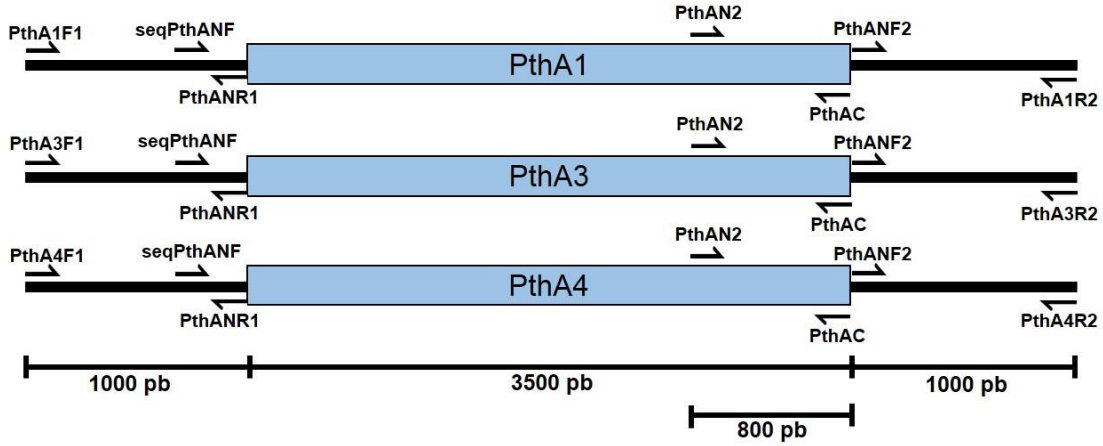

Figura 10. Esquema da disposição dos oligonucleotídeos utilizados para obtenção e confirmação dos mutantes de deleção. O esquema ilustra as regiões de 1000 pb *upstream* e *downstream* dos genes *pthA*s em azul, com 3500 pb, evidenciando a posição dos oligonucleotídeos utilizados para a construção do cassete de deleção e confirmação dos mutantes de deleção de *pthA*s. Os oligonucleotídeos PthA1F1, PthA1R2, PthA3F1, PthA3R2, PthA4F1 e PthA4R2 são específicos para cada um dos PthAs, enquanto que PthANR1, PthANF2, seqPthANF, PthAN2 e PthAC são comuns para todos os PthAs.

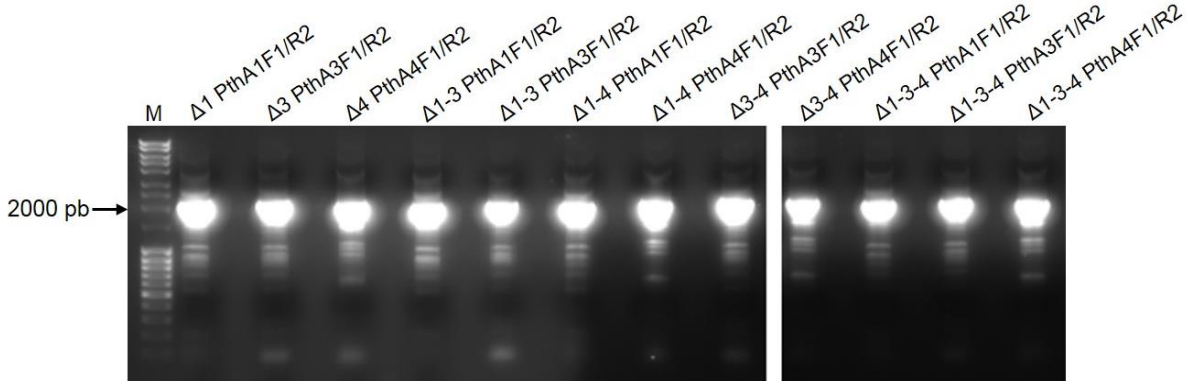

Figura 11. Gel de agarose 1% mostrando os fragmentos de DNA dos mutantes simples, duplos e triplo, gerados por PCR. As bandas de 2000 pb correspondem aos 1000 pb *upstream* e *downstream* dos *pthA*s, indicando a deleção dos *pthA*s. Os primers utilizados foram os respectivos F1 e R2 que anelam nas regiões flanqueadoras de cada gene *pthA*.

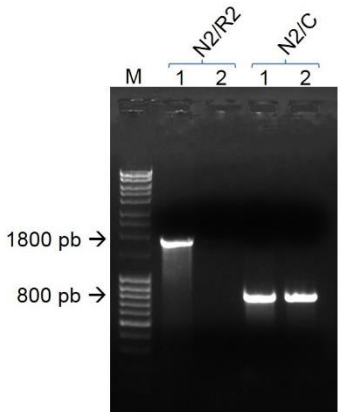

Figura 12. Reações de PCR controle resolvidas em gel de agarose 1%. As bactérias utilizadas nesta reação de PCR foram *X. citri* (1) e o mutante Δ1 (2). O primeiro par de primers utilizado foi o PthAN2 (N2), que anela na região interna de qualquer PthA e o PthA1R2 (R2), que anela na região flanqueadora ao gene *pthA1* (Tabelas 1 e 2, Figura 10). Nota-se que somente na reação com *X. citri* foi possível observar a banda de aproximadamente 1800 pb, indicando que *X. citri* ainda possui o gene *pthA1*, porém o mutante Δ1 possui o gene deletado. Na reação utilizando os primers PthAN2 e PthAC (C) (Tabela 2, Figura 10) foi observada a banda de aproximadamente 800 pb nos dois casos, tanto em *X. citri* quanto no mutante Δ1, comprovando que os outros PthAs (2, 3 e 4) continuam presentes neste mutante. A letra M corresponde ao marcador molecular.

Tabela 2. Oligonucleotídeos utilizados na confirmação dos mutantes de deleção e na complementação dos efetores TAL em vetor de expressão em *Xanthomonas*.

Oligonucleotídeo	**Sequência 5'- 3'**
seqPthANF	CCTCCATGCGGGTCCGTGATCGCC
PthAN2	CATATGGCGTTGACCAACGACCAC
PthAC	GAATTCTCACTGAGGCAATAGCTC
proPthANF	CCTCCATGCGGGTCCGTGATCGCC
PromotA4F	CGCCTTCATGTCTGCGCCTCACCC
M13F	GTAAAACGACGGCCAGTG

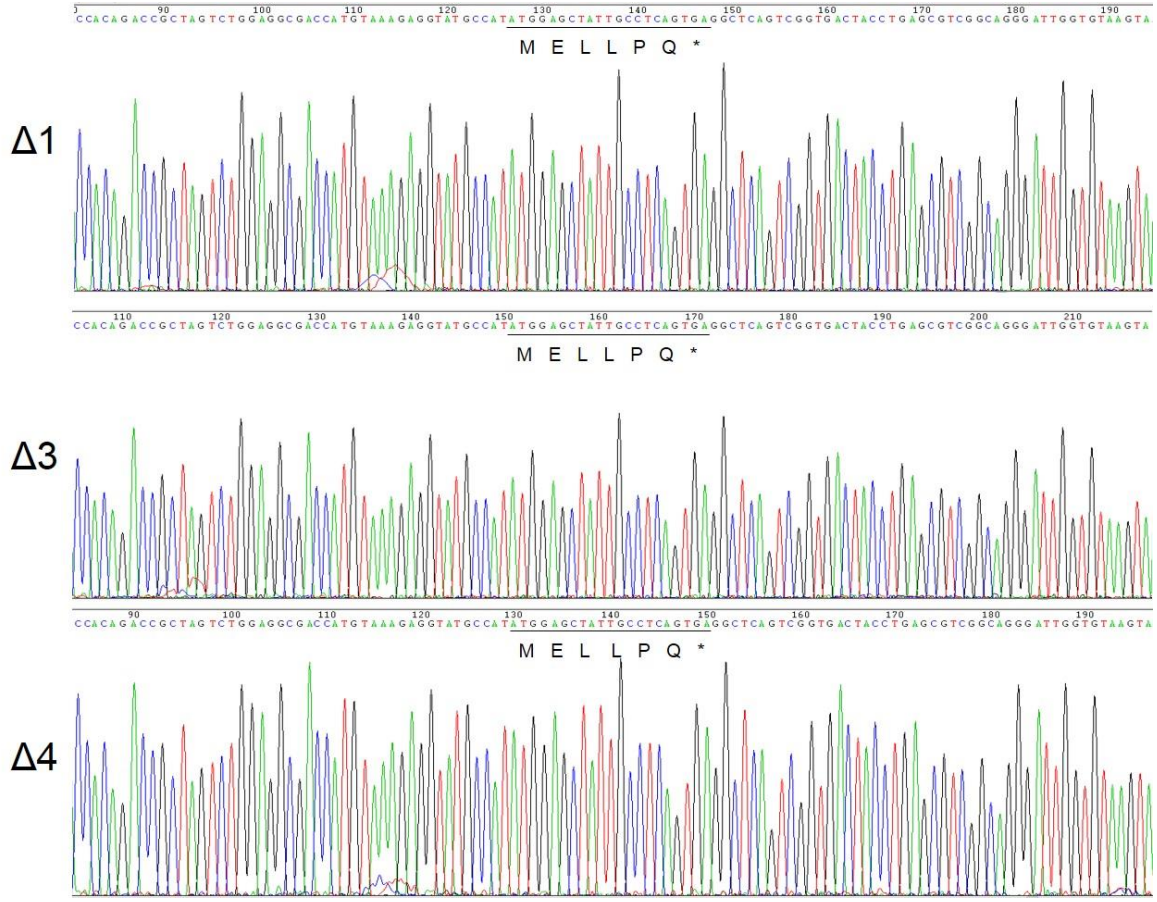

Figura 13. Demonstração do sequenciamento dos mutantes Δ1, Δ3 e Δ4. A região do cromatograma apresentado corresponde a região de deleção do gene, onde foram indicados a sequência de aminoácidos codificada na região do *pthA* mutado. Para o sequenciamento utilizou-se os fragmentos de 2000 pb amplificados por PCR, que foram obtidos utilizando-se os oligonucleotídeos específicos para cada *pthA* (Tabela 1). O oligonucleotídeo utilizado no sequenciamento foi o proPthANF (Tabela 2) que se liga a uma região comum da região promotora dos *pthA*s, pois aproximadamente 250 pb *upstream* aos genes *pthA*s são idênticos em todos os *pthA*s.

3.2 Obtenção de material vegetal

Mudas de laranja doce (*Citrus sinensis*) das variedades Pêra, Valência, Natal, Hamlin e Lima Sorocaba, mudas de limão Tahiti (ou lima ácida, *Citrus latifolia*) e limão Galego (ou lima ácida, *Citrus aurantifolia*), certificadas como livre de patógeno, foram obtidas de viveiros da região (Citrograf) e mantidas em vasos dentro de casa de vegetação. O porta-enxerto corresponde ao limão Cravo (ou lima ácida, *Citrus limonia*).

3.3 Análise funcional dos mutantes de deleção de *pthA*s

Células bacterianas de *X. citri* estirpe 306 e dos 7 mutantes de deleção foram estriadas em placas contendo meio LBON + ampicilina 100 µg/ml a partir de estoques a -80ºC. As placas permaneceram incubadas a 28ºC por 48 h. As células foram ressuspendidas em água milli-Q estéril e a suspensão bacteriana ajustada para a concentração de OD_{600} = 0,01 (aproximadamente 10^5 células/mL). Folhas jovens de plantas sadias foram inoculadas com aproximadamente 0,1 mL da suspensão bacteriana com o auxílio de seringa e agulha. As plantas foram monitoradas diariamente para a observação do progresso da doença e a avaliação dos sintomas foi efetuada aos 14 dias após a inoculação (dpi). O experimento foi realizado três vezes com três repetições por tratamento, sendo observado resultados similares em todas as repetições.

3.4 Quantificação Bacteriana

3.4.1 Infiltração de folhas de citros

Plantas de laranja doce das variedades Pêra, Valência, Lima Sorocaba e plantas de limão Tahiti foram escolhidas para efetuar a análise de crescimento bacteriano. Folhas jovens foram selecionadas para serem infiltradas, tomando-se o cuidado de escolher folhas com aproximadamente mesma idade em todas as repetições.

As bactérias *X. citri* e os 7 mutantes de deleção foram ressuspendidas em água milliQ estéril e a solução bacteriana foi ajustada para uma concentração de OD_{600} = 0,1. As infiltrações das soluções bacterianas foram feitas em seções foliares com o auxílio de seringas e agulhas. Após a infiltração, as soluções foram plaqueadas em LBON + ampicilina 100 µg/ml somente para registrar o número de células vivas no tempo zero, verificando que foram infiltradas cerca de 10^6 células/mL.

3.4.2 Extração bacteriana e quantificação do crescimento bacteriano

As folhas infiltradas das quatro variedades foram coletadas aos 2 e 14 dpi. Discos foliares correspondentes a 1 cm^2 foram retirados das seções foliares infiltradas, os quais foram macerados em cadinhos com 1 mL de água milliQ estéril. Posteriormente foi feita uma diluição seriada de cada amostra em água milliQ estéril e em seguida determinadas diluições foram plaqueadas em meio LBON + ampicilina 100 µg/ml e mantidas em estufa a 28ºC por 48 h (Figura 14). As colônias bacterianas foram então quantificadas e as diferenças entre os tratamentos (folhas infiltradas com a bactéria selvagem *versus* folhas infiltradas com os mutantes de deleção) foram submetidas ao teste estatístico “t de Student” com nível de

significância de 5% ($p < 0,05$). O experimento foi conduzido com três repetições, obtendo-se resultados semelhantes.

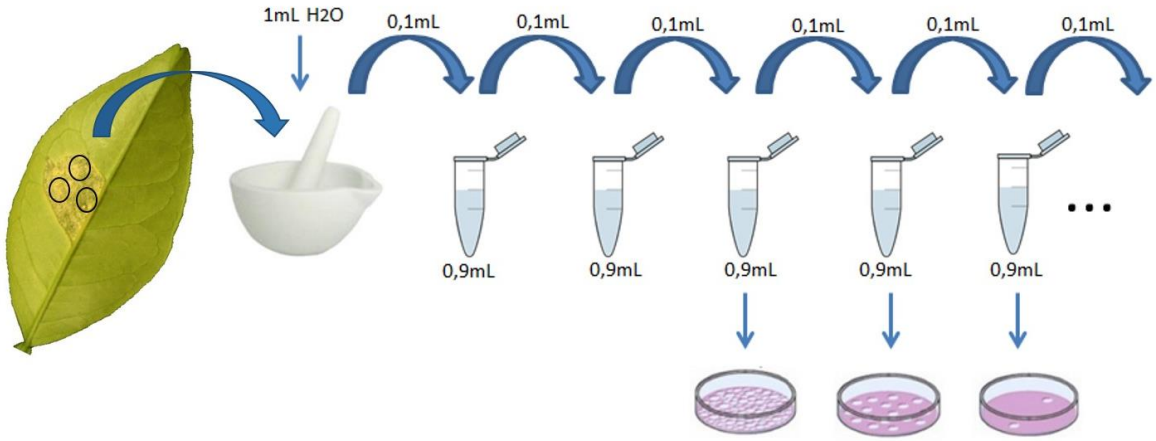

Figura 14. Esquema da extração bacteriana. Discos foliares correspondentes a 1 cm^2 foram retirados das amostras de folhas infiltradas e foram maceradas em cadinho contendo 1 mL de água. Uma alíquota de 0,1 mL foi retirada deste macerado e realizou-se uma diluição seriada e posterior plaqueamento de determinadas diluições.

3.5 Clonagem dos genes *pthA*s e *pthC*s em vetor de expressão de *Xanthomonas*

A clonagem dos genes *pthA*s e *pthC*s foi realizada em dois vetores de expressão de *Xanthomonas*: pMR20 (Skerker *et al.*, 2005) e pUFR047 (DeFeyter *et al.*, 1993).

3.5.1 Clonagem no vetor pMR20

Os genes de *X. citri* estirpe 306 que codificam para as proteínas PthA1 a 4, e os genes de *X. aurantifolii* C, estirpe ICMP 8435, que codificam para as proteínas PthC1 e 2 clonados em vetor de expressão de *E. coli* (pET29a) já estavam disponíveis no laboratório. Os plasmídeos foram então digeridos utilizando-se as enzimas de restrição *XbaI* e *EcoRI* e os fragmentos purificados foram ligados ao vetor pMR20 (Figura 15), utilizando a enzima T4 DNA ligase sob incubação no banho a 16ºC por 16 h. O vetor pMR20 é um vetor de expressão constitutivo usado em *Xanthomonas*, onde o gene a ser expresso está sob controle do promotor lacZ. Por ser este um vetor de baixa cópia, antes da ligação foi feita uma Mid prep, utilizando o kit *Plasmid Midi Kit* (Qiagen) e digestão com as mesmas enzimas de restrição utilizadas para a digestão do inserto. A reação de ligação foi utilizada na transformação de *E. coli* DH5α eletrocompetentes. Estas células foram mantidas a 37ºC, 200 rpm por 1 h e plaqueadas em meio LB ágar seletivo com tetraciclina 15 µg/mL + IPTG + X-Gal e posteriormente incubadas em

estufa a 37°C por 16 h. A seleção dos transformantes foi por meio de PCR de colônia brancas utilizando primers que anelam em uma região comum a todos os PthAs e PthCs (primers PthAN2 e PthAC, Tabela 2), amplificando um inserto de aproximadamente 800 pb.

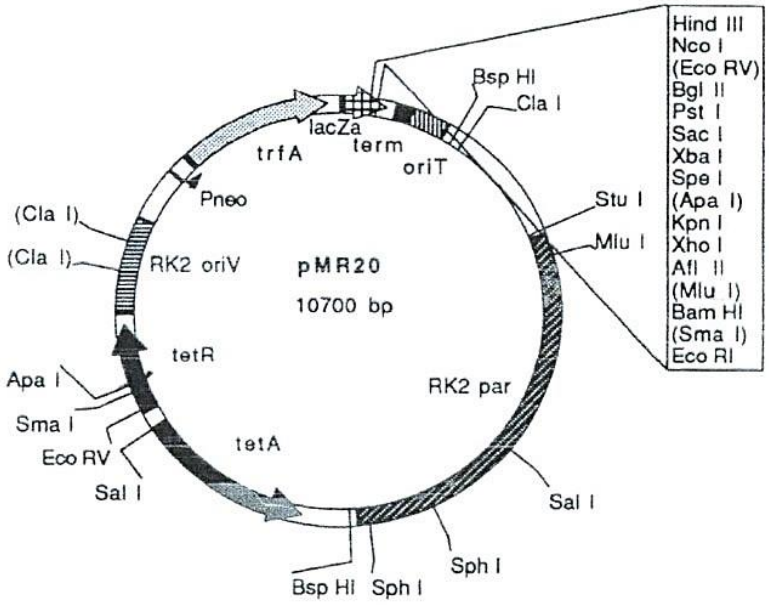

Figura 15. Mapa do vetor pMR20 utilizado para a expressão dos genes *pthAs* e *pthCs* em *Xanthomonas* (Skerker *et al.*, 2005).

3.5.2 Complementação da bactéria B21.2 com os genes *pthA4*, *pthC1* e *pthC2*

Após a clonagem dos genes *pthA*s e *pthC*s em vetor de expressão em *Xanthomonas* (pMR20), a cultura de *E.coli* contendo o vetor foi crescida em meio líquido LB + tetraciclina 15 µg/mL e a extração plasmidial efetuada através do kit Spin Miniprep Kit (Qiagen), seguindo as instruções do fabricante. Inicialmente foi feito um teste somente com a bactéria B21.2, uma cepa de *X. citri* mutante, que possui o gene *pthA4* não funcional, portanto uma bactéria incapaz de causar cancro (gentilmente cedida pelo Dr. Dean Gabriel, da Universidade da Flórida) (Swarup *et al.*, 1991; Swarup *et al.*, 1992; Al-Saadi *et al.*, 2007). Dessa forma, o DNA plasmidial recombinado foi utilizado para a eletroporação da bactéria mutante B21.2. A obtenção de células B21.2 eletrocompetentes e a eletroporação utilizando estas células seguiu o mesmo protocolo utilizado para *X. citri* (item 3.1.2), com a diferença de que as células foram posteriormente plaqueadas em meio LBON + tetraciclina 30 µg/ml.

As bactérias B21.2 foram complementadas somente com os genes *pthA4*, *pthC1* e *pthC2* e infiltradas em folhas de laranja doce variedade Pêra, com o auxílio de seringas e

agulhas. As soluções bacterianas foram preparadas e ajustadas para uma concentração de OD_{600} = 0,3, e as folhas infiltradas foram coletadas aos 12 dpi para a avaliação do fenótipo resultante da infiltração.

3.5.3 Detecção da expressão de PthA4, clonada no vetor pMR20, por meio de *Western blot*

As bactérias *X. citri*, B21.2 e B21.2 complementada com PthA4 foram estriadas em placas de LBON ágar + ampicilina 100 µg/ml ou tetraciclina 30 µg/ml e mantidas a 28ºC por 48 h. A extração proteica foi realizada diretamente das culturas bacterianas utilizando o tampão de extração de proteínas (100 mM DTT, 2% SDS, 0,1% azul de bromofenol, 10% glicerol, 50 mM tris-HCl pH6,8). Os extratos bacterianos totais foram aquecidos a 95ºC por 10 min e permaneceram no sonicador de banho por 1 h. Logo em seguida a etapa de aquecimento foi repetida e depois mantidas por mais 30 min no sonicador de banho. As amostras foram analisadas por eletroforese em gel de poliacrilamida-SDS 10% coradas com *Coomassie blue*. Em seguida, as proteínas contidas no gel de poliagrilamida-SDS 10% (não corado) foram transferidas para uma membrana de PVDF (difluoreto de polivinila) em tampão de transferência (48 mM de tris-base, 39 mM de glicina, 0,037% de SDS e 20% de metanol), onde a transferência foi realizada a 350 mA por 1 h e 15 min. Posteriormente, a membrana foi incubada em solução bloqueadora (5% de leite em pó desnatado em 1x TBS) por 1 h e depois incubada com o anticorpo primário *Anti-PthA* (diluição 1:1000), sendo mantido overnight a 4ºC. Após a incubação com o anticorpo primário, a membrana foi lavada quatro vezes (de 10 min sob leve agitação) em solução TBS (20 mM de Tris-base; 150 mM de NaCl, pH 7,5) e incubada com anticorpo secundário *anti-rabbit* (1:3000) (ECL Kit – *Amersham Biosciences*), por 1 h. A membrana foi novamente lavada quatro vezes por 10 min em solução TBS. A detecção foi feita utilizando-se o método de quimioluminescência do Kit ECL (*Amersham Biosciences*).

3.5.4 Clonagem no vetor pUFR047

O vetor pUFR047 (Figura 16) é um vetor de expressão desprovido de um promotor para a expressão dos genes de interesse em *Xanthomonas*. Assim, com o propósito de expressar os genes que codificam as proteínas PthAs e PthCs, inserimos o promotor do gene *pthA4* no vetor pUFR047 para direcionar a expressão das proteínas de interesse.

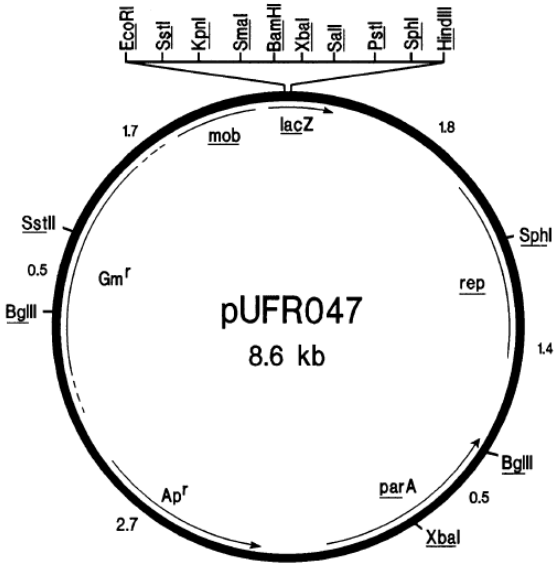

Figura 16. Mapa do vetor de expressão em *Xanthomonas* pUFR047 (DeFeyter *et al.*, 1993).

O inserto contendo a região promotora de *pthA4* corresponde a região de aproximadamente 1000 pb *upstream* ao gene que codifica para *pthA4*. Desta forma, o vetor pGEM-T-Easy contendo a região promotora de *pthA4* foi digerido com as enzimas de restrição *HindIII* e *NdeI*. O inserto liberado, de aproximadamente 1000 pb, foi excisado do gel de agarose 1% e purificado utilizando o kit *Gel Extraction Kit* (Qiagen) de acordo com o protocolo do fabricante.

Os genes de *X. citri* que codificam para as proteínas PthA1 a 4, e os genes de *X. aurantifolii* C que codificam para as proteínas PthC1 e 2 foram digeridos do vetor de expressão de *E. coli* (pET29a) utilizando as enzimas de restrição *NdeI* e *EcoRI*. Os fragmentos de aproximadamente 3500 pb foram excisados do gel de agarose 1% e purificados utilizando o mesmo kit acima.

O vetor pUFR047 também é um vetor de baixa cópia, por isso foi efetuada uma Mid prep, utilizando o kit *Plasmid Midi Kit* (Qiagen), seguindo as especificações do fabricante. Então o vetor foi digerido com as enzimas de restrição *HindIII* e *EcoRI*. A banda de vetor linearizada foi excisada do gel de agarose 1% e purificada.

Para a clonagem da região promotora de *pthA4* e do próprio gene *pthA4* no vetor pUFR047 linearizado efetuou-se uma ligação tripla, utilizando a enzima T4 DNA ligase sob incubação no banho a 16°C por 16 h. A reação de ligação foi utilizada na transformação de *E. coli* DH5α eletrocompetentes com aplicação do pulso de voltagem de 2,5 KV a 25μF, 200Ω, utilizando o equipamento *Gene Pulser Xcell* da Bio-Rad. Imediatamente após o pulso foi adicionado 1 mL de meio LB líquido e depois as células foram mantidas a 37°C, 200 rpm por

1 h. As células foram então plaqueadas em meio LB ágar seletivo com gentamicina 5 µg/mL + IPTG + X-Gal e posteriormente incubadas em estufa a 37°C por 16 h. A seleção dos transformantes foi por meio de PCR de colônias brancas utilizando 2 pares de primers, um que anela na região promotora (PthA4F1 e PthANR1, Tabela 1) e outro que anela em uma região comum a todos os PthAs e PthCs (PthAN2 e PthAC, Tabela 2), amplificando um inserto de aproximadamente 1000 e 800 pb, respectivamente (Figuras 17 e 18). A clonagem foi confirmada por sequenciamento utilizando os primers M13F, que anela no vetor amplificando também a região promotora e o primer PromotA4F, que anela na porção final da região promotora de PthA4, amplificando ainda o início da sequência de PthA4, comprovando a ligação do promotor ao gene (Tabela 2) (Figura 17).

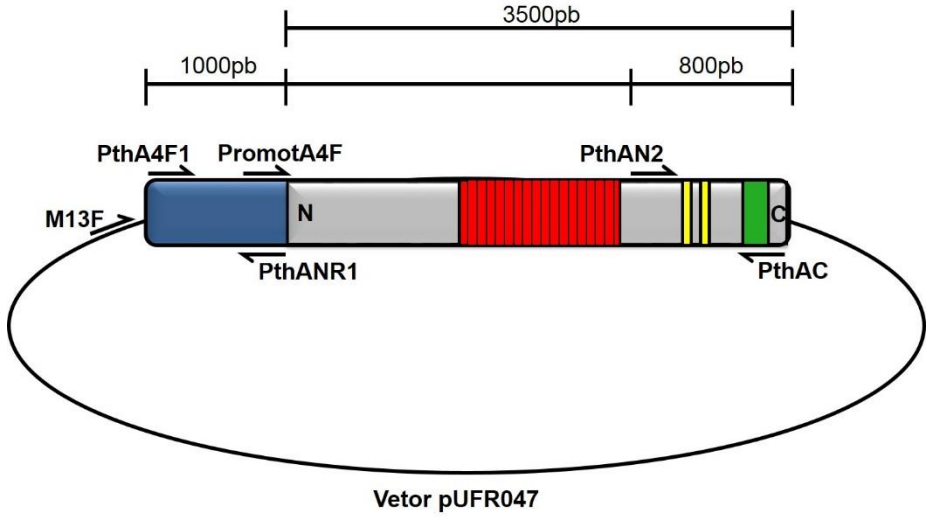

Figura 17. Figura esquemática da construção no vetor pUFR047 demonstrando as regiões de anelamento dos primers. Em azul é ilustrado a região promotora de 1000 pb e em cinza encontra-se toda a região da proteína PthA de 3500 pb, incluindo as regiões de repetição de aminoácidos do domínio interno (vermelho), o sinal de localização nuclear (amarelo) e o domínio de ativação (verde), mostrando ainda a porção N-terminal (N) e C-terminal (C) do PthA. Os primers PthA4F1 e PthANR1 amplificam a região promotora de 1000 pb e PthAN2 e PthAC anela na porção final comum a todos os PthAs e PthCs, amplificando 800 pb. O primer M13F anela no vetor e PromotA4F anela na porção final da região promotora.

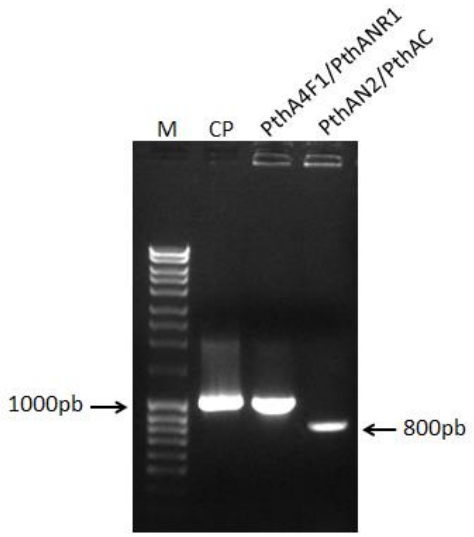

Figura 18. Confirmação da clonagem da região promotora de *pthA4* e do gene *pthA4* em pUFR047 por PCR, resolvido em gel de agarose 1%. A presença da região promotora foi identificada pela amplificação de uma banda de aproximadamente 1000 pb utilizando os primers PthA4F1/PthANR1 e o gene *pthA4* foi identificado utilizando os primers PthAN2/PthAC, obtendo a amplificação de uma banda de aproximadamente 800 pb. "M" corresponde ao marcador molecular e "CP" ao controle positivo, onde foi efetuada uma reação controle para o mix de PCR utilizando um DNA plasmidial contendo a região promotora.

Após a confirmação da construção de pUFR047 + promotor + *pthA4* por sequenciamento, prosseguimos utilizando esta construção como base para as clonagens dos outros PthAs e PthCs. Efetuou-se uma Mid-prep e então uma digestão com as enzimas de restrição *NdeI* e *EcoRI* para liberar uma banda de aproximadamente 3500 pb correspondente ao gene *pthA4*. A banda de aproximadamente 9,6 kb (pUFR047 + promotor) foi purificada do gel de agarose 1% para ser utilizado em uma nova ligação para clonar individualmente os genes *pthA1*, *pthA2*, *pthA3*, *pthC1* e *pthC2* no vetor pUFR047 contendo a região promotora. Desta forma, foram feitas ligações simples do vetor + promotor com os genes *pthA*s e *pthC*s utilizando a enzima T4 DNA ligase sob incubação no banho a 16°C por 16 h. Todas essas construções foram então transformadas em *E. coli* DH5α eletrocompetentes e plaqueadas em meio LB + gentamicina 5 μg/mL + IPTG + X-Gal. A confirmação das colônias transformadas foi feita a partir de PCR e sequenciamento, utilizando-se os pares de primers PthA4F1/PthANR1 e PthAN2/PthAC (Figura 19).

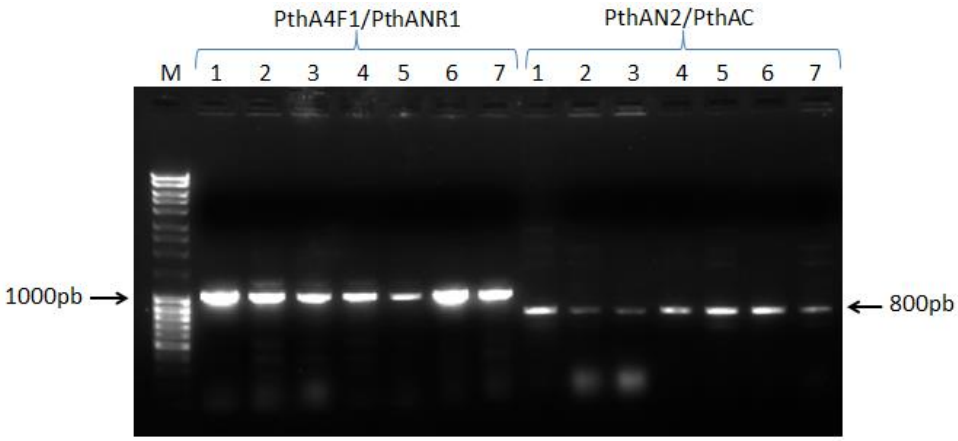

Figura 19. Reações de PCR resolvidas em gel de agarose 1%. Esta figura ilustra como exemplo a confirmação da clonagem do gene *pthA1* no vetor pUFR047 + promotor. Foram utilizados os primers PthA4F1/PthANR1 e PthAN2/PthAC que amplificam um fragmento de 1000 pb e 800 pb, respectivamente.

3.5.6 Complementação das bactérias mutantes com as construções no vetor pUFR047

Após a clonagem dos genes *pthA*s e *pthC*s no vetor pUFR047, as culturas de *E.coli* contendo as contruções no vetor pUFR047 foram crescidas em meio líquido LB + gentamicina 5µg/mL e a extração plasmidial efetuada através do kit *Plasmid Midi Kit* (Qiagen). O DNA plasmidial foi utilizado para a eletroporação dos mutantes de deleção de *pthA*s e do mutante B21.2. No procedimento de eletroporação, foi misturado de 100 a 200 ng do DNA plasmidial com 60 µL de célula competente. A eletroporação foi realizada utilizando o equipamento *Gene Pulser Xcell* da Bio-Rad, sob as seguintes condições: aplicação de pulso na voltagem de 3,0 KV a 25µF, 200Ω. Após a eletroporação, foi adicionado 1 ml de meio líquido LBON, permanecendo as células incubadas por 4 h no shaker a 28ºC, 200 rpm, para a recuperação das células transformantes. Após este período, as células foram plaqueadas em meio LBON ágar seletivo contendo gentamicina 5 µg/ml e mantidas em estufa a 28ºC por 48 h. A confirmação das células transformantes foi através de PCR utilizando o par de primer M13F, que anela no vetor, e PthANR1, que anela na região final do promotor (Figura 20).

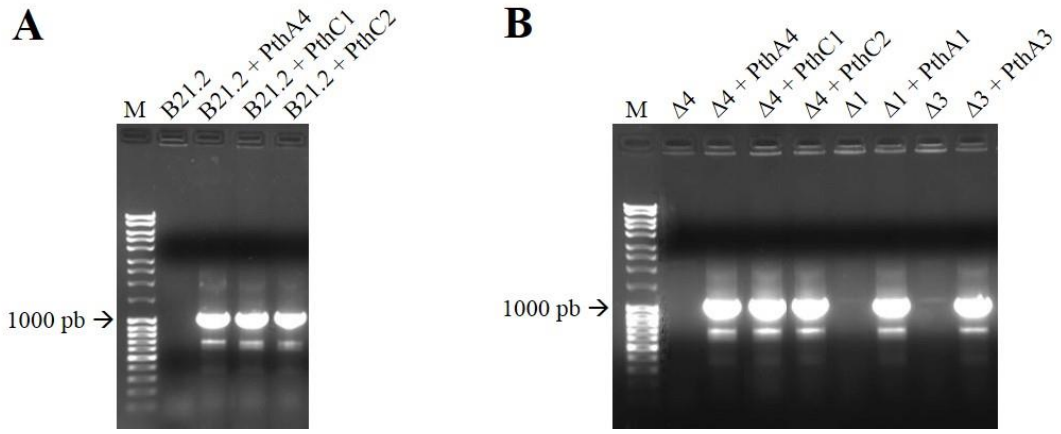

Figura 20. Confirmação da complementação da bactéria mutante B21.2 (**A**) e dos mutantes de deleção simples (Δ1, Δ3 e Δ4) (**B**) com as construções de pUFR047 + promotor contendo os genes *pthA*s e *pthC*s resolvidas em gel de agarose 1%. O par de primers utilizado nesta PCR foi o M13F e PthANR1 que anela no vetor e no final da região promotora, respectivamente, amplificando uma banda de aproximadamente 1000 pb.

3.6 Análise *in planta* das complementações feitas em mutantes de deleção de *pthA*s e no mutante B21.2 com os genes *pthA*s e *pthC*s

Folhas jovens de laranja Pêra e limão Galego foram selecionadas para serem infiltradas com a bactéria selvagem *X. citri*, o mutante B21.2, os mutantes de deleção de *pthA*s, e as bactérias complementadas com os *pthA*s e *pthC*s. As infiltrações foram realizadas com o auxílio de seringa e agulha, e as soluções bacterianas foram ajustadas para uma concentração final de OD_{600} = 0,01 (aproximadamente 10^5 células/mL), sendo que a evolução dos sintomas foi acompanhada diariamente. As folhas foram coletadas aos 21 dpi para a análise dos sintomas. O experimento foi realizado três vezes, com três repetições para cada tratamento, sendo observado resultados semelhantes.

3.7 Extração de RNA e obtenção de cDNA

As folhas de citros infiltradas com as bactérias selvagem, mutantes de deleção, mutantes complementados e água, usada como controle, foram coletadas às 72 h após infiltração (hpi) e congeladas imediatamente em nitrogênio líquido. Posteriormente, as folhas foram maceradas em cadinhos com nitrogênio líquido. Todos os utensílios utilizados nesta etapa, como cadinho, pistilo e espátulas foram tratados com H_2O_2 + H_2O DEPC (Diethyl pyrocarbonate) em uma concentração de 1:5 por 20 min, antes de macerar as amostras.

A extração de RNA foi realizada pelo método de trizol (Invitrogen), seguindo o protocolo e as instruções do fabricante. Ao final, o RNA foi ressupendido em H_2O DEPC e armazenado a -80ºC. A concentração das amostras de RNA foi medida em Espectrofotômetro Nanodrop.

Todas as amostras de RNA foram ajustadas para uma concentração final de 3,0 µg/µL e tratadas com DNase I (Promega). A síntese de cDNA foi efetuada utilizando o kit RevertAid H Minus First Strand cDNA Synthesis kit (Thermo Scientific) seguindo o protocolo do fabricante. Ao final, as amostras de cDNA foram armazenadas a -20ºC.

3.8 RT-qPCR de alvos de PthAs

Para a realização da PCR em tempo real foi utilizado o equipamento 7500 Real Time PCR System (Applied Biosystems), que comporta placas de 96 poços.

Os oligonucleotídeos usados como iniciadores foram desenhados utilizando-se o programa Primer Express 2.0 (Tabela 3). Na reação de qPCR foi utilizado um total de 25 µL, sendo 1 µL do cDNA sintetizado, 1 µL de cada oligonucleotídeo (*Forward* e *Reverse*) a 5 µM, 12,5 µL de SYBR Green 2x Master Mix (Thermo Scientific) e 9,5 µL de H_2O. As condições de ciclagem da reação foram aquelas definidas pelo ciclo "Universal" do programa 7500 System (Applied Biosystems).

O controle utilizado como calibrador nas reações de qPCR foi o cDNA obtido a partir de folhas infiltradas com H_2O, enquanto os normalizadores utilizados como controle interno foram os genes de *C. sinensis* que codificam para o translocador de malato (de Oliveira *et al.*, 2013) e actina (Mafra *et al.*, 2012). No total, foi extraído o RNA de três folhas independentes para cada tratamento utilizado nas reações de qPCR, correspondendo a três réplicas biológicas; e também foram utilizadas três réplicas técnicas para cada réplica biológica. O teste estatístico "t de Student" com nível de significância de 5% ($p < 0,05$), foi aplicado na análise comparativa dos dados.

Tabela 3. Oligonucleotídeos utilizados nas análises de RT-qPCR.

Oligonucleotídeo	**Sequência 5'-3'**
Tumor related protein F	GCTGAAAGGAATTCTCGAAGTT
Tumor related protein R	CCCCGCCAAGAAATCCA
bZIP transcription factor F	GAGGTCCAGGATGCGGAAA
bZIP transcription factor R	ACGAACCACATGGGACCAA
ABI3 F	CGCACCCCAGGCATCA

ABI3 R	CTGACCCTGAAGCTGGTTTTG
NAC transcription factor F	TCTGGGAAAGCCCCTAAAGG
NAC transcription factor R	GCGGCAACCGATACTCGTT
Cytochrome P450 monooxygenase F	TGGATCATTCGCAACCATTG
Cytochrome P450 monooxygenase R	TCTCCGAAGCTGCATCAAAA
Terpene synthase F	TGCCTACGCCCAACAGTTC
Terpene synthase R	CGCGTGTAAGATTGAGAATTCG
HAP3-like protein F	GTTGATAGCGCAGGGCATAAC
HAP3-like protein R	CGCACCCACCGTAAAGTTGT
Gibberellin 20-oxidase F	ACCTGCTGCTGTCTCTTACTTCTG
Gibberellin 20-oxidase R	GCAGCCCCGGGATGGA
Apyrase F	CGCAAGTTTTCCCCCAATT
Apyrase R	GCCGGCGTCAAAAATAACAG
Pm52 F	GGCCGCCGACAAAGG
Pm52 R	TGAGAGGCGGCCATCATC
Pectate lyase F	AATCAGGGAGCGACGTCAGA
Pectate lyase R	CCCAGGCTTCGCAGGTATC
LOB3 F	GGCGTGGCCCGGTTA
LOB3 R	TGTTGGCAGGTCGGATAGCT
LOB3b F	CTCCATGCCTGCAACATACG
LOB3b R	GTGCAGGTTGGACCATTGG
Tobacco 14-3-3 protein F	GCTCAGGATATCGCAAATGCT
Tobacco 14-3-3 protein R	AGAGCCAGTCCTAGCCGGATAG
Dioxygenase (DIOX) F	GGGACTTCACGTGCGAAAAG
Dioxygenase (DIOX) R	CGCTAATTGGAGCGACATGA
Cysteine proteinase F	GGGCACTGTGGAACTCAGTTG
Cysteine proteinase R	GCCTCTGGTAGATCCATATCCAA
NBS-LRR protein F	GTGGTTTGCCTCTTGCACTTATT
NBS-LRR protein R	AGCTCCATTCCTCCTGTGACTTC
SIP1 F	CCTAAAGCGCCAAAGAAACCT
SIP1 R	GCCGCTTTCTTTTGCATGAA
Tobacco Avr9 F	GACATGCACGCCTCTTTCGT
Tobacco Avr9 R	CCGGACTGTTACTGCAGCTAAA
LOB1 F	TTTTCCACCAACCGAACCAT
LOB1 R	TGATATTGCTAGCACCGAAGACTCT

LOB2 F	GGTGCCTTCATTTCCCAGTAGC
LOB2 R	AGCTGATTCCAGTGAGCTCTGC
RNA binding protein F	CCTCAGTCAGGAGGTTCAAAGAC
RNA binding protein R	CATCAGCTTGTTCCACAGAAAAA
Mads box protein F	TGGGAAGCCTTTCTCATTCG
Mads box protein R	CAGGAAGCGGTTTGCAACA
FMO1 F	ACCTTGCCAAGCAGTTTTGC
FMO1 R	AAGTTGGTGTGCGAGAAGGAA
FMO2 F	TTGGGTGAATGGACCTGTCA
FMO2 R	CAGCAGCAACGGCTAAACCT
Actina F	CCCTTCCTCATGCCATTCTTC
Actina R	CGGCTGTGGTGGTAAACATGT
Translocador de malato F	CCTGATGCGCCGAAGCT
Translocador de malato R	CGTGCTCATAGGTCCCATTTTC

3.9 Modelagem molecular de DIOX de citros

O modelo estrutural 3D da proteína DIOX de citros foi gerado através do programa Swiss-Model, disponível no site: http://swissmodel.expasy.org/, aplicando parâmetros padrões e utilizando a estrutura cristalográfica da proteína F6'H1 de Arabidopsis, código PDB 4XAE, como modelo de procura (Sun *et al.*, 2015). Os alinhamentos estruturais do modelo da proteína DIOX com a proteína F6'H1 foram realizados utilizando o programa PyMOL (DeLano, 2002).

3.10 Tratamento com Psoralen em folhas de citros

Psoralen foi dissolvido em etanol absoluto e a solução estoque mantida a 50 mM. Folhas de laranja Pera e limão Tahiti foram infiltradas com uma suspensão de *X. citri*, ajustada para a concentração final de OD_{600}= 0,1, na presença e ausência de psoralen. Psoralen foi então adicionado na suspensão bacteriana numa concentração final de 0,1 e 0,5 mM. Como psoralen foi dissolvido em etanol absoluto, na suspensão bacteriana utilizada como controle do tratamento também foi acrescentado etanol numa concentração final de 0,2 a 1%. Para garantir o efeito do psoralen ao longo do desenvolvimento dos sintomas na planta, psoralen e etanol foram acrescentados a cada três dias nas seções foliares infiltradas.

Psoralen é uma furanocoumarina, um composto natural que é intercalante de DNA e pode causar mutagênese. Com o objetivo de verificar se Psoralen ou etanol, nas concentrações utilizadas para a infiltração, poderiam afetar o crescimento de *X. citri in vitro*, as soluções de

X. citri + psoralen ou etanol foram plaqueadas em meio de cultura e foi observado que não houve interferência no crescimento de *X. citri* em meio de cultura.

Para efetuar a contagem de bactérias, discos foliares correspondendo a 1cm^2 da região inoculada foram macerados em cadinhos contendo 1 mL de água e depois foi efetuada uma diluição seriada e plaqueamento de determinadas diluições, como ilustrado na Figura 14. As fotos do tratamento com psoralen e a quantificação bacteriana foram feitas aos 10 dpi e o experimento foi executado com três repetições. Foi aplicado a análise estatística "t de Student", com nível de significância de 5% ($p < 0,05$).

3.11 Clonagem e sequenciamento das regiões promotoras dos genes alvos *LOB1*, *LOB2* e *DIOX*

Folhas jovens de laranja Pêra e limão Tahiti foram coletadas para a realização da extração do seu DNA genômico utilizando o método CTAB de extração de DNA (Doyle & Doyle, 1987). A qualidade e a quantidade de DNA foram verificadas no equipamento nanodrop e em gel de agarose. Oligonucleotídeos que anelam nas regiões promotoras dos genes *LOB1*, *LOB2* e *DIOX* foram desenhados baseados nas sequências de DNA do genoma de citros (Xu *et al.*, 2013; Wu *et al.*, 2014) e encontram-se na Tabela 4. Em seguida, as regiões promotoras dos genes *LOB1*, *LOB2* e *DIOX* foram amplificadas por PCR utilizando 1 µg do DNA genômico juntamente com 125 nM de cada iniciador, obtidos para cada gene alvo, 2,5 mM de cada dNTP, 1,5 mM de $MgCl_2$ e 1 U de *Taq* DNA polimerase para um volume final de 20 µL. As condições de amplificação foram: 1 ciclo de 4 min a 94ºC, seguido de 35 ciclos de 30 s a 94ºC, 30 s a 55ºC e 1 min e 10 s a 72ºC. Os fragmentos de PCR de aproximadamente 1000 pb foram excisados do gel de agarose 1% e purificados utilizando o kit *Gel Extraction Kit* (Qiagen) de acordo com o protocolo do fabricante. O produto de PCR purificado foi ligado ao vetor pGEM-T-Easy e esta ligação foi utilizada na transformação de *E. coli* DH5α quimiocompetentes. Estas células foram mantidas a 37ºC, 200 rpm por 1 h e plaqueadas em meio LB ágar seletivo com ampicilina 100 µg/mL + IPTG + X-Gal e posteriormente incubadas em estufa a 37°C por 16 h. A seleção dos transformantes foi por meio de PCR de colônias brancas utilizando os primers das regiões promotoras dos genes alvos. Em seguida, a cultura foi crescida em meio líquido LB + ampicilina 100 µg/mL por 16 h e a extração plasmidial efetuada através do kit Spin Miniprep Kit (Qiagen), seguindo as instruções do fabricante. A região promotora foi sequenciada utilizando-se os primers T7 e SP6 que se anelam no vetor. As sequências das regiões promotoras dos genes *LOB1*, *LOB2* e *DIOX* das variedades Valência e Clemenules (depositadas nos bancos de dados "*Citrus Genome Database*" e "*NCBI*") foram comparadas com as nossas sequências

obtidas de laranja Pêra e limão Tahiti. Desta forma, essas sequências das regiões promotoras dos genes *LOB1*, *LOB2* e *DIOX* das variedades Pêra, Tahiti, Valência e Clemenules foram alinhadas utilizando o software Clustal Omega (http://www.ebi.ac.uk/Tools/msa/clustalo/). As regiões de ligação dos PthAs nos promotores dos genes *LOB1*, *LOB2* e *DIOX* foram obtidos através do programa TALgetter (http://galaxy2.informatik.uni-halle.de:8976/tool_runner?tool_id=TALgetter) e os elementos regulatórios também identificados nas regiões promotoras desses genes foram obtidos através do programa PlantPAN 2.0 (Chang *et al.*, 2008), disponível no site: http://plantpan2.itps.ncku.edu.tw.

Tabela 4. Oligonucleotídeos utilizados na amplificação das regiões promotoras dos genes *LOB1*, *LOB2* e *DIOX*.

Primer	**Sequência 5' – 3'**
LOB1pro_F	GAACAGCTAATAAGCAAGAGGTGG
LOB1pro_R	GGGATTGCTACATTAATTTTGTGTTTGC
LOB2pro_F	CTTCAAAGTTCAAGGCAATAGGACCG
LOB2pro_R	GAGCAATAATCAACACTCAAGAACG
DIOXpro_F1	AGATGCATGAGGCGTAGCTGCCTAGC
DIOXpro_F2	GATTATTCCAAAGAGTCTTTATTG
DIOXpro_F3	TTAAAAATAATAATACTGAAGAAATCG
DIOXPro_F4	GGTACCACAGTTGGATCCAGCC
DIOXpro_R1	GCCAGGATAGAGCCATTTGTTGTTGCC
DIOXpro_R2	CCAGGACTGGGTTGCCAGGATAG

4. RESULTADOS

4.1 Contribuição dos *pthA*s no desenvolvimento do cancro cítrico em diferentes hospedeiras

Com o objetivo de avaliar o papel ou contribuição de cada *pthA* no desenvolvimento do cancro cítrico, foram obtidos mutantes de deleção dos genes *pthA*s. No total foram obtidos três mutantes simples (Δ1, Δ3 e Δ4), três mutantes duplos (Δ1-3, Δ1-4 e Δ3-4) e um mutante triplo (Δ1-3-4) que foram infiltrados em folhas de sete diferentes variedades de citros (laranja Pêra, Valência, Hamlin, Natal, lima Sorocaba, limão Taiti e Galego). Os sintomas do cancro causados pelos mutantes de deleção foram comparados àqueles causados pela bactéria selvagem *X. citri* estirpe 306.

De acordo com dados da literatura (Al-Saadi *et al.*, 2007; Yan & Wang, 2012; Soprano *et al.*, 2013; Hu *et al.*, 2014), foi observado que *pthA4* é indispensável para a elicitação do cancro, uma vez que nenhuma das hospedeiras de citros inoculadas com o mutante Δ4, ou qualquer outro mutante em que o gene *pthA4* foi deletado, apresentaram hiperplasia ou hipertrofia nas folhas (Figuras 21, 22 e 23). Entretanto, a deleção no gene *pthA1* resultou numa redução substancial no número de pústulas em todas as variedades de laranja doce testadas, particularmente nas variedades Hamlin e Pêra, mas não no limão Tahiti (Figura 21). Similarmente, a deleção de *pthA3* reduziu a severidade das lesões de cancro em Pêra e, em menor grau, em Hamlin, Sorocaba e limão Galego, mas não nas variedades Valência, Natal ou Tahiti (Figuras 21 e 23). As lesões de cancro foram mais reduzidas na maioria das hospedeiras inoculadas com o mutante Δ1-3, sugerindo que *pthA1* e *pthA3* possuem um efeito aditivo na formação de pústulas elicitadas por *pthA4* (Figuras 22 e 23).

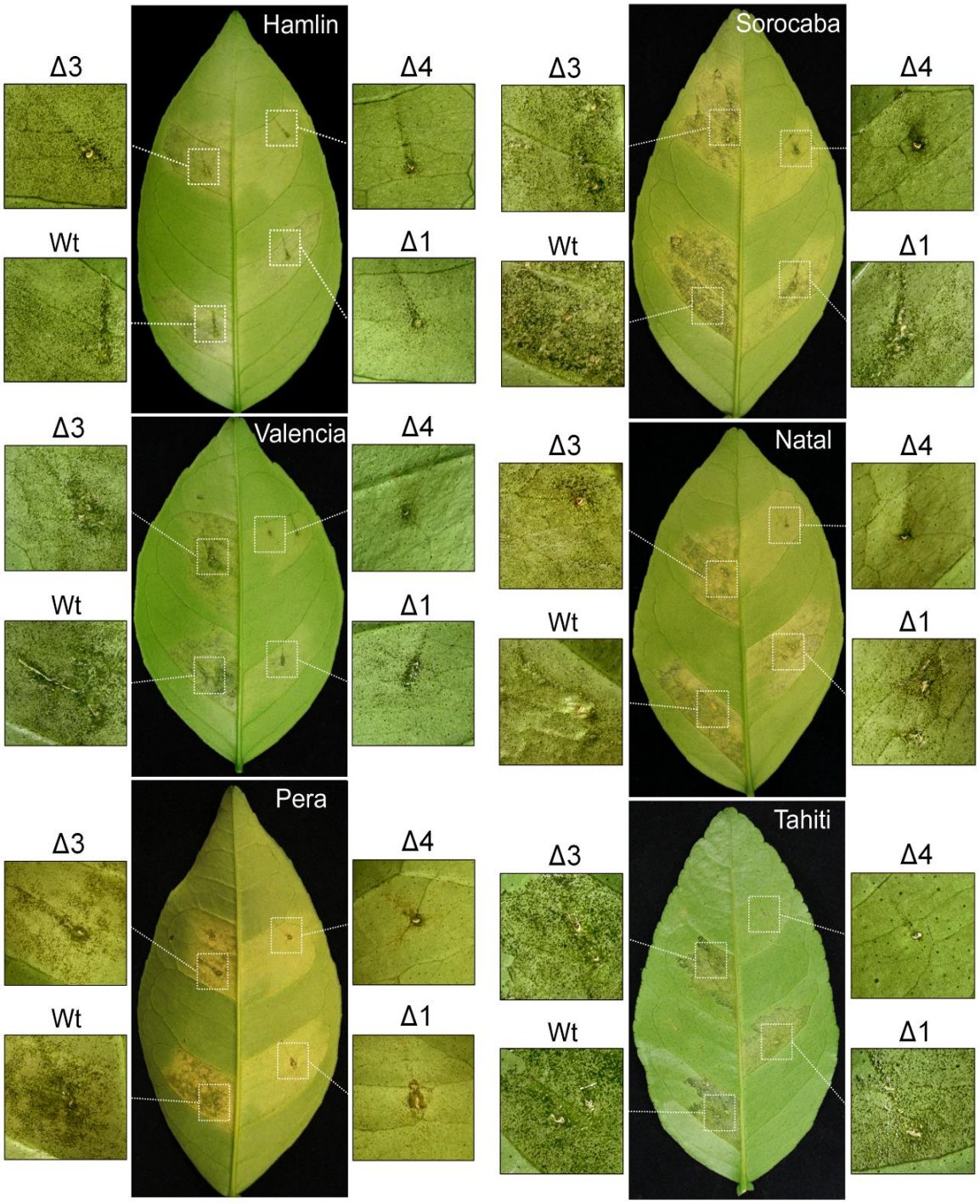

Figura 21. Folhas de citros variedades Pêra, Hamlin, Valência, Natal, Sorocaba e Taiti infiltradas com os mutantes de deleção simples e a bactéria selvagem *X. citri* (Wt). Nas seções foliares infiltradas com o mutante Δ4 não foram observados os sintomas do cancro, enquanto que na presença de PthA4 há a formação de pústulas, mostrando que PthA4 é essencial para a elicitação do cancro em todas as variedades testadas. PthA1 e PthA3 também possuem papel significativo no desenvolvimento da doença, atuando de forma aditiva ou sinergística a elicitação do cancro por PthA4, variando de acordo com a planta hospedeira testada. Todas as fotos foram tiradas aos 14 dpi, sendo que foi utilizado um aumento de 10x nas imagens ampliadas.

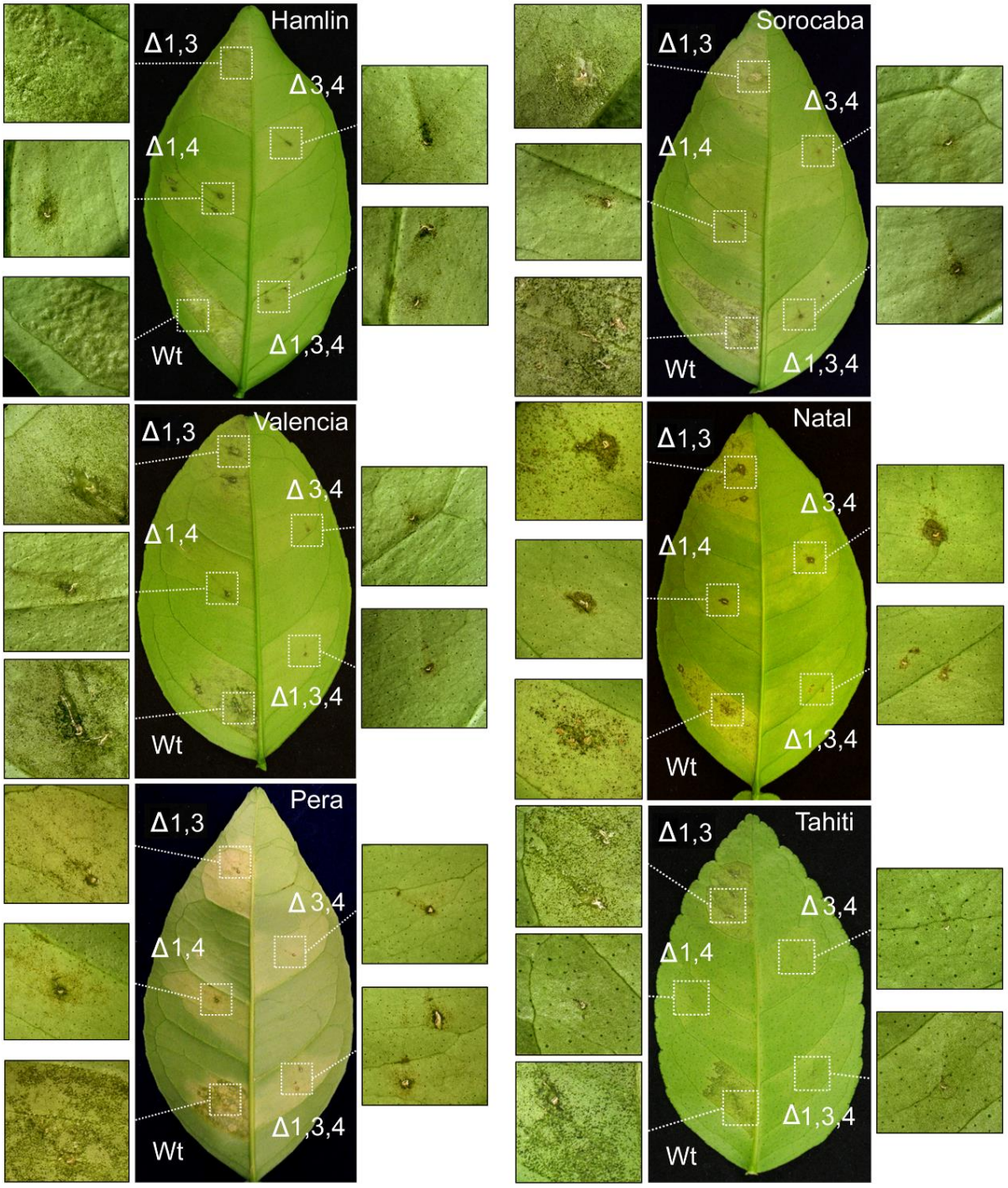

Figura 22. Folhas de citros variedades Pêra, Hamlin, Valência, Natal, Sorocaba e Taiti infiltradas com os mutantes de deleção duplo, triplo e a bactéria selvagem *X. citri* (Wt). Na infiltração com os mutantes Δ1-4, Δ3-4 e Δ1-3-4 não há a formação de pústulas, evidenciando que PthA4 é essencial para a elicitação do cancro. Na infiltração com o mutante Δ1-3 há cancro, porém reduzido em relação a *X. citri*, indicando uma função aditiva de PthA1 e PthA3. As fotos foram tiradas aos 14 dpi, sendo utilizado um aumento de 10x nas imagens ampliadas.

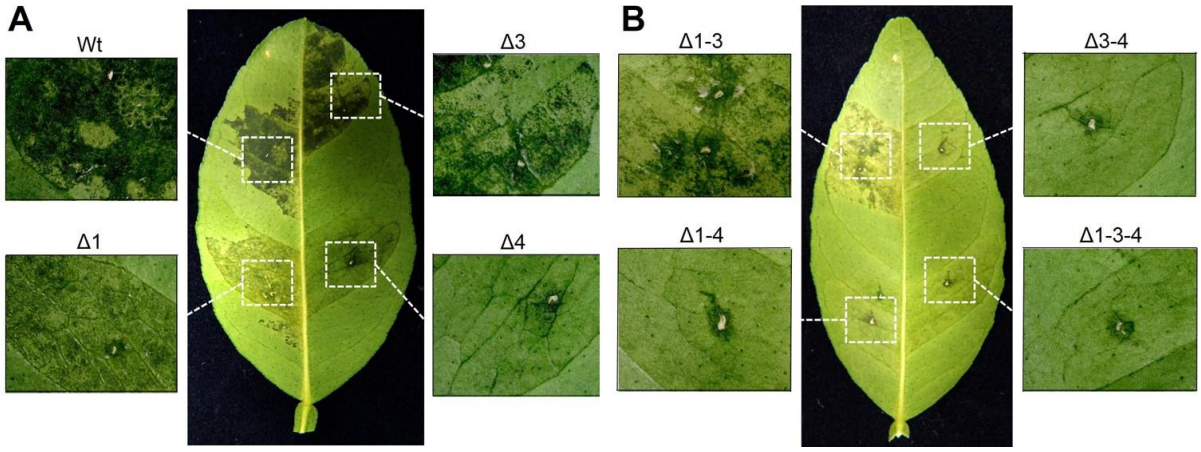

Figura 23. Folhas de limão Galego infiltradas com os sete mutantes de deleção de *pthA*s e a bactéria selvagem *X. citri*. **A)** Infiltração com os mutantes simples e *X. citri* (Wt). **B)** Infiltração com os mutantes duplo e triplo. O fenótipo da infiltração foi avaliado aos 14 dpi e as fotos ampliadas possuem um aumento de 10x.

Conjuntamente, estes resultados indicam que as proteínas PthA1 e PthA3 apresentam efeito aditivo ou sinergístico no desenvolvimento dos sintomas de cancro em algumas hospedeiras, apesar de PthA4 ser necessário e suficiente para induzir hipertrofia e hiperplasia nas sete variedades de citros testadas. O fato da infiltração com o mutante triplo (Δ1-3-4) não induzir sintomas em nenhuma das variedades testadas sugere que o gene *pthA2* apenas não é suficiente para a elicitação do cancro (Figuras 21, 22 e 23).

4.2 Efetores TAL influenciam o crescimento bacteriano *in planta*

A observação de que o PthA1 e PthA3 contribuem para o desenvolvimento do cancro em algumas variedades de citros como Pêra, Valência e Sorocaba, mas não no limão Tahiti, nos levou a investigar se essas proteínas também podem influenciar o crescimento bacteriano na planta.

Para analisar o padrão de crescimento bacteriano dos mutantes de deleção em relação a bactéria selvagem, foram realizadas duas coletas de folhas infiltradas, aos 2 dpi, para registrar o crescimento inicial e a sobrevivência da bactéria após a inoculação, e aos 14 dpi, quando as folhas já apresentavam sintomas de cancro.

A Figura 24 mostra o padrão de crescimento de *X. citri* e dos mutantes de deleção nas quatro hospedeiras testadas (variedades Pêra, Tahiti, Valência e Sorocaba). Em todas as hospedeiras, há uma tendência de maior crescimento de *X. citri* em relação aos mutantes, tanto aos 2 quanto aos 14 dpi. Além disso, observamos também que, ao longo do tempo, *X. citri*

possui um crescimento mais acelerado em relação aos mutantes (dados não apresentados), atingindo seu máximo de crescimento na ordem de $1x10^9$ CFU/cm^2 (Unidades Formadoras de Colônia). Os dados mostram também que as mutações dupla e tripla reduzem significativamente o crescimento bacteriano em relação as mutações simples e a infiltração com *X. citri* nestas hospedeiras (Figura 24). Estes dados indicam que cada efetor PthA pode ter o seu papel no crescimento bacteriano atuando de forma aditiva também na patogenicidade e no "fitness" bacteriano.

Outro fato observado é que, apesar das seções foliares infiltradas com mutantes sem o gene *pthA4* não apresentarem sintomas de hipertrofia ou hiperplasia, a bactéria permanece viva e consegue se multiplicar, chegando a atingir um crescimento da ordem de $1x10^8$ CFU/cm^2 (Figura 24). Esse mesmo fato foi observado na curva de crescimento bacteriano do mutante B21.2, que também não causa cancro em folhas infiltradas, mas ainda assim é capaz de se multiplicar dentro da célula da planta (Figura 25).

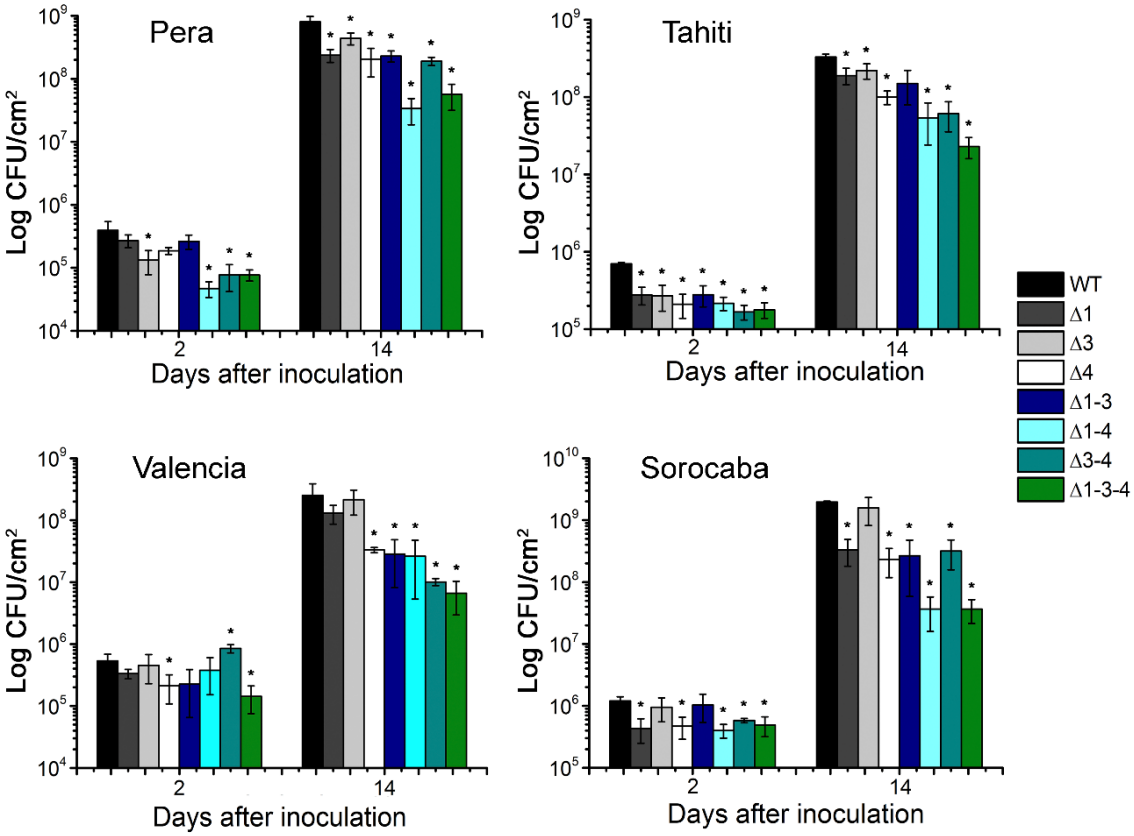

Figura 24. Gráficos com os padrões de crescimento bacteriano de quatro hospedeiras (Pêra, Tahiti, Valência e Sorocaba) infiltradas com *X. citri* (WT) e os sete mutantes de deleção. A quantidade de células infiltradas foi da ordem de $1x10^6$ células/mL e as folhas infiltradas foram coletadas aos 2 e 14 dpi. A quantificação bacteriana foi realizada em unidades formadoras de colônia (CFU) por cm^2.

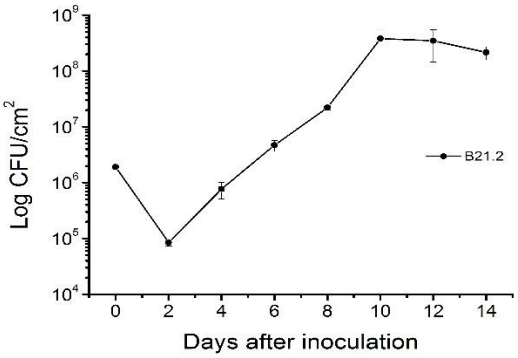

Figura 25. Gráfico da curva de crescimento da bactéria mutante B21.2 na laranja Pêra. A solução bacteriana infiltrada foi ajustada para uma concentração de OD600 = 0,1. É possível observar um decaimento da população bacteriana nos dois primeiros dias após a inoculação devido a um período de adaptação. Depois há um crescimento exponencial atingindo a ordem de 10^8 CFU/cm^2 e aos 10 dpi há o início da fase estacionária. O experimento foi realizado com três repetições.

4.3 Análise da expressão dos genes *pthA4*, *pthC1* e *pthC2* clonados no vetor pMR20

Com o objetivo de testar se PthC1 e PthC2 funcionam como proteínas Avr em laranja doce, o mutante B21.2 foi complementado com os genes *pthA4* (como controle), *pthC1* e *pthC2* clonados no vetor pMR20.

O mutante B21.2 de *X. citri* foi obtido a partir da estirpe selvagem 3213, que também possui 4 variantes da proteína PthA, assim como *X. citri* 306. O mutante B21.2 não é patogênico a plantas de laranja doce, pois possui o gene *pthA4* não funcional (Swarup *et al.*, 1991; Swarup *et al.*, 1992; Al-Saadi *et al.*, 2007).

Folhas de laranja Pêra foram infiltradas com as bactérias *X. citri*, B21.2 e B21.2 complementadas com os genes *pthA4*, *pthC1* e *pthC2*, para avaliação da progressão dos sintomas na planta (Figura 26). Nas folhas infiltradas com *X. citri* é possível observar uma grande proliferação celular, com hipertrofia e hiperplasia de células, correspondente ao principal sintoma do cancro cítrico. No entanto, nas folhas infiltradas com a bactéria B21.2 complementada com *pthA4*, *pthC1* e *pthC2*, não foi observada nenhuma alteração significativa nos sintomas em relação ao controle infiltrado com o mutante B21.2 (Figura 26). Apesar de ter sido observado uma maior anasarca na região infiltrada com B21.2 + PthA4, não houve formação de pústulas (Figura 26).

Figura 26. Corte transversal de folhas de laranja Pêra com aumento de 30x. Em todas as quatro folhas, o lado esquerdo da nervura central foi infiltrado com o mutante B21.2, como controle, e do lado direito as infiltrações foram as seguintes: (**A)** *X. citri*, (**B)** B21.2 + PthA4, (**C**) B21.2 **+** PthC1 e (**D)** B21.2 + PthC2. As fotos foram tiradas aos 12 dpi. A concentração bacteriana correspondeu a OD_{600}= 0,3 para o inóculo do mutante B21.2 e B21.2 complementado e OD_{600}= 0,01 para *X. citri*.

O esperado era que pelo menos na infiltração com B21.2 + PthA4 houvesse algum sintoma aparente de cancro, pois o gene *pthA4* é o homólogo funcional ao gene *pthA4* mutado em B21.2 (Al-Saadi *et al.*, 2007). Este experimento foi repetido, o qual apresentou resultados semelhantes. Consultando outros profissionais experientes no uso do vetor pMR20, foi relatado que este vetor pode ser pouco estável dentro da bactéria, de forma que as proteínas PthAs e PthCs podem não estar sendo expressas. Para tentar verificar se a proteína PthA4 estava sendo expressa foram feitas análises de *western blot* a partir de extrato total de bactérias. Porém, o anticorpo *anti-PthA* utilizado não foi capaz de diferenciar as variantes de PthAs, pois mesmo o mutante B21.2 possui as proteínas PthA1, PthA2 e PthA3 (Figura 27). Portanto, como alternativa, os genes *pthA*s e *pthC*s foram clonados no vetor pUFR047 (DeFeyter *et al.*, 1993).

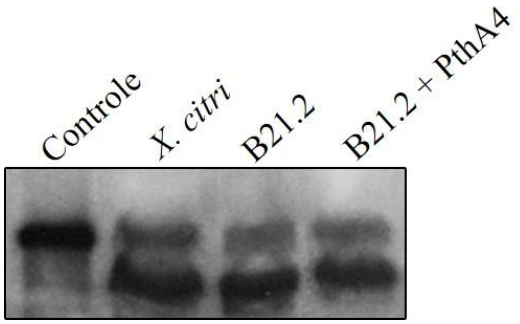

Figura 27. *Western blot* para identificação da expressão de PthA4 clonado no vetor pMR20. É possível observar que não houve diferença entre *X. citri*, B21.2 e B21.2 + PthA4, onde foi encontrada a presença de PthAs mesmo na bactéria B21.2. O controle corresponde a proteína PthA2 purificada.

4.4 PthC1 não atua como proteína Avr em laranja doce

Como não foi possível analisar a expressão dos genes *pthC1* e *pthC2* clonados no vetor pMR20, estes genes foram então clonados no vetor pUFR047. Desta forma, os mutantes de deleção e o mutante B21.2 foram complementados com os respectivos *pthA*s e *pthC*s e foram infiltrados em folhas de laranja Pêra e limão Galego, a fim de analisar o fenótipo resultante da infiltração e verificar se houve a complementação dos sintomas nas folhas.

A Figura 28 ilustra os fenótipos das folhas de laranja Pêra infiltradas com os mutantes B21.2 e Δ4, além das complementações desses dois mutantes com *pthA4*, *pthC1* e *pthC2*, em relação a *X. citri*. Como visto anteriormente, os mutantes B21.2 e Δ4 não causam cancro. Embora a complementação dos sintomas na infiltração com os mutantes contendo o gene *pthA4* de *X. citri* era esperada, por algum motivo não foi possível observar a restauração dos sintomas do cancro nas áreas infiltradas (Figura 28). Alguns trabalhos indicam a dificuldade de uma efetiva complementação em *X. citri*, sendo muitas vezes somente uma complementação parcial (Hausner *et al.*, 2013; Zimaro *et al.*, 2014).

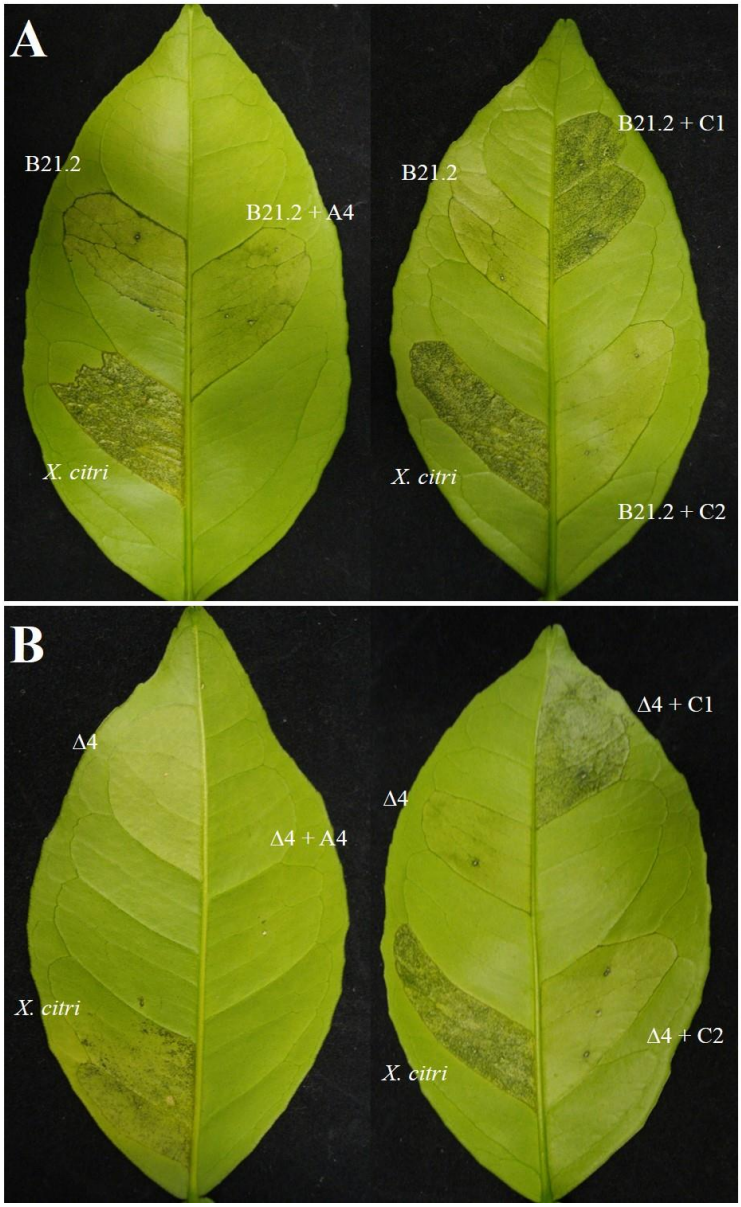

Figura 28. Fenótipo das infiltrações, em folhas de laranja Pêra, dos mutantes Δ4 e B21.2 complementados com os genes *pthA4*, *pthC1* e *pthC2*, em relação a *X. citri*. **A)** Complementações da bactéria B21.2. **B**) Complementações do mutante Δ4. As fotos foram tiradas aos 21 dpi.

As complementações Δ4 + *pthC1*, Δ4 + *pthC2,* B21.2 + *pthC1* e B21.2 + *pthC2* foram feitas com o objetivo de elucidar os mecanismos de virulência de *X. aurantifolii* C. Nossa hipótese era de que esses genes poderiam atuar como genes *avr* em laranja doce, pois quando *X. aurantifolii* C é infiltrado em folhas de limão Galego, causa cancro, porém ao ser infiltrado em laranja doce, há o desencadeamento de uma resposta de defesa (Figura 29). No entanto, ao infiltrar Δ4 + *pthC1* e B21.2 + *pthC1* em laranja Pêra foi observado a formação de pústulas, reproduzindo os sintomas do cancro, semelhante ao da bactéria selvagem *X. citri* (Figura 28). Este fato nos permite afirmar que, contrariamente ao que imaginávamos, PthC1 não atua como

proteína Avr, pois ao ser expressa em laranja Pêra não houve reação de hipersensibilidade ou resposta de defesa, pelo contrário, os dados mostram que *pthC1* complementa os sintomas do cancro em Δ4 e em B21.2, exercendo o papel do gene *pthA4*. Curiosamente, ambos PthA4 e PthC1 possuem 17,5 repetições na região do domínio interno e estudos prévios mostraram que efetores com esse número de repetições são necessários para a elicitação do cancro (Brunings & Gabriel, 2003; Al-Saadi *et al.*, 2007). Por outro lado, ao infiltrar as construções Δ4 + *pthC2* e B21.2 + *pthC2* em laranja Pêra, não foi observada a formação de pústulas (Figura 28). Neste caso, pode não ter ocorrido a complementação do mutante com PthC2 ou PthC2 sozinho realmente não é capaz de restaurar os sintomas do cancro em laranja doce, levando em consideração que este possui 14,5 repetições na região do domínio interno, e não deve ser suficiente para causar cancro.

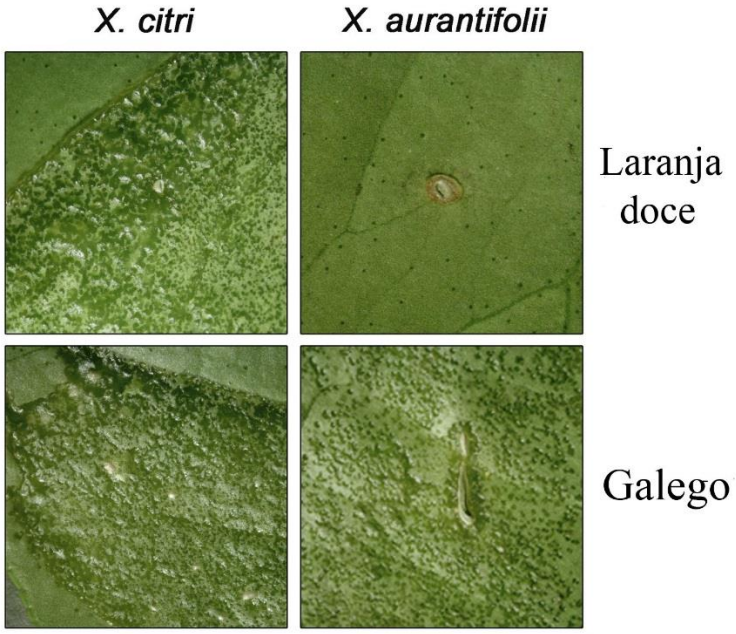

Figura 29. Fenótipo da infiltração das bactérias *X. citri* e *X. aurantifolii* patotipo C em laranja doce variedade Pêra, e em limão Galego. A bactéria *X. citri* causa cancro nas duas variedades testadas, no entanto, *X. aurantifolii* C causa cancro somente em limão Galego, desencadeando resposta de defesa em laranja doce. A infiltração foi realizada com uma concentração bacteriana de 10^6 células/mL e os sintomas foram avaliados aos 14 dpi.

Da mesma forma, o mesmo estudo das complementações de Δ4 e B21.2 com os genes *pthA4*, *pthC1* e *pthC2* foi realizado em limão Galego, no entanto, não foram observados sintomas de cancro em nenhuma das infiltrações. Apesar de ter sido observada uma maior anasarca na complementação com *pthC1*, não houve formação de pústulas (dados não

apresentados). Construções como Δ1 + *pthA1* e Δ3 + *pthA3* também foram desafiadas com laranja Pêra e limão Galego, porém não foi observado um aumento do cancro, ou cancro similar a *X. citri* em nenhuma destas hospedeiras, uma vez que os mutantes Δ1 e Δ3 já causam cancro nestas hospedeiras, ainda que reduzido (dados não apresentados).

4.5 A bactéria *X. aurantifolii* C não é patogênica ao limão Tahiti

Sabe-se que *X. aurantifolii*, responsável pela cancrose C presente exclusivamente no Brasil, causa cancro no limão Galego (Amaral, 2003; Shubert *et al.*, 2003; Cernadas *et al.*, 2008). Já em outras hospedeiras, como laranja doce, há um desencadeamento de resposta de defesa (Figura 29). No entanto, não está descrito na literatura se *X. aurantifolii* C pode causar cancro também no limão Tahiti.

Como pode ser visto na Figura 30, *X. aurantifolii* C não causa cancro no limão Tahiti. Neste caso, houve uma resposta de defesa, assim como ocorre nas laranjas doces. Apesar de o limão Tahiti ser mais próximo filogeneticamente ao limão Galego em relação à laranja doce (Bayer *et al.*, 2009; Penjor *et al.*, 2013), em algum momento evolutivo, os efetores presentes em *X. aurantifolii* C deixaram de causar cancro em limão Tahiti ou passaram a causar virulência no limão Galego.

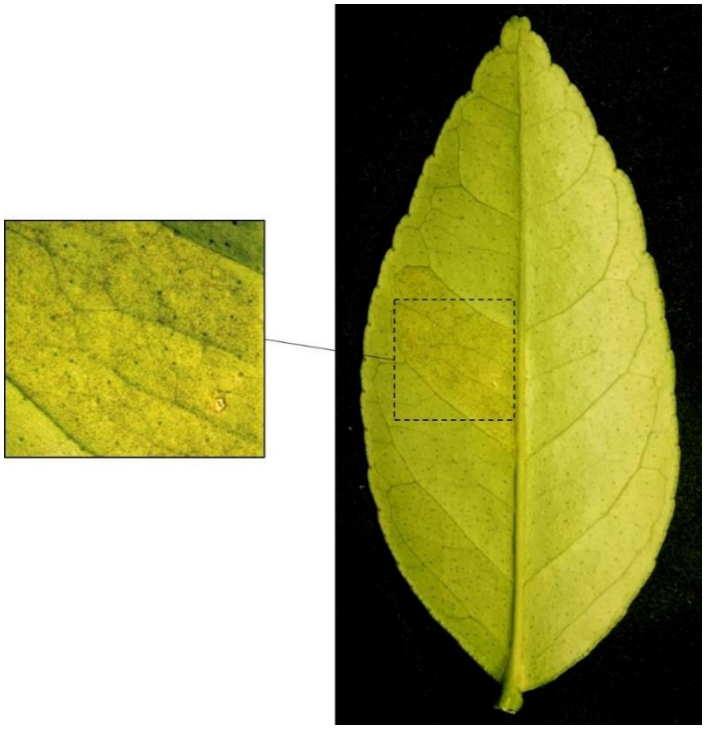

Figura 30. Fenótipo de limão Tahiti ao ser infiltrado com *X. aurantifolii* C. A concentração da solução bacteriana infiltrada foi de OD600 = 0,1 e as fotos foram tiradas aos 21 dpi. A figura do lado esquerdo foi tirada com um aumento de 10x.

4.6 Identificação de alvos diretos das proteínas PthAs e PthCs

Estudos prévios visando a identificação de alvos dos efetores PthA e PthC apontaram potenciais alvos na planta hospedeira *C. sinensis* (Pereira *et al.*, 2014). Desta forma, procurou-se aprofundar os conhecimentos sobre esses potenciais alvos para tentar compreender como as proteínas PthAs e PthCs atuam na célula hospedeira, quais genes podem ser ativados e como isso pode influenciar no desenvolvimento do cancro.

Inicialmente um experimento piloto foi realizado para avaliar o melhor tempo de coleta das folhas, após a infiltração com as bactérias, para avaliar o nível de expressão dos genes alvos. Os tempos de coleta testados foram 48 horas após a inoculação (hpi), 72 hpi e 5 dpi. Após análise da expressão do gene *LOB1*, validado no trabalho de Pereira *et al.*, (2014), chegou-se a conclusão de que o tempo de 72 hpi era o tempo mais adequado para detectar a transativação dos genes alvos.

Nas análises de folhas de laranja Pêra e de limão Tahiti infiltradas com os mutantes de deleção foi observado que, nas seções foliares infiltradas com os mutantes Δ1 e Δ3 havia uma redução substancial no desenvolvimento do cancro em folhas de laranja Pêra, ao passo que em folhas de limão Tahiti, os sintomas causados por esses mutantes não diferiram em relação a cepa selvagem *X. citri* (Figura 21). Desta forma, estas duas hospedeiras foram selecionadas para a comparação dos níveis de expressão de potenciais genes alvos de PthAs e PthC1.

A princípio foram testados oito primers referentes a candidatos preditos como alvos de PthA1 (*Tumor related protein*, *bZIP transcription factor*, *Gibberellin 20-oxidase*, *ABI3*, *NAC transcription factor*, *Cytochrome P450 monooxygenase*, *Terpene synthase* e *HAP3-like protein*), outros sete primers alvos de *pthA3* (*Gibberellin 20-oxidase*, *Apyrase*, *Terpene synthase*, *Pm52*, *Pectate lyase*, *LOB3* e *LOB3b*), 9 alvos de *pthA4* (*Tobacco 14-3-3 protein*, *Dioxygenase*, *Tobacco cysteine proteinase*, *NBS-LRR protein*, *Tomato self pruning-interacting protein 1* (*SIP1*), *Tobacco Avr9*, *LOB1* e *LOB2* e *RNA binding-protein*) e 4 alvos de *pthC1* (*LOB1*, *Mads box protein* e *Flavina monoxigenase* (*FMO*) 1 e 2), todos descritos em Pereira *et al.*, 2014 (Tabela 3).

Apesar das várias análises de expressão dos potenciais genes alvos, neste estudo foram destacados 4 genes: *LOB1*, o único gene *S* de cancro cítrico descrito até o momento (Hu *et al.*, 2014; Li *et al.*, 2014; Pereira *et al.*, 2014), além dos genes *LOB2*, *LOB3* e *DIOX* (Pereira *et al.*, 2014) (Figura 31).

Nestes estudos verificou-se que a expressão do gene *LOB1*, em folhas de limão Tahiti infiltradas com os mutantes simples, reduziu significativamente em relação as folhas infiltradas com a bactéria selvagem (WT) (Figura 31A), indicando que não só PthA4, mas

também PthA1 e PthA3 possuem papel na ativação de *LOB1*. Por outro lado, em folhas de laranja Pêra, observou-se que a expressão de *LOB1* é reduzida em pelo menos metade da expressão na ausência de PthA4, em relação a expressão com *X. citri*, indicando que PthA4 ativa a expressão de *LOB1*, corroborando dados já publicados (Hu *et al.*, 2014; Li *et al.*, 2014; Pereira *et al.*, 2014). Contrariamente, PthA1 parece reprimir *LOB1*, uma vez que na ausência de PthA1 a expressão de *LOB1* está aumentada em relação a WT. Não houve diferença significativa entre a expressão de *LOB1* em folhas infiltradas com o mutante Δ3, em relação a WT, sugerindo que PthA3 somente induz *LOB1* em folhas de limão Tahiti.

A expressão de *LOB2* não é influenciada por PthA1, PthA3 ou PthA4 em folhas de Tahiti (Figura 31B), ao passo que na laranja Pêra a expressão de *LOB2* parece ser dependente de PthA1, pois o nível de expressão de *LOB2* reduz significativamente quando as folhas são infiltradas com o mutante Δ1, em relação a infiltração com WT. Em contrapartida, PthA4 parece reprimir a expressão de *LOB2*, uma vez que a expressão de *LOB2*, induzida por Δ4, é aumentada em relação a WT. Fato contrário ao que tinha sido observado em Pereira *et al.*, 2014.

A expressão de *LOB3* em laranja Pêra não parece ser influenciada por PthAs e em limão Tahiti, apesar do pequeno aumento na expressão, PthA1 e PthA4 parecem reprimir *LOB3* (Figura 31C).

O gene *DIOX*, identificado previamente como um potencial alvo direto de PthA4 e PthA^{w}, é fortemente induzido em epicótilos de citros expressando *pthA4* (Hu *et al.*, 2014; Pereira *et al.*, 2014). Contudo, foi testado se PthA1 e PthA3 também modulam a transcrição de *DIOX* em laranja Pêra em relação ao limão Tahiti. Assim, foi observado que *DIOX* foi fortemente induzido por *X. citri* em laranja Pêra, mas quando infiltradas com os mutantes de deleção simples há uma redução significativa na expressão de *DIOX* (Figura 31D), indicando que PthA1, PthA3 e PthA4 influenciam a expressão de *DIOX* em laranja Pêra, mas não em limão Tahiti, onde não foi observada indução substancial de *DIOX*.

Conjuntamente estes dados sugerem que os genes *LOB2* e *DIOX* também podem funcionar como genes *S* e que PthAs 1 e 3 contribuem com suas expressões em laranja Pêra, mas não em limão Tahiti.

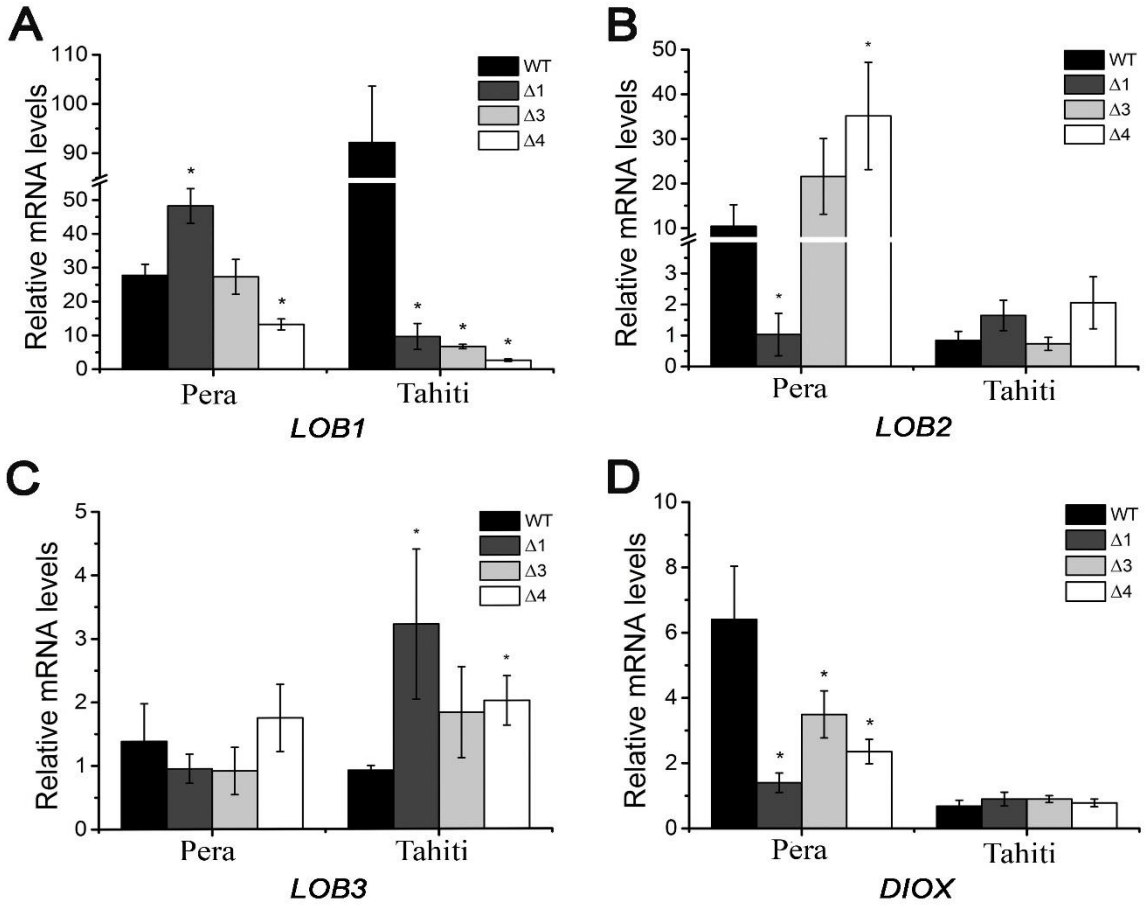

Figura 31. Expressão diferencial dos genes *LOB* e *DIOX* em laranja Pêra e limão Tahiti. Níveis de expressão de *LOB1* **(A)**, *LOB2* **(B)**, *LOB3* **(C)** e *DIOX* **(D)** em folhas de plantas Pêra e Tahiti infiltradas com a bactéria selvagem *X. citri* (WT) e com os mutantes de deleção simples (Δ1, Δ3 e Δ4).

Considerando que PthC1 não atua como uma proteína Avr, pois a expressão de *pthC1* nos mutantes Δ4 e B21.2 restaura os sintomas do cancro, decidiu-se analisar se PthC1 poderia ativar a expressão do gene *LOB1* em laranja Pêra, assim como no limão Galego (Figura 32). Em folhas de laranja Pêra foi observado uma superexpressão de *LOB1* induzida por Δ4 + PthC1, em relação a indução por *X. citri*, *X. aurantifolii* C e Δ4. Apesar de *X. aurantifolii* C também possuir a proteína PthC1, a expressão de *LOB1* é muito maior no mutante complementado, indicando que na bactéria *X. aurantifolii* C possa existir alguma outra proteína que reprima a expressão de *LOB1*, ou ainda pode ter ocorrido um efeito de dose, uma vez que no mutante complementado a expressão de PthC1 está sob o controle do promotor de PthA4. Em folhas de limão Galego, também é possível observar uma maior expressão de *LOB1* induzida por Δ4 + PthC1, em relação a indução por *X. citri*, *X. aurantifolii* C e Δ4, porém essa expressão é bem menor em relação ao que foi observado em laranja Pêra. Este resultado indica

que o gene *LOB1* é alvo de PthC1 e pode estar influenciando na formação do cancro, assim como PthA4, em laranja Pêra (Hu *et al.*, 2014; Pereira *et al.*, 2014).

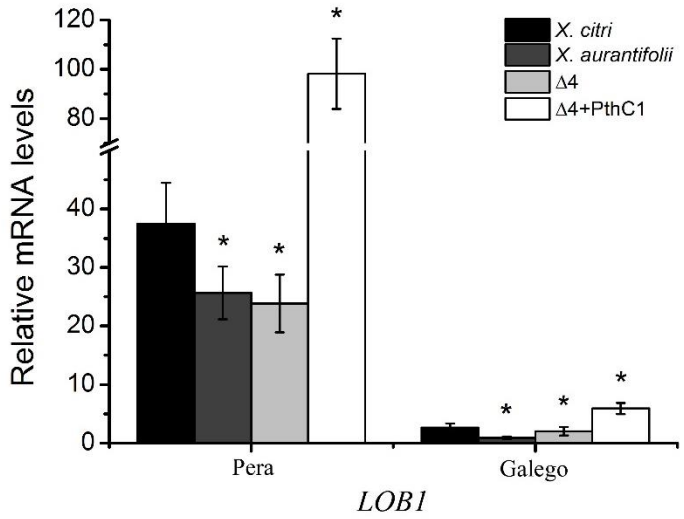

Figura 32. Níveis de expressão de *LOB1* em folhas de laranja Pêra e limão Galego. *LOB1* é alvo de PthC1, pois sua expressão está aumentada em relação a *X. citri*, *X. aurantifolii* C e Δ4 nas duas variedades de citros.

4.7 A indução de LOB1 não é suficiente para causar cancro em citros

Neste trabalho foi observado que os níveis de expressão do gene *LOB1* são bastante reduzidos em folhas de limão Tahiti infiltradas com os mutantes Δ1 e Δ3, em relação a *X. citri* (Figura 31A), mas os sintomas de cancro não se alteram (Figura 21). Por outro lado, em laranja Pêra, a expressão de *LOB1* é altamente induzida pelos mutantes Δ1 e Δ3 (Figura 31A), mesmo sendo observado que os sintomas de cancro são reduzidos na infiltração com esses mutantes (Figura 21). Da mesma forma, quando infiltradas com o mutante Δ4, a expressão de *LOB1* é reduzida em aproximadamente 95% em folhas de Tahiti e 50% em folhas de Pêra, em relação a *X. citri*. Isto coloca em evidência que, mesmo que reduzida, ainda há a expressão de *LOB1* sem a elicitação de cancro (Figuras 21 e 31A).

Diante destes dados, resolveu-se investigar a expressão de *LOB1* nas plantas Pêra e limão Galego infiltradas com *X. citri* e *X. aurantifolii* C, uma vez que *X. aurantifolii* C causa cancro somente em limão Galego (interação compatível) e desencadeia resposta de defesa em laranja Pêra (interação incompatível) (Figuras 29 e 33) (Cernadas *et al.*, 2008). Foi observado que em limão Galego há pouca indução de *LOB1*, mesmo sendo uma interação compatível onde tanto *X. citri* quanto *X. aurantifolii* C causam cancro. Por outro lado, em laranja Pêra há alta indução de *LOB1*, tanto na interação compatível, quanto na incompatível, apesar desta última

ser significativamente menor (Figura 33). Desta forma, a expressão de *LOB1* nem sempre está relacionada à formação do cancro em plantas de citros.

Semelhantemente, decidiu-se verificar também os níveis de expressão de *LOB2*, *LOB3* e *DIOX* em folhas de laranja Pêra e limão Galego em resposta a infecção por *X. citri* e *X. aurantifolii* C. Enquanto as expressões de *LOB2* e *LOB3* não parecem estar relacionados com desenvolvimento do cancro, nem com resposta de defesa nestas hospedeiras, a expressão de *DIOX* foi significativamente reduzida na resposta de HR elicitada por *X. aurantifolii* C em laranja Pêra (Figura 33).

Conjuntamente, estes dados sugerem que pode existir um limiar de expressão de *LOB1* necessário para causar cancro, ou *LOB1* sozinho não é suficiente para promover o desenvolvimento da doença nestas hospedeiras. Contudo, *DIOX* pode contribuir para o desenvolvimento do cancro em laranja Pêra.

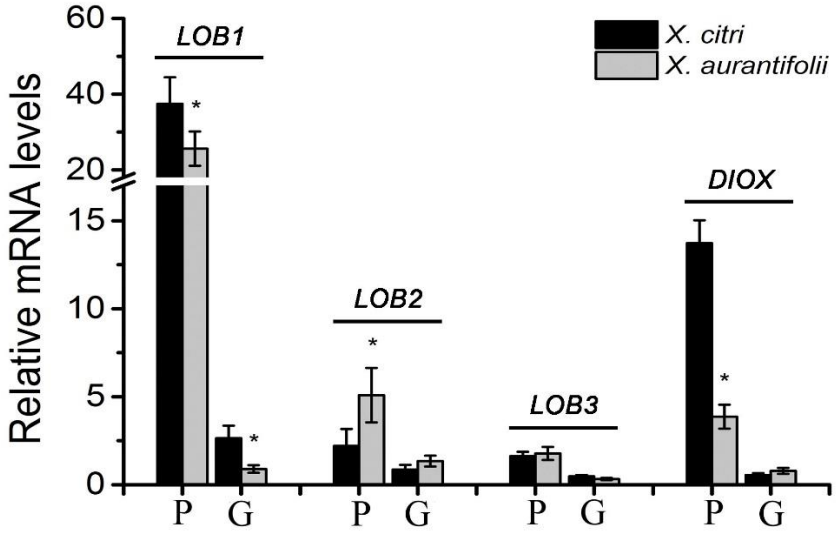

Figura 33. Níveis de expressão de *LOB1*, *LOB2*, *LOB3* e *DIOX* em folhas de laranja Pêra (P) e limão Galego (G) em resposta a infecção por *X. citri* e *X. aurantifolii*. *LOB1* é fracamente induzido na interação compatível em limão Galego e altamente induzido em laranja Pêra, tanto na interação compatível e incompatível. Somente os níveis de expressão de *DIOX* estão bastante reduzidos na interação incompatível entre Pêra e *X. aurantifolii*.

4.8 DIOX de citros é estruturalmente relacionada com 2-oxoglutarato/Fe(II) dioxigenase dependente

A proteína DIOX de citros pertence à família das dioxigenases dependentes de 2-oxoglutarato/Fe(II) (2OGD) as quais utilizam o 2-oxoglutarato e oxigênio molecular como co-substratos e o Fe(II) como cofator para catalisar diversas reações como hidroxilação,

halogenação, desnaturação, epimerização, demetilação, entre outros (Farrow & Facchini, 2014). Essa família de proteínas é a segunda maior família no genoma de plantas, e possuem um importante papel na biossíntese e metabolismo de numerosos componentes como coumarinas, flavonoides, glucosinolatos, hormônios de plantas (giberelina, auxina, etileno, ácido salicílico), etc (Farrow & Facchini, 2014; Kawai *et al.*, 2014).

DIOX de citros é semelhante à enzima ferruloil-CoA 6' hidroxilase (F6'H1) de Arabidopsis e tabaco. F6'H1 catalisa a conversão de ferruloil-CoA em 6'-hidroxiferruloil-CoA, que por sua vez sofre rotação e lactonização espontânea produzindo scopoletina (Figura 34) (Kai *et al.*, 2008; Sun *et al.*, 2014; Farrow & Facchini, 2014; Sun *et al.*, 2015). Scopoletina faz parte do grupo das coumarinas, importantes componentes que contribuem para a adaptação de plantas contra estresse biótico e abiótico (Vialart *et al.*, 2012).

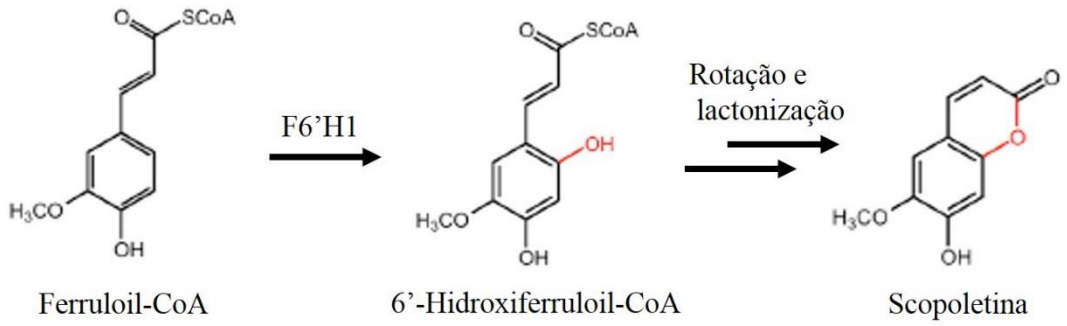

Figura 34. Representação da reação catalisada por F6'H1. Esta enzima cataliza a conversão de ferruloil-CoA em 6'-hidroxiferruloil-CoA, que por sua vez sofre rotação e lactonização espontânea produzindo scopoletina (adaptação de Farrow & Facchini, 2014).

Visando esclarecer a possível função bioquímica e a especificidade de substrato de DIOX, foi gerado um modelo estrutural de DIOX baseado na estrutura cristalográfica de F6'H1 de Arabidopsis (Sun *et al.*, 2015). O modelo molecular obtido sugere que DIOX é estruturalmente similar a F6'H1, com dobramento e topologia típica de uma proteína da família 2OGD (Figura 35A). Além disso, foi possível observar que todos os resíduos de aminoácidos responsáveis pela ligação do átomo de ferro (H234, D236, H292), 2-oxoglutarato (N217, Y219, R302, S304) e do substrato ferruloil-CoA (F150, S152, R213, N215, I237, F308) estão estruturalmente conservados no modelo de DIOX (Figura 35B). Estes resultados indicam que DIOX de citros é o ortólogo de F6'H1 de Arabidopisis e possivelmente utiliza ferruloil-CoA como substrato para sua reação.

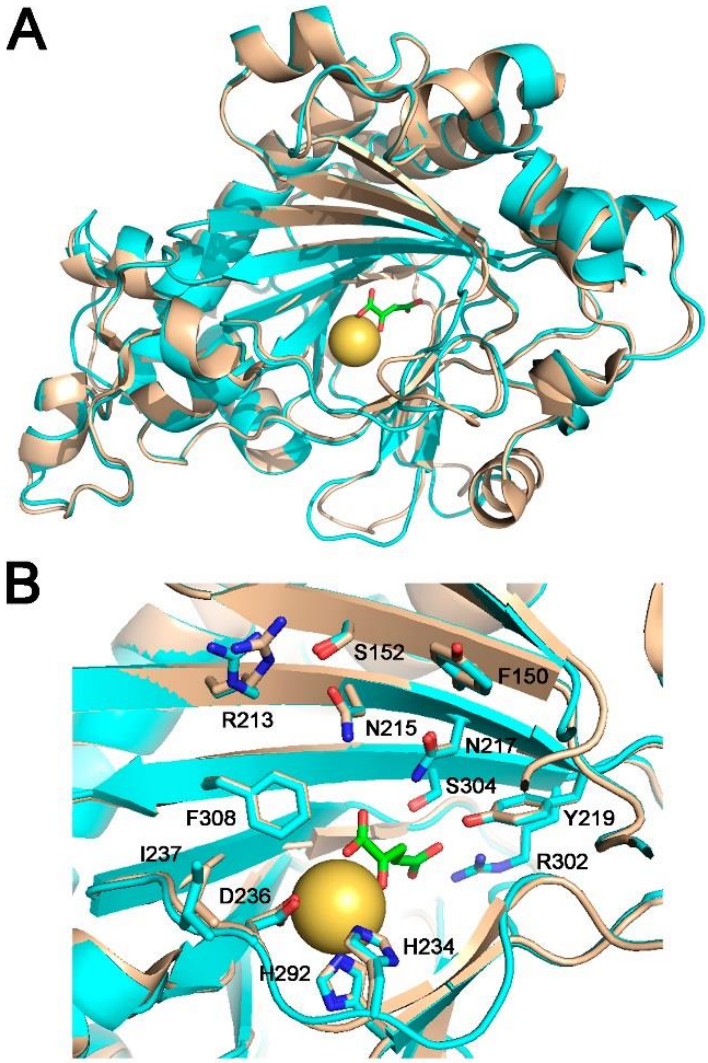

Figura 35. Modelo estrutural de DIOX de citros baseado na estrutura cristalográfica de F6'H1 de Arabidopsis. **A)** Sobreposição do modelo estrutural de DIOX (ciano) com a estrutura cristalográfica da proteína F6'H1 (bege), evidenciando o átomo de ferro (amarelo) e 2-oxoglutarato (verde), mostrando que CsDIOX possui o mesmo dobramento e topologia de F6'H1. **B**) Resíduos de aminoácidos responsáveis pela ligação do átomo de ferro (H234, D236, H292), 2-oxoglutarato (N217, Y210, R302, S304) e ferruloil-CoA (F150, S152, R213, N215, I237, F308) estão estruturalmente conservados no modelo de CsDIOX.

4.9 Psoralen inibe a formação de cancro em laranja Pêra

DIOX de citros é também 82% idêntica a proteína 2OGD de *Ruta graveolens.* Esta converte ferruloil-CoA em scopoletina e *p*-coumaroil-CoA em ácido 2,4-dihidroxicinamico (Vialart *et al.*, 2012). Experimentos cinéticos revelaram que psoralen, uma furanocoumarina, inibe a reação de hidroxilação de ferruloil-CoA e *p*-coumaroil-CoA (Vialart *et al.*, 2012).

Sendo assim, tendo em vista os resultados que sugerem que *DIOX* pode ter um importante papel no desenvolvimento do cancro (Figuras 31D e 33), foi testado o efeito de psoralen em folhas infiltradas com *X. citri*. Duas concentrações diferentes de psoralen foram testadas (0,1 e 0,5 mM) avaliando-se o desenvolvimento da doença e o crescimento bacteriano nas hospedeiras laranja Pêra e limão Tahiti (Figura 36). Foi observado que psoralen inibiu o desenvolvimento do cancro e o crescimento bacteriano nas folhas de laranja Pêra, mas não de limão Tahiti (Figuras 36A e B), onde a expressão de *DIOX* não foi dependente de PthAs (Figura 31D). Ainda foi observado que psoralen agiu de forma dose dependente na laranja Pêra, de maneira que quando se utilizou uma concentração maior de psoralen (0,5 mM), houve redução ainda maior do crescimento bacteriano e dos sintomas do cancro (Figuras 36A e B).

Conjuntamente, estes dados sugerem que *DIOX* atua como gene *S* em laranja Pêra.

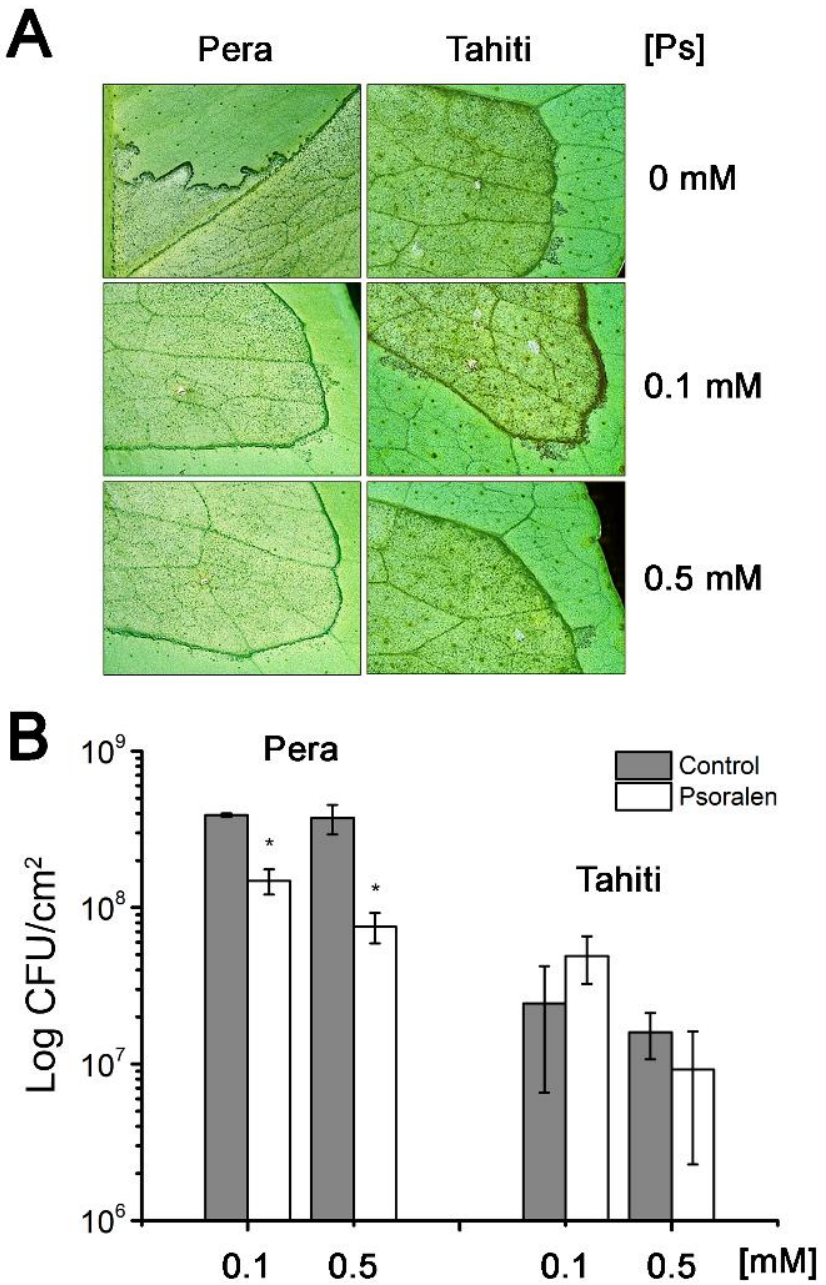

Figura 36. Inibição do cancro em laranja Pêra pelo uso de psoralen. Folhas de laranja Pêra e limão Tahiti foram infiltradas com uma suspensão de *X. citri* numa concentração de OD_{600} = 0,1 na ausência e na presença de psoralen (Ps) nas concentrações de 0,1 e 0,5 mM. Os sintomas nas folhas de Pêra e Tahiti **(A)** e a quantificação bacteriana **(B)** foram avaliados aos 10 dpi. Psoralen inibiu significativamente o desenvolvimento do cancro e o crescimento bacteriano na laranja Pêra, mas não no limão Tahiti.

4.10 Promotores de *LOB1*, *LOB2* e *DIOX* possuem polimorfismos na região de ligação dos PthAs

A expressão diferencial dependente de PthAs dos genes *LOB1*, *LOB2* e *DIOX* observada entre as plantas Pêra e Tahiti (Figura 31) sugere a existência de polimorfismos na região de ligação do efetor ao DNA das plantas. Desta forma, as regiões promotoras desses três genes foram sequenciadas, sendo amplificadas do DNA genômico das plantas Pêra e Tahiti, para comparar com as sequências já publicadas do genoma das variedades Valência (*C. sinensis*) e Clemenules (*C. clementina*) (Xu *et al.*, 2013; Wu *et al.*, 2014).

Nas regiões promotoras dos genes alvos *LOB1*, *LOB2* e *DIOX* foram encontradas múltiplas regiões de ligação dos efetores PthAs (Figura 37). Na região promotora do gene *LOB1* pudemos observar, entre os promotores de Pêra, Tahiti, Valência e Clemenules, uma troca de nucleotídeo (T/C) e uma deleção (G/-) na região que flanqueia o já caracterizado sítio de ligação de PthA4, que se sobrepõe a região do TATA box (Figura 34) (Hu *et al.*, 2014; Pereira *et al.*, 2014). Além disso, foi observado uma região de deleção de 11 nucleotídeos localizada exatamente 25 pb *downstream* ao sítio de ligação de PthA4 na variedade Tahiti em relação as variedades Pêra, Valência e Clemenules. Também foram verificados SNPs (*Single Nucleotide Polymorphisms*) nas regiões de ligação dos efetores PthA1 (A/C) e PthA3 (A/C) no Tahiti em relação as variedades Pêra, Valência e Clemenules (Figura 37).

Na região promotora do gene *LOB2*, além do sítio de ligação de PthA2 identificado anteriormente (Pereira *et al.*, 2014), outros dois sítios de ligação, um de PthA1 e outro de PthA3 foram identificados sobrepondo a região do TATA box (Figura 37). Adicionalmente, foi observada a presença de SNPs nos sítios de ligação de PthA1 (A/G), PthA2 (T/C) e PthA3 (C/T), além da deleção de 7 nucleotídeos em um dos sítios de ligação de PthA2, sendo todos os polimorfismos encontrados no limão Tahiti em relação a Pêra, Valência e Clemenules (Figura 37).

Apesar dos esforços, infelizmente não foi possível obter a sequência da região promotora do gene *DIOX* da variedade Pêra. Foram testados seis pares de oligonucleotídeos distintos (desenhados a partir do genoma de Valência depositado no banco de dados) com DNAs genômicos extraídos de quatro diferentes plantas Pêra em múltiplas reações de PCR, porém sem resultado positivo. Este fato sugere que esta região promotora deve ser uma região altamente polimórfica. Desta forma, somente foram alinhadas as sequências das regiões promotoras de Tahiti, Valência e Clemenules (Figura 37). Em adição ao sítio de ligação de PthA4 descrito anteriormente (Pereira *et al.*, 2014), foi encontrado um sítio de ligação de PthA2 contendo um SNP (T/C) entre os promotores de Tahiti em relação a Valência e Clemenules

(Figura 37). Além disso, semelhantemente ao que foi observado no promotor de *LOB1*, no promotor do gene *DIOX* também foi observado uma deleção de 14 pb flanqueando o sítio de ligação de PthA4 no promotor de Tahiti, em relação aos promotores de Valência e Clemenules, e esta região de deleção contêm o W box de sequência 'TGAC' que é reconhecida por fatores de transcrição WRKY, capazes de controlar genes responsivos a giberelina e relacionados a patogenicidade (Figura 37) (Eulgem *et al.*, 1999; Zhang *et al.*, 2004).

Além do elemento regulatório W box encontrado no promotor de *DIOX*, também foram identificadas, através do algoritmo PlantPAN 2.0, várias outras regiões putativas de ligação de fatores de transcrição nos promotores de *LOB1*, *LOB2* e *DIOX*. O fato mais marcante encontrado foi o fator Dof, pois os sítios de Dof foram encontrados perto dos sítios de ligação dos PthAs nos três promotores estudados (Figura 37). Algumas trocas de nucleotídeos ou deleções próximo aos sítios Dof foram encontradas entre as sequências de laranja doce e limão Tahiti. Além disso, no promotor de *DIOX* observou-se dois sítios Dof invertidos formando um palíndrome, localizados a 28 pb *downstream* do sítio de ligação de PthA4. Conjuntamente, estes resultados indicam que a expressão diferencial e PthAs dependente dos genes *LOB1*, *LOB2* e *DIOX* observadas entre as plantas Pêra e Tahiti podem ser influenciadas pelos polimorfismos encontrados nos sítios de ligação dos PthAs e que os fatores de transcrição WRKY e Dof podem ter um importante papel na regulação transcricional desses genes.

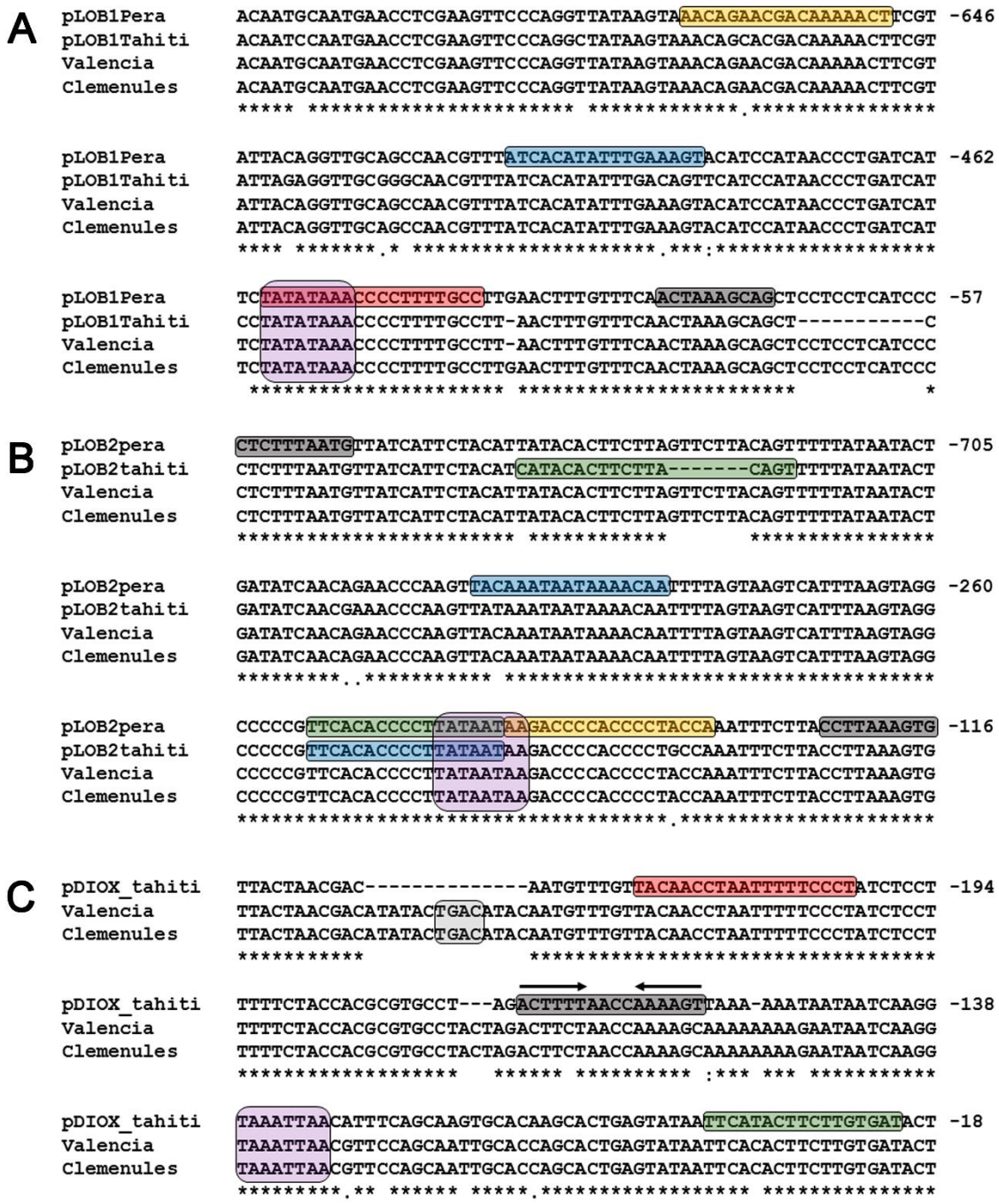

Figura 37. Alinhamento das regiões promotoras dos genes *LOB1*, *LOB2* e *DIOX*. As sequências das regiões promotoras dos genes *LOB1* **(A)**, *LOB2* **(B)** e *DIOX* **(C)** de citros foram amplificadas a partir do DNA genômico de plantas de laranja Pêra e limão Tahiti e comparadas com as sequências das variedades Valência e Clemenules. As regiões de ligação das proteínas PthA1, 2, 3 e 4 preditas estão dispostas na coloração amarelo, verde, azul e vermelho, respectivamente. Os sítios de ligação dos fatores Dof e WRKY estão em cinza escuro e cinza claro, respectivamente, enquanto que o TATA box encontra-se na coloração roxa. As setas em **C** representam a sequência palindrômica de Dof. A maioria dos SNPs encontrados em Pêra em relação a Tahiti, também está presente nas variedades Valência e Clemenules.

6. DISCUSSÃO

O estudo dos mecanismos de patogenicidade dos fitopatógenos permite uma maior compreensão dos fatores específicos capazes de causar doença na planta. Muitos patógenos do gênero *Xanthomonas*, incluindo *X. citri*, *X. aurantifolii* e *X. oryzae*, possuem múltiplos efetores TAL, porém a função de cada um desses efetores na patogenicidade ainda é pouco conhecida, uma vez que poucos efetores têm sido demonstrados como principais fatores de virulência (Yang & White, 2004; Al-Saadi *et al.*, 2007; Wilkins *et al.*, 2015). No caso da bactéria *X. citri* estirpe 306 e *X. aurantifolii* C estirpe ICMP 8435 foram encontradas quatro variantes da proteína PthA e duas variantes da proteína PthC, respectivamente (da Silva *et al.*, 2002; Cernadas *et al.*, 2008). Neste trabalho, buscou-se elucidar a contribuição de cada uma dessas proteínas efetoras no desenvolvimento da doença, ou ainda em um provável desencadeamento de resposta de defesa em algumas hospedeiras de citros.

Desta forma, mutantes de deleção para as proteínas PthAs foram obtidos e os fenótipos nas folhas resultante das infiltrações com esses mutantes foram analisados em relação a infiltração com a bactéria selvagem, em sete hospedeiras de citros distintas (Figuras 21, 22 e 23). Em todas as variedades testadas é indiscutível o papel fundamental que PthA4 exerce na indução do cancro, sendo indispensável para a formação de pústulas, corroborando dados da literatura (Al-Saadi *et al.*, 2007; Yan & Wang, 2012; Soprano *et al.*, 2013; Hu *et al.*, 2014). Muitos autores indicam que *pthA4* é o fator determinante de *X. citri* para causar cancro (Swarup *et al.*, 1992; Duan *et al.*, 1999, Yan & Wang, 2012; Hu *et al.*, 2014). Uma das explicações para PthA4 ser uma proteína importante para o surgimento e desenvolvimento do cancro, é que ela interage especificamente com a proteína MAF1 de citros (CsMAF1), um repressor de RNA polimerase III que controla a biogênese de ribossomos e o crescimento celular (Soprano *et al.*, 2013). Experimentos onde folhas de laranja Pêra foram infiltradas com *X. citri* e a bactéria mutante Δ4 mostraram que, em seções foliares infiltradas com *X. citri* ocorreu uma diminuição nos níveis de CsMAF1, de acordo com o desenvolvimento de hipertrofia e hiperplasia celular. Em contrapartida, em seções foliares onde não se desenvolveu a doença, infiltrada com o mutante Δ4, os níveis de CsMAF1 permaneceram inalterados (Soprano *et al.*, 2013). Dessa forma, é provável que PthA4 previna a interação de CsMAF1 com a RNA polimerase III, permitindo o desenvolvimento do cancro.

Apesar do papel fundamental de PthA4, neste trabalho foram demonstrados, pela primeira vez, que outros PthAs também possuem um papel importante no desenvolvimento de sintomas de cancro em algumas hospedeiras de citros. Estes resultados indicam que os PthAs de *X. citri* possuem um papel aditivo ou complementar na patogenicidade, de forma hospedeiro

dependente, e sugere que PthA1 e PthA3 potencializam o papel de PthA4 na elicitação do cancro. Diante deste fato, também foi analisado o padrão de crescimento das bactérias mutantes em relação a *X. citri* e foi verificado que os PthAs, de um modo geral, também contribuem no crescimento bacteriano, sendo que a perda de dois ou mais PthAs influenciam de forma aditiva (Figura 24). Curiosamente, mesmo quando não é observado o sintoma de cancro nas folhas infiltradas, ainda assim há um crescimento bacteriano elevado (da ordem de 10^8 CFU/cm^2), como foi observado no padrão de crescimento dos mutantes Δ4 e B21.2 (Figuras 24 e 25). Em acordo com estes dados, Yan & Wang (2012) reportaram que um mutante nocaute *pthA4*, que causava somente clorose em folhas de citros variedade Grapefruit, também teve um crescimento perto de 10^8 CFU/cm^2 de folha aos 4 dpi. Estes dados indicam que provavelmente a função principal dos PthAs não é o crescimento bacteriano, mas são necessários para a elicitação e desenvolvimento do cancro e consequente dispersão da bactéria pelas rupturas provenientes das pústulas.

Neste trabalho, após a obtenção dos mutantes de deleção de PthAs, buscou-se também a complementação destes mutantes com os respectivos genes deletados, porém não observamos a restauração dos sintomas. No entanto, na complementação do mutante Δ4 e B21.2 com o gene *pthC1* foi possível observar sintomas de cancro em laranja Pêra, semelhante aos sintomas causados por *X. citri*. Estes dados corroboram os estudos feitos com *X. aurantifolii* C estirpe C340, onde o mutante B21.2 foi complementado com uma proteína PthC contendo 17,5 repetições do domínio central e ao ser infiltrada em folhas de Grapefruit, houve a restauração dos sintomas (Al-Saadi *et al.*, 2007). É provável que o gene PthC2 não seja essencial para *X. aurantifolii* C na elicitação do cancro, mas assim como as proteínas PthA1 e PthA3, PthC2 possa ter um papel aditivo no desenvolvimento do cancro, em limão Galego. Além disso, Al-Saadi *et al.* (2007) demonstraram que a inativação do PthC de *X. aurantifolii* estirpe C340 resultou em perda de patogenicidade no limão Galego, mas não perda de avirulência em Grapefruit. Estes dados indicam que o gene *pthC* não é o responsável por desencadear resposta de defesa em laranja Pêra e que algum outro gene presente em *X. aurantifolii* C possa estar limitando sua gama de hospedeiros.

Neste estudo também procurou-se identificar alvos diretos de PthAs em citros. Potenciais alvos, obtidos em nosso laboratório (Pereira *et al.*, 2014), foram testados em folhas de laranja Pêra e limão Tahiti infiltradas com os mutantes de deleção de PthAs. Estas hospedeiras foram escolhidas devido ao distinto padrão do fenótipo da infiltração observado, de forma que na laranja Pêra foi verificado que PthA1 e PthA3 possuem um efeito aditivo no desenvolvimento do cancro elicitado por PthA4 e em Tahiti, somente verificou-se o efeito de

PthA4 (Figura 21). Estes dados são consistentes com o fato de que PthA1 e PthA3 não foram necessários na indução de *LOB1* em laranja Pêra, mas sim na ativação de outros alvos, como os genes *LOB2* e *DIOX* (Figura 31), e a expressão de *LOB1* em limão Tahiti foi drasticamente reduzida na infiltração com os mutantes de deleção simples (Figura 31A), apesar do cancro ter se desenvolvido normalmente nesta hospedeira em relação a laranja Pêra.

Notavelmente, foi verificado que a indução de *LOB1* por *X. citri* nem sempre se correlaciona com a formação de cancro. Da mesma forma, *LOB1* foi fortemente induzido durante a interação incompatível de *X. aurantifolii* C em laranja Pêra (Figura 33). Estes dados indicam que a indução de *LOB1* por si só não é suficiente para a elicitação do cancro, o que está em acordo com a observação de que a superexpressão de *LOB1* em citros transgênico não resultou na formação de pústulas (Hu *et al.*, 2014). Além disso, Jia *et al.* (2015) geraram plantas transgênicas, da variedade Grapefruit, com mutações no promotor de *LOB1*, mais especificamente na região de ligação de PthA4 ao DNA. A infiltração dessas plantas transgênicas com *X. citri* resultou na típica formação de cancro, semelhante a infiltração de uma planta não transgênica (Jia *et al*., 2015). Este fato mais uma vez indica que, apesar de *LOB1* aparecer como indutor de vários genes relacionados a remodelamento de parede que também são induzidos por PthA4 durante o desenvolvimento de cancro (Hu *et al.*, 2014), não é provável que sua ativação de forma isolada possa desencadear todo o processo de formação do cancro.

O gene *DIOX* de citros foi identificado como alvo de PthA4 em dois estudos independentes visando a identificação de alvos de efetores TAL de *X. citri* (Hu *et al.*, 2014; Pereira *et al.*, 2014). Em outro estudo paralelo visando a identificação de alvos de efetores TAL de *X. oryzae*, foi identificado um ortólogo da *DIOX* de citros como alvo de Tal2d, um efetor TAL de *X. oryzae* (Cernadas *et al.*, 2014). A identificação do gene *DIOX* em diversos estudos reforça a idéia de que este gene possa ter um papel fundamental no desenvolvimento de doenças, talvez atuando como gene de suscetibilidade. Neste estudo, foram apresentadas evidências, sugerindo que *DIOX* pode ter um importante papel no desenvolvimento do cancro. A expressão de *DIOX* foi dependente de PthA1, 3 e 4 em folhas de laranja Pêra, mas não de limão Tahiti (Figura 31D). Além disso, psoralen, um inibidor de 2OGD (Vialart *et al.*, 2012), significativamente reduziu os sintomas de cancro e o crescimento bacteriano em laranja Pêra, mas não em limão Tahiti (Figura 36). Em um estudo envolvendo o fungo *Fusarium fujikuroi* foi descoberto que uma giberelina desaturase (DES), necessária na biossíntese de ácido giberélico, possui características de uma 2OGD. A expressão de DES sob o controle do promotor 35S de "cauliflower mosaic virus" em plantas das espécies *Solanum nigrum*, *Solanum dulcamara* e *Nicotiana sylvestris* resultaram em uma estimulação do crescimento da planta

(Bhattacharya *et al.*, 2012), indicando que proteínas 2OGD podem ter um papel no estímulo de crescimento celular.

Embora a função biológica e o substrato específico da DIOX de citros não tenha sido demonstrada, os estudos com o modelo molecular sugerem fortemente que DIOX é o ortólogo da enzima F6'H1 de Arabidopsis e *R. graveolens* (Figura 35) e pode catalisar a orto-hidroxilação de ferruloil-CoA e/ou *p*-coumaroil-CoA (Kai *et al.*, 2008; Vialart *et al.*, 2012; Sun *et al.*, 2015). Desta forma, a questão que se coloca é como a atividade da DIOX pode conduzir ou contribuir para o desenvolvimento do cancro em laranja Pêra.

Um possível mecanismo pode envolver a ação de cinamoil-CoA redutases (CCR), que converte cinamoil-CoA ésteres, incluindo ferruloil-CoA, *p*-coumaroil-CoA e cafeoil-CoA em seus correspondentes cinamil aldeídos durante a síntese de monômeros de lignina (Zhou *et al.*, 2010; Xue *et al.*, 2015). Foi descrito que a enzima CCR1 de Arabidopsis media a proliferação celular para o desenvolvimento da folha e que o mutante *ccr1* apresentou aumento da proliferação celular e altos níveis de ácido ferrúlico (Xue *et al.*, 2015). Como CCR1 usa preferencialmente ferruloil-CoA como substrato, é possível que 6'-hidroxiferruloil-CoA, o produto da reação da DIOX de citros, iniba a atividade de CCR1, permitindo uma resposta de proliferação celular semelhante a perda de CCR1 (Zhou *et al.*, 2010; Xue *et al.*, 2015). Além disso, o papel de CCR1 na biossíntese de lignina e divisão celular também está relacionado com a atividade de ácido cafeico O-metiltransferases (COMT) e cafeoil-CoA 3-O-metiltransferases (CCOAOMT) que fornece o substrato para CCR1 (Zhou *et al.*, 2010; Xue *et al.*, 2015). A inibição de COMT e CCOAOMT em Arabidopsis resultou em baixos níveis de ácido ferrúlico e diminuição da divisão celular (Xue *et al.*, 2015). Como ácido ferrúlico por si só induz proliferação celular em Arabidopsis, seria interessante investigar se ácido 6-hidroxiferrulico também pode estimular divisão celular durante a formação do cancro.

Outra observação notável é que genes como *COMT*, *CCOAOMT* e *CCR* foram preferencialmente induzidos por *X. aurantifolii* C durante a interação incompatível em laranja Pêra (Cernadas *et al.*, 2008). Isto indica que a via de *COMT*, *CCOAOMT* e *CCR* de citros também pode contribuir na restrição da divisão celular durante a formação do cancro. O fato de *DIOX* ter sido induzido em laranja Pêra em níveis muito menores por *X. aurantifolii* C em relação a *X. citri* (Figura 33) é consistente com a idéia que *DIOX* tem um papel contrário na via de *COMT*, *CCOAOMT* e *CCR*.

Nas regiões promotoras dos genes *LOB1*, *LOB2* e *DIOX* foram encontradas múltiplas regiões de ligação dos efetores PthAs ao DNA, além das regiões de ligação preditas em Pereira *et al.* (2014). A presença dessas regiões de ligação de diferentes PthAs reforça a

idéia da ação em conjunto desses efetores na indução de genes que influenciam no desenvolvimento do cancro. A expressão diferencial e PthA dependente de *LOB1*, *LOB2* e *DIOX* observada entre as plantas de laranja Pêra e limão Tahiti está associada não somente com a presença ou ausência de específicas regiões de ligação do PthA no promotor desses genes, mas também com a ocorrência de SNPs ou deleção de nucleotídeos próximo ou dentro da região de ligação do PthA (Figura 34). Uma única deleção nucleotídica na região de ligação de PthXo2, um efetor de *X. oryzae*, no promotor do gene *S* de crestamento bacteriano, *Xa25* (OsSWEET13), foi suficiente para revogar a ativação desse gene (Zhou *et al.*, 2015). Em um outro gene *S* de crestamento bacteriano (OsSWEET14), uma deleção de 18 pb entre os sítios de ligação de vários efetores TAL também conferiram resistência contra várias estirpes de *X. oryzae* de várias origens geográficas (Hutin *et al.*, 2015). Desta forma, a presença de polimorfismos nos sítios de ligações dos PthAs é uma forte evidência da adaptação do hospedeiro em escapar do reconhecimento do gene alvo pelo efetor.

De certa forma, a mutação na região promotora de um único gene, em alguns casos, pode impedir o reconhecimento do efetor e resultar na resistência da planta (Hutin *et al.*, 2015). Porém, no caso do cancro cítrico, é provável que a inativação de um único gene não irá resultar na resistência da planta. Assim como foi observado nas plantas com mutação no promotor de *LOB1*, onde quatro mutantes de um dos alelos do promotor de *LOB1* foram suscetíveis ao cancro cítrico (Jia *et al.*, 2015). Sendo assim, talvez seja necessária a inativação de múltiplos genes *S*, assim como o *DIOX*, para impedir a formação e desenvolvimento do cancro. No entanto, a obtenção de plantas com mutações em várias regiões promotoras ao mesmo tempo poderia tornar inviável a geração de plantas resistentes ao cancro cítrico. Uma alternativa seria a clonagem de um promotor de um gene que é especificamente ativado na presença de *X. citri*, ligando esse promotor a um gene de resistência de citros, de modo que a região promotora desse gene de resistência fosse subtituído, para desencadear resposta de defesa. Isso faria com que os PthAs atuassem como genes de avirulência ativando genes relacionados a defesa, como inibidores de endoglucanases, biossíntese de fenilpropanóides, MAPKs, entre outros (Cernadas *et al.*, 2008; de Oliveira *et al.*, 2013).

Analisando as regiões de ligação dos PthAs nos promotores dos genes *LOB1*, *LOB2* e *DIOX* observou-se que os PthAs se ligam preferencialmente próxima ou na região do TATA-box. Assim como o gene *AvrBs3* que também se liga na região do TATA-box no promotor do gene *Bs3* (Römer *et al.*, 2007). Estudos prévios mostraram que a maioria das regiões de ligação preditas para os PthAs e PthCs apresentaram uma tendência de se sobreporem ao TATA-box,

sugerindo que os efetores TAL podem ter uma função semelhante ao das proteínas que se ligam ao TATA-box (Pereira *et al.*, 2014).

Ainda nas regiões promotoras dos genes *LOB1*, *LOB2* e *DIOX*, foram encontrados vários sítios Dof próximos das regiões de ligação dos PthAs. Os fatores Dof controlam a transcrição de vários genes de plantas. Em Arabidopsis, Dof5.8 reprime a resposta de auxina ocasionando má formação de veias foliares (Konishi & Yanagisava, 2015), enquanto DAG1 (*Dof affecting germination 1*) regula negativamente o gene da biossíntese de giberelina AtGA3ox1, que codifica uma 2OGD relacionada com DIOX de citros (Gabriele *et al.*, 2010). Em milho, os fatores Dof interagem com proteínas HMGB (*High Mobility Group B*) facilitando a ligação de Dof ao DNA (Yanagisawa, 1997; Krohn *et al.*, 2002; Cavalar *et al.*, 2003; Grasser *et al.*, 2007).

A interação entre Dof e HMGB é de particular importância uma vez que todos os PthAs de *X. citri* interagiram com a proteína de citros HMGB1 (de Souza *et al.*, 2012). A proteína HMGB1 de mamíferos interage com TBP (TATA-binding protein) para reprimir a transcrição, enquanto o fator transcricional TFIIA se liga à TBP para romper o complexo HMGB/TBP e ativar a transcrição (Sutrias-Grau *et al.*, 1999; Das & Scovell, 2001; Dasgupta & Scovell, 2003). Considerando que os fatores Dof atuam como repressores da transcrição e que os PthAs se ligam próximo ou no elemento TATA-box de promotores de citros, é possível que, semelhante ao TFIIA, os PthAs possam substituir Dof/HMGB ou alterar o recrutamento de fatores no sítio TBP para promover o início da transcrição.

7. CONCLUSÕES

O estudo funcional dos efetores TAL de *X. citri* e *X. aurantifolii* nos permite uma maior compreensão de suas ações dentro da planta hospedeira e assim elaborar estratégias de controle da doença. Neste presente estudo, buscou-se elucidar a função de cada um dos efetores TAL presentes nestas bactérias, além de avaliar a expressão de potenciais genes alvos dessas proteínas efetoras. Desta forma, os resultados apresentados neste trabalho permitiram concluir-se que:

I. A proteína PthA4 é essencial e suficiente para a elicitação do cancro em todas as hospedeiras testadas, e PthA1 e PthA3 tem um importante papel no desenvolvimento dos sintomas, atuando de forma aditiva e hospedeiro dependente;
II. Os PthAs afetam o crescimento bacteriano *in planta* de maneira aditiva;
III. PthC1 atua como efetor de patogenicidade, e não como proteína Avr na laranja Pêra;
IV. *X. aurantifolii* patotipo C não causa cancro em limão Tahiti;
V. A expressão de *LOB1*, principal gene de suscetibilidade do cancro cítrico descrito na literatura, não se correlaciona com o desenvolvimento das lesões do cancro em hospedeiras de citros testadas;
VI. Os genes *LOB2* e sobretudo *DIOX* atuam como prováveis genes de suscetibilidade para o cancro cítrico em laranja Pêra;
VII. A expressão gênica diferencial de alvos de PthAs, encontrada em diferentes hospedeiras de citros, está associada a polimorfismos encontrados nos promotores dos genes alvos, nas regiões adjacentes ou de ligação dos efetores PthAs.

8. REFERÊNCIAS BIBLIOGRÁFICAS

Abramovitch, R. & Martin, G. (2004) Strategies used by bacterial pathogens to suppress plant defenses. *Curr. Opin. Plant Biol.* 7, 356-364.

Abramovitch, R.B., Anderson, J.C., Martin, G.B. (2006) Bacterial elicitation and evasion of plant innate immunity. *Nat. Rev. Mol. Cell Biol.* 7, 601-611.

Al-Saadi, A., Reddy, J., Duan, Y., Brunings, A., Yuan, Q., Gabriel, D. (2007) All five host-range variants of *Xanthomonas citri* carry one *pthA* homolog with 17.5 repeats that determines pathogenicity on citrus, but none determine host-range variation. *Mol. Plant-Microbe Interact*. 20, 934-943.

Amaral, A. (2003) Cancro cítrico: permanente preocupação da citricultura no Brasil e no mundo. Comunicado Técnico. Brasília, Embrapa: p.1-5.

Andrade, M.O. (2011) Estudo da sinalização celular envolvendo a via do quorum-sensing e os segundos mensageiros c-diGMP e (p)ppGpp no fitopatógeno *Xanthomonas axonopodis* pv *citri*. Tese de doutorado defendida em 13/07/2011 no Instituto de Química da Universidade de São Paulo, Departamento de Bioquímica, São Paulo–SP.

Andrade, M.O., Farah, C.S., Wang, N. (2014) The post-transcriptional regulator *rsmA/csrA* activates T3SS by stabilizing the 59 UTR of *hrpG*, the master regulator of *hrp/hrc* genes, in *Xanthomonas*. *PLoS Pathog*. 10, e1003945.

Bayer, R. J., Mabberley, D. J., Morton, C., Miller, C.H., Sharma, I. K., Pfeil, B. E., Rich, S., Hitchcock, R., Sykes, S. (2009) A molecular phylogeny of the orange subfamily (Rutaceae:Aurantioideae) using nine cpDNA sequences. *Am. J. Bot.* 96, 668-685.

Behlau, F. & Belasque Jr., J. (2014) Cancro cítrico: a doença e seu controle. Fundecitrus.

Behlau, F., Junior, J., Filho, A. B., Junior, R. P. L. (2007) Incidência e Severidade de Cancro Cítrico em Laranja 'Pêra Rio' sob Condições de Controle Químico e Proteção com Quebra-Vento. *Fitopatol. Bras.* 32, 311-317.

Belasque Jr., J., Parra-Pedrazzoli, A.L., Rodrigues Neto, J., Yamamoto, P.T., Chagas, M.C.M., Parra, J.R.P., Vinyard, B.T., Hartung, J.S. (2005) Adult citrus leafminers (*Phyllocnistis citrella*) are not efficient vectors for *Xanthomonas axonopodis* pv. *citri*. *Plant Dis.* 89, 590-594.

Birch, P.R., Rehmany, A.P., Pritchard, L., Kamoun, S., Beynon J.L. (2006) Trafficking arms: Oomycete effectors enter host plant cells. *Trends Microbiol.* 14, 8-11.

Bittel, P. & Robatzek, S. (2007) Microbe-associated molecular patterns (MAMPs) probe plant immunity. *Curr. Opin. Plant Biol.* 10, 335-341.

Block, A., Li, G., Fu, Z.Q., Alfano, J.R. (2008) Phytopathogen type III effector weaponry and their plant targets. *Curr. Opin. Plant Biol*. 11, 396-403.

Boch, J. & Bonas, U. (2010) Xanthomonas AvrBs3 family-type III effesctors: discovery and function. *Annu. Rev. Phytopathol*. 48, 419-436.

Boch, J., Scholze, H., Schornack, S., Landgraf, A., Hahn, S., Kay, S., Lahaye, T., Nickstadt, A., Bonas, U. (2009) Breaking the code of DNA binding specificity of TAL-type III effectors. *Science*, 326, 1509-1512.

Bogdanove, A.J. & Voytas, D.F. (2011) TAL effectors: customizable proteins for DNA targeting. *Science*, v. 333, p. 1843-1846.

Bonas, U., Stall, R.E., Staskawicz, B. (1989) Genetic and structural characterization of the avirulence gene *avrBs3* from *Xanthomonas campestris* pv. *vesicatoria*. *Mol. Gen. Genet.* 218, 127-136.

Brattacharya, A., Kourmpetli, S., Ward, D.A., Thomas, S.G., Gong, F., Powers, S.J., Carrera, E., Taylor, B., Gonzalez, F.N.C., Tudzynski, B., Phillips, A.L., Davey, M.R., Hedden, P. (2012) Characterization of the fungal gibberellin desaturase as a 2-oxoglutarate-dependent dioxygenase and its utilization for enhancing plant growth. *Plant Physiol*. 160, 837-845.

Brunings, A.M. & Gabriel, D.W. (2003) *Xanthomonas citri*: breaking the surface. *Mol. Plant Pathol*. 4, 141-157.

Büttner, D. & Bonas, U. (2009) Regulation and secretion of *Xanthomonas* virulence factors. *FEMS Microbiology Reviews*, 34, 107-133.

Büttner, D. & He, S.Y. (2009) Type III protein secretion in plant pathogenic bacteria. *Plant Physiol.* 150, 1656-1664.

Cavalar, M., Möller, C., Offermann, S., Krohn, N.M., Grasser, K.D., Peterhänsel, C. (2003) The interaction of DOF transcription factors with nucleosomes depends on the positioning of the binding site and is facilitated by maize HMGB5. *Biochemistry*, 42, 2149-2157.

Cernadas, R.A., Camillo, L.R., Benedetti, C.E. (2008) Transcriptional analysis of the sweet orange interaction with the citrus canker pathogens *Xanthomonas axonopodis* pv. *citri* and *Xanthomonas axonopodis* pv. *aurantifolii*. *Mol. Plant Pathol.* 9, 609-631.

Cernadas, R.A., Doyle, E.L., Ninõ-Liu, D.O., Wilkins, K.E., Bancroft, T., Wang, L., Schmidt, C.L., Caldo, R., Yang, B., White, F.F., Nettleton, D., Wise, R.P., Bogdanove, A.J. (2014) Code-assisted discovery of TAL effector targets in bacterial leaf streak of rice reveals contrast with bacterial blight and a novel susceptibility gene. *Plos Pathog.* 10(2):e1003972.

Chang, W.C., Lee, T.Y., Huang, H.D., Huang, H.Y., Pan, R.L. (2008) PlantPAN: Plant Promoter Analysis Navigator, for identifying combinatorial cis-regulatory elements with distance constraint in plant gene group. *BMC Genomics*, 9, 561.

Chiesa, M.A., Siciliano, M.F., Ornella, L., Roeschlin, R.A., Favaro, M.A., Delgado, N.P., Sendín, L.N., Orce, I.G., Ploper, L.D., Vojnov, A.A., Vacas, J.G., Filippone, M.P., Castagnaro, A.P., Marano, M.R. (2013) Characterization of a variant of *Xanthomonas citri* subsp. *citri* that triggers a host-specific defense response. *Phytopathology*, 103, 555-564.

CitrusBR: Associação Nacional dos Exportadores de Sucos Cítricos. Disponível em: <http://www.citrusbr.com/>. Acesso em 25 de Janeiro de 2016.

da Silva, A., Ferro, J., Reinach, F.C., Farah, C.S., Furlan, L.R., Quaggio, R.B., Monteiro-Vitorello, C.B., Van Sluys, M.A., Almeida, N.F., Alves, L.M., do Amaral, A.M., Bertolini, M.C., Camargo, L.E., Camarotte, G., Cannavan, F., Cardozo, J., Chambergo, F., Ciapina, L.P., Cicarelli, R.M., Coutinho, L.L., Cursino-Santos, J.R., El-Dorry, H., Faria, J.B., Ferreira, A.J., Ferreira, R.C., Ferro, M.I., Formighieri, E.F., Franco, M.C., Greggio, C.C., Gruber, A., Katsuyama, A.M., Kishi, L.T., Leite, R.P., Lemos, E.G., Lemos, M.V., Locali, E.C., Machado, M.A., Madeira, A.M., Martinez-Rossi, N.M., Martins, E.C., Meidanis, J., Menck, C.F., Miyaki, C.Y., Moon, D.H., Moreira, L.M., Novo, M.T., Okura, V.K., Oliveira, M.C., Oliveira, V.R., Pereira, H.A., Rossi, A., Sena, J.A., Silva, C., de Souza, R.F., Spinola, L.A., Takita, M.A., Tamura, R.E., Teixeira, E.C., Tezza, R.I., Trindade dos Santos, M., Truffi, D., Tsai, S.M., White, F.F., Setubal, J.C., Kitajima, J.P. (2002) Comparison of the genomes of two *Xanthomonas* pathogens differing host specificities. *Nature*, 417, 459-463.

Dangl, J.L & Jones, J.D.G. (2001) Plant pathogens and integrated defence responses to infection. *Nature*, 411, 826-833.

Das, D. & Scovell, W.M. (2001) The binding interaction of HMG-1 with the TATAbinding protein/TATA complex. *J. Biol. Chem*. 276, 32597–32605.

Dasgupta, A. & Scovell, W.M. (2003) TFIIA abrogates the effects of inhibition by HMGB1 but not E1A during the early stages of assembly of the transcriptional preinitiation complex. *Biochim. Biophys. Acta*. 1627, 101–110.

de Oliveira, M.L.P., Silva, C.C.L., Abe, V.Y., Costa, M.G.C., Cernadas, R.A., Benedetti, C.E. (2013) Increased resistence against citrus canker mediated by a citrus mitogen-activated protein kinase. *Mol. Plant-Microbe Interact.* 26, 1190-1199.

de Souza, T.A., Soprano, A.S., de Lira N.P.V., Quaresma, A.J.C., Pauletti, B.A., Leme, A.F.P., Benedetti, C.E. (2012) The TAL effector PthA4 interacts with nuclear factors involved in

RNA dependent processes including a HMG protein that selectively binds poly(U) RNA. *PLoS ONE,* 7, e32305.

De Wit, P.J.G.M. (2007) How plants recognize pathogens and defend themselves. *Cell. Mol. Life Sci.* 64, 2726-2732.

De Wit, P.J.G.M., Mehrabi, R., Van Den Burg, H.A., Stergiopoulos, I. (2009) Fungal effector proteins: past, present and future. Review. *Mol. Plant Pathol*. 10, 735-747.

DeFeyter, R., Yang, Y., Gabriel, D.W. (1993) Gene-for-gene interactions between cotton *R* genes and *Xanthomonas campestris* pv. *malvacearum avr* genes. *Mol. Plant-Microbe Interact.* 6, 225-237.

DeLano, W.L. (2002) The PyMOL molecular graphics system. San Carlos, CA: DeLano Scientific.

Dodds, P.N. & Rathjen, J.P. (2010) Plant immunity: towards an integrated view of plant-pathogen interactions. *Nat. Rev. Genet.* 11, 539-548.

Doyle, J.J. & Doyle, J.L. (1987) A rapid isolation procedure for small quantities of fresh leaf tissue. *Phytochem. Bull.* 19, 11-15.

Duan, Y., Castañeda, A., Zhao, G., Erdos, G., Gabriel, D.(1999) Expression of a single, host-specific, bacterial pathogenicity gene in plant cells elicits division, enlargement, and cell death. *Mol. Plant-Microbe Interact.* 12, 556-560.

Eulgem, T., Rushton, P.J., Schmelzer, E., Hahlbrock, K., Somssich, I.E. (1999) Early events in plant defence signaling: rapid gene activation by WRKY transcription factors. *EMBO J*. 18, 4689-4699.

Farrow, S.C. & Facchini, P.J. (2014) Functional diversity of 2-oxoglutarate/Fe(II)-dependent dioxygenases in plant metabolism. *Front. Plant Sci*. 5, 524.

Gabriele, S., Rizza, A., Martone, J., Circelli, P., Costantino, P., Vittorioso, P. (2010). The DOF protein DAG1 mediates PIL5 activity on seed germination by negatively regulating the GA biosynthetic gene *AtGA3ox1*. *Plant J*. 61, 312–323.

Grasser, M., Christensen, J.M., Peterhänsel, C., Grasser, K.D. (2007) Basic and acidic regions flanking the HMG-Box domain of maize HMGB1 and HMGB5 modulate the stimulatory effect on the DNA binding of transcription factor Dof2. *Biochemistry*, 46, 6375-6382.

Grau, J., Wolf, A., Reschke, M., Bonas, U., Posch, S., Boch, J. (2013) Computational predictions provide insights into the biology of TAL effector target sites. *PLOS Comput. Biol*. 9(3):e1002962.

Hausner, J., Hartmann, N., Lorenz, C., Buttner, D. (2013) The periplasmic HrpB1 protein from *Xanthomonas* binds to peptidoglycan and to components of the type III secretion system. *Appl. Environ. Microbiol*. 79, 6312–6324.

Hu, Y., Zhang, J., Jia, H., Sosso, D., Li, T., Frommer, W.B., Yang, B., White, F.F., Wang, N., Jones, J.B. (2014) Lateral organ boundaries 1 is a disease susceptibility gene for citrus bacterial canker disease. *Proc. Natl. Acad. Sci. U.S.A*. 111, 521-529.

Hutin, M., Sabot, F., Ghesquière, A., Koebnik, R., Szurek, B. (2015) A knowledge-based molecular screen uncovers a broad spectrum *OsSWEET14* resistance allele to bacterial blight from wild rice. *Plant J*. 84, 694-703.

Jacobs, C., Domian, I.J., Maddock, J.R., Shapiro, L. (1999) Cell cycle–dependent polar localization of an essential bacterial histidine kinase that controls DNA replication and cell division. *Cell*, 97, 111–120.

Jia, H., Orbovic, V., Jones, J.B., Wang, N. (2015) Modification of the PthA4 effector binding elements in Type I *CsLOB1* promoter using Cas9/sgRNA to produce transgenic Duncan grapefruit alleviating XccDpthA4: dCsLOB1.3 infection. *Plant Biotech. J.* 1–11.

Jones, J. D. & Dangl J. L. (2006) The plant immune system. *Nature*, 444, 323-329.

Kai, K., Mizutani, M., Kawamura, N., Yamamoto, R., Tamai, M., Yamaguchi, H., Sakata, K., Shimizu, B. (2008) Scopoletin is biosynthesized via orthohydroxylation of feruloyl CoA by a 2-oxoglutarate-dependent dioxygenase in *Arabidopsis thaliana*. *Plant J.* 55, 989–999.

Kamoun, S. (2009) The secretome of plant-associated fungi and oomycetes. In: Deising, H. & Essey, K. *The Mycota*, 173-180.

Kawai, Y., Ono, E., Mizutani, M. (2014) Evolution and diversity of the 2-oxoglutarate-dependent dioxygenase superfamily in plants. *Plant J.* 78, 328-343.

Kay, S. & Bonas, U. (2009) How *Xanthomonas* type III effectors manipulate the host plant. *Curr. Opin.Microbiol*. 12, 1-7.

Kay, S., Hahn, S., Marois, E., Hause, G., Bonas, U. (2007) A bacterial effector acts as a plant transcription factor and induces a cell size regulator. *Science*, 318, 648-651.

Koller, O., Oliveira, R., Nunes, D. S., Soglio, F. D., Panzenhagen, N. V., Sartori, I. A., Manteze, F. (2006) Controle químico do cancro cítrico em plantas jovens sob manejo convencional e orgânico. *Ciênc. Rural*, 36, 1043-1048.

Konishi, M. & Yanagisawa, S. (2015) Transcriptional repression caused by Dof5.8 is involved in proper vein network formation in *Arabidopsis thaliana* leaves. *J. Plant Res.* 128, 643-652.

Krohn, N.M., Yanagisawa, S., Grasser, K.D. (2002) Specificity of the stimulatory interaction between chromosomal HMGB proteins and the transcription factor Dof2 and its negative

regulation by protein kinase CK2-mediated phosphorylation. *J. Biol. Chem*. 277, 32438-32444.

Kubori, T.; Sukhan, A.; Aizawa, S.I.; Galan, J.E. (2000) Molecular characterization and assembly of the needle complex of the Salmonella typhimurium type III protein secretion system. *Proc. Natl. Acad. Sci. U.S.A*. 97, 10225–10230.

Leite, R. J.; Egel, D.; Stall, R. E. (1994) Genetic analysis of hrp-related DNA sequences of *Xanthomonas campestris* strains causing diseases of citrus. *Appl Environ Microbiol.* 60, 1078-1086.

Li, Z., Zou, L., Ye, G., Xiong, L., Ji, Z., Zakria, M., Hong, N., Wang, G., Chen, G. (2014) A potential disease susceptibility gene *CsLOB* of citrus is targeted by a major virulence effector PthA of *Xanthomonas citri* subsp. *citri*. *Mol. Plant.* 7, 912-915.

Mafra, V., Kubo, K.S., Alves-Ferreira, M., Ribeiro-Alves, M., Stuart, R.M., Boava, L.P., Rodrigues, C.M., Machado, M.A. (2012) Reference genes for accurate transcript normalization in citrus genotypes under different experimental conditions. *PLoS ONE*, 7, e31263.

MAPA: Ministério da Agricultura, Pecuária e Abastecimento. Disponível em <http://www.agricultura.gov.br/vegetal/culturas/citrus>. Acesso em 25 de Janeiro de 2016.

Moscou, M. & Bogdanove, A. (2009) A simple cipher governs DNA recognition by TAL effectors. *Science*, 326, 1501.

Neves, M., Trombin, V.G., Milan, P., Lopes, F.F., Cressoni, F., Kalaki, R. (2010) O retrato da citricultura brasileira. Ribeirão Preto: Markestrat.

Oliva, R., Win, J., Raffaele, S., Boutemy, L., Bozkurt, T.O., Chaparro-Garcia, A., Segretin, M.E., Stam, R., Schornack, S., Cano, L.M., van Damme, M., Huitema, E., Thines, M., Banfield, M.J., Kamoun, S. (2010) Recent developments in effector biology of filamentous plant pathogens. *Cell. Microbiol.* 12, 705-715.

Oshiro, E.E., Nepomuceno, R.S.L., Faria, J.B., Ferreira, L.C.S., Ferreira, R.C.C. (2006) Site-direct gene replacement of the phytopathogen *Xanthomonas axonopodis* pv. *citri*. *J. Microbiol. Methods.* 65, 171-179.

Penjor, T., Yamamoto, M., Uehara, M., Ide, M., Matsumoto, N., Matsumoto, R., Nagano, Y. (2013) Phylogenetic relationships of *Citrus* and its relatives based on *matK* gene sequences. *PLoS ONE*, 8(4): e62574.

Pereira, A.L., Carazzolle, M.F., Abe, V.Y., de Oliveira, M.L., Domingues, M.N., Silva, J.C., Cernadas, R.A., Benedetti, C.E. (2014) Identification of putative TAL effector targets of the

citrus canker pathogens shows functional convergence underlying disease development and defense response. *BMC Genomics*. 15, 157.

Pitino, M., Armstrong, C.M., Duan, Y. (2015) Rapid screening for citrus canker resistance employing pathogen-associated molecular pattern-triggered immunity responses. *Horticulture Research*, 2, 15042.

Prates, H.S., Nakano, O., Gravena, S. (1996). Minadora das folhas dos citros *Phyllocnistis citrella*. Comunicado Técnico, 129. Campinas, CATI.

Richter, A., Streubel J., Blücher, C., Szurek, B., Reschke, M., Grau, J., Boch, J. (2014) A TAL effector repeat architecture for frameshift binding. *Nat. Commun*. 11;5:3447.

Römer, P., Hahn, S., Jordan, T., Strauss, T., Bonas, U. and Lahaye, T. (2007) Plant pathogen recognition mediated by promoter activation of the pepper Bs3 resistance gene. *Science*, 318, 645-648.

Ryan, R.P., Vorhölter, F.J., Potnis, N., Jones, J.B., Sluys, M.A.V., Bogdanove, A.J., Dow, M. (2011) Pathogenomics of *Xanthomonas*: understanding bacterium–plant interactions. *Nature*, 9, 344-355.

Schubert, T. & Sun, X. (2003) Bacterial Citrus Canker. *Plant Pathol.* 377, 1-6.

Shiotani, H., Fujikawa, T., Ishihara, H., Tsuyumu, S., Ozaki, K. (2007) A *pthA* homolog from *Xanthomonas axonopodis* pv. *citri* responsible for host-specific suppression of virulence. *J Bacteriol*. 189, 3271-3279.

Shubert, T.S., Rizvi, S.A., Sun. X., Gottwald, T.R., Graham, J.H., Dixon, W.N. (2003) Meeting the challenge of eradicating citrus canker in Florida again. *Plant Dis.* 85, 340-356.

Skerker, J.M., Prasol, M.S., Perchuk, B.S., Biondi, E.G., Laub, M.T. (2005) Two-component signal transduction pathways regulating groeth and cell cycle progression in a bacterium: a system-level analysis. *Plos Biol.* 3(10):e334.

Soprano, A.S., Abe, V.Y., Smetana, J.H., Benedetti, C.E. (2013) Citrus MAF1, a repressor of RNA Pol III, binds the *Xanthomonas citri* canker elicitor PthA4 and suppresses citrus canker development. *Plant Physiol.* 163, 232-242.

Stergiopoulos, I. & De Wit, P. (2009) Fungal effector proteins. *Annu. Rev. Phytopathol*. 47, 233-63.

Sun, H., Wang, L., Zhang, B., Ma, J., Hettenhausen, C., Cao, G., Sun, G., Wu, J., Wu, J. (2014) Scopoletin is a phytoalexin against *Alternaria alternata* in wild tobacco dependent on jasmonate signalling. *J. Exp. Bot*. 65, 4305-4315.

Sun, X., Stall, R.E., Jones, J.B., Cubero, J., Gottwald, T.R., Graham, J.H., Dixon, W.N., Schubert, T.S., Chaloux, P.H., Stromberg, V.K., Lacy, G.H., Sutton, B.D. (2004) Detection

and characterization of a new strain of citrus bacteria from Key/Mexican lime and alemow in South Florida. *Plant Dis.* 88, 1179-1188.

Sun, X., Zhou, D., Kandavelu, P., Zhang, H., Yuan, Q., Wang, B.C., Rose, J., Yan, Y. (2015) Structural insights into substrate specificity of feruloyl-CoA 6'-hydroxylase from *Arabidopsis thaliana*. *Sci. Rep*. 5, 10355.

Sutrias-Grau, M., Bianchi, M.E., Bernue´s, J. (1999) High mobility group protein 1 interacts specifically with the core domain of human TATA box-binding protein and interferes with transcription factor IIB within the pre-initiation complex. *J. Biol. Chem*. 274, 1628–1634.

Swarup, S., De Feyter, R., Brlansky, R.H., Gabriel, D.W. (1991) A pathogenicity locus from *Xanthomonas citri* enables strains from several pathovars of *Xanthomonas campestris* to form cankerlike lesions on citrus. *Phytopathology*, 81, 802-809.

Swarup, S., Yang, Y., Kingsley, M.T., Gabriel, D.W. (1992) An *Xanthomonas citri* pathogenicity gene, *pthA*, pleiotropically encodes gratuitous avirulence on nonhosts. *Mol. Plant-Microbe Interact*. 5, 204-213.

Szurek, B., Rossier, O., Hause, G., Bonas, U. (2002) Type III-dependent translocation of the *Xanthomonas* AvrBs3 protein into the plant cell. *Mol. Microbiol.* 46, 13-23.

Torto, T. A., Li, S. A., Styer, A., Huitema, E., Testa, A., Gow, N. A. R., van West, P., Kamoun, S. (2003) EST mining and functional expression assays identify extracellular effector proteins from the plant pathogen *Phytophthora. Genome Res.* 13, 1675–1685.

Verniere, C., Hartung, J.S., Pruvost, O.P., Civerolo, E.L., Alvarez, A.M., Maestri, P., Luisetti, J. (1998) Characterization of phenotypically distinct strains of *Xanthomonas axonopodis* pv. *citri* from Southwest Asia. *Eur. J. Plant Pathol.* 104, 477-487.

Vialart, G., Hehn, A., Olry, A., Ito, K., Krieger, C., Larbat, R., Paris, C., Shimizu, B., Sugimoto, Y., Mizutani, M., Bourgaud, F. (2012) A 2-oxoglutarate-dependent dioxygenase from *Ruta graveolens* L. exhibits p-coumaroyl CoA 2'-hydroxylase activity (C2'H): a missing step in the synthesis of umbelliferone in plants. *Plant J*. 70, 460–470.

Wilkins, K.E., Booher, N.J., Wang, L., Bogdanove, A.J. (2015) TAL effectors and activation of predicted host targets distinguish Asian from African strains of the rice pathogen *Xanthomonas oryzae* pv. *oryzicola* while strict conservation suggests universal importance of five TAL effectors. *Front. Plant Sci*. 6, 536.

Wu, G.A., Prochnik, S., Jenkins, J., Salse, J., Hellsten, U., Murat, F., Perrier, X., Ruiz, M., Scalabrin, S., Terol, J., Takita, M.A., Labadie, K., Poulain, J., Couloux, A., Jabbari, K., Cattonaro, F., Del Fabbro, C., Pinosio, S., Zuccolo, A., Chapman, J., Grimwood, J., Tadeo, F.R., Estornell, L.H., Muñoz-Sanz, J.V., Ibanez, V., Herrero-Ortega, A., Aleza, P., Pérez-

Pérez, J., Ramón, D., Brunel, D., Luro, F., Chen, C., Farmerie, W.G., Desany, B., Kodira, C., Mohiuddin, M., Harkins, T., Fredrikson, K., Burns, P., Lomsadze, A., Borodovsky, M., Reforgiato, G., Freitas-Astúa, J., Quetier, F., Navarro, L., Roose, M., Wincker, P., Schmutz, J., Morgante, M., Machado, M.A., Talon, M., Jaillon, O., Ollitrault, P., Gmitter, F., Rokhsar, D. (2014) Sequencing of diverse mandarin, pummelo and orange genomes reveals complex history of admixture during citrus domestication. *Nat Biotechnol*. 32, 656-662.

Xu, Q., Chen, L.L., Ruan, X., Chen, D., Zhu, A., Chen, C., Bertrand, D., Jiao, W.B., Hao, B.H., Lyon, M.P., Chen, J., Gao, S., Xing, F., Lan, H., Chang, J.W., Ge, X., Lei, Y., Hu, Q., Miao, Y., Wang, L., Xiao, S., Biswas, M.K., Zeng, W., Guo, F., Cao, H., Yang, X., Xu, X.W., Cheng, Y.J., Xu, J., Liu, J.H., Luo, O.J., Tang, Z., Guo, W.W., Kuang, H., Zhang, H.Y., Roose, M.L., Nagarajan, N., Deng, X.X., Ruan, Y. (2013) The draft genome of sweet orange (*Citrus sinensis*). *Nat Genet*. 45, 59-66.

Xue, J., Luo, D., Xu, D., Zeng, M., Cui, X., Li, L., Huang, H. (2015) CCR1, an enzyme required for lignin biosynthesis in Arabidopsis, mediates cell proliferation exit for leaf development. *Plant J*. 83, 375–387.

Yan, Q. & Wang, N. (2012) High-throughput screening and analysis of genes of *Xanthomonas citri* subsp. *citri* involved in citrus canker symptom development. *Mol. Plant-Microbe Interact.* 25, 69-84.

Yanagisawa, S. (1997) Dof DNA-binding domains of plant transcription factors contribute to multiple protein-protein interactions. *Eur. J. Biochem*. 250, 403-410.

Yang, B. & White, F.F. (2004) Diverse members of the AvrBs3/PthA family of type III effectors are major virulence determinants in bacterial blight disease of rice. *Mol. Plant-Microbe Interact*. 17, 1192-1200.

Yin, C. & Hulbert, S. (2010) Prospects for functional analysis of effectors from cereal rust fungi. *Euphytica.* 179, 57-67.

Zhang, Z.L., Xie, Z., Zou, X., Casaretto, J., Ho, T.D., Shen, Q.J. (2004) A rice WRKY gene encodes a transcriptional repressor of the gibberellin signaling pathway in aleurone cells. *Plant Physiol*. 134, 1500–1513.

Zhou, J., Peng, Z., Long, J., Sosso, D., Liu, B., Eom, J.S., Huang, S., Liu, S., Vera Cruz, C., Frommer, W.B., White, F.F., Yang, B. (2015) Gene targeting by the TAL effector PthXo2 reveals cryptic resistance gene for bacterial blight of rice. *Plant J*. 82, 632-643.

Zhou, R., Jackson, L., Shadle, G., Nakashima, J., Temple, S., Chen, F., Dixon, R.A. (2010) Distinct cinnamoyl CoA reductases involved in parallel routes to lignin in *Medicago truncatula*. *Proc. Natl. Acad. Sci. U.S.A*. 107, 17803-17808.

Zimaro, T.; Thomas, L.; Marondedze, C.; Sgro, G.G.; Garofalo, C.G.; Ficarra, F.A.; Gehring, C.; Ottado, J.; Gottig, N. (2014) The type III protein secretion system contributes to *Xanthomonas citri* subsp. *citri* biofilm formation. *BMC Microbiology*. 14, 1471-2180.

Zipfel, C. & Felix, G. (2005) Plant and animal: a different taste for microbes. *Curr. Opin. Plant Biol.* 8, 353-360.

9. ANEXOS

ANEXO I – Artigo publicado em março de 2016 na revista '*Molecular Plant Pathology*', no qual sou a primeira autora do trabalho. O conteúdo deste artigo corresponde a quase todos os resultados obtidos nesta tese.

Molecular Plant Pathology

MOLECULAR PLANT PATHOLOGY DOI: 10.1111/mpp.12359

Additive roles of PthAs in bacterial growth and pathogenicity associated with nucleotide polymorphisms in effector-binding elements of citrus canker susceptibility genes

VALERIA YUKARI ABE AND CELSO EDUARDO BENEDETTI*

Laboratório Nacional de Biociências, Centro Nacional de Pesquisa em Energia e Materiais, Campinas, SP CP6192, Brazil

SUMMARY

Citrus canker, caused by *Xanthomonas citri*, affects most commercial citrus varieties. All *X. citri* strains possess at least one transcription activator-like effector of the PthA family that activates host disease susceptibility (*S*) genes. The *X. citri* strain 306 encodes four PthA effectors; nevertheless, only PthA4 is known to elicit cankers on citrus. As none of the PthAs act as avirulence factors on citrus, we hypothesized that PthAs 1–3 might also contribute to pathogenicity on certain hosts. Here, we show that, although PthA4 is indispensable for canker formation in six Brazilian citrus varieties, PthAs 1 and 3 contribute to canker development in 'Pera' sweet orange, but not in 'Tahiti' lemon. Deletions in two or more *pthA* genes reduce bacterial growth *in planta* more pronouncedly than single deletions, suggesting an additive role of PthAs in pathogenicity and bacterial fitness. The contribution of PthAs 1 and 3 in canker formation in 'Pera' plants does not correlate with the activation of the canker *S* gene, *LOB1* (*LATERAL ORGAN BOUNDARIES* 1), but with the induction of other PthA targets, including *LOB2* and citrus dioxygenase (*DIOX*). *LOB1*, *LOB2* and *DIOX* show differential PthA-dependent expression between 'Pera' and 'Tahiti' plants that appears to be associated with nucleotide polymorphisms found at or near PthA-binding sites. We also present evidence that *LOB1* activa- tion alone is not sufficient to elicit cankers on citrus, and that *DIOX* acts as a canker *S* gene in 'Pera', but not 'Tahiti', plants. Our results suggest that the activation of multiple *S* genes, such as *LOB1* and *DIOX*, is necessary for full canker development.

Keywords: citrus canker, citrus dioxygenase, *LATERAL ORGAN BOUNDARIES* genes, *pthA*, TAL effectors, *Xanthomonas citri*, *Xanthomonas aurantifolii*.

INTRODUCTION

Citrus canker, caused by strains of *Xanthomonas citri* (also known as *X. citri* ssp. *citri*), is one of the most economically important citrus diseases that not only affects the commercial citrus plantations, but also the citrus markets worldwide (Brunings and Gabriel, 2003; Graham *et al.*, 2004). The *X. citri* 'A' strains (Asiatic group) cause the most severe types of canker and have a broad host range, affecting sweet oranges (*Citrus sinensis*), grapefruits (*Citrus paradisi*) and lemons (*Citrus limon*). However, the citrus canker pathogens *Xanthomonas aurantifolii* (also known as *X. fuscans* ssp. *aurantifolii*) pathotypes 'B' and 'C' have a much narrower range of citrus hosts and are responsible for the 'B' and 'C' types of canker, respectively, which are restricted to some regions of South America (Brunings and Gabriel, 2003; Shubert *et al.*, 2003). In particular, a 'C' strain of *X. aurantifolii*, isolated in Brazil, infects 'Mexican' lime only (*Citrus aurantifolia*) and induces a hypersensitive response (HR) in several citrus hosts, including sweet oranges and lemons (Brunings and Gabriel, 2003; Cernadas *et al.*, 2008; Chiesa *et al.*, 2013).

The disease symptoms caused by *X. citri* and *X. aurantifolii* 'C' are characterized by water-soaked and eruptive lesions on the surface of leaves, twigs and fruits (Brunings and Gabriel, 2003; Cernadas *et al.*, 2008; Shubert *et al.*, 2003). The vigorous growth of the host cells, as a result of infection, causes the epidermis to break open, favouring pathogen spread and disease dissemination (Brunings and Gabriel, 2003; Wichmann and Bergelson, 2004). Although the precise mechanism by which these *Xanthomonas* pathogens induce canker is unknown, it is well known that members of the PthA/AvrBs3 family of transcriptional activator-like (TAL) effectors play a central role in the activation of host genes implicated in cell division and growth (Al-Saadi *et al.*, 2007; Duan *et al.*, 1999; Hu *et al.*, 2014; Pereira *et al.*, 2014; Soprano *et al.*, 2013; Swarup *et al.*, 1992; Yan and Wang, 2012).

TAL effectors function as transcription factors in plant cells. These proteins have a variable DNA-binding domain made up of tandem repeats of 33–34 amino acids that recognizes specific promoter elements of host target genes (Boch and Bonas, 2010). The DNA-binding specificity of TAL effectors is provided primarily by the highly polymorphic residues located at positions 12–13 of the repeats, known as repeat variable diresidues, or RVDs (Boch *et al.*, 2009; Moscou and Bogdanove, 2009). Structural studies have revealed that the DNA-binding domain of TAL effectors folds into a super-helical structure that wraps around the DNA, and that the 13th RVD residue of each repeat makes direct contact with one DNA base in a linear fashion (Deng *et al.*, 2012; Mak

*Correspondence: Email: celso.benedetti@lnbio.cnpem.br

et al., 2012; Murakami *et al*., 2010). Therefore, as distinct RVDs show preferential binding to certain DNA bases, one can predict the DNA-binding sequence or effector-binding element (EBE) of a TAL effector by knowing its RVD composition (Boch *et al*., 2009; Moscou and Bogdanove, 2009).

TAL effectors play critical roles in disease development, acting as major pathogenicity determinants; however, they can also act as avirulence factors through the activation of defence-related genes (Antony *et al*., 2010; Kay *et al*., 2007; Römer *et al*., 2007; Yang *et al*., 2006; Yu *et al*., 2011). Although some PthA variants have been suggested to act as avirulence factors on citrus (Chiesa *et al*., 2013; Shiotani *et al*., 2007), PthAs are generally thought to function as pathogenicity determinants that transactivate the host genes required for disease susceptibility and canker formation (Al-Saadi *et al*., 2007; Cernadas *et al*., 2008; Hu *et al*., 2014; Pereira *et al*., 2014).

The citrus *LATERAL ORGAN BOUNDARIES 1* (*LOB1*) gene is, to our knowledge, the only citrus canker susceptibility (*S*) gene known to date (Hu *et al*., 2014; Li *et al*., 2014; Pereira *et al*., 2014). It was found that certain PthA variants bind specifically to a region of the citrus *LOB1* gene promoter enhancing *LOB1* expression, and that the PthA-dependent expression of *LOB1* correlates with canker symptom development (Hu *et al*., 2014). In addition to *LOB1*, however, several citrus genes implicated in cell division, cell wall remodelling and auxin and gibberellin synthesis and action, including *LOB2*, *LOB3* and *DIOX* (citrus dioxygenase), have been identified as potential direct targets of PthAs (Pereira *et al*., 2014). Nevertheless, the functional role played by these genes in canker elicitation and development remains to be elucidated.

All strains of *X. citri* and *X. aurantifolii* causing hyperplastic lesions on citrus carry at least one PthA variant that activates host *S* genes, including *LOB1* (Al-Saadi *et al*., 2007; Hu *et al*., 2014). For instance, the *X. citri* 'A' strains 306 and 3213 contain four *pthA* genes that encode highly homologous PthA proteins that differ from each other primarily in their DNA-binding domain. Nevertheless, pathogenicity studies have shown that only *pthA4* is necessary and sufficient for canker elicitation on 'Valencia' sweet orange and 'Duncan' grapefruit (Al-Saadi *et al*., 2007; Hu *et al*., 2014; da Silva *et al*., 2002; Yan and Wang, 2012). In addition, none of the PthA proteins from these strains appear to act as avirulence factors on citrus plants (Al-Saadi *et al*., 2007; Yan and Wang, 2012). Therefore, the existence of multiple *pthA* genes in a single bacterial strain suggests that each might contribute to disease development or pathogen fitness on certain hosts. The observation that PthAs form homo- and heterodimers in yeast cells, and that the transient expression of PthA2 or PthA4 in citrus epicotyls induces a similar category of functionally related genes associated with cell division and growth, supports this idea (Domingues *et al*., 2010; Pereira *et al*., 2014). Moreover, in spite of the differences in their RVD composition, transiently expressed PthAs 2 and 4 activate many common targets in citrus epicotyls (Pereira *et al*., 2014).

Here, we present evidence indicating that PthAs from *X. citri* strain 306 have additive roles in canker development and bacterial growth in some citrus hosts, including 'Pera' sweet orange. In addition to PthA4, PthAs 1 and 3 contribute to symptom development in 'Pera' leaves and this correlates with a PthA-dependent activation of citrus *DIOX*, but not *LOB1*. Importantly, we show that, although *LOB1* is regarded as an important citrus canker *S* gene (Hu *et al*., 2014; Li *et al*., 2014; Pereira *et al*., 2014), its induction is not always accompanied by canker formation, indicating that the activation of additional PthA targets is needed for full disease symptoms. In line with this idea, we present evidence suggesting that citrus *DIOX*, which encodes a member of the 2-oxoglutarate/Fe(II)-dependent dioxygenase (2OGD) family, also functions as a canker *S* gene, as psoralen, an inhibitor of this class of enzymes, inhibits canker formation. Furthermore, we found many nucleotide polymorphisms in the citrus *LOB1*, *LOB2* and *DIOX* promoters that overlap with PthA sites, which might explain the differential PthA-dependent expression of these genes in distinct citrus hosts.

RESULTS

Host-dependent contribution of PthAs 1 and 3 to canker formation

Six commercial citrus varieties largely cultivated in Brazil, including the sweet oranges 'Hamlin', 'Valencia', 'Pera', 'Sorocaba' and 'Natal' (Washington Navel), and the 'Tahiti' lemon cultivar, were infiltrated with the single (Δ1, Δ3, Δ4), double (Δ1-3, Δ1-4, Δ3-4) and triple (Δ1-3-4) *pthA*-deletion mutants, and the canker symptoms were compared with those caused by the wild-type bacterium (Figs 1 and 2). In agreement with previous studies (Al-Saadi *et al*., 2007; Hu *et al*., 2014; Soprano *et al*., 2013; Yan and Wang, 2012), we found that *pthA4* is indispensable for canker elicitation, as none of the citrus hosts inoculated with the Δ4 mutant, or with any of the mutants lacking *pthA4*, showed hyperplastic lesions on leaves (Figs 1 and 2). However, a deletion in *pthA1* also caused a substantial reduction in the number of canker pustules in all the sweet orange varieties, particularly in 'Hamlin' and 'Pera', but not in 'Tahiti' lemon (Fig. 1). Similarly, a deletion in *pthA3* reduced the severity of the canker lesions in 'Pera' and, to a lesser extent, in 'Hamlin' and 'Sorocaba', but not in 'Valencia', 'Natal' or 'Tahiti' plants (Fig. 1). Canker lesions were further reduced in most of the hosts inoculated with the Δ1-3 mutant, suggesting that *pthA*s 1 and 3 have additive effects on pustule formation elicited by *pthA4* (Fig. 2). The fact that the Δ1-3-4 mutant did not induce any symptoms

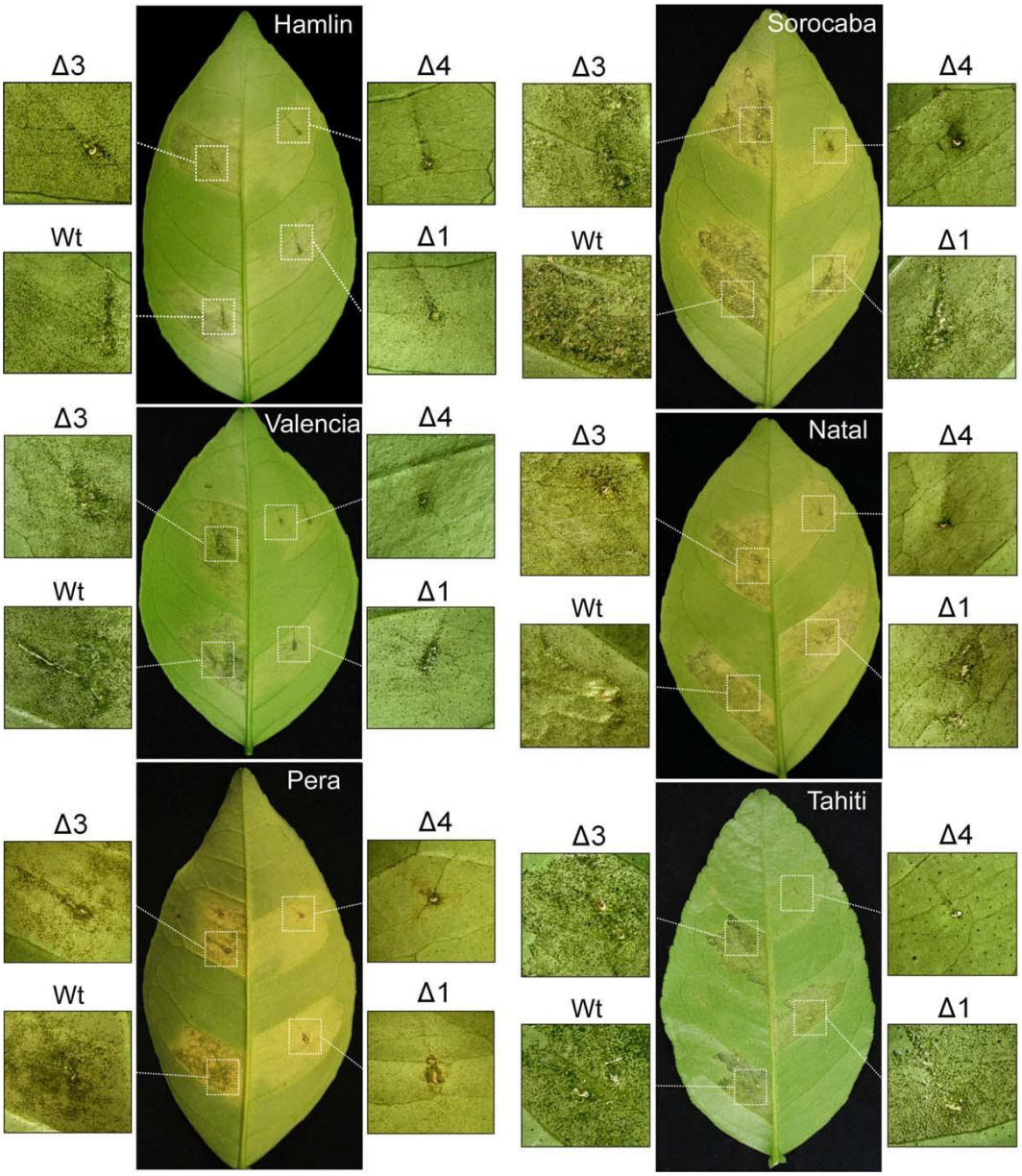

Fig. 1 Host-dependent effect of single *pthA* deletions in canker development. Leaves of the sweet orange varieties 'Hamlin', 'Valencia', 'Natal', 'Pera' and 'Sorocaba', and 'Tahiti' lemon, were infiltrated with bacterial suspensions (10^5 cells/mL) of wild-type (Wt) *Xanthomonas citri* and respective single *pthA*-deletion mutants (Δ1, Δ3, Δ4). Canker symptoms were evaluated 14 days after bacterial inoculation. *pthA4* is essential to elicit cankers in all citrus hosts; nevertheless, *pthA1* also contributes significantly to symptom development in 'Hamlin', 'Valencia' and 'Pera', but not in 'Tahiti' plants. Similarly, a deletion in *pthA3* also reduces canker formation in 'Pera' and, to a lesser extent, in 'Hamlin' and 'Sorocaba', but not in 'Valencia', 'Natal' or 'Tahiti' plants.

in any of the citrus plants tested also suggests that *pthA2* alone is not sufficient to elicit canker on citrus (Fig. 2). Together, these data show that PthAs 1 and 3 contribute to symptom development elicited by PthA4 in certain citrus hosts.

PthAs affect bacterial growth *in planta* in an additive manner

The observation that PthAs 1 and 3 contribute to canker formation, particularly in 'Pera' sweet orange, but not 'Tahiti' lemon,

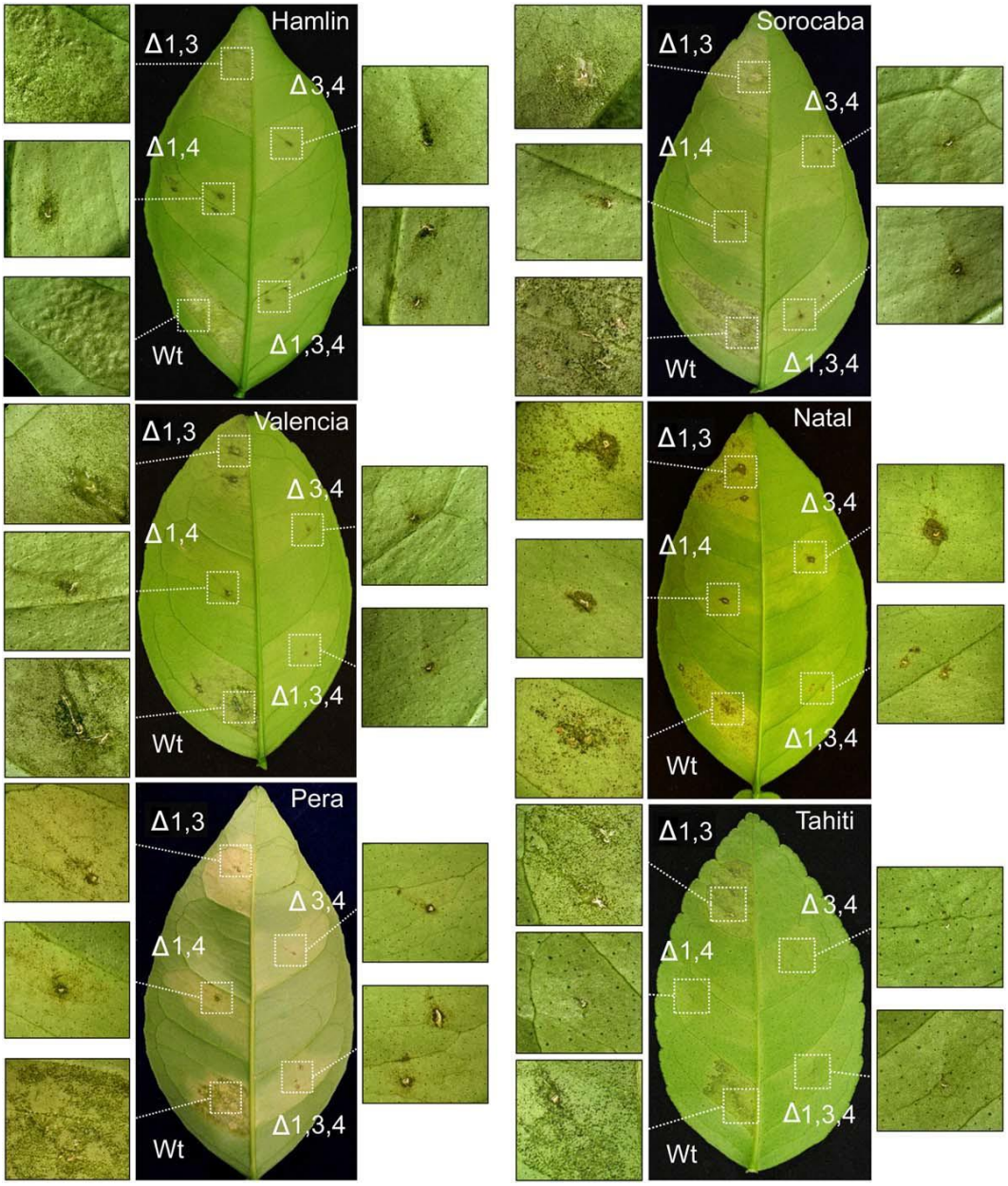

Fig. 2 Host-dependent effect of double and triple *pthA* deletions in canker development. Leaves of 'Hamlin', 'Valencia', 'Natal', 'Pera', 'Sorocaba' and 'Tahiti' plants were infiltrated with bacterial suspensions (10^5 cells/mL) of wild-type (Wt) *Xanthomonas citri* and respective double (Δ1-3, Δ1-4, Δ3-4) and triple (Δ1-3-4) *pthA*-deletion mutants, and canker symptoms were evaluated 14 days after bacterial inoculation. Although a deletion in *pthA4* is sufficient to abolish cankers in all the citrus hosts, an additive effect of *pthA*s 1 and 3 in disease development is noted in 'Pera', 'Natal' and 'Sorocaba' plants.

led us to investigate whether they would also affect bacterial growth *in planta*. To test this, we infiltrated leaves of 'Pera' and 'Tahiti' plants with the *pthA* mutants and followed their growth compared with that of the wild-type bacterium (Fig. 3). We found that all the *pthA* mutations reduced bacterial growth in both 'Pera' and 'Tahiti' leaves at 2 and 14 days post-inoculation (dpi) relative to the wild-type bacterium (Fig. 3). In addition, the double (Δ1-4, Δ3-4) and triple (Δ1-3-4) *pthA*-deletion mutants grew

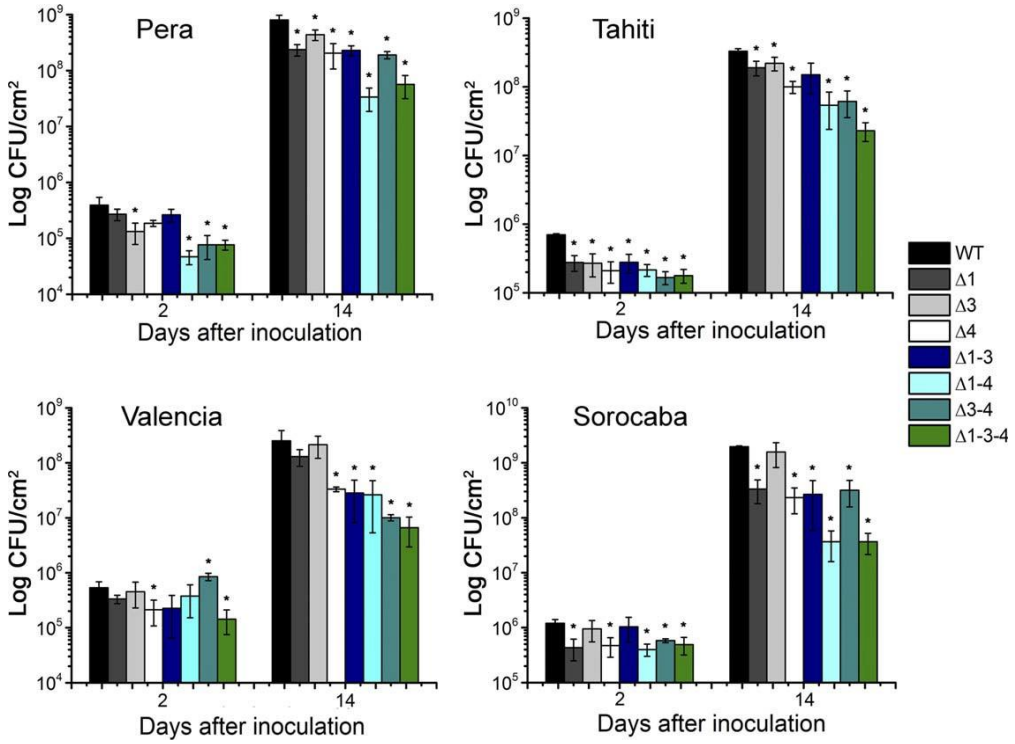

Fig. 3 Additive effect of PthAs on bacterial growth *in planta*. Leaves of sweet orange and lemon plants were infiltrated with bacterial suspensions (10^6 cells/mL) and the growth of wild-type *Xanthomonas citri* (WT) and respective *pthA*-deletion mutants (Δ) was monitored at 2 and 14 days after bacterial inoculation. The double (Δ1-4 and Δ3-4) and triple (Δ1-3-4) *pthA*-deletion mutants grew significantly less well than the respective single mutants and the WT bacteria in all the citrus hosts tested, suggesting an additive effect of PthAs on bacterial growth *in planta*. Bacterial growth, expressed in colony-forming units (CFU)/cm^2 of leaf, is the mean of three biological replicates. The error bars denote standard deviations, whereas the asterisks above the bars indicate statistically significant differences between *X. citri* and mutant-inoculated plants ($P < 0.05$).

significantly less well than the respective single mutants or the wild-type bacterium in these hosts (Fig. 3). Similar results were observed in 'Valencia' and 'Sorocaba' plants (Fig. 3), indicating that PthAs 1, 3 and 4 exert an additive effect on bacterial growth *in planta*. Interestingly, however, although there seems to be a correlation between bacterial growth and the induction of cell hypertrophy, the Δ4 mutant reached bacterial titres higher than 10^8 cells/cm^2 of leaf at 14 dpi in most of the hosts without causing any canker symptoms (Figs 1 and 3). In agreement with these results, Yan and Wang (2012) also reported that a *pthA4* knockout mutant, which only caused chlorosis in grapefruit leaves, reached almost 10^8 bacterial cells/cm^2 of leaf at 4 dpi.

PthA-induced genes are differentially regulated in a host-dependent manner

The evidence that PthAs 1 and 3 have additive effects on canker development elicited by PthA4 in 'Pera' sweet orange, but not 'Tahiti' lemon (Figs 1 and 2), suggested that PthAs 1 and 3 could activate additional canker *S* genes or help to enhance *LOB1* expression in 'Pera' leaves. Thus, in addition to *LOB1*, we evaluated the expression levels of *LOB2*, *LOB3* and *DIOX*, identified previously as putative PthA targets (Pereira *et al*., 2014). We found that *LOB1* expression was significantly reduced in 'Tahiti' leaves infiltrated with each of the single *pthA* mutants, indicating that not only PthA4, but also PthAs 1 and 3, activate *LOB1* transcription in this host (Fig. 4A). However, although PthA4 activates *LOB1* in 'Pera' leaves, confirming previous results (Hu *et al*., 2014; Li *et al*., 2014; Pereira *et al*., 2014), PthA1 seems to repress *LOB1* transcription in this host, as higher *LOB1* expression levels were detected in 'Pera' leaves infiltrated with the Δ1 mutant relative to the wild-type bacterium (Fig. 4A). No significant differences in *LOB1* expression were observed in 'Pera' plants challenged with the Δ3 mutant relative to the wild-type bacterium, suggesting that PthA3 induces *LOB1* transcription only in 'Tahiti' plants (Fig. 4A).

LOB2 (orange1.1g040761m.g) and *LOB3* (orange1.1g 036534m) were also induced by *X. citri* in 'Pera' sweet orange and 'Tahiti' lemon; however, PthAs 1, 3 and 4 do not seem to

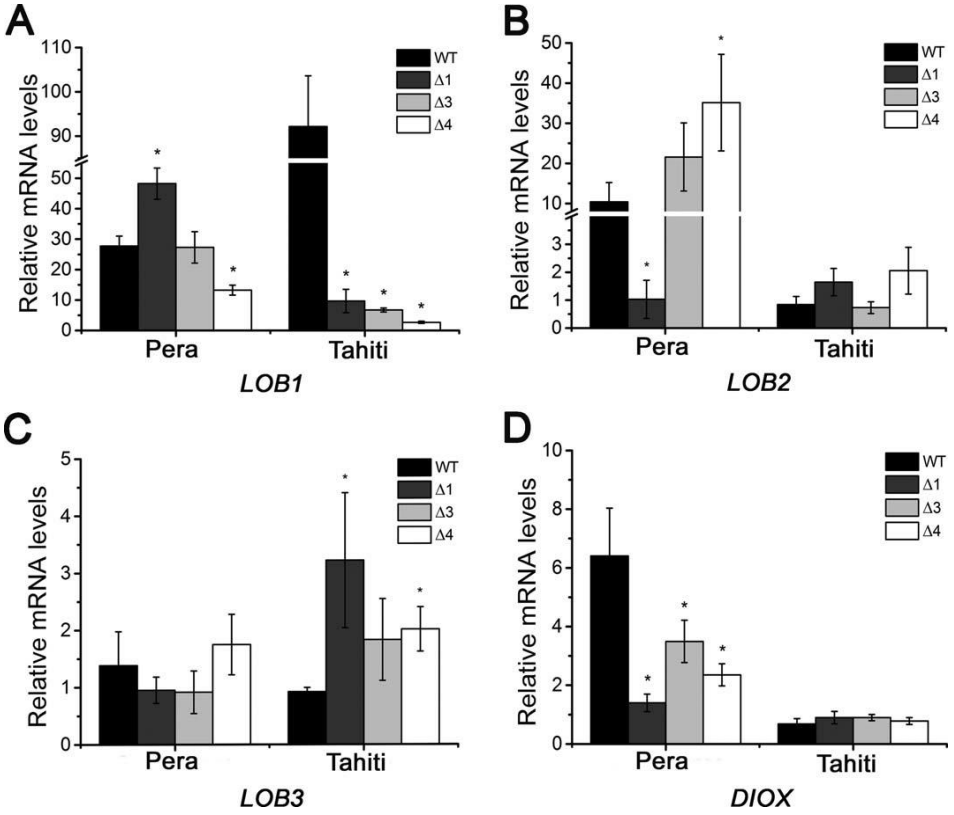

Fig. 4 Differential PthA-dependent induction of *LOB* (*LATERAL ORGAN BOUNDARIES*) and *DIOX* (citrus dioxygenase) genes in sweet orange and lemon plants. Expression levels of *LOB1*, *LOB2*, *LOB3* and *DIOX* in 'Pera' and 'Tahiti' leaves infiltrated with the wild-type (WT) *Xanthomonas citri* or the single *pthA*-deletion mutants (Δ1, Δ3 and Δ4), 72 h post-inoculation. (A) PthAs 1, 3 and 4 are required for *LOB1* induction in lemon, whereas only PthA4 is important for *LOB1* induction in 'Pera' sweet orange. However, PthA1 seems to repress *LOB1* transcription in this host. (B, C) *LOB2* and *LOB3* are induced by *X. citri* in 'Pera' and 'Tahiti' plants; however, PthAs 1, 3 and 4 do not alter significantly *LOB2* expression in 'Tahiti' or *LOB3* expression in 'Pera' plants. *LOB2* expression in 'Pera' sweet orange appears to require PthA1, but not PthA3 or PthA4. (D) The *DIOX* gene is also induced by *X. citri* WT and respective single *pthA* mutants in 'Pera' and 'Tahiti' leaves; however, deletion in *pthA* 1, 3 or 4 significantly reduces *DIOX* expression in 'Pera', but not in 'Tahiti', leaves. The error bars denote standard deviations, whereas the asterisks above the bars indicate statistically significant differences between *X. citri* and mutant-inoculated plants ($P < 0.05$).

influence *LOB2* expression in 'Tahiti' or *LOB3* expression in 'Pera' plants (Fig. 4B,C). *LOB2* expression in sweet orange appears to depend on PthA1, as significantly lower levels of *LOB2* transcripts were detected in 'Pera' leaves in response to the Δ1 mutant relative to the wild-type *X. citri* (Fig. 4B). On the other hand, and contrary to previous observations (Pereira *et al*., 2014), a deletion in *pthA4* enhanced *LOB2* expression in 'Pera' leaves. The slight increase in *LOB3* expression in 'Tahiti' plants infiltrated with the single *pthA* mutants also suggests that PthAs 1, 3 and 4 repress *LOB3* expression in this host (Fig. 4C).

The citrus *DIOX* gene (orange1.1g017949m), identified previously as a potential direct target of PthA4 and PthAw, is highly induced in citrus epicotyls expressing PthA4 (Hu *et al*., 2014; Pereira *et al*., 2014). Therefore, we tested whether PthA1 or PthA3 could also modulate *DIOX* transcription in 'Pera' relative to 'Tahiti' plants. We found that, although *DIOX* is up-regulated by *X. citri* and by the single *pthA* mutants in 'Pera' and 'Tahiti' leaves, deletion in *pthA*s 1, 3 or 4 substantially reduces *DIOX* expression in 'Pera', but not 'Tahiti', leaves (Fig. 4D). These results confirm previous data showing that *DIOX* is induced in response to *X. citri* infection in 'Pera' leaves and that its expression is not altered by PthA2, nor entirely dependent on PthA4, in citrus epicotyls (Pereira *et al*., 2014). Taken together, these results indicate that *LOB2* and *DIOX* might also function as canker *S* genes and that PthAs 1 and 3 contribute to their expression in 'Pera', but not 'Tahiti', plants.

LOB1 induction is not sufficient to elicit canker on citrus

We observed that, in spite of the high levels of *LOB1* induced by the Δ1 and Δ3 mutants in 'Pera' compared with 'Tahiti' leaves,

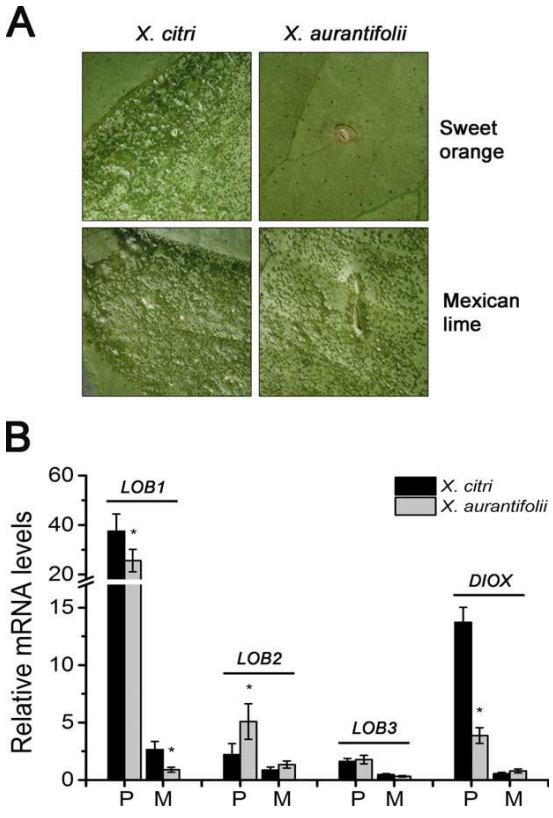

Fig. 5 *LOB1* (*LATERAL ORGAN BOUNDARIES 1*) induction does not always correlate with canker development. (A) Leaves of 'Pera' sweet orange and 'Mexican' lime were infiltrated with *Xanthomonas citri* and *X. aurantifolii* 'C', and canker symptoms were evaluated 14 days after bacterial infiltration (10^6 cells/mL). In contrast with a hypersensitive response (HR) elicited by *X. aurantifolii* 'C' in sweet orange compared with lemon, canker lesions developed in both 'Pera' and 'Mexican' lime inoculated with *X. citri*. (B) Expression levels of *LOB1*, *LOB2*, *LOB3* and *DIOX* (citrus dioxygenase) genes in 'Pera' (P) relative to 'Mexican' lime (M) leaves in response to *X. citri* or *X. aurantifolii* 'C' infection. *LOB1* is weakly induced in the compatible interactions in 'Mexican' lime and highly induced in both the compatible and incompatible interactions in 'Pera'. The expression level of *DIOX*, but not of *LOB1*, *LOB2* or *LOB3*, is significantly reduced in the incompatible interaction between 'Pera' and *X. aurantifolii* 'C'. The error bars denote standard deviations, whereas the asterisks above the bars indicate statistically significant differences between *X. citri*- and *X. aurantifolii*-inoculated plants ($P < 0.05$).

canker pustules developed normally in 'Tahiti', but were reduced in 'Pera' leaves, when challenged with the *pthA1*- and *pthA3*-knockout mutants (Figs 1 and 4A). In addition, although *LOB1* expression decreased by approximately 95% in 'Tahiti' compared with a 50% reduction in 'Pera' leaves infiltrated with the Δ4 mutant, canker lesions did not develop in any of these hosts (Figs 1 and 4A). These results suggest that there is either a threshold of *LOB1* expression necessary to promote canker or that *LOB1* induction alone is not sufficient for canker development in these hosts.

To investigate this idea, we measured the expression levels of *LOB1* in 'Pera' sweet orange and 'Mexican' lime leaves infiltrated with *X. aurantifolii* 'C', in comparison with *X. citri*, as *X. aurantifolii* 'C' causes canker in 'Mexican' lime, but HR in 'Pera' (Fig. 5A) (Cernadas *et al*., 2008). We found, surprisingly, that *LOB1* was weakly induced in the compatible interaction in 'Mexican' lime, and highly induced in both the compatible and incompatible interactions in 'Pera' (Fig. 5B). Therefore, *LOB1* induction does not always correlate with canker development in citrus plants.

We also investigated the expression levels of *LOB2*, *LOB3* and *DIOX* in 'Pera' and 'Mexican' lime leaves in response to *X. citri* or *X. aurantifolii* 'C' infection. Although *LOB2* and *LOB3* expression did not seem to correlate with either canker development or defence response in these hosts, the expression of *DIOX* was substantially reduced in the HR response elicited by *X. aurantifolii* 'C' in 'Pera' leaves (Fig. 5B). Together, these results suggest that *LOB1* induction *per se* is not sufficient for canker formation and that *DIOX* might contribute to disease development.

CsDIOX is structurally related to 2OGDs

The protein encoded by the citrus *DIOX* gene belongs to the 2OGD family of enzymes that use iron and 2-oxoglutarate as cofactors. Members of this family catalyse many different reactions, including hydroxylation, halogenation, demethylation, epimerization, among others (Farrow and Facchini, 2014; Martinez and Hausinger, 2015). In plants, 2OGDs play important roles in the biosynthesis and metabolism of numerous compounds, such as flavonoids, coumarins, glucosinolates, gibberellins, ethylene, auxin and salicylic acid (Farrow and Facchini, 2014).

The citrus DIOX protein (CsDIOX) is closely related to the Arabidopsis and tobacco feruloyl-CoA 6'-hydroxylase 1 (F6'H1), which catalyses the conversion of feruloyl-CoA into 6'-hydroxylferuloyl-CoA during the synthesis of the coumarin scopoletin (Sun *et al*., 2014, 2015). To gain insights into the possible biochemical function and substrate specificity of CsDIOX, we generated a structural model of CsDIOX based on the Arabidopsis AtF6'H1 crystal structure (Sun *et al*., 2015). Our molecular model suggests that CsDIOX is structurally very similar to AtF6'H1 (Fig. 6A). In addition to having the typical protein fold and topology of the 2OGD family, all the amino acid residues responsible for the binding of the iron atom (H234, D236, H292), 2-oxoglutarate (N217, Y219, R302, S304) and substrate feruloyl-CoA (F150, S152, R213, N215, I237, F308) are structurally conserved in the CsDIOX model (Fig. 6B). These observations indicate that CsDIOX is the orthologue of AtF6'H1 (Kai *et al*., 2008; Sun *et al*., 2015) and possibly uses feruloyl-CoA and *p*-coumaroyl-CoA as substrates.

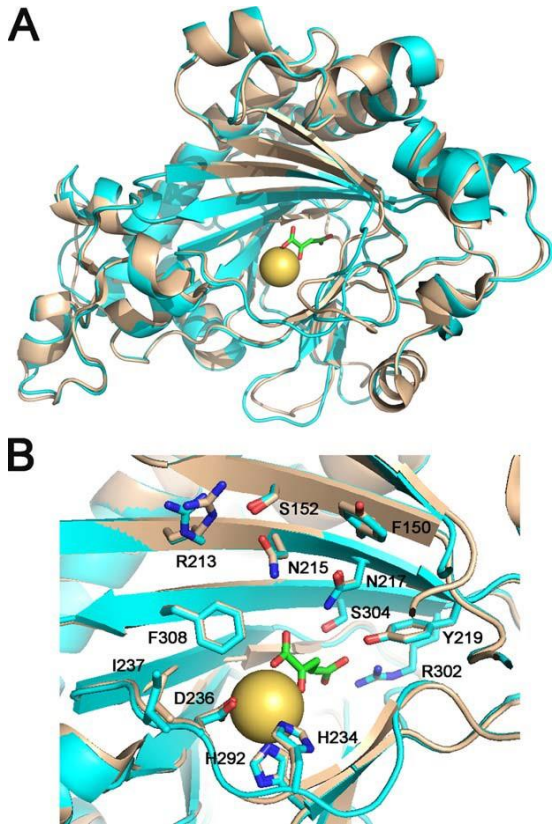

Fig. 6 The citrus DIOX protein (CsDIOX) is structurally related to Arabidopsis feruloyl-CoA 6'-hydroxylase 1 (F6'H1). (A) Superposition of the CsDIOX structural model (cyan) with the Arabidopsis AtF6'H1 crystal structure (sand), depicting the iron atom (yellow) and 2-oxoglutarate (green) (PDB code 4XAE; Sun *et al*., 2015), showing that CsDIOX displays the same folding and topology as AtF6'H1. (B) All of the amino acid residues responsible for the binding of the iron atom (H234, D236, H292), 2-oxoglutarate (N217, Y219, R302, S304) and feruloyl CoA (F150, S152, R213, N215, I237, F308) are structurally conserved in the CsDIOX model.

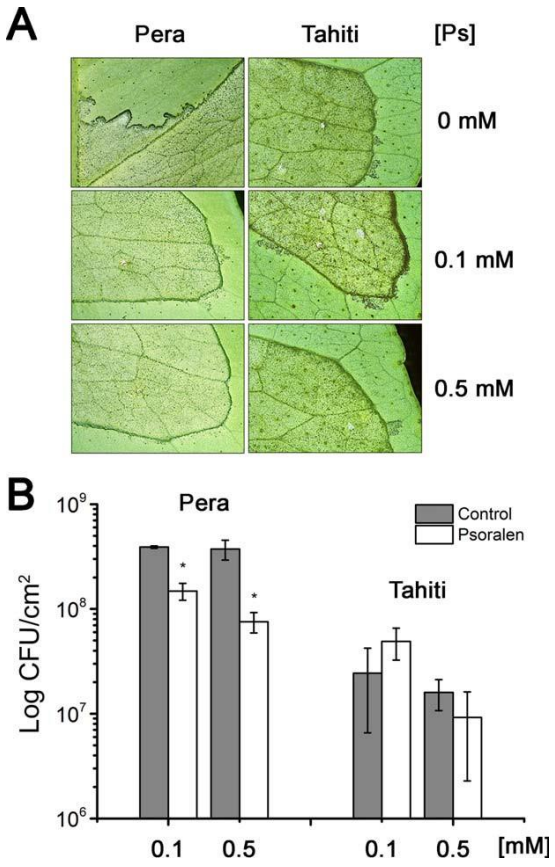

Fig. 7 Psoralen inhibits canker formation in 'Pera' sweet orange. Leaves of 'Pera' sweet orange and 'Tahiti' lemon were infiltrated with a suspension of *Xanthomonas citri* (10^6 cells/mL) in the absence or presence of 0.1 or 0.5 mM psoralen (Ps). Canker symptoms (A) and bacterial counts (B) were evaluated 10 days after bacterial inoculation. Psoralen significantly inhibited canker development and bacterial growth in 'Pera' sweet orange, but not in 'Tahiti' lemon. Bacterial growth, expressed in colony-forming units (CFU)/cm^2 of leaf, is the mean of three biological replicates. The error bars denote standard deviations, whereas the asterisks above the bars indicate statistically significant differences between means ($P < 0.05$).

Psoralen inhibits canker formation in 'Pera' sweet orange

CsDIOX is also 82% identical to the *Ruta graveolens* 2OGD, which converts feruloyl-CoA into scopoletin and *p*-coumaroyl-CoA into 2,4-dihydroxycinnamic acid (Vialart *et al*., 2012). As the results shown in Figs 4D and 5B suggest that *DIOX* could play a role in canker development, and psoralen, a furanocoumarin, inhibits the *p*-coumaroyl- and feruloyl-CoA hydroxylase activities of *R. graveolens* 2OGD at concentrations of 50–200 μM (Vialart *et al*., 2012), we tested the effect of 0.1 and 0.5 mM psoralen on *X. citri* growth and disease development. Notably, we found that psoralen inhibited canker formation and the growth of *X. citri* in a dose-dependent manner in leaves of 'Pera' sweet orange, but not 'Tahiti' lemon (Fig. 7), where the expression of *DIOX* was not dependent on PthAs or significantly induced in response to *X. citri* infection (Fig. 4D). Taken together, these results suggest that citrus *DIOX* acts as a canker *S* gene in 'Pera' sweet orange.

Promoters of *LOB1*, *LOB2* and *DIOX* show polymorphisms at PthA sites

The differential PthA-dependent expression of *LOB1*, *LOB2* and *DIOX* genes observed between 'Pera' and 'Tahiti' plants suggests the existence of nucleotide polymorphisms at effector-binding sites. Thus, we sequenced the promoter regions of these genes amplified from 'Pera' and 'Tahiti' plants and compared them with

those of the published genomes of *C. sinensis* 'Valencia' and *C. clementina* 'Clemenules' (Wu *et al*., 2014; Xu *et al*., 2013).

In the *LOB1* promoter, we found a single nucleotide change (C/T) and a single nucleotide deletion (G/–) flanking the characterized PthA4-binding site (Hu *et al*., 2014; Pereira *et al*., 2014) among the 'Tahiti', 'Valencia', 'Pera' and 'Clemenules' promoters (Fig. 8A). We also found an 11-nucleotide deletion 25 bp downstream of the PthA4 site in the 'Tahiti' relative to the 'Pera', 'Valencia' or 'Clemenules' promoters. In addition to the PthA4 site, we found putative PthA1 and PthA3 sites located 667 and 498 bp upstream of the ATG, respectively, both carrying single nucleotide polymorphisms (SNPs) between the 'Pera' (A/C) and 'Tahiti' (A/C) promoters (Fig. 8A).

The *LOB2* promoter also seems to cluster multiple PthA sites. In addition to the PthA2 site identified previously (Pereira *et al*., 2014), which overlaps with the predicted TATA box element, we found additional PthA1, PthA2 and PthA3 sites which also present nucleotide deletions or SNPs between the 'Pera' and 'Tahiti' sequences (Fig. 8B).

Despite many efforts, the *DIOX* promoter could not be amplified from several 'Pera' individuals, even though we tested six distinct pairs of oligos derived from the 'Valencia' genome (Table S1, see Supporting Information) in multiple polymerase chain reaction (PCRs). This suggests that this genomic region is highly polymorphic. Indeed, when we compared the sequence of the *DIOX* promoter obtained from 'Tahiti' plants with those of 'Valencia' and 'Clemenules', we found nucleotide insertions ranging from 150 to 1230 bp located at approximately 270 bp upstream of the ATG (not shown). Thus, the ~260-bp sequence of the 'Tahiti' promoter was aligned with the corresponding sequences of the 'Valencia' and 'Clemenules' promoters (Fig. 8C). In addition to the PthA4 site described previously (Pereira *et al*., 2014), we found a PthA2 site that also shows an SNP between the 'Tahiti' and 'Valencia' or 'Clemenules' promoters (Fig. 8C). Moreover, as observed in the *LOB1* promoter, there is a 14-bp deletion flanking the PthA4 site in the 'Tahiti' relative to the 'Valencia' or 'Clemenules' promoters (Fig. 8C). According to the PlantPAN 2.0 algorithm (Chang *et al*., 2008), this deletion comprise a 'TGAC' core-containing W box which is bound by WRKY factors that control pathogenesis-related and gibberellin response genes (Eulgem *et al*., 1999; Zhang *et al*., 2004).

In addition to the predicted W box found in the *DIOX* promoter, a PlantPAN 2.0 search identified several putative transcription factor-binding sites in the *LOB1*, *LOB2* and *DIOX* promoters. One particular factor, Dof, attracted our attention, because Dof sites were found near PthA sites in all three promoters (Fig. 8). Most notably, in the *DIOX* promoter, two inverted Dof sites form a palindrome located 28 bp downstream of the PthA4 site (Fig. 8C). We also observed single nucleotide changes or deletions near or at the Dof sites between the sweet orange and lemon sequences (Fig. 8). Together, these results indicate that the differential PthA-dependent expression of *LOB1*, *LOB2* and *DIOX* observed between 'Pera' and 'Tahiti' plants might be influenced by the polymorphisms found at the PthA sites, and that WRKY and Dof factors might play an important role in the transcriptional regulation of these genes.

DISCUSSION

Although many *Xanthomonas* pathogens, including *X. citri* and *X. oryzae*, carry multiple TAL effector genes, the precise role or contribution of each of these effectors to pathogenicity is poorly understood, as only a few have been shown to act as major virulence factors (Al-Saadi *et al*., 2007; Wilkins *et al*., 2015; Yang and White, 2004). In the case of *X. citri* strain 306, which carries four PthA effectors, only PthA4 is known to play a fundamental role in canker elicitation, whereas none seem to act as avirulence factors on citrus (Al-Saadi *et al*., 2007; Hu *et al*., 2014; da Silva *et al*., 2002; Yan and Wang, 2012).

In this study, we have shown that, although PthA4 is indispensable for canker formation in all citrus varieties tested, corroborating literature data (Al-Saadi *et al*., 2007; Hu *et al*., 2014; Soprano *et al*., 2013; Yan and Wang, 2012), PthAs 1 and 3 also contribute to disease symptom development and bacterial growth in some citrus hosts, including 'Pera' sweet orange. These results indicate that TAL effectors of *X. citri* have a host-dependent additive or complementary role in pathogenicity, and suggest that PthAs 1 and 3 potentiate the role played by PthA4 in canker elicitation. This idea is consistent with the fact that PthAs 1 and 3 are not required for *LOB1* induction in 'Pera' plants, but for the activation of other targets, including *LOB2* and *DIOX*. Importantly, we show that *LOB1* induction by *X. citri* does not always correlate with canker formation. The expression of *LOB1* is, for instance, drastically reduced in 'Tahiti' leaves infiltrated with the *pthA*-deletion mutants (Fig. 4A), although canker lesions develop normally in this host relative to 'Pera' sweet orange (Figs 1 and 2). Conversely, *LOB1* is strongly up-regulated during the incompatible interaction between *X. aurantifolii* 'C' and 'Pera' plants (Fig. 5). These data indicate that *LOB1* induction *per se* is not sufficient for canker elicitation, which is in agreement with the observation that the transient overexpression of *LOB1* in transgenic citrus does not result in the formation of canker pustules (Hu *et al*., 2014). Therefore, although *LOB1* appears to directly up-regulate many cell wall-remodelling genes which are also induced by PthA4 during canker development (Hu *et al*., 2014), it is unlikely that *LOB1* activation alone would trigger the whole process of canker formation.

In line with this idea, we present evidence suggesting that citrus *DIOX*, identified as a PthA4 target in two independent studies (Hu *et al*., 2014; Pereira *et al*., 2014), might also play an important role in canker development. The expression of *DIOX* is dependent on PthAs 1, 3 and 4 in 'Pera' sweet orange, but not in 'Tahiti'

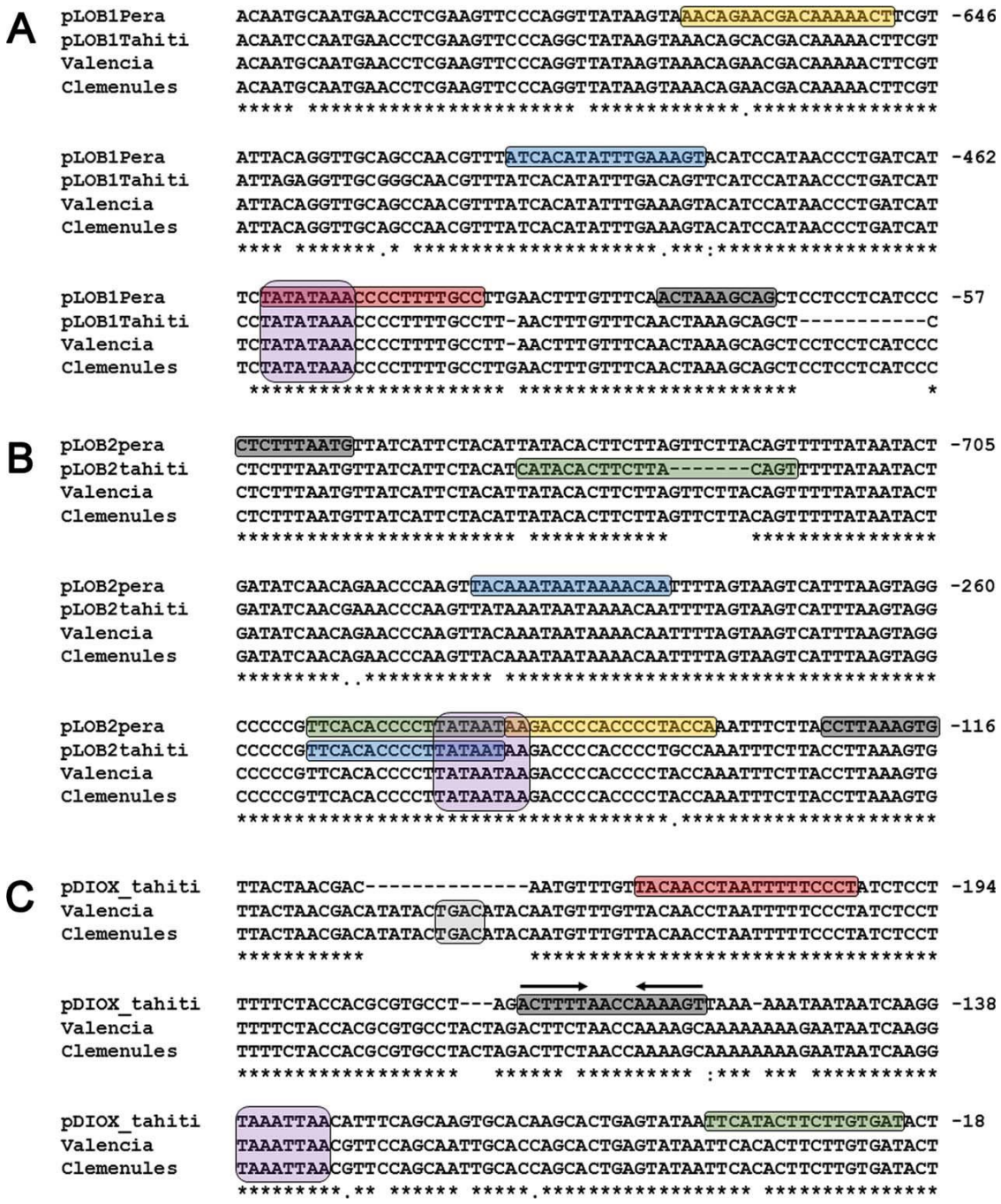

Fig. 8 Promoters of *LOB1* (*LATERAL ORGAN BOUNDARIES 1*), *LOB2* and *DIOX* (citrus dioxygenase) genes show nucleotide polymorphisms at PthA sites. The promoter regions of the citrus *LOB1* (A), *LOB2* (B) and *DIOX* (C) genes were amplified from 'Pera' and 'Tahiti' plants and compared with those of the *Citrus sinensis* 'Valencia' and *C. clementine* 'Clemenules' cultivars (Wu *et al*., 2014; Xu *et al*., 2013). The predicted PthA1-, PthA2-, PthA3- and PthA4-binding sites are boxed in yellow, green, blue and red, respectively. The Dof- and WRKY-binding sites are coloured in grey and light grey, respectively, whereas the TATA box elements are in purple. Arrows in (C) represent a Dof palindromic sequence. Most of the single nucleotide polymorphisms (SNPs) found in 'Pera' relative to 'Tahiti' plants are also present in 'Valencia' and 'Clemenules' cultivars.

lemon (Fig. 4D). In addition, psoralen, an inhibitor of 2OGD (Vialart *et al*., 2012), significantly attenuates canker formation and bacterial growth in 'Pera', but not 'Tahiti', plants (Fig. 7). Although the biological function and substrate specificity of CsDIOX have not yet been demonstrated, our molecular modelling studies strongly suggest that CsDIOX is the orthologue of the Arabidopsis and *R. graveolens* F6'H1 enzymes (Fig. 6), and can thus catalyse the *ortho*-hydroxylation of feruloyl-CoA and/or *p*-coumaroyl-CoA (Kai *et al*., 2008; Sun *et al*., 2015; Vialart *et al*., 2012). The question that arises is therefore how the CsDIOX activity could lead or contribute to citrus canker development in 'Pera' sweet orange.

One possible mechanism might involve the action of cinnamoyl-CoA reductases (CCRs), which convert cinnamoyl-CoA esters, including feruloyl-CoA, *p*-coumaroyl-CoA and caffeoyl-CoA, into their corresponding cinnamyl aldehydes during the synthesis of lignin monomers (Xue *et al*., 2015; Zhou *et al*., 2010). It has been shown that the Arabidopsis CCR1 enzyme mediates the cell proliferation exit for leaf development and that the *ccr1* mutant exhibits increased cell proliferation and high levels of ferulic acid (Xue *et al*., 2015). Because CCR1 preferentially uses feruloyl-CoA as substrate, it is possible that 6-hydroxylferuloyl-CoA, the product of the CsDIOX reaction, inhibits the activity of CCR1, leading to a cell proliferation response similar to that of the loss of CCR1 (Xue *et al*., 2015; Zhou *et al*., 2010). Moreover, the role of CCR1 proteins in lignin biosynthesis and cell division is also linked to the activities of caffeic acid *O*-methyltransferases (COMTs) and caffeoyl-CoA 3-*O*-methyltransferases (CCOAOMTs), which provide the substrates for CCR1 (Xue *et al*., 2015; Zhou *et al*., 2010). Inhibition of COMT and CCOAOMT in Arabidopsis results in low levels of ferulic acid and decreased cell division (Xue *et al*., 2015). As ferulic acid itself induces cell proliferation in Arabidopsis, it would be interesting to investigate whether 6-hydroxylferulic acid can also stimulate cell division during canker formation.

It is also notable that many *COMT*, *CCOAOMT* and *CCR* genes are preferentially up-regulated by *X. aurantifolii* 'C' during its incompatible interaction in 'Pera' sweet orange (Cernadas *et al*., 2008). We initially interpreted this pattern of *COMT*, *CCOAOMT* and *CCR* gene induction as part of the *X. aurantifolii*-elicited HR, in which increased lignin biosynthesis reinforces the plant cell wall to restrict pathogen attack (Cernadas *et al*., 2008). However, in the light of the data reported by Xue *et al*. (2015), it is possible that the citrus *COMT*, *CCOAOMT* and *CCR* pathway also helps to restrict cell division during canker formation. The fact that the citrus *DIOX* gene is induced in 'Pera' leaves at much lower levels by *X. aurantifolii* 'C' relative to *X. citri* (Fig. 5B) is consistent with the idea that *DIOX* plays an opposing role in the *COMT*, *CCOAOMT* and *CCR* pathway. Moreover, the observation that PthA4 up-regulates a second *F6'H1* gene (XP_006488907.1) and that EBEs for PthAs are found in a number of citrus *DIOX*-related 2OGD genes (Pereira *et al*., 2014) also suggests that this lignin biosynthetic pathway is differentially modulated by *X. citri*, leading to cell hyperplasia.

The differential PthA-dependent expression of *LOB1*, *LOB2* and *DIOX* observed between 'Pera' sweet orange and 'Tahiti' lemon plants is not only associated with the presence or absence of specific PthA sites in the promoters of these genes, but also with the occurrence of SNPs or nucleotide deletions found adjacent to or within such PthA sites (Fig. 8). A single nucleotide deletion in the *X. oryzae* PthXo2 EBE in the rice bacterial blight *S* gene *Xa25* (*OsSWEET13*) is, for instance, sufficient to abrogate effector-associated gene activation (Zhou *et al*., 2015). In another rice bacterial blight *S* gene, *OsSWEET14*, an 18-bp deletion within the binding sites targeted by several TAL effectors also confers resistance against many *X. oryzae* strains of various geographical origins (Hutin *et al*., 2015). Therefore, the presence of nucleotide polymorphisms at PthA sites is strong evidence of a host adaptation to evade effector target recognition.

Near the PthA sites, we also found several putative Dof sites in the *LOB1*, *LOB2* and *DIOX* promoters. Dof factors control the transcription of many plant genes. In Arabidopsis, Dof5.8 represses the auxin response, leading to impaired vein formation in leaves (Konishi and Yanagisawa, 2015), whereas DAG1 negatively regulates the gibberellin biosynthetic gene *AtGA3ox1*, which encodes a CsDIOX-related 2OGD (Gabriele *et al*., 2010). In maize, Dof factors interact with HMGB (high-mobility group B) proteins, which facilitate Dof binding to naked DNA or to nucleosomes (Cavalar *et al*., 2003; Grasser *et al*., 2007; Krohn *et al*., 2002; Yanagisawa, 1997).

The interaction between Dof and HMGBs is of particular note, as all PthAs from strain 306 interact with the citrus HMGB1 protein (de Souza *et al*., 2012). Mammalian HMGB1 interacts with the TATA-binding protein (TBP) to repress transcription, whereas transcription factor TFIIA binds TBP to disrupt the HMGB/TBP complex and activate transcription (Das and Scovell, 2001; Dasgupta and Scovell, 2003; Sutrias-Grau *et al*., 1999). Considering that Dof factors act as transcription repressors and that PthAs bind at or close to TATA box elements of citrus promoters, it is possible that, similar to TFIIA, PthAs could displace Dof/HMGB or alter the recruitment of factors at TBP sites to promote transcription initiation.

EXPERIMENTAL PROCEDURES

Bacterial strains and growth conditions

Escherichia coli DH5α cells were grown in Luria–Bertani (LB) medium at 37 °C for 16 h, whereas *X. citri* strain 306 (da Silva *et al*., 2002) and *X. aurantifolii* 'C' strain ICMP 8435 (Cernadas *et al*., 2008) were grown in LB medium without NaCl (LBON) at 28 °C for 48 h. When required, ampicillin

(100 μg/mL) and/or kanamycin (50 μg/mL) were added to the growth medium.

Construction of *pthA*-deletion mutants

The single (Δ1, Δ3), double (Δ1-3, Δ1-4, Δ3-4) and triple (Δ1-3-4) *pthA*-knockout mutants of *X. citri* were obtained by homologous recombination following the same procedure as used to obtain the *pthA4*-deletion mutant (Δ4), described previously (Soprano *et al*., 2013). To generate the Δ1 and Δ3 mutants, DNA fragments of ~1.0 kb, flanking the coding regions of *pthA1* and *pthA3*, were amplified using the pairs of oligos PthA1F1/PthANR1 and PthANF2/PthA1R2, and PthA3F1/PthANR1 and PthANF2/PthA3R2, respectively (Table S1 and Fig. 1A). The PCR fragments corresponding to the upstream and downstream regions of each *pthA* gene were ligated through the *Nde*I sites and cloned into the *Hind*III and *Eco*RI sites of the suicide vector pNPTS138 to create an in-frame deletion (Andrade *et al*., 2014). The constructs were verified by DNA sequencing and used to transform *X. citri* cells by electroporation. Bacterial colonies were selected on LBON plates supplemented with ampicillin and kanamycin, or with ampicillin and 5% sucrose. Kanamycin-sensitive colonies that grew in the presence of sucrose were selected and PCR tested for the absence of *pthA* genes after two recombination events (Fig. S1B, see Supporting Information). Despite many efforts, we were unable to select a *pthA2*-deletion mutant. To confirm the *pthA1* and *pthA3* knockouts, the DNA fragments encompassing the deleted loci were amplified with oligos PthA1F1/PthA1R2 and PthA3F1/PthA3R2, respectively, and sequenced with oligo seqPthANF, which covers the in-frame deletion regions (Table S1 and Fig. S1A, C).

The double (Δ1-3, Δ1-4, Δ3-4) and triple (Δ1-3-4) *pthA*-deletion mutants were generated using the single mutants in successive rounds of deletion. The double and triple *pthA* mutants were also confirmed by PCR analysis and DNA sequencing (Fig. S1B).

Plant growth and bacterial inoculations

The sweet orange ('Pera', 'Valencia', 'Hamlin', 'Sorocaba' and 'Natal') and lemon ('Tahiti' and 'Mexican' lime) varieties were obtained from certified nurseries as 'pathogen free' and maintained in glasshouse conditions. Leaves were infiltrated with water suspensions of 10^5 or 10^6 cells/mL of *X. citri*, *X. aurantifolii* 'C' or the *pthA*-deletion mutants, previously grown on LBON plates for 48 h at 28 °C. The wild-type bacteria and corresponding *pthA*-deletion mutants were infiltrated in nine distinct leaves from three independent plants of the same citrus variety. The inoculated plants were monitored daily for the appearance of canker symptoms.

Bacterial growth analysis

The growth of *X. citri* and *pthA*-deletion mutants in leaf tissues was evaluated as described previously (Cernadas *et al*., 2008). Discs of leaf sectors infiltrated with approximately 10^6 bacterial cells were removed at 2 and 14 days after bacterial inoculation and ground in 1 mL of sterile water. Serial dilutions of the bacterial suspensions were plated on LBON supplemented with ampicillin, and bacterial colonies were counted from three independent leaf extractions. The experiment was repeated three times and statistically significant differences between treatments (*X. citri* vs. mutant-inoculated plants) were calculated using Student's *t*-test with $P < 0.05$.

Plant RNA extraction and reverse transcription-quantitative polymerase chain reaction (RT-qPCR) analysis

Total RNA extraction and RT-qPCR analyses were conducted as described previously (Pereira *et al*., 2014). The oligonucleotides used as primers were designed using Applied Biosystems (Foster City, CA, USA) Primer Express 2.0 software (Table S1). PCR amplifications were carried out using the 7500 system 'Universal' cycle condition in an ABI Prism 7300 instrument (Applied Biosystems), and the gene encoding citrus actin was used as internal control for normalization (Mafra *et al*., 2012). Total RNAs from three different leaves were used in the PCRs as independent biological replicates, and three technical replicates for each biological sample were considered for statistical two-tailed Student's *t*-test to compare the changes in gene expression between treatments. The relative gene expression levels among samples were determined using 7000 System SDS software (Applied Biosystems) with default parameters.

Psoralen treatment

Leaves of 'Pera' sweet orange and 'Tahiti' lemon were infiltrated with a water suspension of *X. citri* (10^6 cells/mL) in the absence or presence of psoralen. Psoralen at 50 mM was dissolved in 100% ethanol and added to the bacterial cell suspensions at 0.1 and 0.5 mM final concentrations. Ethanol was also added to the bacterial cell suspensions at 0.2% or 1.0% final concentrations to serve as controls for psoralen treatments. Psoralen or ethanol at the concentrations used did not affect the growth of *X. citri* in culture medium (not shown). To maintain the active pools of the inhibitor, psoralen or ethanol was infiltrated into the inoculated leaf sectors on the third and sixth days of bacterial inoculation. The experiment was performed using nine infiltrated leaves from three plants of each citrus cultivar. Canker symptoms and bacterial counts were evaluated at 10 days after bacterial infiltration. Statistically significant differences between treatments were calculated using Student's *t*-test with $P < 0.05$.

Cloning and sequencing of promoter regions of citrus genes

Genomic DNA of 'Pera' sweet orange and 'Tahiti' lemon was extracted from leaves using the cetyltrimethylammonium bromide (CTAB) method (Doyle and Doyle, 1987). The quality and quantity of DNA were verified by gel electrophoresis and UV spectroscopy. The promoter regions of *LOB1*, *LOB2* and *DIOX* were amplified by PCR using 1.0 μg of genomic DNA, 125 nM of each primer and Platinum Taq, following the recommendations of the manufacturer (Thermo Fisher Scientific Inc., Waltham, MA). The oligonucleotides used as primers for *LOB1*, *LOB2* and *DIOX* (Table S1) were designed based on the DNA sequences of the citrus genomes (Wu *et al*., 2014; Xu *et al*., 2013). After amplification (1 × 94 °C for 4 min, followed by 35 × 94 °C for 30 s, 55 °C for 30 s and 72 °C for 70 s), the PCR fragments were cloned into the pGEM T-Easy vector (Promega, Madison, WI, USA) and sequenced. The promoter sequences were aligned using CLUSTAL Omega software at http://www.ebi.ac.uk/Tools/msa/clustalo/.

Molecular modelling studies

The three-dimensional structural model of CsDIOX was generated with the SWISS-MODEL server at http://swissmodel.expasy.org/, applying default parameters and using the *Arabidopsis thaliana* AtF6′H1 crystal structure (PDB code 4XAE; Sun *et al*., 2015) as the search model. Structural alignments of the CsDIOX model with AtF6^{0}H1 were performed with PyMOL (DeLano, 2002).

ACKNOWLEDGEMENTS

This work was supported by the São Paulo Research Foundation (FAPESP Grants 2011/20468-1 and 2011/19988-0) and Conselho Nacional de Desenvolvimento Científico e Tecnológico (CNPq Grant 300937/2012-1).

REFERENCES

Al-Saadi, A., Reddy, J., Duan, Y., Brunings, A., Yuan, Q. and Gabriel, D. (2007) All five host-range variants of *Xanthomonas citri* carry one *pthA* homolog with 17.5 repeats that determines pathogenicity on citrus, but none determine host-range variation. *Mol. Plant–Microbe Interact.* 20, 934–943.

Andrade, M.O., Farah, C.S. and Wang, N. (2014) The post-transcriptional regulator *rsmA/csrA* activates T3SS by stabilizing the 59 UTR of *hrpG*, the master regulator of *hrp/hrc* genes, in *Xanthomonas*. *PLoS Pathog.* 10, e1003945.

Antony, G., Zhou, J., Huang, S., Li, T., Liu, B., White, F. and Yang, B. (2010) Rice *xa13* recessive resistance to bacterial blight is defeated by induction of the disease susceptibility gene Os-11N3. *Plant Cell*, 22, 3864–3876.

Boch, J. and Bonas, U. (2010) *Xanthomonas* AvrBs3 family-type III effectors: discovery and function. *Annu. Rev. Phytopathol.* 48, 419–436.

Boch, J., Scholze, H., Schornack, S., Landgraf, A., Hahn, S., Kay, S., Lahaye, T., Nickstadt, A. and Bonas, U. (2009) Breaking the code of DNA binding specificity of TAL-type III effectors. *Science*, 326, 1509–1512.

Brunings, A.M. and Gabriel, D.W. (2003) *Xanthomonas citri*: breaking the surface. *Mol. Plant Pathol.* 4, 141–157.

Cavalar, M., Möller, C., Offermann, S., Krohn, N.M., Grasser, K.D. and Peterhänsel, C. (2003) The interaction of DOF transcription factors with nucleosomes depends on the positioning of the binding site and is facilitated by maize HMGB5. *Biochemistry*, 42, 2149–2157.

Cernadas, R.A., Camillo, L.R. and Benedetti, C.E. (2008) Transcriptional analysis of the sweet orange interaction with the citrus canker pathogens *Xanthomonas axonopodis* pv. *citri* and *Xanthomonas axonopodis* pv. *aurantifolii*. *Mol. Plant Pathol.* 9, 609–631.

Chang, W.C., Lee, T.Y., Huang, H.D., Huang, H.Y. and Pan, R.L. (2008) PlantPAN: Plant Promoter Analysis Navigator, for identifying combinatorial cis-regulatory elements with distance constraint in plant gene group. *BMC Genomics*, 9, 561.

Chiesa, M.A., Siciliano, M.F., Ornella, L., Roeschlin, R.A., Favaro, M.A., Delgado, N.P., Sendín, L.N., Orce, I.G., Ploper, L.D., Vojnov, A.A., Vacas, J.G., Filippone, M.P., Castagnaro, A.P. and Marano, M.R. (2013) Characterization of a variant of *Xanthomonas citri* subsp. *citri* that triggers a host-specific defense response. *Phytopathology*, 103, 555–564.

Das, D. and Scovell, W.M. (2001) The binding interaction of HMG-1 with the TATA-binding protein/TATA complex. *J. Biol. Chem.* 276, 32 597–32 605.

Dasgupta, A. and Scovell, W.M. (2003) TFIIA abrogates the effects of inhibition by HMGB1 but not E1A during the early stages of assembly of the transcriptional preinitiation complex. *Biochim. Biophys. Acta*, 1627, 101–110.

DeLano, W.L. (2002) *The PyMOL Molecular Graphics System*. San Carlos, CA: DeLano Scientific.

Deng, D., Yan, C., Pan, X., Mahfouz, M., Wang, J., Zhu, J.K., Shi, Y. and Yan, N. (2012) Structural basis for sequence-specific recognition of DNA by TAL effectors. *Science*, 335, 720–723.

Domingues, M.N., Souza, T.A., Cernadas, R.A., de Oliveira, M.L.P., Docena, C., Farah, C.S. and Benedetti, C.E. (2010) The *Xanthomonas citri* effector protein PthA interacts with citrus proteins involved in nuclear transport, protein folding and ubiquitination associated with DNA repair. *Mol. Plant Pathol.* 11, 663–675.

Doyle, J.J. and Doyle, J.L. (1987) A rapid isolation procedure for small quantities of fresh leaf tissue. *Phytochem. Bull.* 19, 11–15.

Duan, Y., Castañeda, A., Zhao, G., Erdos, G. and Gabriel, D. (1999) Expression of a single, host-specific, bacterial pathogenicity gene in plant cells elicits division, enlargement, and cell death. *Mol. Plant–Microbe Interact.* 12, 556–560.

Eulgem, T., Rushton, P.J., Schmelzer, E., Hahlbrock, K. and Somssich, I.E. (1999) Early events in plant defence signaling: rapid gene activation by WRKY transcription factors. *EMBO J.* 18, 4689–4699.

Farrow, S.C. and Facchini, P.J. (2014) Functional diversity of 2-oxoglutarate/Fe(II)-dependent dioxygenases in plant metabolism. *Front. Plant Sci.* 5, 524.

Gabriele, S., Rizza, A., Martone, J., Circelli, P., Costantino, P. and Vittorioso, P. (2010) The DOF protein DAG1 mediates PIL5 activity on seed germination by negatively regulating the GA biosynthetic gene *AtGA3ox1*. *Plant J.* 61, 312–323.

Graham, J.H., Gottwald, T.R., Cubero, J. and Achor, D.S. (2004) *Xanthomonas axonopodis* pv. *citri*: factors affecting successful eradication of citrus canker. *Mol. Plant Pathol.* 5, 1–15.

Grasser, M., Christensen, J.M., Peterhänsel, C. and Grasser, K.D. (2007) Basic and acidic regions flanking the HMG-Box domain of maize HMGB1 and HMGB5 modulate the stimulatory effect on the DNA binding of transcription factor Dof2. *Biochemistry*, 46, 6375–6382.

Hu, Y., Zhang, J., Jia, H., Sosso, D., Li, T., Frommer, W.B., Yang, B., White, F.F., Wang, N. and Jones, J.B. (2014) Lateral organ boundaries 1 is a disease susceptibility gene for citrus bacterial canker disease. *Proc. Natl. Acad. Sci. USA*, 111, 521–529.

Hutin, M., Sabot, F., Ghesquière, A., Koebnik, R. and Szurek, B. (2015) A knowledge-based molecular screen uncovers a broad spectrum *OsSWEET14* resistance allele to bacterial blight from wild rice. *Plant J.* 84, 694–703. doi: 10.1111/tpj.13042. [Epub ahead of print]

Kai, K., Mizutani, M., Kawamura, N., Yamamoto, R., Tamai, M., Yamaguchi, H., Sakata, K. and Shimizu, B. (2008) Scopoletin is biosynthesized via orthohydroxylation of feruloyl CoA by a 2-oxoglutarate-dependent dioxygenase in *Arabidopsis thaliana*. *Plant J.* 55, 989–999.

Kay, S., Hahn, S., Marois, E., Hause, G. and Bonas, U. (2007) A bacterial effector acts as a plant transcription factor and induces a cell size regulator. *Science*, 318, 648–651.

Konishi, M. and Yanagisawa, S. (2015) Transcriptional repression caused by Dof5.8 is involved in proper vein network formation in *Arabidopsis thaliana* leaves. *J. Plant Res.* 128, 643–652.

Krohn, N.M., Yanagisawa, S. and Grasser, K.D. (2002) Specificity of the stimulatory interaction between chromosomal HMGB proteins and the transcription factor Dof2 and its negative regulation by protein kinase CK2-mediated phosphorylation. *J. Biol. Chem.* 277, 32 438–32 444.

Li, Z., Zou, L., Ye, G., Xiong, L., Ji, Z., Zakria, M., Hong, N., Wang, G. and Chen, G. (2014) A potential disease susceptibility gene *CsLOB* of citrus is targeted by a major virulence effector PthA of *Xanthomonas citri* subsp. *citri*. *Mol. Plant.* 7, 912–915.

Mafra, V., Kubo, K.S., Alves-Ferreira, M., Ribeiro-Alves, M., Stuart, R.M., Boava, L.P., Rodrigues, C.M. and Machado, M.A. (2012) Reference genes for accurate transcript normalization in citrus genotypes under different experimental conditions. *PLoS One*, 7, e31263.

Mak, A.N.S., Bradley, P., Cernadas, R.A., Bogdanove, A.J. and Stoddard, B.L. (2012) The crystal structure of TAL effector PthXo1 bound to its DNA target. *Science*, 335, 716–719.

Martinez, S. and Hausinger, R.P. (2015) Catalytic mechanisms of Fe(II)- and 2-oxoglutarate-dependent oxygenases. *J. Biol. Chem.* 290, 20 702–20 711.

Moscou, M. and Bogdanove, A. (2009) A simple cipher governs DNA recognition by TAL effectors. *Science*, 326, 1501.

Murakami, M.T., Sforça, M.L., Neves, J.L., Paiva, J.H., Domingues, M.N., Pereira, A.L.A., Zeri, A.C.M. and Benedetti, C.E. (2010) The repeat domain of the type III effector protein PthA shows a TPR-like structure and undergoes conformational changes upon DNA interaction. *Proteins*, 78, 3386–3395.

Pereira, A.L., Carazzolle, M.F., Abe, V.Y., de Oliveira, M.L., Domingues, M.N., Silva, J.C., Cernadas, R.A. and Benedetti, C.E. (2014) Identification of putative TAL effector targets of the citrus canker pathogens shows functional convergence underlying disease development and defense response. *BMC Genomics*, 15, 157.

Römer, P., Hahn, S., Jordan, T., Strauss, T., Bonas, U. and Lahaye, T. (2007) Plant pathogen recognition mediated by promoter activation of the pepper Bs3 resistance gene. *Science*, 318, 645–648.

Shiotani, H., Fujikawa, T., Ishihara, H., Tsuyumu, S. and Ozaki, K. (2007) A *pthA* homolog from *Xanthomonas axonopodis* pv. *citri* responsible for host-specific suppression of virulence. *J. Bacteriol.* 189, 3271–3279.

Shubert, T.S., Rizvi, S.A., Sun, X., Gottwald, T.R., Graham, J.H. and Dixon, W.N. (2003) Meeting the challenge of eradicating citrus canker in Florida again. *Plant Dis.* 85, 340–356.

da Silva, A., Ferro, J., Reinach, F.C., Farah, C.S., Furlan, L.R., Quaggio, R.B., Monteiro-Vitorello, C.B., Van Sluys, M.A., Almeida, N.F., Alves, L.M., do Amaral, A.M., Bertolini, M.C., Camargo, L.E., Camarotte, G., Cannavan, F., Cardozo, J., Chambergo, F., Ciapina, L.P., Cicarelli, R.M., Coutinho, L.L., Cursino-Santos, J.R., El-Dorry, H., Faria, J.B., Ferreira, A.J., Ferreira, R.C., Ferro, M.I., Formighieri, E.F., Franco, M.C., Greggio, C.C., Gruber, A., Katsuyama, A.M., Kishi, L.T., Leite, R.P., Lemos, E.G., Lemos, M.V., Locali, E.C., Machado, M.A., Madeira, A.M., Martinez-Rossi, N.M., Martins, E.C., Meidanis, J., Menck, C.F., Miyaki, C.Y., Moon, D.H., Moreira, L.M., Novo, M.T., Okura, V.K., Oliveira, M.C., Oliveira, V.R., Pereira, H.A., Rossi, A., Sena, J.A., Silva, C., de Souza, R.F., Spinola, L.A., Takita, M.A., Tamura, R.E., Teixeira, E.C., Tezza, R.I., Trindade dos Santos, M., Truffi, D., Tsai, S.M., White, F.F., Setubal, J.C. and Kitajima, J.P. (2002) Comparison of the genomes of two *Xanthomonas* pathogens differing in host specificities. *Nature*, 417, 459–463.

Soprano, A.S., Abe, V.Y., Smetana, J.H. and Benedetti, C.E. (2013) Citrus MAF1, a repressor of RNA Pol III, binds the *Xanthomonas citri* canker elicitor PthA4 and suppresses citrus canker development. *Plant Physiol.* 163, 232–242.

de Souza, T.A., Soprano, A.S., de Lira N.P.V., Quaresma, A.J.C., Pauletti, B.A., Leme, A.F.P. and Benedetti, C.E. (2012) The TAL effector PthA4 interacts with nuclear factors involved in RNA dependent processes including a HMG protein that selectively binds poly(U) RNA. *PLoS One*, 7, e32305.

Sun, H., Wang, L., Zhang, B., Ma, J., Hettenhausen, C., Cao, G., Sun, G., Wu, J. and Wu, J. (2014) Scopoletin is a phytoalexin against *Alternaria alternata* in wild tobacco dependent on jasmonate signalling. *J. Exp. Bot.* 65, 4305–4315.

Sun, X., Zhou, D., Kandavelu, P., Zhang, H., Yuan, Q., Wang, B.C., Rose, J. and Yan, Y. (2015) Structural insights into substrate specificity of feruloyl-CoA 6′-hydroxylase from *Arabidopsis thaliana*. *Sci. Rep.* 5, 10 355.

Sutrias-Grau, M., Bianchi, M.E. and Bernue's, J. (1999) High mobility group protein 1 interacts specifically with the core domain of human TATA box-binding protein and interferes with transcription factor IIB within the pre-initiation complex. *J. Biol. Chem.* 274, 1628–1634.

Swarup, S., Yang, Y., Kingsley, M.T. and Gabriel, D.W. (1992) An *Xanthomonas citri* pathogenicity gene, *pthA*, pleiotropically encodes gratuitous avirulence on nonhosts. *Mol. Plant–Microbe Interact.* 5, 204–213.

Vialart, G., Hehn, A., Olry, A., Ito, K., Krieger, C., Larbat, R., Paris, C., Shimizu, B., Sugimoto, Y., Mizutani, M. and Bourgaud, F. (2012) A 2-oxoglutarate-dependent dioxygenase from *Ruta graveolens* L. exhibits p-coumaroyl CoA 2'-hydroxylase activity ($C2^0H$): a missing step in the synthesis of umbelliferone in plants. *Plant J.* 70, 460–470.

Wichmann, G. and Bergelson, J. (2004) Effector genes of *Xanthomonas axonopodis* pv. *vesicatoria* promote transmission and enhance other fitness traits in the field. *Genetics*, 166, 693–706.

Wilkins, K.E., Booher, N.J., Wang, L. and Bogdanove, A.J. (2015) TAL effectors and activation of predicted host targets distinguish Asian from African strains of the rice pathogen *Xanthomonas oryzae* pv. *oryzicola* while strict conservation suggests universal importance of five TAL effectors. *Front. Plant Sci.* 6, 536.

Wu, G.A., Prochnik, S., Jenkins, J., Salse, J., Hellsten, U., Murat, F., Perrier, X., Ruiz, M., Scalabrin, S., Terol, J., Takita, M.A., Labadie, K., Poulain, J., Couloux, A., Jabbari, K., Cattonaro, F., Del Fabbro, C., Pinosio, S., Zuccolo, A., Chapman, J., Grimwood, J., Tadeo, F.R., Estornell, L.H., Muñoz-Sanz, J.V., Ibanez, V., Herrero-Ortega, A., Aleza, P., Pèrez-Pèrez, J., Ramòn, D., Brunel, D., Luro, F., Chen, C., Farmerie, W.G., Desany, B., Kodira, C., Mohiuddin, M., Harkins, T., Fredrikson, K., Burns, P., Lomsadze, A., Borodovsky, M., Reforgiato, G., Freitas-Astùa, J., Quetier, F., Navarro, L., Roose, M., Wincker, P., Schmutz, J., Morgante, M., Machado, M.A., Talon, M., Jaillon, O., Ollitrault, P., Gmitter, F. and Rokhsar, D. (2014) Sequencing of diverse mandarin, pummelo and orange genomes reveals complex history of admixture during citrus domestication. *Nat. Biotechnol.* 32, 656–662.

Xu, Q., Chen, L.L., Ruan, X., Chen, D., Zhu, A., Chen, C., Bertrand, D., Jiao, W.B., Hao, B.H., Lyon, M.P., Chen, J., Gao, S., Xing, F., Lan, H., Chang, J.W., Ge, X., Lei, Y., Hu, Q., Miao, Y., Wang, L., Xiao, S., Biswas, M.K., Zeng, W., Guo, F., Cao, H., Yang, X., Xu, X.W., Cheng, Y.J., Xu, J., Liu, J.H., Luo, O.J., Tang, Z., Guo, W.W., Kuang, H., Zhang, H.Y., Roose, M.L., Nagarajan, N., Deng, X.X. and Ruan, Y. (2013) The draft genome of sweet orange (*Citrus sinensis*). *Nat. Genet.* 45, 59–66.

Xue, J., Luo, D., Xu, D., Zeng, M., Cui, X., Li, L. and Huang, H. (2015) CCR1, an enzyme required for lignin biosynthesis in Arabidopsis, mediates cell proliferation exit for leaf development. *Plant J.* 83, 375–387.

Yan, Q. and Wang, N. (2012) High-throughput screening and analysis of genes of *Xanthomonas citri* subsp. *citri* involved in citrus canker symptom development. *Mol. Plant–Microbe Interact.* 25, 69–84.

Yanagisawa, S. (1997) Dof DNA-binding domains of plant transcription factors contribute to multiple protein–protein interactions. *Eur. J. Biochem.* 250, 403–410.

Yang, B., Sugio, A. and White, F.F. (2006) *Os8N3* is a host disease-susceptibility gene for bacterial blight of rice. *Proc. Natl. Acad. Sci. USA*, 103, 10 503–10 508.

Yang, B. and White, F.F. (2004) Diverse members of the AvrBs3/PthA family of type III effectors are major virulence determinants in bacterial blight disease of rice. *Mol. Plant–Microbe Interact.* 17, 1192–1200.

Yu, Y., Streubel, J., Balzergue, S., Champion, A., Boch, J., Koebnik, R., Feng, J., Verdier, V. and Szurek, B. (2011) Colonization of rice leaf blades by an African strain of *Xanthomonas oryzae* pv. *oryzae* depends on a new TAL effector that induces the rice nodulin-3 *Os11N3* gene. *Mol. Plant–Microbe Interact.* 24, 1102–1113.

Zhang, Z.L., Xie, Z., Zou, X., Casaretto, J., Ho, T.D. and Shen, Q.J. (2004) A rice WRKY gene encodes a transcriptional repressor of the gibberellin signaling pathway in aleurone cells. *Plant Physiol.* 134, 1500–1513.

Zhou, J., Peng, Z., Long, J., Sosso, D., Liu, B., Eom, J.S., Huang, S., Liu, S., Vera Cruz, C., Frommer, W.B., White, F.F. and Yang, B. (2015) Gene targeting by the TAL effector PthXo2 reveals cryptic resistance gene for bacterial blight of rice. *Plant J.* 82, 632–643.

Zhou, R., Jackson, L., Shadle, G., Nakashima, J., Temple, S., Chen, F. and Dixon, R.A. (2010) Distinct cinnamoyl CoA reductases involved in parallel routes to lignin in *Medicago truncatula*. *Proc. Natl. Acad. Sci. USA*, 107, 17 803–17 808.

SUPPORTING INFORMATION

Additional Supporting Information may be found in the online version of this article at the publisher's website:

Fig. S1 Construction of *pthA*-deletion mutants. (A) Strategy used for the deletion of the *pthA* genes in *Xanthomonas citri* strain 306. Schematic view of *pthA1*, *pthA3* and *pthA4* loci depicting the oligonucleotides (arrows) used to generate the 1.0-kb fragments flanking the *pthA* coding regions (blue). The oligonucleotides PthA1F1, PthA1R2, PthA3F1, PthA3R2, PthA4F1 and PthA4R2 are specific for each *pthA* locus, whereas PthANR1 and PthANF2 are common to all *pthA*s. The bars below represent the approximate length of the DNA fragments. (B) Confirmation of the *pthA* deletions by polymerase chain reaction (PCR). DNAs from the single (Δ1, Δ3 and Δ4), double (Δ1-3, Δ1-4 and Δ3-4) and triple (Δ1-3-4) mutants were amplified using the indicated oligonucleotides shown in
(A) and resolved on agarose gel. The approximately 2.0-kb PCR bands corresponding to the 1.0-kb fragments flanking the *pthA* genes are indicative of the specific *pthA* deletions in each mutant background. (C) Examples of sequencing chromato- grams of Δ1, Δ3 and Δ 4 mutants showing the respective in- frame *pthA* deletions. The amino acid sequences encoded by the mutated *pthA* loci are indicated. The 2.0-kb fragments obtained with the specific PthAF and PthAR oligos were sequenced using oligo seqPthANF.

Table S1 Oligonucleotides used for the gene expression analyses, promoter cloning and sequencing, and *pthA*-deletion mutant construction and verification.

ANEXO II – Artigo publicado no ano de 2014 na revista '*BMC Genomics*', no qual participo como terceira autora. A minha contribuição neste trabalho foi a realização do estudo da expressão de potenciais genes alvos da proteína PthA4 em laranja doce, que gerou a figura 5 do artigo.

Pereira *et al. BMC Genomics* 2014, 15:157
http://www.biomedcentral.com/1471-2164/15/157

BMC Genomics

RESEARCH ARTICLE Open Access

Identification of putative TAL effector targets of the citrus canker pathogens shows functional convergence underlying disease development and defense response

Andre LA Pereira[1†], Marcelo F Carazzolle[1,2†], Valeria Y Abe[1], Maria LP de Oliveira[1,3], Mariane N Domingues[1], Jaqueline C Silva[1], Raul A Cernadas[1,4] and Celso E Benedetti[1*]

Abstract

Background: Transcriptional activator-like (TAL) effectors, formerly known as the AvrBs3/PthA protein family, are DNA-binding effectors broadly found in *Xanthomonas spp.* that transactivate host genes upon injection via the bacterial type three-secretion system. Biologically relevant targets of TAL effectors, i.e. host genes whose induction is vital to establish a compatible interaction, have been reported for xanthomonads that colonize rice and pepper; however, citrus genes modulated by the TAL effectors PthA"s" and PthC"s" of the citrus canker bacteria *Xanthomonas citri* (Xc) and *Xanthomonas aurantifolii* pathotype C (XaC), respectively, are poorly characterized.
Of particular interest, XaC causes canker disease in its host lemon (*Citrus aurantifolia*), but triggers a defense response in sweet orange.

Results: Based on, 1) the TAL effector-DNA binding code, 2) gene expression data of Xc and XaC-infiltrated sweet orange leaves, and 3) citrus hypocotyls transformed with PthA2, PthA4 or PthC1, we have identified a collection of *Citrus sinensis* genes potentially targeted by Xc and XaC TAL effectors. Our results suggest that similar with other strains of *Xanthomonas* TAL effectors, PthA2 and PthA4, and PthC1 to some extent, functionally converge.
In particular, towards induction of genes involved in the auxin and gibberellin synthesis and response, cell division, and defense response. We also present evidence indicating that the TAL effectors act as transcriptional repressors and that the best scoring predicted DNA targets of PthA"s" and PthC"s" in citrus promoters predominantly overlap with or localize near to TATA boxes of core promoters, supporting the idea that TAL effectors interact with the host basal transcriptional machinery to recruit the RNA pol II and start transcription.

Conclusions: The identification of PthA"s" and PthC"s" targets, such as the *LOB* (*LATERAL ORGAN BOUNDARY*) and *CCNBS* genes that we report here, is key for the understanding of the canker symptoms development during host susceptibility, or the defenses of sweet orange against the canker bacteria. We have narrowed down candidate targets to a few, which pointed out the host metabolic pathways explored by the pathogens.

Keywords: TAL effectors, PthA, PthC, *Xanthomonas citri*, *Xanthomonas aurantifolii*, Citrus canker, Target genes

*Correspondence: celso.benedetti@lnbio.cnpem.br
†Equal contributors
[1]Laboratório Nacional de Biociências, Centro Nacional de Pesquisa em Energia e Materiais, R. Giuseppe Máximo Scolfaro 10000, Campinas, SP 13083-970, Brazil
Full list of author information is available at the end of the article

Background

Transcriptional activator-like (TAL) effectors of *Xanthomonas spp.* had been featured as central determinants of both bacterial pathogenicity and avirulence in numerous plant species or cultivars [1-6]. However, it was not until recently that the biochemical function of TAL effectors as transcriptional regulators was discovered [6-13].

The tridimensional structure of TAL effectors showed that these proteins are distinct from any other bacterial effectors that are targeted to the interior of the host cell by the type-III secretion system [14-17]. TAL effectors striking signature is made by the polymorphisms in positions 12-13th of the 33-34 amino acids tandem repeats, referred as repeat-variable diresidues (RVDs), which comprise the DNA-binding domain of the effector [12,13]. The consecutive repeats wrap around the DNA double helix, accommodating the RVDs adjacent to the target DNA bases in a one-to-one RVD-DNA base fashion, which are stabilized by hydrogen bonds and/or Wan-der Waals forces between the 13th RVD residue and the DNA base [15-17]. These TAL effector-targeted sequences have been initially called UPT (up-regulated by TAL effector) boxes, and later more broadly, Effector Binding Elements (EBEs) [6,9]. The discovery of the TAL effector code has provided an invaluable tool for genome engineering by user-designed TAL effectors fused to catalytic domains, or designer TAL effectors to activate gene expression and explore their function during bacterial infection processes [18-20].

Based on host-range, *Xanthomonas citri* strains belong into different pathotypes being the Asian group A the most aggressive that exhibit wide-host range. Strains from groups B and C form a phylogenetically distinct clade originated in South America that exhibit limited host range [4,21]. The TAL effectors identified in *X. citri* strains were designated PthA"s", PthB"s" and PthC"s", and despite they are inherent in pathogenicity, the corresponding host gene targets remain uncharacterized [2,4,21-23]. Interestingly, a pioneering study showed that pathotypes A, B and C carry at least one isofunctional PthA, PthB or PthC effector of 17.5 repeat domains, which is essentially required to elicit hyperplastic canker lesions on citrus [4,21]. On the other hand, none of the TAL effectors from the limited-host-range strains (pathotypes B and C) was able to trigger the hypersensitive response (HR) observed in grapefruit plants when expressed heterologously in other strain, suggesting that TAL effectors from citrus canker pathogens do not limit host range but rather contribute to virulence associated functions [4,21].

Recent reports have focused on the computational- based prediction of EBEs in plant genomes to identify the putative host gene targets of TAL effectors [13,24,25]. For citrus, the *in silico* analyses to predict PthA"s" targets in sweet orange provided a set of candidates but additional experimental evidence of, e.g. gene expression, is still needed to validate such predictions [24]. Also, those studies did not include PthB"s" or PthC"s" effectors from the restricted host-range strains like *Xanthomonas aurantifolii* pathotype C (XaC), which in turn trigger a defense response in sweet oranges. Such analyses could provide molecular candidates that regulate the citrus defense response against *Xanthomonas spp.* [24,26]. In other pathosystems, the identification of TAL effector- induced genes of *X. vesicatoria* and *X. oryzae* has revealed novel virulence mechanisms of plant bacteria mediated by the targeted transcriptional induction of key regulators of host susceptibility [3,6,8,11]. Therefore, identification of TAL effector targeted factors that regulate citrus canker susceptibility is a milestone to understand and improve disease resistance.

Using microarray analyses, we have previously shown that the genes up-regulated by XaC in sweet orange leaves are involved in basal defense. In contrast, *X. citri* (Xc) induced genes associated with cell division and growth at the beginning of the infection process [26]. We also found that many of the rapidly Xc-induced genes, including cellulases, expansins and other cell-wall remodeling proteins, are co-regulated by auxin and gibberellin, hormones that are required for canker development [27] and control cell growth and expansion in other plant species [28]. TAL effectors not only play a central role as major determinants of host susceptibility, but are also capable of eliciting a resistance response when targeting HR-executor genes [3,6-8,29,30]. Based on these evidences, we hypothesized that TAL effectors from Xc and XaC are directly regulating the transcription of sweet orange genes involved in canker formation and defense response, respectively.

In this study, we present a combination of bioinformatics, microarray analyses, and molecular assays to identify sweet orange genes targeted by PthA2, PthA4 and PthC1 proteins. We show that the ectopic expression of PthA2, PthA4 or PthC1 in citrus epicotyls resulted in the up- regulation of a group of genes involved in auxin and gibberellin response, cell growth, and defense response. Our *in silico* studies using the TAL effector code, predicted many EBEs for the PthA"s" and/or PthC effectors in the promoter regions of genes induced in epicotyls expressing the corresponding TAL effector. Interestingly, we noticed that the EBEs overlap with, or localize close to TATA box elements of the promoters. In addition, despite the different RVD composition between PthA"s" and PthC"s", our results indicate a targeting of functionally-related genes, which further support a model where TAL effectors display the functional convergence by selective evolution as general TATA-binding proteins [24,25]. Finally, we present experimental evidence suggesting that TAL effectors from citrus canker pathogens also function as transcriptional repressors.

Results

Transcriptional changes in sweet orange triggered by Xc TAL effectors

By extensive gene expression analyses, we had identified numerous genes up-regulated during the canker disease development of sweet orange leaves infiltrated with Xc [26]. To test whether any of those genes are direct targets of TAL effectors, we have undertaken two complementary approaches. First, we performed microarrays assays of orange leaves after bacterial infiltration in the presence or absence of the protein synthesis inhibitor, cycloheximide (Ch), a strategy that has early pinpointed AvrBs3 targets in pepper plants [10,31]. We found that many of the genes induced by Xc at 6 and/or 48 h after infiltration [26] are also induced by Xc in the presence of Ch (Additional file 1), thus indicating that Xc elicit major transcriptional reprograming independent of protein synthesis. Several of these differentially expressed genes are likely involved in terpene and gibberellin synthesis, ethylene production and signaling, cell-wall remodeling, cell division and defense responses (Additional file 1). In particular, we noticed that the ethylene synthesis pathway represented by orthologs of ACC synthase, ACC oxidase and AP2 factor genes, which play roles in cell wall softening [32-34], appears to be a primary mechanism elicited in the host after Xc sensing. On the other hand, defense response genes encoding chitinases, WRKY factors and pathogenesis-related (PR) proteins are also rapidly induced (Additional file 1).

Second, we transiently expressed the Xc TAL effectors PthA2 and PthA4 in sweet orange epicotyls and compared the transcriptional changes relative to epicotyls transformed with GUS as a control (Figure 1A). We selected PthA2 and PthA4 because they form heterodimers and interact with several citrus proteins implicated in transcriptional control [23,35-37]. By inspecting the RVD sequences of PthA2 and PthA4 (Figure 1B), we presumed that they would target common host genes. Consistent with this observation, we found that the transient expression of PthA2 or PthA4 resulted in the up-regulation of a similar group of genes that are functionally related to both defense and disease development (Additional file 2). The genes associated with canker development that were most strongly induced by both PthA2 and PthA4, encode cell-wall synthesis and remodeling enzymes, including a glycosyl transferase ortholog of *upa15* (CV709535) that is readily up-regulated by AvrBs3 in pepper plants [10]. In addition, the defense response induced genes encode chitinases, PR proteins and an ACC synthase, which are also up-regulated by Xc in the presence of Ch, thus providing initial evidence that they might be functional targets of PthA2 and PthA4 (Additional files 1 and 2). Notably, numerous genes up-regulated in response to PthA2 or PthA4 are functionally related to auxin and gibberellin synthesis and signaling, cell division and growth, and defense responses (Additional file 2). In particular, we noticed a strong PthA4-dependent induction of genes encoding cell division and expansion proteins including kinesins, tubulins, histones, ribosomal proteins, and orthologs of *dem* (*defective embryo and meristems*) and LOB (lateral organ boundary) (Additional file 2). Besides, the transcriptional profile of epicotyls expressing PthA4 is remarkably similar to that of citrus leaves infiltrated with Xc 48 h post-inoculation [26], as shown by the up-regulation of a large number of genes related to auxin synthesis, mobilization, and signaling, including two homologs of the auxin influx carrier protein AUX1 (CV706455, CX053885) [38-40] (see Venn diagram in Additional file 2). In contrast, epicotyls expressing PthA2 showed the up-regulation of many genes implicated in cell-wall remodeling and gibberellin synthesis and signaling, including orthologs of *upa6* and *upa7* (alpha-expansins), and *upa22* (GA-like protein), respectively, which are putative targets of AvrBs3 in pepper [10,31] (Additional file 2). PthA2 also induced several genes encoding retrotransposons (Additional file 2), which were also reported as off-targets of AvrXa7 in rice [25].

Gene onthology (GO) enrichment analysis showed that while PthA2 modulate several genes categorized in cell-wall organization and RNA-dependent DNA replication and integration, PthA4 affected the expression of genes grouped under the microtubule-based movement and cell growth category. In addition, the GO analysis showed that PthA2 and PthA4 commonly regulate a large number of genes involved in carbohydrate (sucrose, glucan and glycoside) metabolism, and cell-wall organization and biogenesis (Figure 2 and Additional file 2). These evidences support the functional convergence between Xc TAL effectors, and is in agreement with recent reports of *X. oryzae* TAL effectors [24,25]. In addition, the common targeting of PthA2 and PthA4 is a strong indicator that they may have additive or even synergistic roles for activation of host genes required for citrus canker susceptibility.

Transcriptional changes in sweet orange triggered by PthC1, a TAL effector of *X. aurantifolii*

We have shown previously that XaC elicit an HR-type response in sweet orange leaves, which is characterized by the up-regulation of multiple defense-related genes [26]. To examine whether XaC TAL effectors are involved in the host transcriptional defense response, we cloned two TAL effectors from XaC strain ICMP 8354, designated PthC1 and PthC2. The essential differences between XaC TAL effectors occur in the number of repeat domains and the nature of the repeat variable diresidues (RVDs), which altogether form the DNA-binding domain of the protein [12,13]. PthC1 has 18 RVDs or 17.5 repeat domains, and PthC2 is shorter with only 15 RVDs or 14.5 repeat domains (Figure 1B). Despite the overall structural

Results

Transcriptional changes in sweet orange triggered by Xc TAL effectors

By extensive gene expression analyses, we had identified numerous genes up-regulated during the canker disease development of sweet orange leaves infiltrated with Xc [26]. To test whether any of those genes are direct targets of TAL effectors, we have undertaken two complementary approaches. First, we performed microarrays assays of orange leaves after bacterial infiltration in the presence or absence of the protein synthesis inhibitor, cycloheximide (Ch), a strategy that has early pinpointed AvrBs3 targets in pepper plants [10,31]. We found that many of the genes induced by Xc at 6 and/or 48 h after infiltration [26] are also induced by Xc in the presence of Ch (Additional file 1), thus indicating that Xc elicit major transcrip- tional reprograming independent of protein synthesis. Several of these differentially expressed genes are likely involved in terpene and gibberellin synthesis, ethylene production and signaling, cell-wall remodeling, cell div- ision and defense responses (Additional file 1). In par- ticular, we noticed that the ethylene synthesis pathway represented by orthologs of ACC synthase, ACC oxidase and AP2 factor genes, which play roles in cell wall soften- ing [32-34], appears to be a primary mechanism elicited in the host after Xc sensing. On the other hand, defense re- sponse genes encoding chitinases, WRKY factors and pathogenesis-related (PR) proteins are also rapidly induced (Additional file 1).

Second, we transiently expressed the Xc TAL effectors PthA2 and PthA4 in sweet orange epicotyls and compared the transcriptional changes relative to epicotyls transformed with GUS as a control (Figure 1A). We selected PthA2 and PthA4 because they form heterodimers and interact with several citrus proteins implicated in transcriptional control [23,35-37]. By inspecting the RVD sequences of PthA2 and PthA4 (Figure 1B), we presumed that they would target common host genes. Consistent with this observation, we found that the transient expression of PthA2 or PthA4 resulted in the up-regulation of a similar group of genes that are functionally related to both defense and disease development (Additional file 2). The genes associated with canker development that were most strongly induced by both PthA2 and PthA4, encode cell-wall synthesis and remodeling enzymes, including a glycosyl transferase ortholog of *upa15* (CV709535) that is readily up-regulated by AvrBs3 in pepper plants [10]. In addition, the defense response induced genes encode chitinases, PR proteins and an ACC synthase, which are also up-regulated by Xc in the presence of Ch, thus providing initial evidence that they might be functional targets of PthA2 and PthA4 (Additional files 1 and 2). Notably, numerous genes up-regulated in response to PthA2 or PthA4 are functionally related to auxin and gibberellin synthesis and signaling, cell division and growth, and defense responses (Additional file 2). In particular, we noticed a strong PthA4-dependent induction of genes encoding cell division and expansion proteins including kinesins, tubulins, histones, ribosomal proteins, and orthologs of *dem* (*defective embryo and meristems*) and LOB (lateral organ boundary) (Additional file 2). Besides, the transcriptional profile of epicotyls expressing PthA4 is remarkably similar to that of citrus leaves infiltrated with Xc 48 h post-inoculation [26], as shown by the up-regulation of a large number of genes related to auxin synthesis, mobilization, and signaling, including two homologs of the auxin influx carrier protein AUX1 (CV706455, CX053885) [38-40] (see Venn diagram in Additional file 2). In contrast, epicotyls expressing PthA2 showed the up-regulation of many genes implicated in cell-wall remodeling and gibberellin synthesis and signaling, including orthologs of *upa6* and *upa7* (alpha-expansins), and *upa22* (GA-like protein), respectively, which are putative targets of AvrBs3 in pepper [10,31] (Additional file 2). PthA2 also induced several genes encoding retrotransposons (Additional file 2), which were also reported as off-targets of AvrXa7 in rice [25].

Gene onthology (GO) enrichment analysis showed that while PthA2 modulate several genes categorized in cell-wall organization and RNA-dependent DNA replication and integration, PthA4 affected the expression of genes grouped under the microtubule-based movement and cell growth category. In addition, the GO analysis showed that PthA2 and PthA4 commonly regulate a large number of genes involved in carbohydrate (sucrose, glucan and glycoside) metabolism, and cell-wall organization and biogenesis (Figure 2 and Additional file 2). These evidences support the functional convergence between Xc TAL effectors, and is in agreement with recent reports of *X. oryzae* TAL effectors [24,25]. In addition, the common targeting of PthA2 and PthA4 is a strong indicator that they may have additive or even synergistic roles for activa- tion of host genes required for citrus canker susceptibility.

Transcriptional changes in sweet orange triggered by PthC1, a TAL effector of *X. aurantifolii*

We have shown previously that XaC elicit an HR-type response in sweet orange leaves, which is characterized by the up-regulation of multiple defense-related genes [26]. To examine whether XaC TAL effectors are involved in the host transcriptional defense response, we cloned two TAL effectors from XaC strain ICMP 8354, desig- nated PthC1 and PthC2. The essential differences between XaC TAL effectors occur in the number of repeat domains and the nature of the repeat variable diresidues (RVDs), which altogether form the DNA-binding domain of the protein [12,13]. PthC1 has 18 RVDs or 17.5 repeat do- mains, and PthC2 is shorter with only 15 RVDs or 14.5 repeat domains (Figure 1B). Despite the overall structural

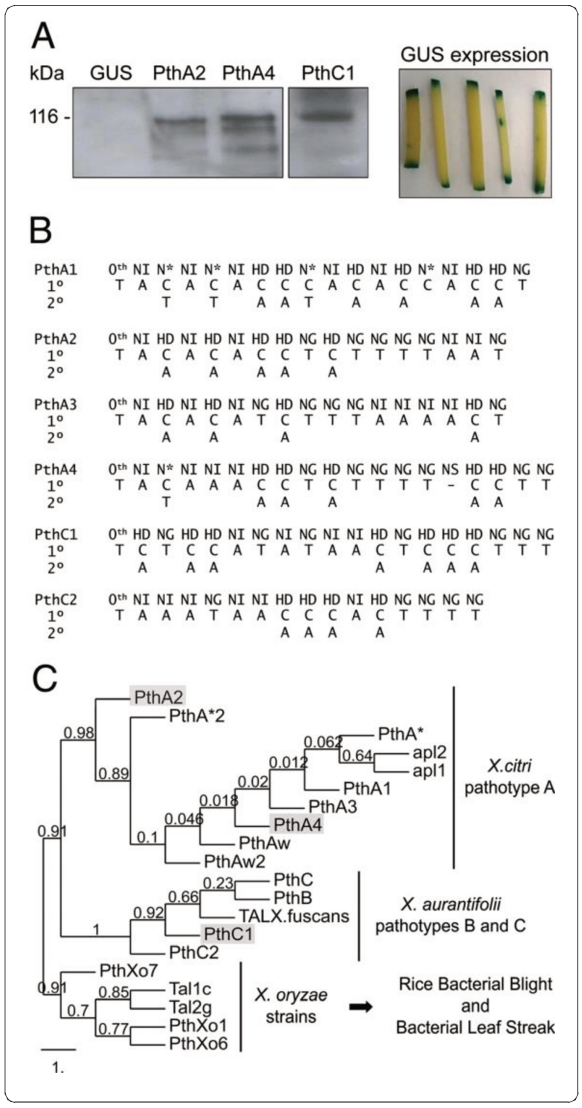

Figure 1 Heterologous expression in citrus epicotyls, RVD sequences and phylogeny of TAL effectors PthA2, PthA4 and PthC1. (A) Western blot of protein extracts from sweet orange epicotyls transfected with *A. tumefaciens* EHA105 carrying pBI121-35S::*pthA2* (PthA2), pBI121-35S::*pthA4* (PthA4), pBI121-35S::*pthC1* (PthC1), or the native plasmid pBI121-35S::*uidA* (GUS) for control of TAL effectors expression. Total protein from epicotyls expressing PthA2, PthA4 or, PthC1 proteins (~116 kDa) were separated by electrophoresis on 10% SDS-polyacrylamide gels, transferred to PVDF membranes, and detected with anti-PthA2 serum (left panel). The expression of *uidA* gene was assayed histochemically for β-glucuronidase (GUS) activity using 5-bromo-4-chloro-3-indolyl-β-D-glucuronic acid (X-Gluc) as substrate (right panel). (B) RVD sequence composition of *X. citri* isolate 306 TAL effectors PthA1, PthA2, PthA3 and PthA4, and PthC1 and PthC2 from *X. aurantifolii* ICMP 8435, aligned with the corresponding predicted DNA targets. According to the TAL effector code, only the first and second bases associated with higher frequency for each RVD are represented. (C) Phylogenetic tree of TAL effectors from different *Xanthomonas* strains that cause citrus canker disease and blight or leaf streak of rice. The maximum likelihood analysis was built with the PhyML tool using a bootstrapping procedure of 500 repetitions. Only the C-terminal domains (~278 residues) of TAL effectors from *Xanthomonas spp.* were used for the analysis. The four PthA"s" of Xc strain 306 belong into a group close to other TAL effectors from pathotype A strains; meanwhile, PthCs and PthBs from *X. aurantifolii* integrate a distinct group of pathotypes B and C strains, respectively. The tree is displayed with the TAL effectors from *X. oryzae* strains rooted as outgroup. Amino acid sequences were aligned using MUSCLE and analyzed on phylogenetic pipeline of *Phylogeny.fr* [41].

similarities with PthA"s" of Xc, PthC1 and PthC2 are phylogenetically more closely related to PthB"s" and PthC"s" from other pathotype B and C strains, respectively (Figure 1C), that are distinguished by their limited host range [4,21]. In terms of the RVD composition, PthC1 appears also more similar to PthB and PthC of other citrus canker strains reported to induce weak disease symptoms or hypersensitive response in sweet oranges [4,21]. Despite the fact that PthC from a group C strain was not required for the HR elicited on grapefruit [4], we decided to test whether PthC1 induce the expression of defense-related genes in sweet orange, as we observed during XaC infection [26]. Therefore, we transfected PthC1 in sweet orange epicotyls and compared the transcriptional changes relative to epicotyls expressing PthA2, PthA4, or the GUS gene as reference (Figure 1A). We found that PthC1 elicit not only a different but also an opposite effect of PthA2 and PthA4, because its expression resulted in a general down regulation of genes involved in auxin and gibberellin synthesis and signaling, cell-wall remodeling, cell division, and defense responses (Additional file 3). The fact that auxin and gibberellin promote initial canker pustule formations [27] indicate that PthC1, in contrast to PthA2 and PthA4, do not contribute to canker symptoms in sweet orange. Nevertheless, we found Aux/IAA and bZip orthologous genes repressed by PthC1 (CV713157, CV704184, CK701644, CN182471), which function as

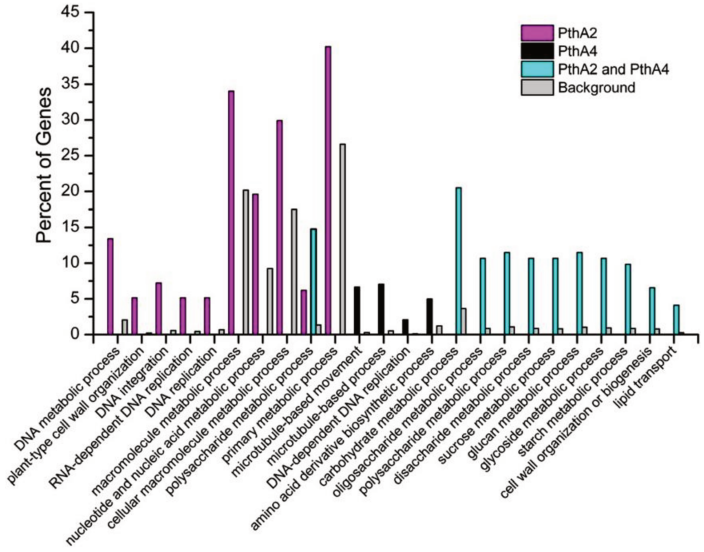

Figure 2 GO enrichment analysis for PthA2 and/or PthA4-regulated genes. GO enrichment analysis performed with agriGO [42], showing that PthA2 and PthA4 modulate several genes in sweet orange associated with canker development. Despite the fact that PthA2 and PthA4 regulate distinct, but related sets of genes implicated in cell-wall remodeling, cell division and growth, they both altered group of genes involved in carbohydrate metabolism and cell-wall organization and biogenesis. The identity of the enriched genes can be found in Additional file 2.

negative regulators of the auxin and gibberellin signaling pathways affecting plant growth and development [43-45]. In addition, the down-regulation of genes encoding GH3-like enzymes (CF837666, CF837443) [46] and indole-3-acetic acid amido synthase (CV714093) suggest that PthC1 operates to increase the active pools of free auxin. On the other hand, we found no obvious HR-like executor among the genes up-regulated by PthC1 in sweet orange epicotyls (Additional file 3), although an AP2-domain transcription factor orthologous of the tomato Pti4 [47] might be an interesting candidate (Additional file 3).

Together, these data show that PthC1, in contrast to PthA2 and PthA4, regulate a different set of genes in sweet orange. Although these genes may not significantly favor host susceptibility, they do not appear to be elicitors of an HR response either. This idea is consistent with the observation that a knockout mutation of *pthC* in a group C strain resulted in loss of pathogenicity on lime, but still triggers the HR response on grapefruit [4].

Computational prediction of EBEs for PthA and PthC in citrus genomes

The public release of the *Citrus sinensis* and *Citrus clementina* genomes together with the TAL effector code of DNA binding [12,13], provides a suitable model to investigate *in silico* the TAL effector-targeted genes in citrus. Because the computational tools available for TAL effector targets prediction do not yet support analyses of the citrus genomes [24,25,48], we designed a position weight matrix based on TAL effector-DNA association frequencies to predict and score EBEs for Xc and XaC TAL effectors in citrus gene promoters (Additional file 4). Putative EBEs for the four PthA"s" and the 2 PthC"s" of strains Xc 306 and XaC ICMP 8354, respectively, were identified in nearly one thousand promoters. We then selected the top one hundred best scoring *C. sinensis* promoters ranging from 8.5 to 17.4 for further analysis (Additional file 5). In order to test the performance of our computational matrix analysis, we used the target finder function of the TAL Effector-Nucleotide Targeter 2.0 (TALE-NT) tools [48] to search for PthA"s" and PthC"s" EBEs in the top twenty best scoring promoters. We retrieved virtually the same EBE predictions with equivalent score values [data not shown], indicating a similar achievement between our prediction method and the TALE-NT tools.

Next, we functionally categorized our candidates based on sequence homology to plant, yeast, or animal gene orthologs with known biological function (Additional file 5). In addition to genes implicated in auxin and gibberellin synthesis and signaling, and in cell-wall remodeling, we found a substantial number of genes involved in cell division and morphogenesis, transcription regulation and defense (Additional file 5). Although most of our best scoring promoters do not correspond with the genes identified in our microarray analyses (see below), these data seem to be meaningful because the predicted

candidates belong to the same functional categories of those up-regulated in citrus epicotyls in response to PthA/PthC expression or in Xc-infiltrated leaves in the presence of Ch (Additional files 1, 2, 3). Remarkably, we predicted two PthC1 targets, orange1.1g035902m.g and orange1.1g035488m.g (Additional file 5), with a strong similarity to the *Bs3* gene of pepper, which is an HR executor transcriptionally activated by AvrBs3 of *X. vesicatoria* [7]. We also found that several PthA"s" putative targets are involved in abscisic acid (ABA) synthesis, signaling and response, particularly for PthA1 (Additional file 5). Interestingly, some of these genes, including an ABA8-hydroxilase (orange1.1g012199m.g), ABI3 (orange1.1g038867m.g) and ABI3-interacting protein-1 (orange1.1g044737m.g), also participate in the cross-talk between auxin and gibberellin, and in plant growth and development [49-51] (Additional file 5).

Experimental validation of putative gene targets of PthA and PthC effectors

Although computational identification of TAL effector-targeted genes have been recently conducted for TAL effectors of *X. oryzae* and Xc in their corresponding host genomes, the studies for Xc are largely deficient on experimental validation for novel candidate targets [24,25]. Nevertheless, the combination of *in silico* predictions with gene expression data, demonstrated to be a suitable strategy to identify new biologically relevant TAL effector targets [52]. Thus, in order to verify our *in silico* target predictions, we used the whole set of microarray data in our hands to search for experimental evidence of gene regulation of our predicted TAL effector targets. We found that nearly 20% and 3% of the computational- predicted targets were up and down-regulated, respectively, indicating that TAL effectors not only induce but may ultimately repress the expression of host predicted targets (Additional files 1, 2, 3 and 5). Using a cross-check criteria we were able to select targets that 1) are differentially expressed in epicotyls expressing the corresponding TAL effector, 2) are also differentially expressed after infiltration of Xc in the presence of Ch, and 3) are functionally associated with the mechanisms of canker development or defense response (Table 1).

To verify these data, we first confirmed the TAL effector protein accumulation in epicotyls transiently expressing *pthA2*, *pthA4* or *pthC1* (Figure 1A), and subsequently examined the mRNA levels of the predicted targets by quantitative RT-PCR on the transgenic tissues. Totally, sixteen

Table 1 Predicted TAL effector targeted genes in *C. sinensis* that are transcriptionally regulated by Xc in the presence of Ch or, by the heterologous expression of the TAL effector

Microarray data (fold change)	Sweet orange genes with	Homologous gene description	Functional category	References
	PthA2 binding sites			
PthA2 x GUS (4.0)	orange1.1g032466m.g	Pepper UPA22 (UPA22)	GA response	[10,31]
	orange1.1g031880m.g	Tobacco rac-like GTPase 1 (RAC)	Auxin response	[53]
	orange1.1g001197m.g	Rat transcription activator BRG1 (BRG1)	Cell growth	[54]
PthA2 x GUS (-3.1)	orange1.1g023431m.g	Xyloglucan endotransglucosylase (XET)	Cell growth	[55]
	orange1.1g040761m.g	Castor bean LOB domain protein (LOB2)	Defense	[56]
PthA2 x GUS (-3.1)	orange1.1g037640m.g	Tobacco UDP-glucosyltransferase (UDPGT)	Defense	[57]
	PthA4 binding sites			
Xc + Ch x Ch (3.8)	orange1.1g024897m.g	Tobacco 14-3-3 protein (14-3-3)	Cell growth	[58-60]
PthA4 x GUS (11.4)	orange1.1g017949m.g	*Citrus limetta* dioxygenase (DIOX)	Cell growth	[61,62]
PthA4 x GUS (5.2)	orange1.1g018649m.g	Tobacco cysteine proteinase (CP)	Defense	[63,64]
	orange1.1g037138m.g	*C. trifoliata* NBS-LRR protein (CCNBS1)	Defense	[65]
	PthC1 binding sites			
	orange1.1g041266m.g	Tomato self pruning-interacting protein 1 (SIP1)	Cell growth	[66]
	orange1.1g010756m.g	Potato Ca^{+2}-dependent protein kinase (CDPK)	Cell growth	[67]
	orange1.1g039072m.g	Potato CC-NBS-LRR protein (CCNBS2)	Defense	[68]
	orange1.1g042296m.g	Sunflower CC-NBS-LRR protein (CCNBS3)	Defense	[69]
	Multiple EBEs			
	PthA2, PthA4, PthC1			
	orange1.1g046669m.g	Tobacco Avr9/Cf9 elicited protein 146 (AE146)	Defense	[70]
	PthA4, PthC1			
Xc + Ch x Ch (8.8)	orange1.1g026556m.g	Aspen LOB domain 1 (LOB1)	Cell growth	[71]

genes implicated in symptom development or defense response, were selected for target validation (Table 1). These candidates were differentially expressed in response to Xc infiltration and also after TAL effector expression in epicotyls, and encoded at least one predicted EBE for the corresponding TAL effector in their promoters. Initially, we tested the expression of four putative PthA2 targets, including an ortholog of the pepper *upa22*, which encodes a xyloglucan endotransglucosylase (*XET*), a RAC- GTPase gene (*RAC*), and an ortholog of the rat BRG1, implicated in cell wall strengthening, auxin response, and tumor development, respectively (Table 1). Consistent with the microarray data (Table 1), the citrus *upa22* and the *BRG1* genes were slightly but preferentially up-regulated by PthA2 compared to PthA4, PthC1 or GUS in epicotyls; in contrast, *XET* was significantly down-regulated in response to PthA2 (Figure 3A). The *RAC* gene, which was induced in epicotyls expressing PthA2 and PthA4, also appeared down-regulated in tissues expressing PthC1 (Figure 3A). Despite the strong induction of *RAC* by PthA4 (Figure 3A), we found no good scoring candidate EBEs for PthA4 in the *RAC* promoter. Presumably, this is part of false negative predictions that account for the current limitations of computational analyses of TAL effector targets [17,52,72,73].

To test the PthA4 candidate targets, we selected 4 genes encoding orthologous of a tobacco 14-3-3 protein, a two-domain dioxygenase (DIOX), a cysteine protease (CP), and a CC-NBS-LRR protein (CCNBS1), which play roles in gibberellin synthesis, cell elongation and defense (Table 1). Consistent with the microarray data (Table 1), we found that the four selected genes were strongly (more than 6 fold-change) up-regulated in epicotyls expressing PthA4, which support the computational prediction of best scoring targets of PthA4 (Figure 3B). Although *14-3-3* and *DIOX* were induced moderately (between 2 to 3 fold-change) in epicotyls expressing PthC1, no EBEs for PthC1 were identified in these targets.

We also tested the PthC1 predictions using 4 selected candidate genes, including the orthologs of a potato Ca^{+2}-dependent protein kinase (*CDPK*) and tomato self-pruning interacting protein 1 (*SIP1*), and two CC-NBS-LRR resistance genes (*CCNBS2* and *3*) (Table 1). An ortholog of the pepper *Bs3* gene (orange1.1g035488m.g) was also tested; however, we were not able to detect this gene by qPCR analysis, even using large amounts of cDNA input. We found that *SIP1* and *CCNBS3* genes were significantly induced in response to PthC1 expression relative to GUS, although *CCNBS3* was also up-regulated by PthA2 and 4 (Figure 3C). In addition, *SIP1* and *CCNBS2* appeared also induced in response to PthA4 expression. Interestingly, we found an EBE for PthA4 in the *SIP1* promoter with a score value of 6.2 that explains the observation. In contrast, *CDPK* was 3-fold repressed by PthC1 (Figure 3C).

Altogether, these results partially confirm the TAL effector targets prediction but also suggest that more than one TAL effector might induce the same gene, and that TAL effectors can ultimately cause transcriptional repression of targets, although we have not tested whether this is a direct or indirect (secondary) effect of the protein.

To further investigate these observations, we evaluated the expression of a predicted PthA2 target, a phenylpropanoid:UDP-glucosyltransferase (*UDPGT*), which was nearly 3-folds down-regulated in PthA2-expressing epicotyls (Table 1). We also tested a predicted target of PthA2, PthA4 and PthC1 encoding an Avr9/Cf9-elicited protein 146 homolog, *AE146*, as well as two Lateral Organ Boundaries genes, *LOB1* and *LOB2*, indentified as targets of PthA4/PthC1 and PthA2, respectively (Table 1). A previous report predicted that the citrus *LOB1* was targeted by PthA4 [24]. We found that *AE146* is induced in response to PthA2 and PthA4 expression, but in contrast, PthA2, PthA4 and PthC1, down-regulate the expression of *UDPGT* (Figure 4A). Consistent with our microarray data (Table 1), *LOB1* was predominantly induced by PthA4, but repressed by PthC1, while all the three TAL effectors tested induce the expression of *LOB2* (Figure 4B).

We also used a *pthA4* knockout derivative of Xc, which is not pathogenic in sweet orange neither it induces hyperplasic lesions [23], to analyze the expression levels of candidate PthA4 targets. We found that three of the predicted PthA4 targets, *DIOX*, *CP* and *14-3-3*, are induced at higher levels in leaves infiltrated with the wild type Xc strain relative to the *pthA4*-deletion mutant; however, these genes were also up-regulated by the *pthA4* mutant relative to water infiltration, which indicates that these genes present a more complex mechanism of induction where PthA4 is not absolutely required (Figure 5A).

We also evaluated the expression of two PthA2 predicted targets *RAC* and *LOB2*, and two PthC1 targets *LOB1* and *SIP1*, which were highly up-regulated in epicotyls expressing PthA4 (Figure 3A and C). Although *RAC* expression was under the level of detection by quantitative PCR (not shown), we found that the transcript accumulation of *SIP1* was lower in response to *pthA4*-deletion mutant relative to leaves infiltrated with the wild type Xc (Figure 5A). Similarly, the expression levels of *LOB1* and *LOB2* were significantly lower in leaves infiltrated with the *pthA4*-deletion mutant (Figure 5B). Nevertheless, *LOB1*, *LOB2* and *SIP1* were also up-regulated in leaves infiltrated with the *pthA4*-deletion mutant relative to water-infiltrated leaves, suggesting an alternative mechanism of target induction, potentially by other TAL effectors that our analysis failed to predict.

Taken together these results confirm our previous observations, and point out to *LOB1*, *LOB2, SIP1, CP* and *DIOX* as primary targets of Xc and XaC TAL effectors, in particular of PthA4 (Figure 5).

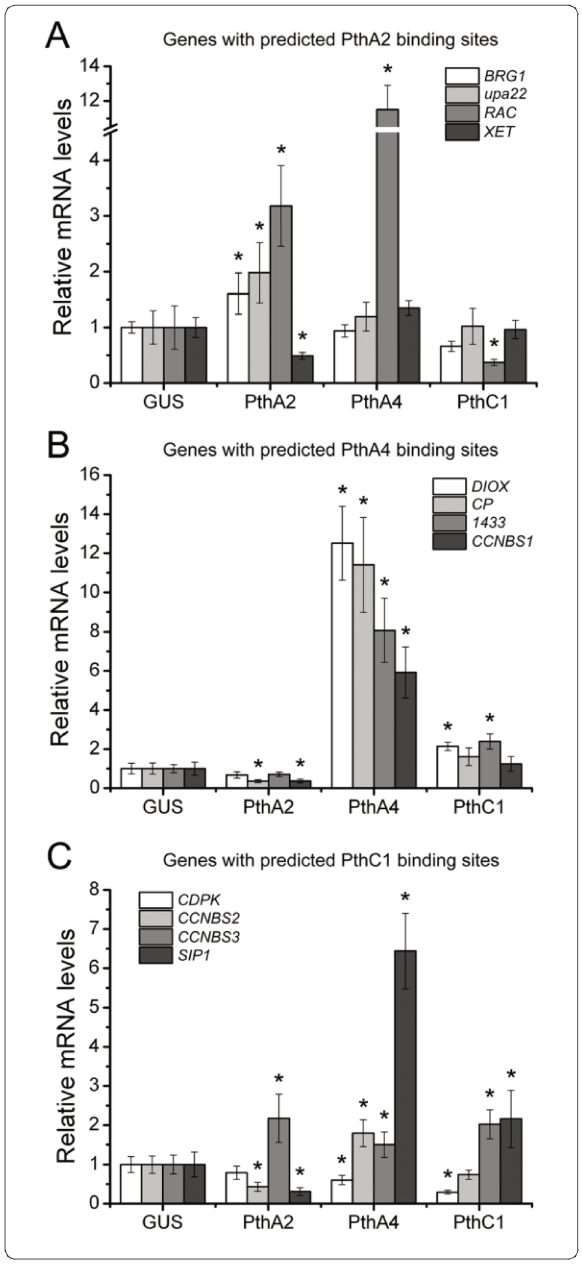

Figure 3 Gene expression levels of predicted targets of PthA2, PthA4 and PthC1 in epicotyls transfected with the corresponding TAL effector. (A) Quantitative RT-PCR (qPCR) of four sweet orange genes with best-scoring effector-binding elements (EBEs) predicted for PthA2 in their promoters. (B) qPCR of four sweet orange genes with best-scoring EBEs predicted for PthA4 in their promoters. Predicted PthA4 target genes are significantly and predominantly up-regulated by PthA4 expression. (C) qPCR of four sweet orange genes with best-scoring EBEs predicted for PthC1 of XaC in their promoters. The expression levels are the mean of three independent biological replicates. The error bars denote standard deviations whereas asterisks indicate statistically significant differences ($p < 0.05$) in the mRNA levels in epicotyls expressing the TAL effectors relative to GUS.

PthA and PthC EBEs overlap with or localize close to TATA box elements in citrus promoters

Including AvrBs3, several TAL effectors bind to EBEs that overlap with TATA-like sequences [6-8,29]. In some cases this causes a downstream shift of the transcriptional start site in the targeted gene, suggesting that TAL effectors might have a similar function of TATA-binding proteins [6-10]. Here, we found that approximately 73% of the predicted EBEs for PthA"s" and PthC"s" localize between 16 and 300 bp upstream the translation start codon of the genes (Additional file 5). This observation and a recent study in rice suggesting that TAL effectors of *X. oryzae* are predicted to bind within 300 bp upstream the start codon and frequently overlap with TATA-box elements of the promoter [24], prompted us to evaluate whether the overlap or close proximity between TATA boxes and EBE positions, also occurs for TAL effectors of Xc and XaC in citrus promoters. We found that most of the EBEs predicted for PthA"s" and PthC"s" show a tendency to overlap with, or localize within 30 bp of putativeTATA- box elements (Figure 6 and Additional file 5). For instance, in five of the candidate targets (*LOB1*, *LOB2*, *AE146, CCNBS1* and *CDPK*) the EBEs overlapped with a putative TATA box (Additional file 5). Thus, our data suggest that despite the RVD variations among these TAL effectors, they are likely to have an evolutionary selection pressure towards the targeting of TATA-rich regions of host sequences that are critical for the transcriptional regulation.

Discussion

Despite the fact that many TAL effectors targets and their molecular functions have been coming to light in recent years [3,6-11,74,75], citrus genes directly activated by PthA"s" or PthC"s" effectors, and their role in canker development or host defense against *Xanthomonas spp.*, remain poorly characterized. In this study, we have identified a number of genes putatively targeted by PthA"s" and PthC"s" in sweet orange, and shown that most of them impinge on disease and/or host defense responses. We also observed that PthA2 and PthA4, yet bearing distinct

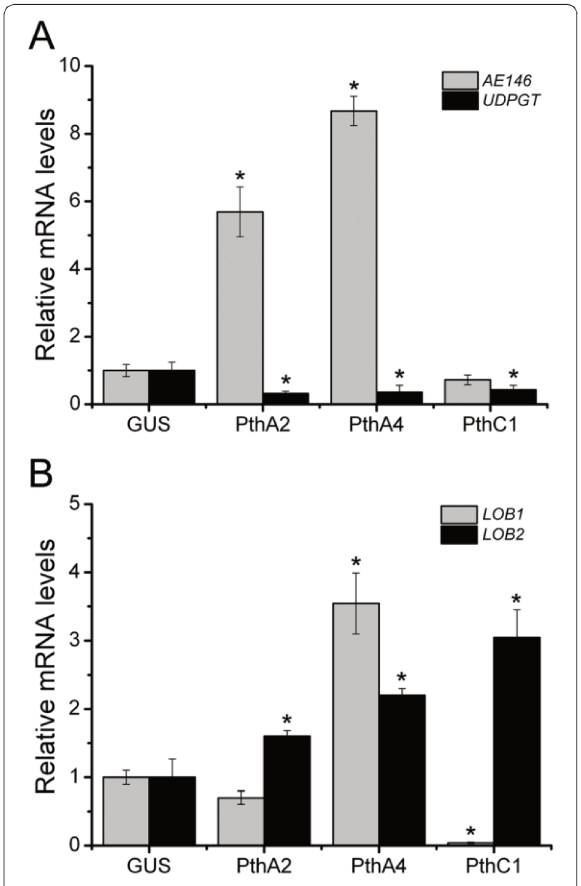

Figure 4 Expression levels of possible common targets of PthA2, PthA4 and/or PthC1. (A) Expression levels of the Avr9/Cf9-elicited 146 (*AE146*) and *UDPGT* genes in response to TAL effector expression in citrus epicotyls. Although binding sites for PthA2, PthA4 and PthC1 were identified in the *AE146* gene promoter, *AE146* is strongly induced by PthA2 and 4 only. The UDPGT gene, which was down-regulated by PthA2 in microarray experiments, and has a predicted PthA2-binding site in its promoter, is repressed by all three effector proteins. (B) Expression levels of two citrus *LOB* genes (*LOB1* and *LOB2*) in response to TAL effector expression in citrus epicotyls. LOB1, identified as a target of PthA4 and PthC1 was preferentially modulated by these effectors, whereas *LOB2*, identified as a PthA2 target by EBE prediction is apparently up-regulated by all three effectors. The expression levels are the mean of three independent biological replicates. The error bars denote standard deviations whereas asterisks indicate statistically significant differences ($p < 0.05$) in the mRNA levels in epicotyls expressing the TAL effectors relative to GUS.

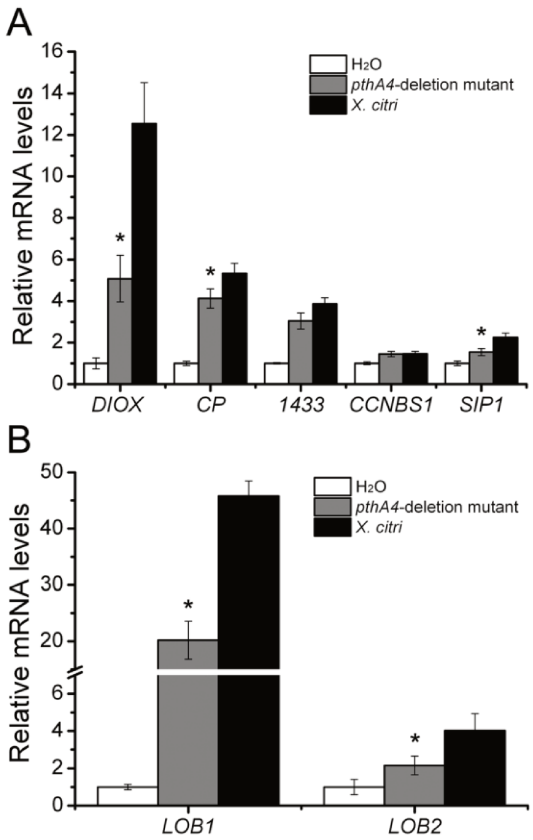

Figure 5 Expression levels of potential targets of PthA4. Expression levels of *DIOX*, *CP*, *14-3-3* (1433), *CCNBS1* and *SIP1* (A), or *LOB1* and *LOB2* (B), in sweet orange leaves infiltrated with Xc or its mutant derivative lacking *pthA4* (*pthA4*-deletion mutant), 72 h post-inoculation, relative to water-infiltrated leaves. All target genes were induced by Xc and *pthA4*-deletion mutant, relative to water infiltration; however, the expression levels of most genes, including *DIOX*, *SIP1*, *LOB1* and *LOB2*, were significantly lower in the leaves infiltrated with the *pthA4* mutant, suggesting a role of PthA4 in gene activation. The expression levels are the mean of three independent biological replicates. The error bars denote standard deviations whereas asterisks indicate statistically significant differences ($p < 0.05$) between the mRNA levels found in the leaves infiltrated with the *pthA4* mutant, relative to the wild type *X. citri*.

RVDs composition (Figure 1B), exhibit functional convergence, in particular to regulate genes of the auxin and gibberellin synthesis and response pathways, as well as their downstream signaling cascade genes like those for cell wall remodeling, cell division and expansion. In citrus, targeting these hormonal pathways appear to be the headline of canker-causing *Xanthomonas spp.* since endogenous auxin and gibberellin are required for initial canker formation in leaves infiltrated with the pathogen, and the exogenous application of the hormones transcriptionally regulate specific genes also induced by Xc during the onset of infection [26,27]. How these hormones contribute to the canker disease needs further exploration, but it is clear their relationship with the canker symptoms, hypertrophy and hyperplasia of mesophyll cells [2], which generate enough internal pressure to prompt the epidermal rupture and facilitate pathogen release to the leaf surface for disease propagation [21,27]. Besides, auxin also increase the

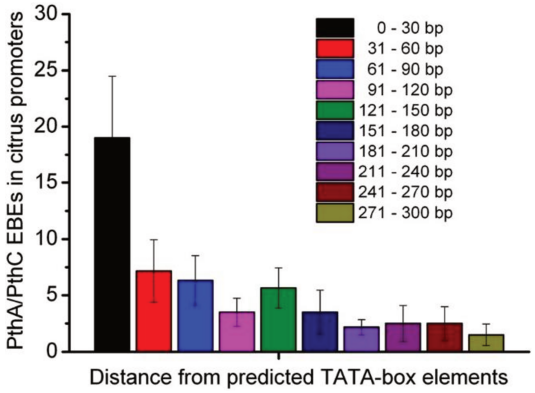

Figure 6 Distribution of average distance of predicted EBEs relative to TATA-like elements in citrus promoters. Possible overlap between TATA box and PthA/PthC-binding site positions in the citrus promoters predicted as targets of PthA/PthC proteins. The great majority of PthA and PthC-binding sites overlap with, or are located within 30 bp of the predicted TATA-box elements in the corresponding citrus promoters.

host susceptibility on other plant-pathogen interactions [76-79], pointing it out as a conserved mechanism of biotrophic microbes to elicit cell wall softening to e.g., leak nutrients from the host cell, and/or to improve effectors translocation that promote host susceptibility and bacterial fitness. Overall, it is tempting to speculate that, in the case of the citrus canker pathogens, manipulating the auxin signaling pathway via TAL effector-targeting would be an effective way to disarm host defense responses for bacterial survival and pathogenicity. Notably, many of the AvrBs3 up-regulated (*UPA*) genes are also auxin-responsive and some of them including *upa7*, *upa15*, *upa17* and *upa20*, are known to enhance cell hypertrophy and the synthesis of cell-wall polymers [8,10,31]. These data reflect on recent studies suggesting that the redundancy and convergence in TAL effector repertories occurring within and across *X. oryzae* strains, respectively, may be a conserved feature of TAL effector evolution as a consequence of an arms race of the host-bacteria interaction [24,25]. The biological meaning of such functional redundancy of TAL effectors in strain 306, particularly between PthA2 and PthA4, denote a cooperative, or eventually a synergistic role of these effectors as transcriptional activators (Figures 3, 4, 5, Additional files 2 and 5). In addition, it is interesting to note that PthA2 physically interacts with PthA4, and that both proteins bind independently to the C-terminal domain of RNA Pol II [37]. Hence, TAL effector-mediated transcriptional regulation in citrus appears to be further influenced by the multiple protein-protein interactions occurring at the assembly locus of RNA Pol II. According with this assumption, the up-regulation of *LOB1* and *LOB2* in epicotyls expressing PthA2 or PthA4 (Figure 4B), and in sweet orange leaves infiltrated with Xc or its *pthA4* mutant derivative (Figure 5B), emerges as an evident example of a redundant targeting of a presumably major gene for canker susceptibility. We also predicted another gene encoding a LOB-domain protein targeted by PthA3, orange1.1g048558m.g (Additional file 5). Interestingly, *LOB* genes have been associated to auxin signaling pathways, including cell growth control and organ development [56,71,80]. From an evolutionary point of view, it seems advantageous for a single Xc strain to target a family of potential susceptibility genes, i.e. *LOB* genes with different TAL effectors, which function cooperatively or synergistically, because it will assure the induction of the critical set of genes involved in disease symptoms development. The observation is convincing since it implies a mechanism that the pathogen uses to overcome potential natural polymorphisms in TAL effector targeted promoters, in particular those occurring in susceptibility genes among different host varieties [6].

Beyond the functional redundancy of Xc TAL effectors, we found that PthA4 predominantly induce genes encoding ribosomal proteins and proteins of cell division and growth, like kinesins, tubulins and histones (Additional file 2). This is noteworthy because PthA4 also physically interacts with the citrus MAF1 protein (CsMAF1), which is a negative regulator of RNA Pol III that controls ribosome biogenesis and suppresses canker symptoms [23,36]. Thus, the specific PthA4-induction of ribosomal protein genes appears to be a causal feedback mechanism of ribosome biogenesis that is required for cell division and growth. On the other hand, although PthA2 does not interact with CsMAF1, it binds to and inhibits the prolyl-isomerase activity of the citrus cyclophilin CsCYP, a putative negative regulator of the RNA Pol II complex [23,35,37,81]. Therefore, it remains to be determined how these protein specific interactions between TAL effectors and components of RNA Pol II and III complexes affect the outcome of the host expression profiles in response to bacterial infection.

In contrast to PthA"s"-induced genes, epicotyls expressing PthC1 showed a general down-regulation of auxin and gibberellin response genes suggesting that this TAL effector is not an elicitor of susceptibility. For instance, *LOB1* that is induced by PthA4, appears significantly down-regulated by PthC1 (Figure 4B), which is consistent with the PthC1-mediated repression of auxin response genes, since LOB proteins have also been implicated in auxin signaling [80,82]. However, it remains to be determined whether the general down-regulation of the auxin responsive genes by PthC1 in sweet orange is the major cause for the lack of host susceptibility (i.e. no hyperplasic lesions) after infiltration of sweet orange with XaC [26].

In pepper plants ecotype ECW-30, the *Bs3* resistance gene induced by the *X. vesicatoria* TAL effector AvrBs3, executes an HR response after bacterial infiltration [7]. Our computational analyses have predicted EBEs of PthC1 in the promoters of two sweet orange genes orthologous to *Bs3*, orange1.1g035488m.g and orange1.1g035902m.g (Additional file 5); however, we were not able to detect their expression in response to PthC1 or after XaC infiltration (Additional file 3), and neither were them detected by any other gene expression analyses we conducted before i.e., differential display PCR and suppression subtractive hybridization [26]. Besides, though the results discussed above indicate that XaC cannot induce host susceptibility, we do not yet discard the possibility that an HR-like elicitor is mediating the sweet orange defense against XaC. It has been verified and predicted that nodulin and flavone-3-hydroxylase (F3H) genes, respectively, represent common targets of *Xanthomonas* ssp. TAL effectors [11,24,25]. Here, we found four nodulin-related genes, which are significantly up-regulated in sweet orange leaves infiltrated with Xc in the presence of Ch, DN620509, or in epicotyls expressing PthA2, CX675781, and PthA4, DN958192 and CV710110. However, we were not able to predict EBEs for PthA"s" in their promoters suggesting a potential gap for false negative predictions of computational analyses, or eventually indicating that their induction is consequential of other primary targets of the TAL effectors. On the other hand, we predicted EBEs of PthA and/or PthC in the promoters of the nodulin-related genes orange1.1g007766m.g and orange1.1g042021m.g, but none of these genes were up-regulated in our microarray dataset (Additional files 1, 2 and 5).

One of the predicted targets of PthA4 is the citrus dioxygenase gene *DIOX* (Table 1, Figures 3B and 5A, Additional file 5) that is similar to the rice gene *F3H*, also a predicted target of TAL effectors from *X. oryzae* strains [25]. Although the F3H was linked to flavonoid biosynthesis [25], both *F3H* and *DIOX* are similar to Gibberellin-20-Oxidases (GA20ox), a group of enzymes that catalyze gibberellin biosynthesis [83]. Interestingly, as observed for the *LOB* genes, a citrus gene encoding a putative GA20 oxidase (orange1.1g019643m.g) was identified as a target of PthA1, PthA2 and PthA3 (Additional file 5). This protein has the same domain architecture found in DIOX, which suggests they are functional orthologs. In addition, both PthA4 and PthC1 transactivate a regulator of gibberellin synthesis namely *14-3-3*, and a *SIP1* gene in epicotyls (Figure 3) whose protein products interact with a SELF-PRUNING factor involved in the control plant architecture and flowering of tomato [58,66,84]. These evidences together support the susceptibility effect of inducing gibberellin genes during the process of infection.

Another outcome of our study is the proximity of the predicted EBEs relative to putative TATA boxes of promoter regions (Figure 6). This is in line with the fact that EBEs for *X. oryzae* TAL effectors have been also identified close to TATA elements in rice promoters [6]. Similarly, AvrBs3 binding sites are found within 100 bp upstream of the transcription start site [10], raising the idea that TAL effectors might functionally replace general TATA-binding factors, as recently proposed [24]. In addition, our data indicates that TAL effectors can function as transcriptional repressors, in particular PthC1, as discussed above (Additional files 2 and 3; Figures 3 and 4).

Conclusion

In conclusion, we have identified candidate targets of PthA"s" and PthC"s" in citrus that will not only strengthen our understanding on canker symptoms formation, but also provide novel information about host susceptibility or defenses against *Xanthomonas* pathogens, which will assist in the selection and generation of canker resistant plants.

Methods

Bacterial strains, plasmids and growth conditions

PthA2 and PthA4 were amplified from the Xc strain 306 [85] and cloned into pET28a and pBI121 for bacteria and plant expression, as previously described [35]. Plasmids were introduced into *E. coli* strain DH5alpha and/or *Agrobacterium tumefaciens* strain EHA105 by electroporation. *E. coli* cells were incubated at 37°C in Luria-Bertani (LB) medium, whereas Xc and *A. tumefaciens* were grown in LB without NaCl at 28°C and in YEP (Bacto peptone 10 g/l, NaCl 5 g/l, Yeast extract 10 g/l, and Agar 15 g/l) at 30°C, respectively [86]. Bacterial cultures were grown at different time periods until they reached the desired optical densities. Antibiotics were added to the media in the following final concentrations: ampicillin, 100 μg/ml; kanamycin, 50 μg/ml; rifampicin, 50 μg/ml; streptomycin, 25 μg/ml.

Plant material, bacterial infiltration

Six-month-old plants of sweet orange "Pera" were obtained from certified nurseries and kept in a growth room at 25–28°C with a 14 h light photoperiod. For plant infiltration, Xc strains were inoculated from single colony plates and grown over night at 28°C in liquid LB without NaCl. Cells colonies were suspended in sterile water to an optical density at 600 nm (OD_{600}) of 0.1 (nearly 10^6 CFU/ml). Leaves were infiltrated with bacterial suspensions in water or, in 50 μM cycloheximide (Ch) (Sigma-Aldrich, USA). Water and Ch only were independently infiltrated as mock controls. For quantitative PCR (qPCR) assays, fully expanded "Pera" leaves were infiltrated with a water suspension ($OD_{600} = 0.1$) of wild type Xc strain 306, or its *pthA4*-deletion mutant derivative [23].

Cloning TAL effectors from *X. aurantifolii*

PthC genes were PCR amplified using total DNA extracted from the XaC strain ICMP 8435 [26] as template. Primers targeting conserved 5' and 3' regions were designed based on the four available Xc *pthA* genes (5'-CATATGGATCC CATTCGTTCG-3' and 5'-GAATTCTCACTGAGGCAA TAGCTC-3'). PCR products were amplified using the Pfu turbo DNA polymerase in a 50 μL reaction, following the supplier's instructions (Stratagene, USA), with an annealing temperature of 52°C and extension time of 4 min. PCR products were gel-purified and cloned into of pET28a vector using the restriction sites *Nde*I/*Eco*RI. At least twenty independent clones were analyzed by restriction mapping with *Ssp*I enzyme, or by DNA sequencing and only two different variants designated PthC1 and PthC2 were identified. None of the PthA effectors of Xc isolate 306 were found in our screening of XaC TAL effectors sequences.

Expression of *Xanthomonas* TAL effectors in citrus epicotyls

Agrobacterium strains transformed with pBI121 vector (bearing the *uidA* gene under the control of the CaMV 35S promoter) or its derivative carrying the TAL effectors *pthA2*, *pthA4* or *pthC1* in place of the *uidA* gene, were used to transform sweet orange. Epicotyls from young plantlets of *Citrus sinensis* 'Hamlin' were wounded, transversely sectioned and incubated at room temperature (21°C) for 15 minutes in a fresh suspension of *A. tumefaciens* (OD_{600} = 0.6) containing 100 μM acetosyringone. Co-cultivation assays were conducted on semi-solid 1x Murashige and Skoog medium supplemented with 25 g/l sucrose, vitamin cocktail (10 mg/l thiamine-HCl, 10 mg/l pyridoxine, 1 mg/l nicotinic acid, 0.4 mg/l glycine), 100 mg/l of *myo*-inositol and 0.2 mg/l of 2,4-dichlorophenoxyacetic acid (pH 5.8) during 72 h in dark [87]. Transformation efficiency was confirmed by western blot analyses and histochemical GUS assay prior to RNA isolation for microarray and qPCR analysis.

Western blot detection of PthA/PthC expression

Citrus epicotyls transfected with the native pBI121 vector or, its derivatives carrying the effector genes *pthA2*, *pthA4* or *pthC1*, were grinded to homogeneity in SDS-PAGE sample buffer and resolved on a 10% SDS-polyacrylamide gel. The proteins were transferred onto PVDF membranes and probed with anti-PthA2 serum as previously described [35].

GUS assay

The *A. tumefaciens* strain EHA105 transformed with the pBI121 vector carrying the reporter gene *uidA*, which encodes beta-D-glucuronidase (GUS), was transfected in citrus epicotyls as described previously and the transient expression of GUS was tested using colorimetric assay 72 h after bacteria-tissue co-cultivation [88].

RNA isolation and microarray and RT-qPCR analysis

Messenger RNA (mRNA) was extracted from infiltrated leaves or from transformed epicotyls as described previously [26]. For microarray hybridization, approximately 0.6 μg of mRNA was used to synthesize cDNAs, which were subsequently used as template to generate the biotin-labeled complementary RNAs (cRNAs) using the One-Cycle target labeling assay (Affymetrix). Gene-Chips of citrus genome arrays (Affymetrix) were hybridized with cRNAs following standard instructions of Affymetrix kits. The hybridized arrays were rinsed, stained and scanned with an Affymetrix Genechip Scanner 3000−7G. Two CEL files per treatment, corresponding to biological replicates, were analyzed with the ArrayAssit software package (ArrayAssit x.5, Stratagene, USA) using the MAS5 algorithm.

Total RNA samples were prepared from sweet orange leaves infiltrated with Xc, its *pthA4*-deletion mutant, or water as control, 72 h after bacterial inoculation, using the Trizol method (Invitrogen, Carlsbad, CA) and subsequently treated with DNase I (Promega, Madison, WI). Nearly 10 μg of total RNA was reverse-transcribed using the Maxima First Strand cDNA Synthesis Kit (Fermentas) according to the supplier's instructions, and used as template in real-time qPCR reactions conducted in 96-well plates. Primer sequences (Additional file 6) corresponding to the *Citrus sinensis* genes listed in Table 1 were designed using the Primer Express 2.0 software (ABI, Foster City, CA). Each 25-μL qPCR reaction was composed by 12.5 μL of SYBR green 2× master mix (ABI, Foster City, CA), 1 μL of forward and reverse primer mix (7.5 μM), 1 μL of cDNA and 10.5 μL of diethyl pyrocarbonate-treated water. qPCR amplifications were carried out using the 7500 system "Universal" cycle condition in an ABI Prism 7300 instrument (Applied Biosystems, Foster City, CA). The *Citrus sinensis* gene encoding a malate translocator was selected as internal control for normalization [86]. Total RNA from three different leaves were used in qPCR reactions as independent biological replicates, and three technical replicates for each biological sample were considered for statistical T-tests to determine the significant changes of gene expression across the treatments.

In silico prediction of TAL effector binding sites

A position-specific weight matrix was designed based on the TAL code of associations frequencies between DNA bases and RVDs, and used to score putative effector binding elements (EBEs) of PthA1, PthA2, PthA3 and PthA4 of Xc strain 306, and PthC1 and PthC2 of XaC strain ICMP 8435, considering a thymidine (T) at position-1 of the EBE as preferential base [12,13]. The algorithm was used to perform systematic similarity searches within 1500 bp of promoter regions relative to the translation start site of genes annotated in the

genomes of *C. clementina* (http://www.citrusgenomedb.org/species/clementina/genome1.0) and *C. sinensis* (http://www.citrusgenomedb.org/species/sinensis/genome1.0). Identification of orthologous relationships between these two species was based on nucleotide sequence similarities (BLASTn) and best bidirectional hit (BBH) method [89,90]. Reciprocal sequence similarity searches between *C. clementina* and *C. sinensis* genes were performed using the BLASTn algorithm [91], with an E-value cutoff of $1xE^{-20}$, and a homemade Perl script to parse both BLASTn outputs to identify the BBH BLAST relationships (Additional file 4). The search was performed using the MOODS algorithm [92], which provided a list of possible EBEs for the PthA/PthC TAL effectors with a corresponding score for each sequence. The p-value cutoff was set to 0.001 in order to reduce false positives prediction alignments.

The final set of *C. sinensis* promoters having one or more putative PthA/PthC binding sites (top 100 hits) was derived from a conserved region analysis between the *C. clementina* and *C. sinensis* orthologous promoters, an approach that is widely used to identify new regulatory motifs in many organisms [93-95]. Thus, only the citrus genes with PthA/PthC binding sites in both *C. sinensis* and *C. clementina* promoters were selected.

In *silico* TATA-box prediction

The DNA sequences corresponding to the promoters of *C. sinensis* genes having potential EBEs (top hits) were submitted to the Plant TATA-box prediction server using the TSSP program [96] at the http://linux1.softberry.com/berry.phtml site.

Availability of supporting data

The sequences of PthC1 and PthC2 were deposited in the GeneBank as ADI48327 and ADI48328 accessions, respectively. The microarray data files (Affymetrix CEL files) for all the experiments described here have been deposited to GEO under the superseries GSE51379.

Additional files

Additional file 1: Microarray analyses of sweet orange leaves infiltrated with Xc in the presence or absence of cycloheximide (Ch), 8 h after bacterial inoculation.

Additional file 2: Microarray analyses of sweet orange epicotyls expressing PthA2 or PthA4.

Additional file 3: Microarray analyses of sweet orange epicotyls expressing PthC1.

Additional file 4: Perl script developed to parse both BLASTn outputs to identify the best bidirectional hit (BBH) BLAST relationships.

Additional file 5: Top one hundred best scoring *C. sinensis* promoters with predicted EBEs for PthA and PthC proteins.

Additional file 6: List of primers used in the qPCR experiments.

Competing interests
The authors declare that they have no competing financial interest.

Authors' contribution
Conceived and designed the experiments: ALAP, MFC, RAC and CEB, Performed the experiments: ALAP, MFC, VYA, MLPO, MND, JCS and CEB, Analyzed the data: ALAP, MFC, VYA, MND, RAC and CEB, Wrote the paper: RAC and CEB. All authors read and approved the final manuscript.

Acknowledgements
This work was supported by São Paulo Research Foundation (FAPESP grants 2010/00634-1 and 2011/20468-1) and Conselho Nacional de Desenvolvimento Científico e Tecnológico (CNPq).

Author details
[1]Laboratório Nacional de Biociências, Centro Nacional de Pesquisa em Energia e Materiais, R. Giuseppe Máximo Scolfaro 10000, Campinas, SP 13083-970, Brazil. [2]Departamento de Genética, Evolução e Bioagentes, Instituto de Biologia, Universidade Estadual de Campinas, Campinas, SP 13083-970, Brazil. [3]Present address: U.S. Department of Agriculture, U.S. Horticultural Research Laboratory, 2001 South Rock Road, Fort Pierce, FL 34945, USA. [4]Present address: Department of Plant Pathology and Plant-Microbe Biology, Cornell University, Ithaca, NY 14853, USA.

Received: 21 October 2013 Accepted: 18 February 2014
Published: 25 February 2014

References

1. Bonas U, Stall RE, Staskawicz B: Genetic and structural characterization of the avirulence gene *avrBs3* from *Xanthomonas campestris* pv. *vesicatoria*. *Mol Gen Genet* 1989, 218:127–136.
2. Duan Y, Castañeda A, Zhao G, Erdos G, Gabriel D: Expression of a single, host-specific, bacterial pathogenicity gene in plant cells elicits division, enlargement, and cell death. *Mol Plant Microbe Interact* 1999, 12:556–560.
3. Yang B, Sugio A, White FF: *Os8N3* is a host disease-susceptibility gene for bacterial blight of rice. *Proc Natl Acad Sci U S A* 2006, 103:10503–10508.
4. Al-Saadi A, Reddy J, Duan Y, Brunings A, Yuan Q, Gabriel D: All five host-range variants of *Xanthomonas citri* carry one *pthA* homolog with 17.5 repeats that determines pathogenicity on citrus, but none determine host-range variation. *Mol Plant Microbe Interact* 2007, 20:934–943.
5. Shiotani H, Fujikawa T, Ishihara H, Tsuyumu S, Ozaki K: A *pthA* homolog from *Xanthomonas axonopodis* pv. *citri* responsible for host-specific suppression of virulence. *J Bacteriol* 2007, 189:3271–3279.
6. Antony G, Zhou J, Huang S, Li T, Liu B, White F, Yang B: Rice xa13 recessive resistance to bacterial blight is defeated by induction of the disease susceptibility gene Os-11 N3. *Plant Cell* 2010, 22:3864–3876.
7. Römer P, Hahn S, Jordan T, Strauss T, Bonas U, Lahaye T: Plant pathogen recognition mediated by promoter activation of the pepper *Bs3* resistance gene. *Science* 2007, 318:645–648.
8. Kay S, Hahn S, Marois E, Hause G, Bonas U: A bacterial effector acts as a plant transcription factor and induces a cell size regulator. *Science* 2007, 318:648–651.
9. Römer P, Strauss T, Hahn S, Scholze H, Morbitzer R, Grau J, Bonas U, Lahaye T: Recognition of AvrBs3-like proteins is mediated by specific binding to promoters of matching pepper *Bs3* alleles. *Plant Physiol* 2009, 150:1697–1712.
10. Kay S, Hahn S, Marois E, Wieduwild R, Bonas U: Detailed analysis of the DNA recognition motifs of the *Xanthomonas* type III effectors AvrBs3 and AvrBs3Deltarep16. *Plant J* 2009, 59:859–871.
11. Yu Y, Streubel J, Balzergue S, Champion A, Boch J, Koebnik R, Feng J, Verdier V, Szurek B: Colonization of rice leaf blades by an African strain of *Xanthomonas oryzae* pv. *oryzae* depends on a new TAL effector that induces the rice nodulin-3 *Os11N3* gene. *Mol Plant Microbe Interact* 2011, 24:1102–1113.
12. Boch J, Scholze H, Schornack S, Landgraf A, Hahn S, Kay S, Lahaye T, Nickstadt A, Bonas U: Breaking the code of DNA binding specificity of TAL-type III effectors. *Science* 2009, 326:1509–1512.
13. Moscou M, Bogdanove A: A simple cipher governs DNA recognition by TAL effectors. *Science* 2009, 326:1501.
14. Murakami MT, Sforça ML, Neves JL, Paiva JH, Domingues MN, Pereira AL, Zeri AC, Benedetti CE: The repeat domain of the type III effector protein

PthA shows a TPR-like structure and undergoes conformational changes upon DNA interaction. *Proteins* 2010, 78:3386–3395.

1. Deng D, Yan C, Pan X, Mahfouz M, Wang J, Zhu JK, Shi Y, Yan N: Structural basis for sequence-specific recognition of DNA by TAL effectors. *Science* 2012, 335:720–723.
2. Mak AN, Bradley P, Cernadas RA, Bogdanove AJ, Stoddard BL: The crystal structure of TAL effector PthXo1 bound to its DNA target. *Science* 2012, 335:716–719.
3. Stella S, Molina R, Yefimenko I, Prieto J, Silva G, Bertonati C, Juillerat A, Duchateau P, Montoya G: Structure of the AvrBs3-DNA complex provides new insights into the initial thymine-recognition mechanism. *Acta Crystallogr D Biol Crystallogr* 2013, 69:1707–1716.
4. Li T, Huang S, Jiang WZ, Wright D, Spalding MH, Weeks DP, Yang B: TAL nucleases (TALNs): hybrid proteins composed of TAL effectors and FokI DNA-cleavage domain. *Nucleic Acids Res* 2011, 39:359–372.
5. Miller JC, Tan S, Qiao G, Barlow KA, Wang J, Xia DF, Meng X, Paschon DE, Leung E, Hinkley SJ, Dulay GP, Hua KL, Ankoudinova I, Cost GJ, Urnov FD, Zhang HS, Holmes MC, Zhang L, Gregory PD, Rebar EJ: A TALE nuclease architecture for efficient genome editing. *Nat Biotechnol* 2011, 29:143–148.
6. Zhang F, Cong L, Lodato S, Kosuri S, Church GM, Arlotta P: Efficient construction of sequence-specific TAL effectors for modulating mammalian transcription. *Nat Biotechnol* 2011, 29:149–153.
7. Brunings AM, Gabriel DW: *Xanthomonas citri*: breaking the surface. *Mol Plant Pathol* 2003, 4:141–157.
8. Yan Q, Wang N: High-throughput screening and analysis of genes of *Xanthomonas citri* subsp. *citri* involved in citrus canker symptom development. *Mol Plant Microbe Interact* 2012, 25:69–84.
9. Soprano AS, Abe VY, Smetana JH, Benedetti CE: Citrus MAF1, a repressor of RNA Pol III, binds the *Xanthomonas citri* canker elicitor PthA4 and suppresses citrus canker development. *Plant Physiol* 2013, 163:232–242.
10. Grau J, Wolf A, Reschke M, Bonas U, Posch S, Boch J: Computational predictions provide insights into the biology of TAL effector target sites. *PLoS Comput Biol* 2013, 9:e1002962.
11. Pérez-Quintero AL, Rodriguez-R LM, Dereeper A, López C, Koebnik R, Szurek B, Cunnac S: An improved method for TAL effectors DNA-binding sites prediction reveals functional convergence in TAL repertoires of *Xanthomonas oryzae* strains. *PLoS One* 2013, 8:e68464.
12. Cernadas RA, Camillo LR, Benedetti CE: Transcriptional analysis of the sweet orange interaction with the citrus canker pathogens *Xanthomonas axonopodis* pv. *citri* and *Xanthomonas axonopodis* pv. *aurantifolii*. *Mol Plant Pathol* 2008, 9:609–631.
13. Cernadas RA, Benedetti CE: Role of auxin and gibberellin in citrus canker development and in the transcriptional control of cell-wall remodeling genes modulated by *Xanthomonas axonopodis* pv. *citri*. *Plant Sci* 2009, 177:190–195.
14. Depuydt S, Hardtke CS: Hormone signalling crosstalk in plant growth regulation. *Curr Biol* 2011, 21:R365–R373.
15. Gu K, Yang B, Tian D, Wu L, Wang D, Sreekala C, Yang F, Chu Z, Wang GL, White FF, Yin Z: R gene expression induced by a type-III effector triggers disease resistance in rice. *Nature* 2005, 435:1122–1125.
16. White FF, Yang B: Host and pathogen factors controlling the rice-*Xanthomonas oryzae* interaction. *Plant Physiol* 2009, 150:1677–1686.
17. Marois E, van den Ackerveken G, Bonas U: The *Xanthomonas* type III effector protein AvrBs3 modulates plant gene expression and induces cell hypertrophy in the susceptible host. *Mol Plant Microbe Interact* 2002, 15:637–646.
18. Tatsuki M, Haji T, Yamaguchi M: The involvement of 1-aminocyclopropane-1-carboxylic acid synthase isogene, Pp-ACS1, in peach fruit softening. *J Exp Bot* 2006, 57:1281–1289.
19. Tacken E, Ireland H, Gunaseelan K, Karunairetnam S, Wang D, Schultz K, Bowen J, Atkinson RG, Johnston JW, Putterill J, Hellens RP, Schaffer RJ: The role of ethylene and cold temperature in the regulation of the apple *POLYGALACTURONASE1* gene and fruit softening. *Plant Physiol* 2010, 153:294–305.
20. Yin XR, Allan AC, Chen KS, Ferguson IB: Kiwifruit EIL and ERF genes involved in regulating fruit ripening. *Plant Physiol* 2010, 153:1280–1292.
21. Domingues MN, de Souza TA, Cernadas RA, de Oliveira ML, Docena C, Farah CS, Benedetti CE: The *Xanthomonas citri* effector protein PthA interacts with citrus proteins involved in nuclear transport, protein folding and ubiquitination associated with DNA repair. *Mol Plant Pathol* 2010, 11:663–675.
22. de Souza TA, Soprano AS, de Lira NP, Quaresma AJ, Pauletti BA, Paes Leme AF, Benedetti CE: The TAL effector PthA4 interacts with nuclear factors involved in RNA-dependent processes including a HMG protein that selectively binds poly(U) RNA. *PLoS One* 2012, 7:e32305.
23. Domingues MN, Campos BM, de Oliveira ML, de Mello UQ, Benedetti CE: TAL effectors target the C-terminal domain of RNA polymerase II (CTD) by inhibiting the prolyl-isomerase activity of a CTD-associated cyclophilin. *PLoS One* 2012, 7:e41553.
24. Bennett MJ, Marchant A, Green HG, May ST, Ward SP, Millner PA, Walker AR, Schulz B, Feldmann KA: Arabidopsis AUX1 gene: a permease-like regulator of root gravitropism. *Science* 1996, 1273:948–950.
25. de Billy F, Grosjean C, May S, Bennett M, Cullimore JV: Expression studies on AUX1-like genes in *Medicago truncatula* suggest that auxin is required at two steps in early nodule development. *Mol Plant Microbe Interact* 2001, 14:267–277.
26. Vandenbussche F, Petrásek J, Zádníková P, Hoyerová K, Pesek B, Raz V, Swarup R, Bennett M, Zazímalová E, Benková E, van der Straeten D: The auxin influx carriers AUX1 and LAX3 are involved in auxin-ethylene interactions during apical hook development in *Arabidopsis thaliana* seedlings. *Development* 2010, 137:597–606.
27. Dereeper A, Guignon V, Blanc G, Audic S, Buffet S, Chevenet F, Dufayard JF, Guindon S, Lefort V, Lescot M, Claverie JM, Gascuel O: Phylogeny.fr: robust phylogenetic analysis for the non-specialist. *Nucleic Acids Res* 2008, 36(Web Server issue):W465–W469.
28. Du Z, Zhou X, Ling Y, Zhang Z, Su Z: agriGO: a GO analysis toolkit for the agricultural community. *Nucleic Acids Res* 2010, 38(Web Server issue):W64–W70.
29. Nishimura R, Ohmori M, Fujita H, Kawaguchi M: A Lotus basic leucine zipper protein with a RING-finger motif negatively regulates the developmental program of nodulation. *Proc Natl Acad Sci U S A* 2002, 99:15206–15210.
30. Wang H, Jones B, Li Z, Frasse P, Delalande C, Regad F, Chaabouni S, Latché A, Pech JC, Bouzayen M: The tomato Aux/IAA transcription factor IAA9 is involved in fruit development and leaf morphogenesis. *Plant Cell* 2005, 17:2676–2692.
31. Weller JL, Hecht V, Vander Schoor JK, Davidson SE, Ross JJ: Light regulation of gibberellin biosynthesis in pea is mediated through the COP1/HY5 pathway. *Plant Cell* 2009, 21:800–813.
32. Zhang Z, Li Q, Li Z, Staswick P, Wang M, Zhu Y, He Z: Dual regulation role of GH3.5 in salicylic acid and auxin signaling during *Arabidopsis-Pseudomonas syringae* interaction. *Plant Physiol* 2007, 145:450–464.
33. Zhou J, Tang X, Martin GB: The Pto kinase conferring resistance to tomato bacterial speck disease interacts with proteins that bind a cis-element of pathogenesis-related genes. *EMBO J* 1997, 16:3207–3218.
34. Doyle EL, Booher NJ, Standage DS, Voytas DF, Brendel VP, Vandyk JK, Bogdanove AJ: TAL Effector-Nucleotide Targeter (TALE-NT) 2.0: tools for TAL effector design and target prediction. *Nucleic Acids Res* 2012, 40: W117–W122.
35. Nambara E, Keith K, McCourt P, Naito S: A regulatory role for the *ABI3* gene in the establishment of embryo maturation in *Arabidopsis thaliana*. *Development* 1995, 121:629–636.
36. Nitsch LM, Oplaat C, Feron R, Ma Q, Wolters-Arts M, Hedden P, Mariani C, Vriezen WH: Abscisic acid levels in tomato ovaries are regulated by *LeNCED1* and *SlCYP707A1*. *Planta* 2009, 229:1335–1346.
37. Zeng Y, Zhao T, Kermode AR: A conifer ABI3-interacting protein plays important roles during key transitions of the plant life cycle. *Plant Physiol* 2013, 161:179–195.
38. Noël LD, Denancé N, Szurek B: Predicting promoters targeted by TAL effectors in plant genomes: from dream to reality. *Front Plant Sci* 2013, 4:333.
39. Tao LZ, Cheung AY, Wu HM: Plant Rac-like GTPases are activated by auxin and mediate auxin-responsive gene expression. *Plant Cell* 2002, 14:2745–2760.
40. Sun A, Tawfik O, Gayed B, Thrasher JB, Hoestje S, Li C, Li B: Aberrant expression of SWI/SNF catalytic subunits BRG1/BRM is associated with tumor development and increased invasiveness in prostate cancers. *Prostate* 2007, 67:203–213.
41. O'Donoghue EM, Somerfield SD, Sinclair BK, Coupe SA: Xyloglucan endotransglycosylase: a role after growth cessation in harvested asparagus. *Aust J Plant Physiol* 2001, 28:349–361.
42. Husbands A, Bell EM, Shuai B, Smith HM, Springer PS: LATERAL ORGAN BOUNDARIES defines a new family of DNA-binding transcription factors

and can interact with specific bHLH proteins. *Nucleic Acids Res* 2007, 35:6663–6671.
1. Fraissinet-Tachet L, Baltz R, Chong J, Kauffmann S, Fritig B, Saindrenan P: Two tobacco genes induced by infection, elicitor and salicylic acid encode glucosyltransferases acting on phenylpropanoids and benzoic acid derivatives, including salicylic acid. *FEBS Lett* 1998, 437:319–323.
2. Igarashi D, Ishida S, Fukazawa J, Takahashi Y: 14-3-3 proteins regulate intracellular localization of the bZIP transcriptional activator RSG. *Plant Cell* 2001, 13:2483–2497.
3. Zhang ZT, Zhou Y, Li Y, Shao SQ, Li BY, Shi HY, Li XB: Interactome analysis of the six cotton 14-3-3 s that are preferentially expressed in fibres and involved in cell elongation. *J Exp Bot* 2010, 61:3331–3344.
4. Moriuchi H, Okamoto C, Nishihama R, Yamashita I, Machida Y, Tanaka N: Nuclear localization and interaction of RolB with plant 14-3-3 proteins correlates with induction of adventitious roots by the oncogene rolB. *Plant J* 2004, 38:260–275.
5. Vialart G, Hehn A, Olry A, Ito K, Krieger C, Larbat R, Paris C, Shimizu B, Sugimoto Y, Mizutani M, Bourgaud F: A 2-oxoglutarate-dependent dioxygenase from *Ruta graveolens* L. exhibits p-coumaroyl CoA 2'-hydroxylase activity (C2'H): a missing step in the synthesis of umbelliferone in plants. *Plant J* 2012, 70:460–470.
6. Itoh H, Tanaka-Ueguchi M, Kawaide H, Chen X, Kamiya Y, Matsuoka M: The gene encoding tobacco gibberellin 3beta-hydroxylase is expressed at the site of GA action during stem elongation and flower organ development. *Plant J* 1999, 20:15–24.
7. Beyene G, Foyer CH, Kunert KJ: Two new cysteine proteinases with specific expression patterns in mature and senescent tobacco (*Nicotiana tabacum* L.) leaves. *J Exp Bot* 2006, 57:1431–1443.
8. Zhang XM, Wang Y, Lv XM, Li H, Sun P, Lu H, Li FL: NtCP56, a new cysteine protease in *Nicotiana tabacum* L., involved in pollen grain development. *J Exp Bot* 2009, 60:1569–1577.
9. Yang ZN, Ye XR, Molina J, Roose ML, Mirkov TE: Sequence analysis of a 282-kilobase region surrounding the citrus Tristeza virus resistance gene (*Ctv*) locus in *Poncirus trifoliata* L. *Raf. Plant Physiol* 2003, 131:482–492.
10. Pnueli L, Gutfinger T, Hareven D, Ben-Naim O, Ron N, Adir N, Lifschitz E: Tomato SP-interacting proteins define a conserved signaling system that regulates shoot architecture and flowering. *Plant Cell* 2001, 13:2687–2702.
11. Raíces M, Gargantini PR, Chinchilla D, Crespi M, Téllez-Iñón MT, Ulloa RM: Regulation of CDPK isoforms during tuber development. *Plant Mol Biol* 2003, 52:1011–1024.
12. Chen Y, Liu Z, Halterman DA: Molecular determinants of resistance activation and suppression by *Phytophthora infestans* effector IPI-O. *PLoS Pathog* 2012, 8:e1002595.
13. Radwan O, Mouzeyar S, Nicolas P, Bouzidi MF: Induction of a sunflower CC-NBS-LRR resistance gene analogue during incompatible interaction with *Plasmopara halstedii*. *J Exp Bot* 2005, 56:567–575.
14. Durrant WE, Rowland O, Piedras P, Hammond-Kosack KE, Jones JD: cDNA-AFLP reveals a striking overlap in race-specific resistance and wound response gene expression profiles. *Plant Cell* 2000, 12:963–977.
15. Yordanov YS, Regan S, Busov V: Members of the LATERAL ORGAN BOUNDARIES DOMAIN transcription factor family are involved in the regulation of secondary growth in Populus. *Plant Cell* 2010, 22:3662–3677.
16. Gao H, Wu X, Chai J, Han Z: Crystal structure of a TALE protein reveals an extended N-terminal DNA binding region. *Cell Res* 2012, 22:1716–1720.
17. Meckler JF, Bhakta MS, Kim MS, Ovadia R, Habrian CH, Zykovich A, Yu A, Lockwood SH, Morbitzer R, Elsäesser J, Lahaye T, Segal DJ, Baldwin EP: Quantitative analysis of TALE-DNA interactions suggests polarity effects. *Nucleic Acids Res* 2013, 41:4118–4128.
18. Sugio A, Yang B, Zhu T, White FF: Two type III effector genes of *Xanthomonas oryzae* pv. *oryzae* control the induction of the host genes OsTFIIAγ1 and OsTFX1 during bacterial blight of rice. *Proc Natl Acad Sci U S A* 2007, 104:10720–10725.
19. Streubel J, Pesce C, Hutin M, Koebnik R, Boch J, Szurek B: Five phylogenetically close rice SWEET genes confer TAL effector-mediated susceptibility to Xanthomonas oryzae pv. oryzae. *New Phytol* 2013, 200:808–819.
20. Domingo C, Andrés F, Tharreau D, Iglesias DJ, Talón M: Constitutive expression of OsGH3.1 reduces auxin content and enhances defense response and resistance to a fungal pathogen in rice. *Mol Plant Microbe Interact* 2009, 22:201–210.
21. Navarro L, Dunoyer P, Jay F, Arnold B, Dharmasiri N, Estelle M, Voinnet O, Jones JD: A plant miRNA contributes to antibacterial resistance by repressing auxin signaling. *Science* 2006, 312:436–439.
22. Wang D, Pajerowska-Mukhtar K, Culler AH, Dong X: Salicylic acid inhibits pathogen growth in plants through repression of the auxin signaling pathway. *Curr Biol* 2007, 17:1784–1790.
23. Fu J, Liu H, Li Y, Yu H, Li X, Xiao J, Wang S: Manipulating broad-spectrum disease resistance by suppressing pathogen-induced auxin accumulation in rice. *Plant Physiol* 2011, 155:589–602.
24. Liu H, Wang S, Yu X, Yu J, He X, Zhang S, Shou H, Wu P: ARL1, a LOB-domain protein required for adventitious root formation in rice. *Plant J* 2005, 43:47–56.
25. Campos BM, Sforça ML, Ambrosio AL, Domingues MN, Brasil de Souza T de A, Barbosa JA, Paes Leme AF, Perez CA, Whittaker SB, Murakami MT, Zeri AC, Benedetti CE: A redox 2-cys mechanism regulates the catalytic activity of divergent cyclophilins. *Plant Physiol* 2013, 162:1311–1323.
26. Inukai Y, Sakamoto T, Ueguchi-Tanaka M, Shibata Y, Gomi K, Umemura I, Hasegawa Y, Ashikari M, Kitano H, Matsuoka M: Crown rootless1, which is essential for crown root formation in rice, is a target of an AUXIN RESPONSE FACTOR in auxin signaling. *Plant Cell* 2005, 17:1387–1396.
27. Gallego-Giraldo L, García-Martínez JL, Moritz T, López-Díaz I: Flowering in tobacco needs gibberellins but is not promoted by the levels of active GA1 and GA4 in the apical shoot. *Plant Cell Physiol* 2007, 48:615–625.
28. Nakata M, Yuasa T, Takahashi Y, Ishida S: CDPK1, a calcium-dependent protein kinase, regulates transcriptional activator RSG in response to gibberellins. *Plant Signal Behav* 2009, 4:372–374.
29. da Silva A, Ferro JA, Reinach FC, Farah CS, Furlan LR, Quaggio RB, Monteiro-Vitorello CB, Van Sluys MA, Almeida NF, Alves LM, do Amaral AM, Bertolini MC, Camargo LE, Camarotte G, Cannavan F, Cardozo J, Chambergo F, Ciapina LP, Cicarelli RM, Coutinho LL, Cursino-Santos JR, El-Dorry H, Faria JB, Ferreira AJ, Ferreira RC, Ferro MI, Formighieri EF, Franco MC, Greggio CC, Gruber A, *et al*: Comparison of the genomes of two *Xanthomonas* pathogens with differing host specificities. *Nature* 2002, 417:459–463.
30. de Oliveira ML, Lima Silva CC, Abe VY, Costa MG, Cernadas RA, Benedetti CE: Increased resistance against citrus canker mediated by a citrus MAP kinase. *Mol Plant Microbe Interact* 2013, 26:1190–1199.
31. de Oliveira MLP, Febres VJ, Costa MGC, Moore GA, Otoni WC: High-efficiency *Agrobacterium*-mediated transformation of citrus via sonication and vacuum infiltration. *Plant Cell Rep* 2009, 28:387–395.
32. Jefferson RA, Kavanagh TA, Bevan MW: GUS fusions: beta-glucuronidase as a sensitive and versatile gene fusion marker, in higher plants. *EMBO J* 1987, 6:3901–3907.
33. Altenhoff AM, Dessimoz C: Phylogenetic and functional assessment of orthologs inference projects and methods. *PLoS Comput Biol* 2009, 5:e1000262.
34. Wolf YI, Koonin EV: A tight link between orthologs and bidirectional best hits in bacterial and archaeal genomes. *Genome Biol Evol* 2012, 4:1286–1294.
35. Altschul SF, Gish W, Miller W, Myers EW, Lipman DJ: Basic local alignment search tool. *J Mol Biol* 1990, 215:403–410.
36. Korhonen J, Martinmäki P, Pizzi C, Rastas P, Ukkonen E: MOODS: fast search for position weight matrix matches in DNA sequences. *Bioinformatics* 2009, 25:3181–3182.
37. Solovyev VV, Shahmuradov IA: PromH: promoters identification using orthologous genomic sequences. *Nucleic Acids Res* 2003, 31:3540–3545.
38. Blanco E, Messeguer X, Smith TF, Guigó R: Transcription factor map alignment of promoter regions. *PLoS Comput Biol* 2006, 2:e49.
39. Roy S, Kagda M, Judelson HS: Genome-wide prediction and functional validation of promoter motifs regulating gene expression in spore and infection stages of *Phytophthora infestans*. *PLoS Pathog* 2013, 9:e1003182.
40. Shahmuradov IA, Solovyev VV, Gammerman AJ: Plant promoter prediction with confidence estimation. *Nucleic Acids Res* 2005, 33:1069–1076.

doi:10.1186/1471-2164-15-157
Cite this article as: Pereira *et al.*: Identification of putative TAL effector targets of the citrus canker pathogens shows functional convergence underlying disease development and defense response. *BMC Genomics* 2014 15:157.

ANEXO III – Artigo publicado no ano de 2013 na revista '*Plant Physiology*', no qual participo como segunda autora. Neste trabalho, contribuí com experimentos que resultaram na Figura 6, onde mostramos que a diminuição de CsMAF1 nas lesões de cancro se correlaciona com a presença de PthA4.

Citrus MAF1, a Repressor of RNA Polymerase III, Binds the *Xanthomonas citri* Canker Elicitor PthA4 and Suppresses Citrus Canker Development[1]

Adriana Santos Soprano, Valeria Yukari Abe, Juliana Helena Costa Smetana, and Celso Eduardo Benedetti*

Laboratório Nacional de Biociências, Centro Nacional de Pesquisa em Energia e Materiais, CEP 13083–970, Campinas, São Paulo, Brazil

Transcription activator-like (TAL) effectors from *Xanthomonas* species pathogens act as transcription factors in plant cells; however, how TAL effectors activate host transcription is unknown. We found previously that TAL effectors of the citrus canker pathogen *Xanthomonas citri*, known as PthAs, bind the carboxyl-terminal domain of the sweet orange (*Citrus sinensis*) RNA polymerase II (Pol II) and inhibit the activity of CsCYP, a cyclophilin associated with the carboxyl-terminal domain of the citrus RNA Pol II that functions as a negative regulator of cell growth. Here, we show that PthA4 specifically interacted with the sweet orange MAF1 (CsMAF1) protein, an RNA polymerase III (Pol III) repressor that controls ribosome biogenesis and cell growth in yeast (*Saccharomyces cerevisiae*) and human. CsMAF1 bound the human RNA Pol III and rescued the yeast *maf1* mutant by repressing $tRNA^{His}$ transcription. The expression of PthA4 in the *maf1* mutant slightly restored $tRNA^{His}$ synthesis, indicating that PthA4 counteracts CsMAF1 activity. In addition, we show that sweet orange RNA interference plants with reduced CsMAF1 levels displayed a dramatic increase in tRNA transcription and a marked phenotype of cell proliferation during canker formation. Conversely, CsMAF1 overexpression was detrimental to seedling growth, inhibited tRNA synthesis, and attenuated canker development. Furthermore, we found that PthA4 is required to elicit cankers in sweet orange leaves and that depletion of CsMAF1 in *X. citri*-infected tissues correlates with the development of hyperplastic lesions and the presence of PthA4. Considering that CsMAF1 and CsCYP function as canker suppressors in sweet orange, our data indicate that TAL effectors from *X. citri* target negative regulators of RNA Pol II and Pol III to coordinately increase the transcription of host genes involved in ribosome biogenesis and cell proliferation.

Citrus canker, caused by *Xanthomonas citri*, affects most commercial citrus cultivars, causing significant economic losses worldwide. The bacterium strongly enhances the division and enlargement of plant cells, leading to the formation of water-soaked lesions and raised pustules with extensive epidermal rupture on leaves, stems, and fruit (Brunings and Gabriel, 2003).

The pathogenicity of *X. citri* and its ability to promote cell hypertrophy and hyperplasia depend on the integrity and function of the type III secretion system, which translocates effector proteins into the host cells, and on the action of a special class of *Xanthomonas* spp. effector proteins known as transcriptional activator-like (TAL) effectors (Brunings and Gabriel, 2003; Kay and Bonas, 2009; Guo et al., 2011; Dunger et al., 2012). For instance, the PthA protein, the main TAL effector from *X. citri*, is required for bacterial growth and the induction of cell hypertrophy and hyperplasia in citrus leaves (Swarup et al., 1992; Duan et al., 1999; Al-Saadi et al., 2007; Yan and Wang, 2012). Because rupture of the epidermis significantly favors pathogen spreading and disease dissemination, PthA and related proteins also have been suggested to enhance pathogen fitness in field conditions (Brunings and Gabriel, 2003; Wichmann and Bergelson, 2004).

TAL effectors function as transcription activators in plant cells; however, they can act as pathogenicity or avirulence factors depending on the genes they activate (Gu et al., 2005; Kay et al., 2007; Römer et al., 2007). TAL effectors recognize promoter elements of host genes through their internal repetitive DNA-binding domain, a superhelical structure that embraces the DNA target sequence and provides the specificity for the interactions (Murakami et al., 2010; Deng et al., 2012; Mak et al., 2012). Although the specificity, DNA-binding mode, and numerous targets of TAL effectors have been elucidated, the molecular mechanism by which TAL effectors modulate transcription in the host is still poorly understood.

We addressed this question considering the hypothesis that, to act as transcriptional activators, TAL effectors would necessarily interact with components of the host basal transcriptional machineries. Accordingly, we

[1] This work was supported by the Fundação de Amparo à Pesquisa do Estado de São Paulo (grants 2010/00634-1 and 2011/20468-1) and the Conselho Nacional de Desenvolvimento Científico e Tecnológico.

* Address correspondence to celso.benedetti@lnbio.cnpem.br.

The author responsible for distribution of materials integral to the findings presented in this article in accordance with the policy described in the Instructions for Authors (www.plantphysiol.org) is: Celso Eduardo Benedetti (celso.benedetti@lnbio.cnpem.br).

www.plantphysiol.org/cgi/doi/10.1104/pp.113.224642

identified numerous sweet orange (*Citrus sinensis*) proteins implicated in nuclear import, transcriptional regulation, DNA repair, and mRNA stabilization as possible targets of the *X. citri* PthA proteins (Domingues et al., 2010; de Souza et al., 2012). Moreover, we found that some of the PthA interactors form protein complexes and that distinct PthA proteins, although highly homologous to each other, have differential binding specificity or affinity to certain host targets (Domingues et al., 2010; de Souza et al., 2012). We showed that, while PthA2 and PthA3 preferentially interacted with the sweet orange protein complex comprising the cyclophilin CsCYP, thioredoxin CsTDX, and the CsUEV/UBC13 heterodimer, PthA4 selectively bound to CsVIP2, the citrus homolog of the Arabidopsis (*Arabidopsis thaliana*) VirE-INTERACTING PROTEIN2 (Domingues et al., 2010; de Souza et al., 2012). Importantly, we found that not only CsCYP and CsTDX, but all PthA variants, interact with the C-terminal domain of the citrus RNA polymerase II (CTD), a regulatory domain that plays critical roles in all phases of the transcription cycle (Sobennikova et al., 2007; Domingues et al., 2012; Campos et al., 2013). In addition, we showed that CsCYP complements the function of Ess1, a yeast peptidyl-prolyl cis-trans-isomerase that modulates the rates of RNA polymerase II (Pol II) transcription through the isomerization of Pro residues of the CTD heptad repeats (Domingues et al., 2012). Since PthA2 inhibits the peptidyl-prolyl cis-trans-isomerase activity of CsCYP, and depletion of CsCYP in citrus leaves enhances canker symptoms, we postulated that TAL effectors target negative regulators of transcription to promote cell growth (Domingues et al., 2012).

In line with this idea, we have identified the sweet orange MAF1 homolog (CsMAF1) as a PthA4-interacting protein (de Souza et al., 2012). MAF1 proteins are conserved from yeast to human and play a major role as negative regulators of RNA polymerase III (Pol III), which synthesizes small RNAs, tRNAs, and the 5S ribosomal (r) RNA. MAF1 binds to the clamp domain of RNA Pol III, restricting the recruitment of RNA Pol III and the assembly of the initiation factors TFIIIB, TATA-binding protein, and Brf1 to promoter sites, preventing not only the initiation and elongation but the reinitiation of transcription (Boguta et al., 1997; Upadhya et al., 2002; Desai et al., 2005; Rollins et al., 2007; Vannini et al., 2010).

The association of MAF1 with RNA Pol III is also conserved between yeast and mammals, and it is controlled by reverse phosphorylation reactions mediated by the protein phosphatases PP2A and PP4 and several kinases, including PKA and TARGET OF RAPAMYCIN (TOR; Moir et al., 2006; Oficjalska-Pham et al., 2006; Huber et al., 2009; Wei and Zheng, 2010; Michels, 2011, Oler and Cairns, 2012). Under normal or favorable growth conditions, MAF1 is inactivated by phosphorylation, allowing RNA Pol III transcription, ribosome biogenesis, and cell growth. However, under stress conditions, such as starvation, MAF1 becomes dephosphorylated, and this results in its binding to RNA Pol III, blocking transcription (Moir et al., 2006; Oficjalska-Pham et al., 2006; Roberts et al., 2006; Willis and Moir, 2007).

In both yeast (*Saccharomyces cerevisiae*) and animals, the TOR signaling pathway integrates environmental cues, such as stress signals and nutrient availability, into cell growth and proliferation (Mayer and Grummt, 2006; Willis and Moir, 2007; Wei and Zheng, 2010; Boguta and Graczyk, 2011; Oler and Cairns, 2012). Therefore, as rapid repression of RNA Pol III transcription becomes critical to cell survival during stress or nutrient starvation, MAF1, which is a common element of the yeast and human TOR signaling pathway, plays an important role in controlling ribosome biogenesis, cell growth, and proliferation (Pluta et al., 2001; Upadhya et al., 2002; Johnson et al., 2007). Moreover, since depletion of MAF1 activity in animal cells affected cell morphology and body size, and its overexpression suppressed cell growth and tRNA synthesis in proliferating cells, MAF1 is also considered a tumor-suppressor protein (Johnson et al., 2007; Shor et al., 2010; Rideout et al., 2012).

Although much is known about the function and regulation of MAF1 in yeast and human, the role played by this repressor in plants remains unclear. In fact, MAF1 from plants has not yet been reported. In addition, despite the fact that the TOR signaling pathway in plants has recently been shown to be conserved and also to regulate cell growth, ribosome biogenesis, and metabolism, the association of MAF1 with plant TOR kinases has not yet been described (John et al., 2011; Ren et al., 2011, 2012; Caldana et al., 2013).

Here, we show that CsMAF1, to our knowledge the first plant MAF1 protein to be characterized, specifically interacted with PthA4, bound the human RNA Pol III, and repressed $tRNA^{His}$ synthesis in yeast. Moreover, transgenic citrus with lower CsMAF1 levels accumulated tRNAs and developed much larger canker pustules than normal plants. On the other hand, overexpression of CsMAF1 attenuated canker symptoms and tRNA synthesis and was detrimental to seedling growth. In addition, in agreement with previous reports (Duan et al., 1999; Al-Saadi et al., 2007; Yan and Wang, 2012), we show that PthA4 was required to elicit cankers in sweet orange leaves and that depletion of CsMAF1 in *X. citri*-induced hyperplastic lesions correlates with the presence of PthA4. Thus, our data point to a role of CsMAF1 as a citrus canker suppressor and possibly a novel target of TAL effectors.

RESULTS

CsMAF1 Specifically Interacts with PthA4

We have previously identified CsMAF1 as a PthA4-interacting protein in a yeast two-hybrid screen (de Souza et al., 2012). To confirm this result and test the binding specificity of CsMAF1 to the *X. citri* TAL effectors, we performed additional yeast two-hybrid assays using the four PthA variants as baits. We found that CsMAF1 specifically interacted with PthA4 (Fig. 1A). To map the

PthA4 region that is responsible for this interaction, we tested various PthA4 domains, except the N terminus, which transactivates the yeast reporter genes (Domingues et al., 2010). The results show that the interaction between CsMAF1 and PthA4 appears to require the full-length PthA4 protein, since neither its DNA-binding domain (RD4) nor its Leu-rich repeat (LRR) region or its C-terminal domain plus 5.5 repeat units of the DNA-binding domain (5.5R) were sufficient for a strong interaction (Fig. 1, B and C). The interaction of CsMAF1 with the full-length PthA4 was further confirmed by glutathione *S*-transferase (GST) pulldown (Fig. 1D) and coimmunoprecipitation assays (Fig. 1E). Cell lysates of sweet orange epicotyls transformed with the *pthA4* gene were incubated with the anti-CsMAF1 or preimmune serum, and the immunoprecipitates were analyzed by western blot. We found that anti-CsMAF1, but not the preimmune serum, immunoprecipitated PthA4 transiently expressed in citrus cells, thereby confirming that PthA4 and CsMAF1 interact with each other in vivo (Fig. 1E).

CsMAF1 Shares Conserved Features with the Yeast and Human MAF1

CsMAF1 is a 26-kD protein that is 33% and 38% identical to the *S. cerevisiae* and human MAF1 proteins,

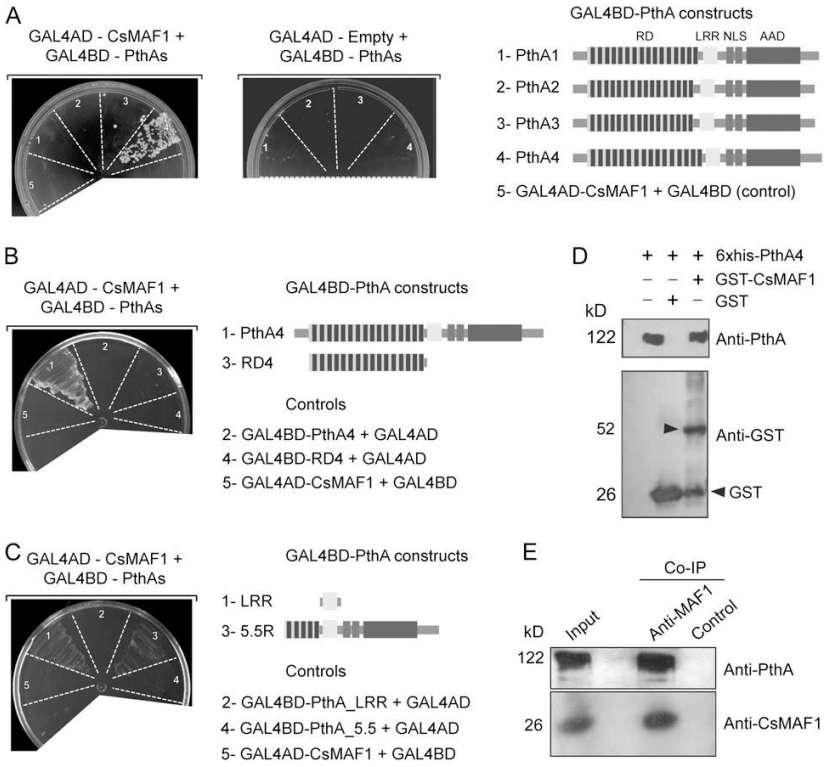

Figure 1. Specific interaction between CsMAF1 and PthA4. A, Yeast two-hybrid assays showing that CsMAF1 specifically interacts with PthA4. Full-length CsMAF1 fused to the yeast GAL4-AD domain or the control plasmid (GAL4AD) was moved into yeast cells carrying one of the four PthA variants (PthA1–PthA4) fused to the GAL4-BD domain (GAL4BD-PthA constructs). The PthA proteins, which lack the first 128 residues and carry the entire repetitive DNA-binding domain (RD), invariable LRR region (LRR), C terminus with the nuclear localization signals (NLS), as well as the acidic activation domain (AAD), are schematically represented. B and C, No interaction was observed between CsMAF1 and RD4 (B), whereas weak interactions were detected with the LRR and the C-terminal domain plus 5.5 repeat units (5.5R) of the DNA-binding domain (C). D, Western-blot detection of the eluted fraction of a GST-pulldown assay using the purified 6xHis-PthA4 as prey and immobilized GST or GST-CsMAF1 as bait, confirming the interaction between PthA4 and CsMAF1. Arrowheads indicate bands corresponding to the GST-CsMAF1 fusion protein (approximately 52 kD) and GST alone (approximately 26 kD) detected by the GST antiserum. PthA4 (approximately 122 kD) was detected by the anti-PthA serum. E, Coimmunoprecipitation (Co-IP) assay of PthA4 and CsMAF1. Cell extracts of citrus epicotyls transiently expressing PthA4 (input) were incubated with the anti-CsMAF1 or preimmune serum (control) and protein A-Sepharose. After washing the beads, bound proteins were resolved on a 10% SDS-polyacrylamide gel and probed with the indicated antibodies. PthA4 was detected in the coimmunoprecipitation performed with the anti-CsMAF1 but not with the preimmune serum.

respectively (Fig. 2A). Although shorter than the yeast and mammalian counterparts, CsMAF1 carries the two signature sequences that characterize the MAF protein family and a nuclear localization signal that is conserved between the yeast and human proteins. In addition, CsMAF1 carries one Thr (Thr-62) and four Ser residues (Ser-59, Ser-64, Ser-66, and Ser-73) that are phosphorylated in the human and/or yeast proteins (Michels, 2011), suggesting that CsMAF1 is similarly regulated by phosphorylation (Fig. 2A). Accordingly, as the yeast and human MAF1 proteins migrate as multiple bands on SDS gels due to their hyperphosphorylation state (Oficjalska-Pham et al., 2006; Huber et al., 2009; Gajda et al., 2010), CsMAF1 from citrus leaves was predominantly detected as a double band on western blots (Fig. 2B).

To test whether CsMAF1 is a phosphoprotein, the recombinant CsMAF1 was incubated with PKA, one of the main kinases that phosphorylates the yeast MAF1 (Moir et al., 2006, 2012). We found that PKA not only phosphorylates CsMAF1, but this causes the protein to migrate with a relatively higher molecular mass, confirming that the slow-migrating CsMAF1 band detected on western blots corresponds to a phosphorylated form of CsMAF1 (Fig. 2C).

To further investigate the relatedness of CsMAF1 with other MAF1 proteins, a phylogenetic analysis was performed (Fig. 2D). We found that CsMAF1, which is the only MAF1 protein in the citrus genome, forms a branch with several uncharacterized plant MAF1 homologs belonging to dicot species. Interestingly, CsMAF1 is

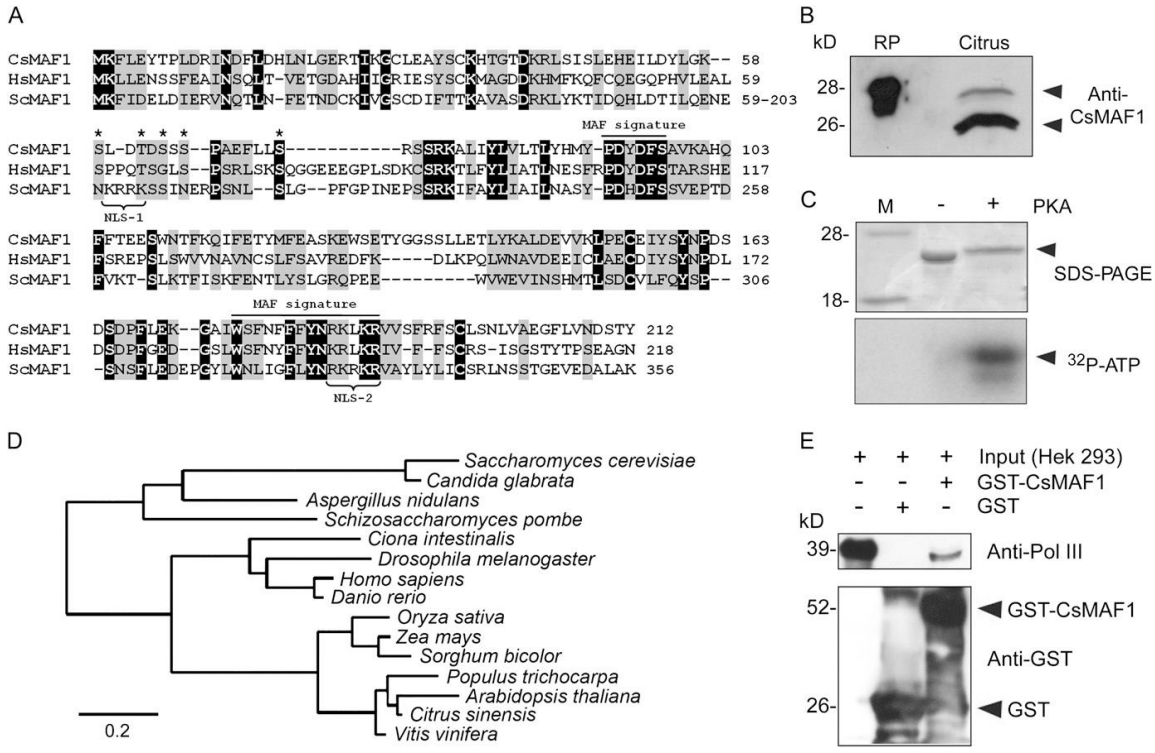

Figure 2. CsMAF1 is a homolog of the human and yeast MAF1 proteins. A, Protein sequence alignment of CsMAF1 with the human (HsMAF1) and yeast (ScMAF1) proteins performed by ClustalW. Identical and similar residues are shaded in black and gray, respectively. The two MAF1 signature sequences, which are conserved in CsMAF1, and the nuclear localization signals (NLS) are indicated. Asterisks indicate Thr and Ser residues that are phosphorylated in the human and/or yeast MAF1 proteins. The sequence comprising amino acid residues 60 to 202 of the yeast protein, as well as some of the C-terminal residues of all three proteins, were omitted to improve the alignment. B, Immunoblot detection of recombinant CsMAF1 (RP) and CsMAF1 from cell extracts of sweet orange leaves (Citrus). Arrowheads indicate two major forms of CsMAF1 in citrus cell extracts. C, SDS-PAGE showing that CsMAF1 phosphorylated by PKA (+) migrates slower than nonphosphorylated (2) CsMAF1 (top panel); the bottom panel shows the radioactive detection of the phosphorylation reaction with [^{32}P]ATP. Arrows indicate the CsMAF1 protein, whereas M indicates the molecular weight marker. D, Phylogenetic analysis of MAF1 proteins from plants (monocots and dicots), animals, yeast, and fungi, showing that CsMAF1 clusters with uncharacterized MAFs from dicot plants. E, GST-pulldown assay showing that GST-CsMAF1, but not GST, binds to the human RNA Pol III from lysed Hek 293 cells. Human RNA Pol III was detected by the monoclonal antibody raised against the human RNA Pol III 39-kD subunit, whereas CsMAF1 was detected by an anti-GST serum (arrowheads).

more closely related to the human than to the yeast MAF1 (Fig. 2D). Given the sequence similarities of CsMAF1 to the human protein, and the availability of a monoclonal antibody raised against the human RNA Pol III 39-kD subunit, we tested whether CsMAF1 could bind the human RNA Pol III. As shown in Figure 2E, CsMAF1 interacted with the RNA Pol III from Hek 293 cells in a GST-pulldown assay, indicating that it is the homolog of human MAF1.

CsMAF1 Inhibits tRNA^{His} Synthesis in the Yeast *maf1* Mutant

The *S. cerevisiae maf1* deletion mutant shows elevated levels of tRNAs, including tRNA^{His}, as a result of the lack of RNA Pol III repression (Boguta et al., 1997; Pluta et al., 2001; Kwapisz et al., 2002). To test whether CsMAF1 could function as an RNA Pol III repressor, we expressed the *CsMAF1* gene in the yeast *maf1* mutant upon copper induction (Fig. 3A) and measured the tRNA^{His} levels in the transformant relative to wild-type and untransformed *maf1* cells. We found that even in the absence of copper, where the accumulation of CsMAF1 was not detected (Fig. 3A), the tRNA^{His} levels in *maf1* cells carrying the *CsMAF1* gene were significantly reduced in comparison with the levels found in untransformed *maf1* cells (Fig. 3B), suggesting that very low levels of CsMAF1 are sufficient to repress RNA Pol III transcription in yeast. Accordingly, the tRNA^{His} levels, which are high in *maf1* relative to wild-type cells, were almost depleted in *maf1* cells treated with copper, indicating that CsMAF1 is the functional homolog of yeast MAF1. Surprisingly, when we coexpressed CsMAF1 with PthA4 in the *maf1* mutant, we observed a slight increase in the tRNA^{His} levels, suggesting that, upon interaction with CsMAF1, PthA4 counteracts the repressor role of CsMAF1 on RNA Pol III transcription (Fig. 3C).

CsMAF1 Controls tRNA Synthesis, Cell Growth, and Canker Development in Sweet Orange

To begin investigating the role of CsMAF1 in RNA Pol III transcription and canker formation, the *CsMAF1* gene was silenced in sweet orange plants. Transgenic lines carrying the *CsMAF1* RNA interference (RNAi) hairpin construct showed reduced levels of the CsMAF1 protein (Fig. 4A). Measurements of the relative area of the upper and lower bands of CsMAF1 revealed that, on average, there was an approximately 45% reduction in the CsMAF1 levels in the RNAi relative to control plants (Fig. 4B).

Next, we determined the relative levels of the tRNA^{His}, tRNA^{Leu}, and tRNA^{Thr}, whose synthesis is controlled by MAF1 in yeast and mammals (Pluta et al., 2001; Cieśla et al., 2007; Shor et al., 2010). Consistent with the reduction in the CsMAF1 levels, the synthesis of the three tRNAs examined, particularly tRNA^{Thr}, was significantly enhanced in the RNAi relative to untransformed plants, indicating that CsMAF1 acts as an RNA

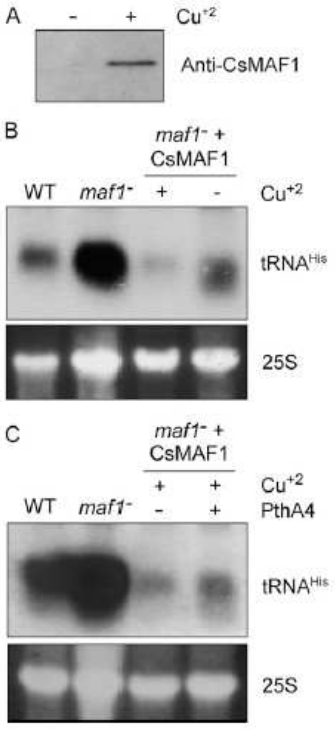

Figure 3. CsMAF1 inhibits tRNA^{His} synthesis in the yeast *maf1* mutant. A, The sweet orange *MAF1* gene was expressed in the yeast *maf1* mutant as a GST fusion (approximately 52 kD) under the control of a copper-induced promoter. After induction with copper sulfate (Cu^{+2}), CsMAF1 was purified and detected with the anti-CsMAF1 serum. B, Northern analysis of tRNA^{His} in the wild-type yeast (WT), the *maf1* deletion mutant (*maf1*$^-$), and *maf1*$^-$ cells complemented with CsMAF1 grown in the presence or absence of copper sulfate (top panel). The expression of CsMAF1 in the *maf1* mutant significantly reduces tRNA^{His} synthesis, which is elevated in the mutant, relative to the wild-type cells. However, upon copper treatment, the tRNA^{His} levels in the mutant are substantially lower, indicating that CsMAF1 complements the function of the yeast MAF1 protein. The 25S rRNA was used as a loading control (bottom panel). C, Northern analysis showing that CsMAF1 represses tRNA^{His} transcription in the *maf1* mutant, whereas its coexpression with PthA4 slightly restores tRNA^{His} synthesis, suggesting that PthA4 inhibits CsMAF1 activity (top panel). The 25S rRNA was used as a loading control (bottom panel).

Pol III repressor in citrus cells (Fig. 4C). Since CsMAF1 specifically interacted with PthA4, which elicits tumors on citrus (Duan et al., 1999), we examined its role in canker development. We found that the citrus plants with reduced levels of CsMAF1 showed a dramatic increase in the number and size of hyperplastic and eruptive lesions caused by *X. citri* infection (Fig. 4D). Canker pustules developed in the RNAi plants were much larger and showed more rupture of the epidermis than those of control plants, indicating that CsMAF1 restricts canker formation in sweet orange (Fig. 4D).

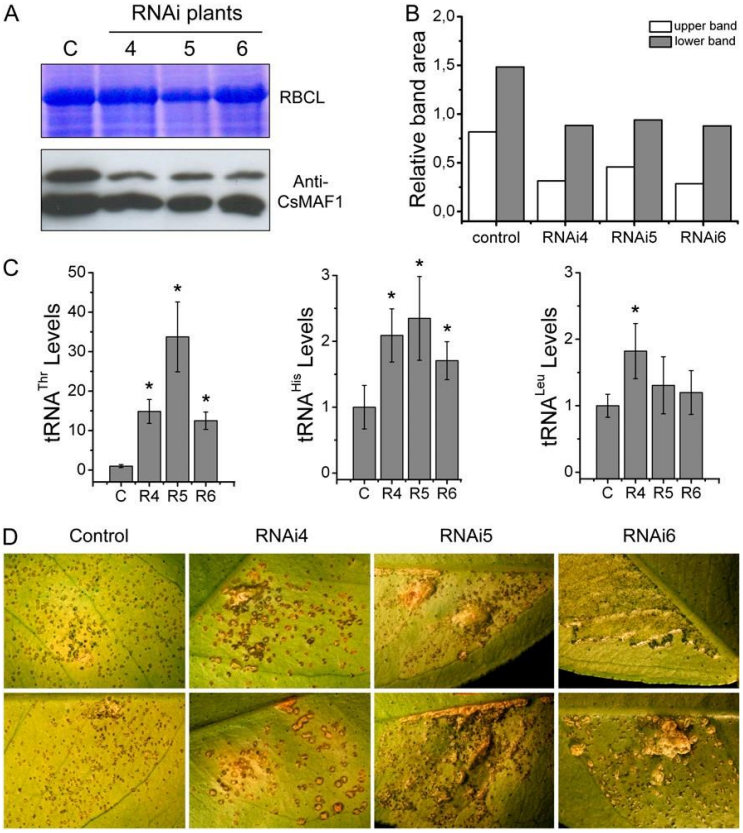

Figure 4. Silencing of CsMAF1 enhances tRNA synthesis and canker development. A, Transgenic plants carrying the CsMAF1 hairpin construct were analyzed by western blot using the anti-CsMAF1 serum (anti-CsMAF1). The CsMAF1 RNAi plants (4, 5, and 6) showed reduced levels of CsMAF1 protein relative to an untransformed control (C). Protein loads were controlled by Coomassie Brilliant Blue staining of the bands corresponding to the large subunit of ribulose-1,5-bisphosphate carboxylase (RBCL). B, Plot of the relative band area of the corresponding top (slow-migrating) and bottom (fast-migrating) bands depicted in A. Measurements of the band areas (in pixels) were performed using ImageJ software. C, Quantitative reverse transcription-PCR analysis of the relative abundance of $tRNA^{His}$, $tRNA^{Leu}$, and $tRNA^{Thr}$ in the CsMAF1 RNAi lines (R4, R5, and R6) and in a control plant (C). The silenced lines showed a significant increase in tRNA expression relative to the control. Asterisks indicate that the differences between the control and transgenic means are statistically significant at $P = 0.05$. D, Sweet orange leaves of control and three CsMAF1 RNAi plants challenged with *X. citri* (approximately 10^4 cells), showing that canker lesions were substantially enhanced in the RNAi compared with control plants. Photographs at 10× magnification were taken 14 d after bacterial infiltration.

To further examine the role of CsMAF1 in canker development, CsMAF1 was overexpressed in sweet orange. Interestingly, we noticed that most of the shoots that emerged from the epicotyls transformed with the *35S::CsMAF1* construct showed a senescing and growth-arrest phenotype, suggesting that CsMAF1 overexpression is lethal or detrimental to seedling growth. In fact, significantly higher levels of CsMAF1 were found in more stunted and yellowing shoots than in more healthy green shoots (Fig. 5A), whereas in plantlets recovered from the selection medium, the levels of CsMAF1 were similar to that of untransformed plants (Fig. 5, B and C). Moreover, we found that in developing shoots, CsMAF1 was detected as a major fast-migrating band corresponding to the dephosphorylated form of CsMAF1, which may reflect the growing and dividing nature of the shoot cells (Fig. 5A). However, among the selected transgenic lines carrying the *35S::CsMAF1* construct, only line 34 showed a relatively higher level of the fast-migrating band of CsMAF1 compared with control plants (Fig. 5, B and C). This transgenic line expressed less $tRNA^{His}$ and $tRNA^{Leu}$ (Fig. 5D) and was less susceptible to *X. citri* infection than control plants (Fig. 5E). Canker lesions developed in line 34 were smaller and showed less epidermal rupture than those in control plants (Fig. 5E), supporting the idea that CsMAF1 restricts canker development.

Taken together, these results indicate that CsMAF1 is a key factor controlling cell growth and proliferation in sweet orange via the repression of RNA Pol III.

CsMAF1 Depletion in Hyperplastic Canker Lesions Correlates with the Presence of PthA4

The results obtained with the transgenic plants led us to investigate the levels of CsMAF1 during canker formation. We found that the levels of CsMAF1 protein were remarkably reduced in hyperplastic canker lesions developed in leaves of normal sweet orange plants (Fig. 6A).

To know whether this depletion was dependent on PthA4, we generated a *X. citri* mutant (strain 306) lacking the *pthA4* gene by homologous recombination. In agreement with previous works showing that PthA4 is required to elicit cankers in grapefruit (*Citrus paradisi*) plants (Duan et al., 1999; Al Saadi et al., 2007; Yan and Wang, 2012), we found that the *pthA4* deletion mutant was not pathogenic to all sweet orange varieties tested, including cv 'Pera', ' Natal', ' Valencia', and 'Hamlin',

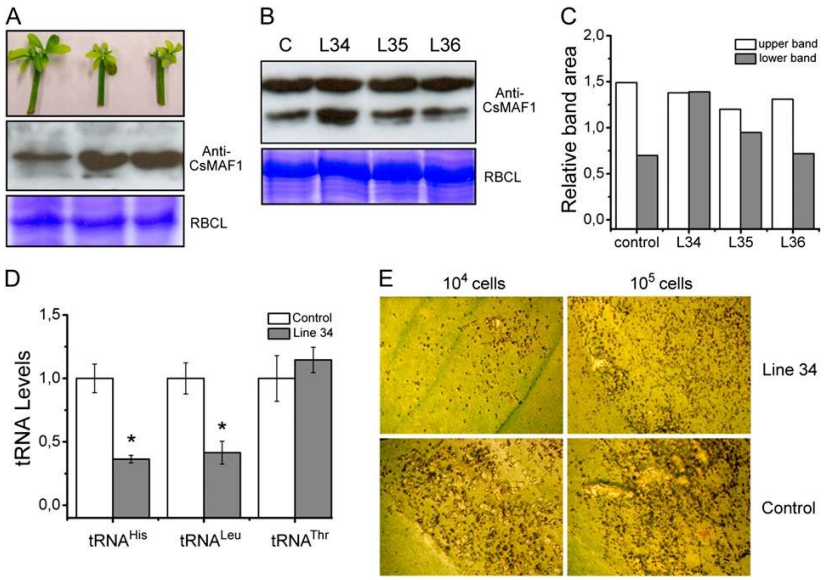

Figure 5. Overexpression of CsMAF1 correlates with seedling growth arrest and the inhibition of canker formation. A, Sweet orange epicotyls transformed with the *35S::CsMAF1* construct showing higher levels of CsMAF1 in more stunted and senescing shoots. RBCL, Ribulose-1,5-bisphosphate carboxylase. B, CsMAF1 levels in young leaves of the transgenic lines recovered after selection for the *35S::CsMAF1* construct. Only line 34 shows a relatively higher level of CsMAF1. C, Control plant. C, Plot of the relative band area of the corresponding top (slow-migrating) and bottom (fast-migrating) bands depicted in B, measured by ImageJ software. D, Quantitative reverse transcription-PCR analysis of the relative abundance of $tRNA^{His}$, $tRNA^{Leu}$, and $tRNA^{Thr}$ in line 34 and a control plant, showing that line 34 accumulates less $tRNA^{His}$ and $tRNA^{Leu}$ than the control plant. Asterisks indicate that the differences between the control and transgenic means are statistically significant at $P = 0.05$. E, Sweet orange leaves of line 34 and a control plant infected with *X. citri* (approximately 10^4 and 10^5 cells) showing that canker lesions are less severe in line 34 than in the control. Photographs at 103 magnification were taken 20 d after bacterial infiltration.

and did not induce cell hypertrophy or hyperplasia, even when leaves were infiltrated with a high density of bacterial cells (Fig. 6, B and C). The *pthA4* deletion mutant was also nonpathogenic to the CsMAF1 RNAi lines (data not shown).

Next, we infiltrated sweet orange cv Pera leaves with the wild type or the *pthA4*-deletion mutant and evaluated the levels of CsMAF1 during canker development. We found that the CsMAF1 levels decreased in the leaf sectors infiltrated with wild-type bacteria, as cell hypertrophy and hyperplasia developed. On the other hand, the CsMAF1 levels in the leaf sectors infiltrated with the *pthA4* mutant remained unaltered relative to those of noninfiltrated tissues (Fig. 6D). Thus, in agreement with the results shown in Figures 4 and 5, reduced CsMAF1 levels correlate with canker formation and the activity of PthA4.

DISCUSSION

In this study, we show that CsMAF1 specifically interacts with the citrus canker elicitor PthA4. We also present evidence that CsMAF1 is the functional homolog of the human and yeast MAF1 proteins, which act as critical regulators of cell growth through the repression of RNA Pol III transcription (Upadhya et al., 2002; Wei and Zheng, 2010; Boguta and Graczyk, 2011).

Although MAF1 proteins have been described as RNA Pol III repressors, human MAF1 has also been shown to function as a negative regulator of RNA polymerase I and to influence RNA Pol II transcription primarily through its ability to down-regulate the synthesis of TATA-binding protein, a common component of the RNA polymerase I, Pol II, and Pol III initiation machineries (Johnson et al., 2007; Vannini and Cramer, 2012). Since ribosome biogenesis and protein synthesis in eukaryotic cells are coupled processes that demand great amounts of energy, they are tightly regulated and coordinated by all three RNA polymerases. Such coordination is not only important to determine the biosynthetic capacity of the cells for growth and proliferation under nutrient availability but also to restrict growth and cell division under stress conditions (Cie´sla et al., 2007; Willis and Moir, 2007; Oler and Cairns, 2012). Not surprisingly, transformed cells subvert these controls and synthesize rRNAs and tRNAs at elevated rates, a recurring feature of many mouse and human tumors (White, 2005; Marshall, 2008). Thus, because MAF1 controls ribosome biogenesis, affects cell morphology and body size, and suppresses cell growth and tRNA synthesis in

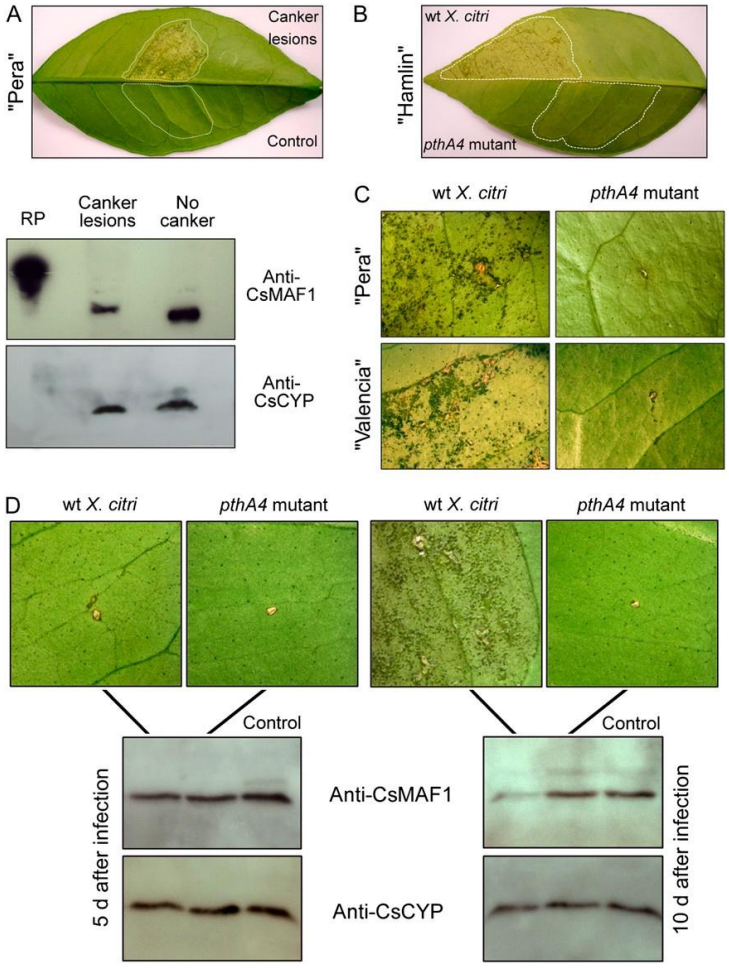

Figure 6. CsMAF1 depletion in canker lesions correlates with the presence of PthA. A, Sweet orange cv Pera infiltrated with a water suspension of *X. citri* (approximately 10^5 cells) showing canker lesions that developed 10 d after bacterial inoculation. Soluble proteins extracted from the indicated leaf sectors (dotted lines) were resolved on a 10% SDS-polyacrylamide gel and probed with anti-CsMAF1. Protein loads were controlled by probing the samples with anti-CsCYP, since the large subunit of ribulose-1,5-bisphosphate carboxylase shows considerable down-regulation during canker formation (Cernadas et al., 2008). CsMAF1 levels are significantly reduced in the hyperplastic lesions relative to CsCYP. B, Leaf sectors of sweet orange cv Hamlin infiltrated with the wild-type (wt) *X. citri* or the *pthA4* deletion mutant (approximately 10^5 cells) showing that PthA4 is required to elicit cankers in sweet orange. C, Detailed view (10× magnification) of sweet orange cv Pera and Valencia leaves challenged with wild-type *X. citri* or the *pthA4* deletion mutant (approximately 10^5 cells) showing the absence of canker symptoms in the leaf sectors infiltrated with the *pthA4* deletion mutant 10 d after bacterial inoculation. D, Soluble proteins from cv Pera leaf sectors infiltrated with wild-type *X. citri* or the *pthA4* deletion mutant (approximately 10^5 cells), or from noninfiltrated leaf sectors (control), were extracted 5 and 10 d after bacterial inoculation (left and right panels, respectively) and analyzed by western blot with the anti-CsMAF1 or anti-CsCYP antiserum. The blots show that depletion of CsMAF1, but not CsCYP, correlates with the development of cell hypertrophy and hyperplasia and with the presence of PthA4.

proliferating cells, it is also considered a tumor-suppressor protein that regulates the transformation state of the cells (Johnson et al., 2007; Shor et al., 2010; Rideout et al., 2012).

Consistent with the role played by the yeast and mammalian MAF1 proteins, CsMAF1 inhibited tRNA synthesis and restricted cell proliferation and canker formation in sweet orange leaves, most likely through the inhibition of ribosome biogenesis. Accordingly, sweet orange genes associated with ribosome biogenesis, cell division, and growth were rapidly and strongly up-regulated by *X. citri* (Cernadas et al., 2008). Moreover, it has been shown that the nucleoli of *Nicotiana benthamiana* cells expressing AvrBs3, a homolog of PthA4, were considerably enlarged and showed nucleolar vacuoles, indicating an increased need for ribosomes in these cells (Gürlebeck et al., 2009). Therefore, considering that PthA4 is required to induce tumors in sweet orange leaves and that depletion of CsMAF1 in *X. citri*-infiltrated tissues correlates with canker formation and the presence of PthA4, we postulate that PthA4 might prevent the interaction of CsMAF1 with the citrus RNA Pol III complex. In addition, as silencing of the PthA interactor and CTD-associated CsCYP in sweet orange also enhanced canker formation (Domingues et al., 2012; Campos et al., 2013), our data support the notion that PthAs from *X. citri* target multiple negative modulators of RNA Pol II and Pol III to coordinately increase the transcription of genes involved in ribosome biogenesis and cell growth.

One of the central regulators of cell growth and ribosome biogenesis in eukaryotes is the kinase TOR, which is also one of the main kinases that control MAF1 activity in yeast and human (Lee et al., 2009, 2012; Marshall et al., 2012). Interestingly, silencing of the Arabidopsis AtTOR caused leaf senescence and seedling growth arrest (Deprost et al., 2007), a phenotype that is reminiscent of that of the citrus shoots overexpressing CsMAF1. Although the association of MAF1

with the TOR kinase has not yet been demonstrated, it is tempting to speculate that CsMAF1 could be phosphorylated by the citrus homolog of AtTOR, an idea supported by the fact that CsMAF1 shares most of the residues that are phosphorylated by the mammalian mTOR or the yeast TORC1-regulated kinase Sch9. In fact, we showed that CsMAF1 is phosphorylated by PKA, which phosphorylates the yeast MAF1 at sites that overlap with those of the TORC1-regulated kinase Sch9 (Moir et al., 2012).

In conclusion, we have identified CsMAF1 as a possible novel target of the TAL effector PthA that functions as a citrus canker suppressor. Nonetheless, despite the advances in the characterization of the first plant MAF1 protein, there are still important questions that need to be addressed. What are the citrus kinases and protein phosphatases that regulate CsMAF1 activity? Is MAF1 a component of the TOR pathway in plants? Does CsMAF1 bind to the citrus RNA Pol III in a similar fashion to the human MAF1/RNA Pol III complex? Does PthA4 block the interaction of CsMAF1 with the RNA Pol III, alter CsMAF1 phosphorylation status, or induce its degradation? The answers to these questions will not only broaden our understanding of how plant cells regulate their growth under stress conditions but also of how TAL effectors manipulate critical host targets for the pathogen's benefit.

MATERIALS AND METHODS

Yeast Two-Hybrid Assays

Yeast two-hybrid assays were performed using the following PthA constructs (pOBD) as baits: PthA1 to PthA4 lacking the first 128 amino acids, the invariable LRR, the internal repetitive domain of PthA4 (RD4), and 5.5R, a construct carrying the last 5.5 repeats of the internal domain of PthA4 plus the C terminus, as described previously (Domingues et al., 2010; de Souza et al., 2012). The sweet orange (*Citrus sinensis*) CsMAF1 (JN600521.1), cloned into pOAD, was used as prey. Bait and prey constructs, including controls (empty pOBD + pOAD prey and pOBD bait + empty pOAD), were cotransformed into the yeast PJ694a cells, which were grown on SC-Trp-Leu-His (SC medium lacking tryptophan, leucine, and histidine) in the presence or absence of adenine and containing 0.3 or 5 mM 3-aminotriazole for 5 d at 30°C.

Protein Purification and GST-Pulldown Assays

The full-length 6xHis-tagged PthA4 was expressed in *Escherichia coli* BL21 (DE3) cells and purified by affinity chromatography (Domingues et al., 2010; de Souza et al., 2012). Full-length CsMAF1 was subcloned into pGEX4T1 as a GST fusion and expressed in BL21(DE3) cells upon isopropylthio-b-galactoside induction for 3 h at 30°C. The cell pellet was suspended in phosphate-buffered saline (PBS) buffer containing 1 mM dithiothreitol and lysozyme (1.0 mg mL^{21}). After sonication and centrifugation, soluble fractions of GST-CsMAF1 were immobilized on glutathione resin and nonbound proteins were removed with four PBS washes. Purified PthA4 (approximately 50 mM) or 1 mL of the soluble extract of human Hek 293 cells lysed in 50 mM HEPES, pH 7.4, containing 150 mM NaCl, 1% Triton X-100, 2 mM EGTA, 2 mM EDTA, 2 mM Na_2SO_4, and 50 mM NaF was incubated with the resins containing immobilized GST or GST-CsMAF1 for 2 h at 4°C. The beads were washed four times with PBS, and the bound proteins were eluted and resolved on 10% SDS-PAGE gels. Proteins were transferred onto polyvinylidene difluoride membranes, probed with anti-PthA (1:5,000), anti-GST (1:3,000), or monoclonal anti-RNA Pol III raised against the human RPC39 subunit (1:500; Santa Cruz Biotechnology) and detected by chemiluminescence.

Coimmunoprecipitation Assays

Agrobacterium tumefaciens transformed with the *pBI121-35S::pthA4* construct was grown in yeast extract and peptone medium to an optical density of 0.6 at 600 nm. Epicotyls of sweet orange cv Hamlin were wounded, transversely sectioned, and incubated at room temperature for 15 min with the *A. tumefaciens* suspension in the presence of 100 mM acetosyringone (Sigma-Aldrich). Cocultivation was performed on solidified Murashige and Skoog medium (Sigma-Aldrich) supplemented with 2.5% Suc, 10 mg L^{21} thiamine-HCl, 10 mg L^{21} pyridoxine, 1 mg L^{21} nicotinic acid, 0.4 mg L^{21} Gly, 100 mg L^{21} myoinositol, and 0.2 mg L^{21} 2,4-dichlorophenoxyacetic acid for 72 h in the dark (de Oliveira et al., 2009). Cell lysates of transformed epicotyls were incubated with the anti- CsMAF1 or preimmune serum, and the immunoprecipitates were analyzed by western blot with the anti-PthA or anti-CsMAF1 serum.

Functional Complementation of Yeast Mutants and Northern Analysis

The yeast wild-type strain BY4742 and the *MAF1* deletion mutant YI3945 (Kwapisz et al., 2002) were transformed with the citrus *CsMAF1* gene cloned into pYEX-4T (Clontech) and/or the *Xanthomonas citri pthA4* gene cloned into pOAD. Transformants were grown on SC-Leu-Ura (SC medium lacking leucine and uracil) plates at 30°C for 4 d. Cells were incubated in PBS buffer containing 20 mg mL^{21} lyticase and disrupted by ultrasonic bath for 30 min. Total RNA (10 mg) isolated using Trizol (Invitrogen) was resolved on denaturing agarose gels, transferred onto nylon membranes (Sambrook and Russel, 2001), and hybridized at 37°C with oligonucleotide probe 5$_9$-GCCATCTCCTAGAATCGAACCAGG-3$_9$ labeled with [g-^{32}P]ATP and T4 polynucleotide kinase (Pluta et al., 2001). After hybridization, membranes were washed in 23 SSC at 37°C (Sambrook and Russel, 2001) and exposed to x-ray films.

Protein Phosphorylation

Purified CsMAF1 (1 mg) was phosphorylated in a 20-mL reaction containing 50 mM Tris (pH 7.5), 10 mM $MgCl_2$, 0.2 mM ATP, 500 mCi $mmol^{21}$ [g-^{32}P]ATP, and 2,500 units of murine PKA (New England Biolabs). The reactions were incubated at 30°C for 30 min and stopped with the addition of 10 mL of 23 SDS sample buffer (Sambrook and Russel, 2001). The samples were heated at 90°C for 5 min and analyzed by SDS-PAGE, followed by autoradiography detection.

Plant Transformation

For silencing of CsMAF1, a DNA fragment of 611 bp of the CsMAF1 complementary DNA (cDNA) was amplified with primers RNAi-F (5$_9$-TCTAGACTCGAGTAGACCGCATCAATGATTTCTTGG-3$_9$) and RNAi-R (5$_9$-ATCGATGGTACCATTGACTAGAAATCCCTCCGCCACC-3$_9$) and cloned in opposite directions in the pHANNIBAL vector (Wesley et al., 2001). The hairpin construct under the control of the 35S promoter was subcloned into the binary pCambia1303 vector (CAMBIA). For CsMAF1 overexpression, the full-length *CsMAF1* gene was subcloned into the pCambia1303 vector under the control of the 35S promoter. The constructs were verified by DNA sequencing and moved into *A. tumefaciens* EHA105.

Etiolated epicotyls of sweet orange cv 'Hamlin' were transformed with the *A. tumefaciens* cells carrying the pCambia plasmids according to de Oliveira et al. (2009). Explants were selected in Murashige and Skoog basal medium containing hygromycin (5 mg L^{21}). Regenerated explants were grafted onto rangpur lime (*Citrus limonia*) root stocks and allowed to develop under growth room conditions (25°C with 10 h of fluorescent light) for acclimatization. Plants were transferred to a greenhouse and analyzed by western blot using the anti-CsMAF1 serum (1:3,000).

Detection of CsMAF1 in Plant Tissues

Young leaves of control and transgenic plants, or shoots regenerated from citrus epicotyls, were macerated in 23 SDS sample buffer (Sambrook and Russel, 2001) and heated at 90°C for 15 min. The samples were centrifuged at 16,000*g* for 10 min and analyzed by SDS-PAGE and immunoblotting.

Generation of the *pthA4* Deletion Mutant

Two DNA fragments of approximately 2,000 bp, flanking the *pthA4* gene (accession no. AAM39311) of *X. citri* strain 306, were amplified

using the oligonucleotide pairs PthA4*Hin*dIII-F (5′-AAGCTTGCGGGAGTCCCTGCGGCACGATGGATCAAG-3′)/PthA*Nde*I-R (5′-GAATGGGATCCATATGGCATACCTCTTTACATGGTCGCC-3′) and PthA*Nde*I-F (5′-GCTCGCATGGCATATGGAGCTATTGCCTCAGTGAGGC-3′)/PthA4*Eco*RI-R (5′-GAATTCCAGTTGAGCGCGCTCGGCCTGGTCGTGAAC-3′). The PCR fragments were ligated through the *Nde*I sites and cloned into the *Hin*dIII and *Eco*RI sites of the suicide vector pNPTS138 (Jenal and Fuchs, 1998). The construct was verified by DNA sequencing. The plasmid was used to transform *X. citri* 306 competent cells, which were selected on Luria-Bertani medium without sodium chloride (LBON), containing ampicillin (100 mg mL^{21}) and kanamycin (50 mg mL^{21}). Selected colonies were subsequently plated on LBON with ampicillin and kanamycin or ampicillin and 5% Suc. Kanamycin-sensitive colonies that grew in the presence of Suc were further selected and PCR tested for the absence of the *pthA4* gene. To confirm the deletion of the *pthA4* gene, the DNA fragment encompassing the deleted *pthA4* locus from two independent bacterial colonies was amplified with oligonucleotides PthA4*Hin*dIII-F and PthA4*Eco*RI-R and sequenced using internal oligonucleotides. Selected mutants were used to challenge sweet orange leaves for canker formation.

Bacterial Infiltration

Wild-type *X. citri* (strain 306) or the *pthA4* deletion mutant was grown for 48 h at 30°C on LBON containing ampicillin. Cells were suspended in water and counted through serial dilutions and plating. Leaves of the transgenic and control plants were infiltrated with 0.1 mL of a water suspension of *X. citri* containing approximately 10^5 or 10^6 bacterial cells mL^{21}.

Plant RNA Isolation and cDNA Synthesis

Total RNA was extracted from leaves using Trizol. The quality and quantity of the RNA was verified by agarose gel and UV spectroscopy. The RNA samples were treated with DNase I (Fermentas) to remove any traces of DNA. cDNAs were synthesized using the Maxima First Strand cDNA Synthesis Kit (Fermentas) according to the supplier's instructions.

Quantitative PCR Analysis

Primers for quantitative PCR were designed using the Primer Express 3.0 software (Applied Biosystems) using the following citrus sequences: $tRNA^{His}$ (5′-GTGGCTGTAGTTTAGTGGTAAGAATTCCACGTTGTGGCCGTGGAGACCTGGGCTCGAATCCCAGCAGCCACA-3′), $tRNA^{Leu}$ (5′-GTCAGGATGGCCGAGTGGTCTAAGGCGCCAGACTCAAGTTCTGGTCCTCGAAAGAGGGCGTGGGTTCAAATCCCACTTCTGACA-3′), and $tRNA^{Thr}$ (5′-GCTCTCGTAGCTCAGTTGGTTAGAGCACCCGTTTAGTAAGCGGGAGGTCTTGAGTTCGACTCTCAACGAGAGCA-3′). The generated cDNAs were diluted and tested for specificity and amplification efficiency of the probes relative to the endogenous control used. The sweet orange succinate dehydrogenase gene (EY722231) was used as an endogenous control. Three quantitative PCRs were performed for each of the mRNA samples (two biological replicates) using the SYBR Green mix and the universal conditions of amplification provided by the 7500 System (Applied Biosystems). The results were analyzed by the 7500 System software (Applied Biosystems) using the relative quantification mode and expressed as the mean of the six PCRs.

Sequence data from this article can be found in the GenBank/EMBL data libraries under accession numbers CsMAF1 (JN600521.1).

ACKNOWLEDGMENTS

We thank Maria Luiza Peixoto de Oliveira for helping with the citrus transformation and Camila Caldana for critical reading of the manuscript.

Received July 10, 2013; accepted July 29, 2013; published July 29, 2013.

LITERATURE CITED

Al-Saadi A, Reddy JD, Duan YP, Brunings AM, Yuan Q, Gabriel DW (2007) All five host-range variants of *Xanthomonas citri* carry one *pthA* homolog with 17.5 repeats that determines pathogenicity on citrus, but none determine host-range variation. Mol Plant Microbe Interact 20: 934–943

Boguta M, Czerska K, Zoładek T (1997) Mutation in a new gene *MAF1* affects tRNA suppressor efficiency in *Saccharomyces cerevisiae*. Gene 185: 291–296

Boguta M, Graczyk D (2011) RNA polymerase III under control: repression and de-repression. Trends Biochem Sci 36: 451–456

Brunings AM, Gabriel DW (2003) *Xanthomonas citri*: breaking the surface. Mol Plant Pathol 4: 141–157

Caldana C, Li Y, Leisse A, Zhang Y, Bartholomaeus L, Fernie AR, Willmitzer L, Giavalisco P (2013) Systemic analysis of inducible target of rapamycin mutants reveal a general metabolic switch controlling growth in *Arabidopsis thaliana*. Plant J 73: 897–909

Campos BM, Sforça ML, Ambrosio AL, Domingues MN, Brasil de Souza TdA, Barbosa JA, Paes Leme AF, Perez CA, Whittaker SB, Murakami MT, et al (2013) A redox 2-cys mechanism regulates the catalytic activity of divergent cyclophilins. Plant Physiol 162: 1311–1323

Cernadas RA, Camillo LR, Benedetti CE (2008) Transcriptional analysis of the sweet orange interaction with the citrus canker pathogens *Xantho- monas axonopodis* pv. *citri* and *Xanthomonas axonopodis* pv. *aurantifolii*. Mol Plant Pathol 9: 609–631

Cieśla M, Towpik J, Graczyk D, Oficjalska-Pham D, Harismendy O, Suleau A, Balicki K, Conesa C, Lefebvre O, Boguta M (2007) Maf1 is involved in coupling carbon metabolism to RNA polymerase III transcription. Mol Cell Biol 27: 7693–7702

Deng D, Yan C, Pan X, Mahfouz M, Wang J, Zhu JK, Shi Y, Yan N (2012) Structural basis for sequence-specific recognition of DNA by TAL effectors. Science 335: 720–723

de Oliveira ML, Febres VJ, Costa MG, Moore GA, Otoni WC (2009) High-efficiency *Agrobacterium*-mediated transformation of citrus via sonication and vacuum infiltration. Plant Cell Rep 28: 387–395

Deprost D, Yao L, Sormani R, Moreau M, Leterreux G, Nicolaï M, Bedu M, Robaglia C, Meyer C (2007) The *Arabidopsis* TOR kinase links plant growth, yield, stress resistance and mRNA translation. EMBO Rep 8: 864–870

Desai N, Lee J, Upadhya R, Chu Y, Moir RD, Willis IM (2005) Two steps in Maf1-dependent repression of transcription by RNA polymerase III. J Biol Chem 280: 6455–6462

de Souza TA, Soprano AS, de Lira NPV, Quaresma AJC, Pauletti BA, Paes Leme AF, Benedetti CE (2012) The TAL effector PthA4 interacts with nuclear factors involved in RNA-dependent processes including a HMG protein that selectively binds poly(U) RNA. PLoS ONE 7: e32305

Domingues MN, de Campos BM, de Oliveira MLP, de Mello UQ, Benedetti CE (2012) TAL effectors target the C-terminal domain of RNA polymerase II (CTD) by inhibiting the prolyl-isomerase activity of a CTD- associated cyclophilin. PLoS ONE 7: e41553

Domingues MN, De Souza TA, Cernadas RA, de Oliveira ML, Docena C, Farah CS, Benedetti CE (2010) The *Xanthomonas citri* effector protein PthA interacts with citrus proteins involved in nuclear transport, protein folding and ubiquitination associated with DNA repair. Mol Plant Pathol 11: 663–675

Duan Y, Castañeda A, Zhao G, Erdos G, Gabriel D (1999) Expression of a single, host-specific, bacterial pathogenicity gene in plant cells elicits division, enlargement, and cell death. Mol Plant Microbe Interact 12: 556–560

Dunger G, Garofalo CG, Gottig N, Garavaglia BS, Rosa MC, Farah CS, Orellano EG, Ottado J (2012) Analysis of three *Xanthomonas axonopodis* pv. *citri* effector proteins in pathogenicity and their interactions with host plant proteins. Mol Plant Pathol 13: 865–876

Gajda A, Towpik J, Steuerwald U, Müller CW, Lefebvre O, Boguta M (2010) Full repression of RNA polymerase III transcription requires in- teraction between two domains of its negative regulator Maf1. J Biol Chem 285: 35719–35727

Gu K, Yang B, Tian D, Wu L, Wang D, Sreekala C, Yang F, Chu Z, Wang GL, White FF, et al (2005) R gene expression induced by a type-III ef- fector triggers disease resistance in rice. Nature 435: 1122–1125

Guo Y, Figueiredo F, Jones J, Wang N (2011) HrpG and HrpX play global roles in coordinating different virulence traits of *Xanthomonas axonopodis* pv. *citri*. Mol Plant Microbe Interact 24: 649–661

Gürlebeck D, Jahn S, Gürlebeck N, Szczesny R, Szurek B, Hahn S, Hause G, Bonas U (2009) Visualization of novel virulence activities of the Xanthomonas type III effectors AvrBs1, AvrBs3 and AvrBs4. Mol Plant Pathol 10: 175–188

Huber A, Bodenmiller B, Uotila A, Stahl M, Wanka S, Gerrits B, Aebersold R, Loewith R (2009) Characterization of the rapamycin- sensitive phosphoproteome reveals that Sch9 is a central coordinator of protein synthesis. Genes Dev 23: 1929–1943

Jenal U, Fuchs T (1998) An essential protease involved in bacterial cell- cycle control. EMBO J 17: 5658–5669

John F, Roffler S, Wicker T, Ringli C (2011) Plant TOR signaling compo- nents. Plant Signal Behav 6: 1700–1705

Johnson SS, Zhang C, Fromm J, Willis IM, Johnson DL (2007) Mammalian Maf1 is a negative regulator of transcription by all three nuclear RNA polymerases. Mol Cell 26: 367–379

Kay S, Bonas U (2009) How *Xanthomonas* type III effectors manipulate the host plant. Curr Opin Microbiol 12: 37–43

Kay S, Hahn S, Marois E, Hause G, Bonas U (2007) A bacterial effector acts as a plant transcription factor and induces a cell size regulator. Science 318: 648–651

Kwapisz M, Smagowicz WJ, Oficjalska D, Hatin I, Rousset JP, Zoładek T, Boguta M (2002) Up-regulation of tRNA biosynthesis affects transla- tional readthrough in maf1-delta mutant of *Saccharomyces cerevisiae*. Curr Genet 42: 147–152

Lee J, Moir RD, McIntosh KB, Willis IM (2012) TOR signaling regulates ribosome and tRNA synthesis via LAMMER/Clk and GSK-3 family kinases. Mol Cell 45: 836–843

Lee J, Moir RD, Willis IM (2009) Regulation of RNA polymerase III transcription involves SCH9-dependent and SCH9-independent branches of the target of rapamycin (TOR) pathway. J Biol Chem 284: 12604–12608

Mak AN, Bradley P, Cernadas RA, Bogdanove AJ, Stoddard BL (2012) The crystal structure of TAL effector PthXo1 bound to its DNA target. Sci- ence 335: 716–719

Marshall L (2008) Elevated RNA polymerase III transcription drives proliferation and oncogenic transformation. Cell Cycle 7: 3327–3329

Marshall L, Rideout EJ, Grewal SS (2012) Nutrient/TOR-dependent regulation of RNA polymerase III controls tissue and organismal growth in Drosophila. EMBO J 31: 1916–1930

Mayer C, Grummt I (2006) Ribosome biogenesis and cell growth: mTOR coordinates transcription by all three classes of nuclear RNA polymerases. Oncogene 25: 6384–6391

Michels AA (2011) MAF1: a new target of mTORC1. Biochem Soc Trans 39: 487–491

Moir RD, Lee J, Haeusler RA, Desai N, Engelke DR, Willis IM (2006) Protein kinase A regulates RNA polymerase III transcription through the nu- clear localization of Maf1. Proc Natl Acad Sci USA 103: 15044–15049

Moir RD, Lee J, Willis IM (2012) Recovery of RNA polymerase III transcription from the glycerol-repressed state: revisiting the role of protein kinase CK2 in Maf1 phosphoregulation. J Biol Chem 287: 30833–30841

Murakami MT, Sforça ML, Neves JL, Paiva JH, Domingues MN, Pereira ALA, Zeri ACM, Benedetti CE (2010) The repeat domain of the type III effector protein PthA shows a TPR-like structure and undergoes con- formational changes upon DNA interaction. Proteins 78: 3386–3395

Oficjalska-Pham D, Harismendy O, Smagowicz WJ, Gonzalez de Peredo A, Boguta M, Sentenac A, Lefebvre O (2006) General repression of RNA polymerase III transcription is triggered by protein phosphatase type 2A-mediated dephosphorylation of Maf1. Mol Cell 22: 623–632

Oler AJ, Cairns BR (2012) PP4 dephosphorylates Maf1 to couple multiple stress conditions to RNA polymerase III repression. EMBO J 31: 1440–1452

Pluta K, Lefebvre O, Martin NC, Smagowicz WJ, Stanford DR, Ellis SR, Hopper AK, Sentenac A, Boguta M (2001) Maf1p, a negative effector of RNA polymerase III in *Saccharomyces cerevisiae*. Mol Cell Biol 21: 5031–5040

Ren M, Qiu S, Venglat P, Xiang D, Feng L, Selvaraj G, Datla R (2011) Target of rapamycin regulates development and ribosomal RNA expression through kinase domain in Arabidopsis. Plant Physiol 155: 1367–1382

Ren M, Venglat P, Qiu S, Feng L, Cao Y, Wang E, Xiang D, Wang J, Alexander D, Chalivendra S, et al (2012) Target of rapamycin signaling regulates metabolism, growth, and life span in *Arabidopsis*. Plant Cell 24: 4850–4874

Rideout EJ, Marshall L, Grewal SS (2012) Drosophila RNA polymerase III repressor Maf1 controls body size and developmental timing by modulating tRNAiMet synthesis and systemic insulin signaling. Proc Natl Acad Sci USA 109: 1139–1144

Roberts DN, Wilson B, Huff JT, Stewart AJ, Cairns BR (2006) Dephosphorylation and genome-wide association of Maf1 with Pol III-transcribed genes during repression. Mol Cell 22: 633–644

Rollins J, Veras I, Cabarcas S, Willis I, Schramm L (2007) Human Maf1 negatively regulates RNA polymerase III transcription via the TFIIB family members Brf1 and Brf2. Int J Biol Sci 3: 292–302

Römer P, Hahn S, Jordan T, Strauss T, Bonas U, Lahaye T (2007) Plant pathogen recognition mediated by promoter activation of the pepper Bs3 re- sistance gene. Science 318: 645–648

Sambrook J, Russel DW (2001) Molecular Cloning: A Laboratory Manual, Ed 3. Cold Spring Harbor Laboratory Press, Cold Spring Harbor, NY

Shor B, Wu J, Shakey Q, Toral-Barza L, Shi C, Follettie M, Yu K (2010) Requirement of the mTOR kinase for the regulation of Maf1 phosphorylation and control of RNA polymerase III-dependent transcription in cancer cells. J Biol Chem 285: 15380–15392

Sobennikova MV, Shematorova EK, Shpakovskiĭ GV (2007) [C-terminal domain (CTD) of the subunit Rpb1 of nuclear RNA polymerase II and its role in the transcription cycle]. Mol Biol (Mosk) 41: 433–449

Swarup S, Yang Y, Kingsley MT, Gabriel DW (1992) An Xanthomonas citri pathogenicity gene, pthA, pleiotropically encodes gratuitous avir- ulence on nonhosts. Mol Plant Microbe Interact 5: 204–213

Upadhya R, Lee J, Willis IM (2002) Maf1 is an essential mediator of diverse signals that repress RNA polymerase III transcription. Mol Cell 10: 1489–1494

Vannini A, Cramer P (2012) Conservation between the RNA polymerase I, II, and III transcription initiation machineries. Mol Cell 45: 439–446

Vannini A, Ringel R, Kusser AG, Berninghausen O, Kassavetis GA, Cramer P (2010) Molecular basis of RNA polymerase III transcription repression by Maf1. Cell 143: 59–70

Wei Y, Zheng XS (2010) Maf1 regulation: a model of signal transduction inside the nucleus. Nucleus 1: 162–165

Wesley SV, Helliwell CA, Smith NA, Wang MB, Rouse DT, Liu Q, Gooding PS, Singh SP, Abbott D, Stoutjesdijk PA, et al (2001) Con- struct design for efficient, effective and high-throughput gene silencing in plants. Plant J 27: 581–590

White RJ (2005) RNA polymerases I and III, growth control and cancer. Nat Rev Mol Cell Biol 6: 69–78

Wichmann G, Bergelson J (2004) Effector genes of *Xanthomonas axonopodis* pv. *vesicatoria* promote transmission and enhance other fitness traits in the field. Genetics 166: 693–706

Willis IM, Moir RD (2007) Integration of nutritional and stress signaling pathways by Maf1. Trends Biochem Sci 32: 51–53

Yan Q, Wang N (2012) High-throughput screening and analysis of genes of *Xanthomonas citri* subsp. *citri* involved in citrus canker symptom development. Mol Plant Microbe Interact 25: 69–84

ANEXO IV – Artigo publicado no ano de 2013 na revista 'MPMI' (*Molecular Plant-Microbe Interactions*), no qual participo como terceira autora. Neste trabalho realizei os experimentos apresentados nas Figuras 4 e 6. Na Figura 4 realizei uma análise de crescimento bacteriano em plantas Troyer transgênicas expressando MAPK1 de citros. Na Figura 6 analisei a expressão de genes relacionados a defesa controlados por MAPK1.

Increased Resistance Against Citrus Canker Mediated by a Citrus Mitogen-Activated Protein Kinase

Maria Luiza Peixoto de Oliveira,[1] Caio Cesar de Lima Silva,[1] Valéria Yukari Abe,[1] Marcio Gilberto Cardoso Costa,[2] Raúl Andrés Cernadas,[1] and Celso Eduardo Benedetti[1]

[1]Laboratório Nacional de Biociências (LNBio), Centro Nacional de Pesquisa em Energia e Materiais (CNPEM), CP6192, CEP 13083-970, Campinas, SP, Brazil; [2]Departamento de Ciências Biológicas, Universidade Estadual de Santa Cruz, Ilhéus, BA, Brazil

Submitted 30 April 2013. Accepted 14 June 2013.

Mitogen-activated protein kinases (MAPK) play crucial roles in plant immunity. We previously identified a citrus MAPK (CsMAPK1) as a differentially expressed protein in response to infection by *Xanthomonas aurantifolii*, a bacterium that causes citrus canker in Mexican lime but a hypersensitive reaction in sweet oranges. Here, we confirm that, in sweet orange, CsMAPK1 is rapidly and preferentially induced by *X. aurantifolii* relative to *Xanthomonas citri*. To investigate the role of CsMAPK1 in citrus canker resistance, we expressed CsMAPK1 in citrus plants under the control of the *PR5* gene promoter, which is induced by *Xanthomonas* infection and wounding. Increased expression of CsMAPK1 correlated with a reduction in canker symptoms and a decrease in bacterial growth. Canker lesions in plants with higher CsMAPK1 levels were smaller and showed fewer signs of epidermal rupture. Transgenic plants also revealed higher transcript levels of defense-related genes and a significant accumulation of hydrogen peroxide in response to wounding or *X. citri* infection. Accordingly, nontransgenic sweet orange leaves accumulate both CsMAPK1 and hydrogen peroxide in response to *X. aurantifolii* but not *X. citri* infection. These data, thus, indicate that CsMAPK1 functions in the citrus canker defense response by inducing defense gene expression and reactive oxygen species accumulation during infection.

Mitogen-activated protein kinases (MAPK) are evolutionarily conserved components of sophisticated signaling cascades or mechanisms used by the cells to transduce extracellular stimuli to intracellular responses. Usually, in these signal transduction pathways, MAPK are activated by MAPK kinases (MAP2K or MEK) that were previously activated by MAPKK kinases (MAP3K or MEKK) in sequential phosphorylation reactions (Melech-Bonfil and Sessa 2010; Rodriguez et al. 2010; Sinha et al. 2011; Vilela et al. 2010). In many plant species, MAPK are known to play crucial roles in plant immunity and to mediate responses to many abiotic stresses, such as cold, drought, and wounding (Jonak et al. 1996; Mizogushi et al. 1996; Ligterink et al. 1997; Seo et al. 2007; Sinha et al. 2011). In response to microbial attack, the MAPK signaling cascade is activated upon the perception of microbe-associated molecular patterns (MAMPs), which, in turn, initiates a coordinated basal defense or immune response characterized by the expression of pathogen-responsive genes, production of reactive oxygen species (ROS), and deposition of callose and lignin at sites of infection (Chisholm et al. 2006). On the other hand, successful microbes overcome these defense responses by deploying a variety of effector molecules that ultimately suppress the immune response (Jones and Dangl 2006).

As initial components of the immune response, MAPK function as serine and threonine kinases that phosphorylate a wide range of protein targets, including members of the WRKY family of transcription factors responsible for the activation of downstream effector genes (Chisholm et al. 2006; Sinha et al. 2011). An example of direct physiological targets of MAPK is the tobacco WRKY factor 8 (WRKY8) that is phosphorylated by the MAPK SIPK, NTF4, and WIPK, involved in innate immunity and regulation of cell death triggered by pathogens (Ishihama et al. 2011; Ren et al. 2006). The MAPK-dependent activation of WRKY8 increases the DNA binding affinity of WRKY8 to its cognate W-box sequences leading to the expression of defense-related genes (Ishihama et al. 2011).

Citrus spp. are susceptible to the bacterial pathogens *Xanthomonas citri* and *Xanthomonas aurantifolii*, the causal agents of citrus canker, an economically important disease characterized by raised pustules on the tissue epidermis (Brunings and Gabriel 2003). Different forms of the disease were characterized; the Asiatic canker (or pathotype A) being the most aggressive and widespread. Asiatic canker is caused by *X. citri*, which infects almost any commercial variety. In contrast, *X. aurantifolii* pathotype C is limited to the Mexican lime alone and induces a hypersensitive response (HR) in sweet oranges (Brunings and Gabriel 2003; Cernadas et al. 2008).

We investigated the differential pathogenicity exhibited by *X. citri* and *X. aurantifolii* pathotype C in sweet oranges by transcriptional analyses of leaves infected with these bacteria (Cernadas et al. 2008). We found that *X. citri* preferentially modulates a set of genes associated with canker development, including those implicated in cell-wall remodeling, cell division, and expansion. On the other hand, *X. aurantifolii* induces

Current address for M. L. P. de Oliveira: U.S. Horticultural Research Laboratory, U.S. Department of Agriculture, Agricultural Research Service, 2001 South Rock Road, Fort Pierce, FL 34945, U.S.A.

Current address for R. A. Cernadas: Department of Plant Pathology and Plant-Microbe Biology, Cornell University, Ithaca, NY 14853, U.S.A.

Corresponding author: C. E. Benedetti; Telephone: +1 55 19 35121111; Fax: +1 55 19 35121006; E-mail address: celso.benedetti@lnbio.org.br

* The *e-X*tra logo stands for "electronic extra" and indicates that Figure 1 appears in color online.

a substantial number of genes associated with a basal defense response consistent with the establishment of an HR through MAPK signaling (Cernadas and Benedetti 2009; Cernadas et al. 2008). In fact, a citrus MAPK (CsMAPK1) related to the tobacco SIPK and WIPK, induced by salicylic acid (SA) and wounding, respectively, was preferentially induced by *X. aurantifolii* at the very early stage of infection (Cernadas et al. 2008). In addition, *X. aurantifolii* induced the expression of WRKY factors similar to pepper WRKY2 and rice OsWRKY71, implicated in resistance against *Xanthomonas vesicatoria* and *Xanthomonas oryzae*, respectively (Liu et al. 2007a; Oh et al. 2006). A MAPKK similar to the SIPK/WIPK/NTF4 activator NtMEK2 (Liu et al. 2007b; Takahashi et al. 2007), and numerous enzymes of the oxidative burst response were also up-regulated preferentially by *X. aurantifolii* in the onset of infection (Cernadas et al. 2008). These results pointed out the CsMAPK1 signaling as an interesting executor candidate of the *X. aurantifolii*–triggered HR in sweet orange. In contrast, we noted that *X. citri* suppresses this pathway within a few hours after bacterial infection as revealed by the downregulation of defense-related genes at 48 h after infiltration (Cernadas et al. 2008).

Considering that MAPK have been implicated in plant defense by boosting hydrogen peroxide production and induction of defense gene expression (Ren et al. 2002, 2006; Sinha et al. 2011), we sought to test whether CsMAPK1 could coordinate a defense response against *X. citri* in sweet oranges. Therefore, we expressed CsMAPK1 in Troyer citrange plants under the control of a *Xanthomonas*-inducible promoter. The results of this study show that the enhanced expression of CsMAPK1 correlates with a decrease in *X. citri* growth and a reduction in canker symptoms. Moreover, we demonstrate that increased expression of CsMAPK1 correlates with the overexpression of defense-related genes and accumulation of hydrogen peroxide. These results suggest that CsMAPK1 contributes to the defense against these *Xanthomonas* pathogens through activation of defense-related genes and production of ROS and that *X. citri* overcomes these CsMAPK1-dependent defense responses during the onset of infection.

RESULTS

CsMAPK1 is preferentially induced in the defense response of *Citrus sinensis* to *X. aurantifolii*.

Previously, we found that the citrus expressed sequence tag CX073386, encoding a MAPK, was specifically up-regulated in the resistance response of sweet orange leaves to *X. aurantifolii* (Cernadas et al. 2008). To further investigate the role of this gene in plant defense, we cloned the corresponding full-length cDNA from sweet orange and named CsMAPK1. *CsMAPK1* encodes a nearly 43-kDa MAPK of the serine and threonine protein kinase subfamily bearing a single kinase do-

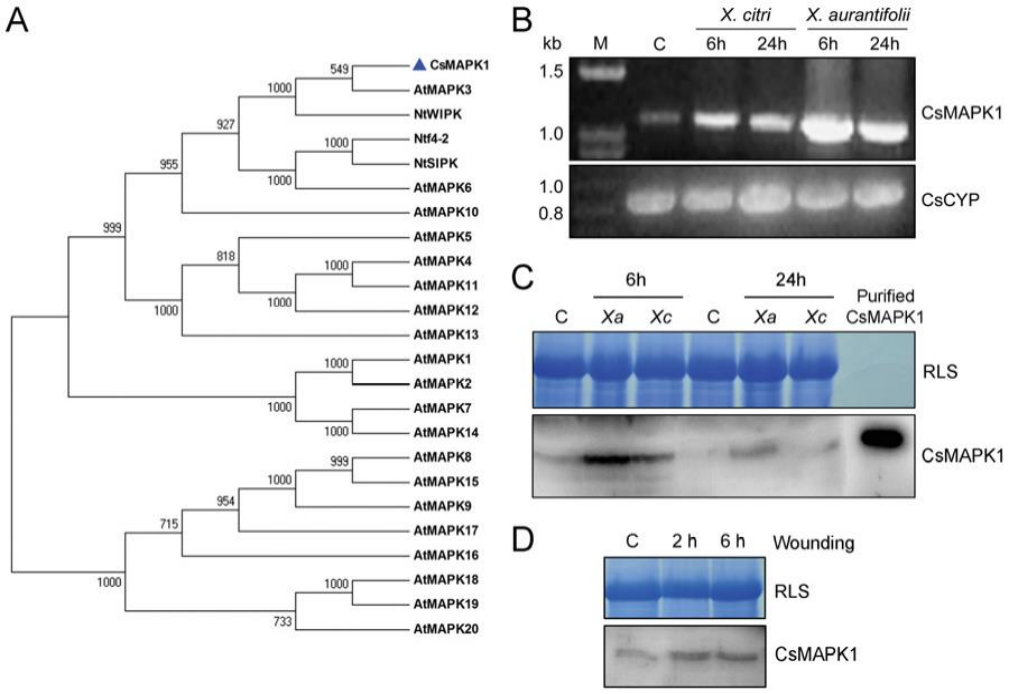

Fig. 1. CsMAPK1 is a single kinase-domain mitogen-activated protein kinases (MAPK) preferentially induced in the defense response of *Citrus sinensis* to *Xanthomonas aurantifolii*. **A,** Phylogenetic tree of MAPK of *Citrus sinensis* (CsMAPK1), *Nicotiana tabacum* (Nt), and *Arabidopsis thaliana* (At). Amino acid sequences were aligned using ClustalX and a maximum likelihood phylogenetic analysis was generated using the MEGA4 program based on the neighbor-joining method. Bootstrap values (above 50%) from 1,000 replicates are indicated at each branch. **B,** Semiquantitative reverse-transcription polymerase chain reaction analysis of *CsMAPK1* expression in sweet orange leaves challenged with *X. citri*, *X. aurantifolii*, or mock control (C). The CsMAPK1 mRNA is preferentially induced in the incompatible interaction between sweet orange and *X. aurantifolii* at 6 and 24 h after bacterial inoculation (approximately 10^4 cells). The citrus gene encoding the CsCYP protein was used as internal control for equal cDNA inputs, and the molecular marker (M) is indicated. **C,** Western blot analysis of sweet orange proteins extracted from leaves inoculated with *X. citri* (*Xc*), X. *aurantifolii* (*Xa*), or noninoculated (C) at 6 and 24 h after infiltration. As positive control, the purified 6xHis-CsMAPK1 protein (approximately 43 kDa) was detected with an antiserum raised against CsMAPK1 (purified CsMAPK1). **D,** Western blot analysis of sweet orange proteins extracted from leaves at 2 and 6 h after wounding. For panels C and D, equal protein loads were verified with Coomassie brilliant blue, included above the corresponding blots. RLS corresponds to the ribulose-1,5-bisphosphate carboxylase large subunit.

main. Phylogenetic analyses revealed that CsMAPK1 belongs to Group A of MAPK (MAPK Group 2002) (Fig. 1A). The CsMAPK1 shares a strong similarity (96% of identity) with PtrMAPK, a *Poncirus trifoliata* MAPK that enhances drought tolerance when overexpressed in tobacco (Huang et al. 2011). Besides, CsMAPK1 belongs to the same phylogenetic group with *Arabidopsis* AtMAPK3 and tobacco WIPK and SIPK kinases, the former regulates environmental stresses responses and was also involved in the resistance against the necrotrophic fungi *Botrytis cinerea* (Galletti et al. 2011; Mizoguchi et al. 1996). In particular, the WIPK and SIPK are components of MAPK cascades implicated in the tomato resistance against *Xanthomonas vesicatoria* (Melech-Bonfil and Sessa 2011). With these evidences, we work on the hypothesis that CsMAPK1 is a functional ortholog of AtMAPK3, WIPK, and SIPK (Fig. 1A).

To confirm our microarray data and to test whether CsMAPK1 is associated with the incompatible interaction, we infiltrated sweet orange leaves with *X. aurantifolii* and *X. citri* and analyzed the mRNA and protein levels of CsMAPK1 at 6 and 24 h after bacterial inoculation. The results show that *CsMAPK1* is induced in response to both *X. citri* and *X. aurantifolii* infections; however, the levels of *CsMAPK1* mRNA are dramatically higher in the incompatible interaction at both 6 and 24 h after infection (Fig. 1B). Consistent with this, the CsMAPK1 polypeptide accumulated at higher levels in response to *X. aurantifolii* than *X. citri* infection at 6 h postinoculation. In addition, CsMAPK1 protein was barely detected in leaves infiltrated with *X. citri* at 24 h postinfection, indicating that this kinase is involved in the incompatible interation (Fig. 1C).

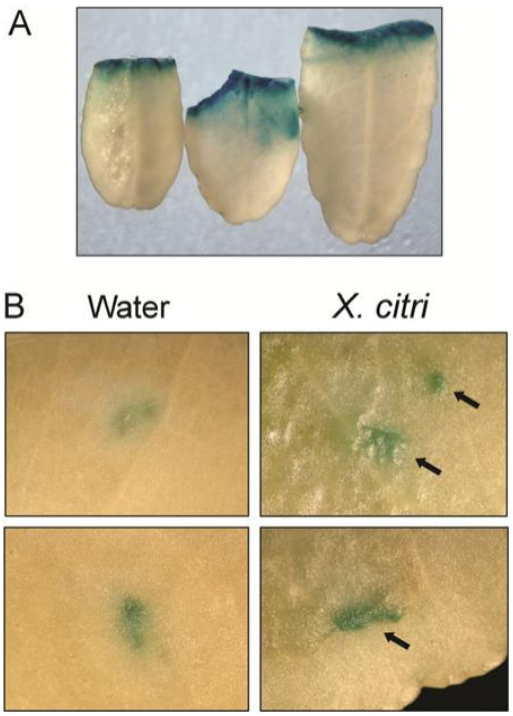

Fig. 2. The citrus *PR5* promoter is induced by wounding and *Xanthomonas citri* infection. **A,** β-Glucuronidase (GUS) activity in leaves of three independent *PR5*::GUS reporter plants in response to wounding. Leaves were chopped with a razor blade and were immediately immersed in the GUS assay buffer for histological detection of GUS activity (blue areas in the vicinity of the wounds). **B,** GUS activity in leaves of reporter plants 10 days after bacterial infiltration (approximately 10 cells). GUS staining is observed in developing pustules (arrows), whereas in leaf sectors infiltrated with water, GUS staining was restricted to the vicinity of the pinprick.

Since BLAST analyses revealed that CsMAPK1 is 83% identical to the NtWIPK, we asked whether the protein would also accumulate upon wounding (Seo et al. 1995). The results revealed that CsMAPK1 is only slightly induced by wounding in sweet orange leaves 2 or 6 h after the treatment (Fig. 1D). Taken together, these data support the idea that CsMAPK1 plays a role in the early defense response triggered by *X. aurantifolii* in sweet orange.

Generation of transgenic citrus lines expressing CsMAPK1 under the control of a *Xanthomonas*-induced promoter.

Considering that *X. citri* suppresses the host basal defenses at early stages of infection (Cernadas et al. 2008) and that *CsMAPK1* is strongly induced during the incompatible interaction, we sought to investigate the role of *CsMAPK1* overexpression in canker development, using the pathogenesis-related *PR5* gene promoter, which is rapidly induced after *X. citri* infiltration (Cernadas et al. 2008). Therefore, we generated two constructs, *PR5::CsMAPK1* and *PR5::uidA* (control), and used them to transform citrus model plants Troyer citrange (*Citrus sinensis* × *Poncirus trifoliata*). We selected Troyer plants because they are susceptible to *X. citri*, efficient to transform, and demand shorter regeneration periods.

To test the responsiveness of the *PR5* promoter to bacterial infection, three independent β-glucuronidase (GUS) reporter plants were infiltrated with suspensions of *X. citri*. We found that the *PR5* promoter is not only induced by *X. citri* infection but also upon wounding (Fig. 2A). In leaf sectors infiltrated with *X. citri,* the *PR5::GUS* activity was predominantly detected in the developing pustules, whereas, in leaf sectors infiltrated with water, the *PR5::GUS* activity was restricted to the vicinity of the pinpricks (Fig. 2B). These results thus show that the *PR5* promoter is capable of driven the expression of a reporter gene in response to both local wounding and canker pustules development after *X. citri* infiltration.

Accumulation of CsMAPK1 hampers *X. citri* growth and decreases canker symptoms in Troyer plants.

To test the function of the *PR5* promoter-induction of CsMAPK1 in response to *X. citri*, we first analyzed the expression levels of CsMAPK1 by quantitative polymerase chain reaction (PCR) in four independent transgenic Troyer plants (*CsMAPK1*-3, *CsMAPK1*-13, *CsMAPK1*-15, and *CsMAPK1*-18) carrying the *PR5::CsMAPK1* cassette after bacterial infiltration. The results were consistent with the previous GUS reporter experiments and demonstrate that all four *CsMAPK1* transgenic lines accumulate higher levels of the *CsMAPK1* mRNA at 6 and 24 h after bacterial infiltration (Fig. 3A). In fact, the *PR5* promoter was capable of driving significantly higher expression of *CsMAPK1* compared with its native promoter upon *X. citri* challenge (Fig. 3A). In agreement with this, we also observed higher accumulation of CsMAPK1 protein in transgenic leaves infiltrated with *X. citri* (Fig. 3B). In addition, our data revealed that the CsMAPK1 protein accumulation was also higher in the transgenic lines in response to wounding, relative to the control plants (Fig. 3C).

To know whether the enhanced expression of CsMAPK1 would affect canker symptom development, we sprayed the lower side of transgenic and control leaves with a suspension of *X. citri* (10^6 cells per milliliter). We observed that canker symptons started to appear within 35 days after spraying and that the *CsMAPK1*-13 plant showed the most significant reduction in canker symptoms (Fig. 3D, upper panel). Neverthe-

less, canker symptoms in *CsMAPK1*-3, *CsMAPK1*-15, and *CsMAPK1*-18 lines were also relatively less severe than in control plants based on the number, morphology, or pigmentation, alone or in combination, of the developed pustules. Moreover, we noticed no rupture of the epidermis in pustules developed on the *CsMAPK1*-13 line, even after 60 days after bacterial infection. On the other hand, canker pustules developed in the *CsMAPK1*-3 and *CsMAPK1*-15 lines were similar to those of line 13 but bigger (Fig. 3D, lower panel). Pustules developed in line 18 were also smaller and fewer than in control plants. However, in contrast with line 13, *CsMAPK1*-3, *CsMAPK1*-15, and *CsMAPK1*-18, showed epidermal rupture later during the infection (Fig. 3D, lower panel).

When leaves were infiltrated with a suspension of *X. citri* (approximately 10^3 cells), we also observed a reduction in the number of rising pustules in the transgenic lines as compared with the control (Fig. 3E). However, epidermal rupture was observed in all transgenic lines, indicating that under more severe conditions of infection, CsMAPK1 overexpression appears to be less effective to inhibit pustule formation.

Next, we performed Western blots to analyze the protein levels of CsMAPK1 on leaves of *CsMAPK1*-13 infiltrated with *X. citri* that showed reduced canker lesions (Fig. 3D and E). We found that the *CsMAPK1*-13 line expresses CsMAPK1 not only early (6 h) after infiltration but, also, later (40 days post-inoculation) in leaves with developing pustules (Fig. 3F). In contrast, the control plants showed reduced CsMAPK1 levels, particularly at 6 h postinfection, and no expression of the protein was detected in leaves with developing canker lesions (Fig. 3F).

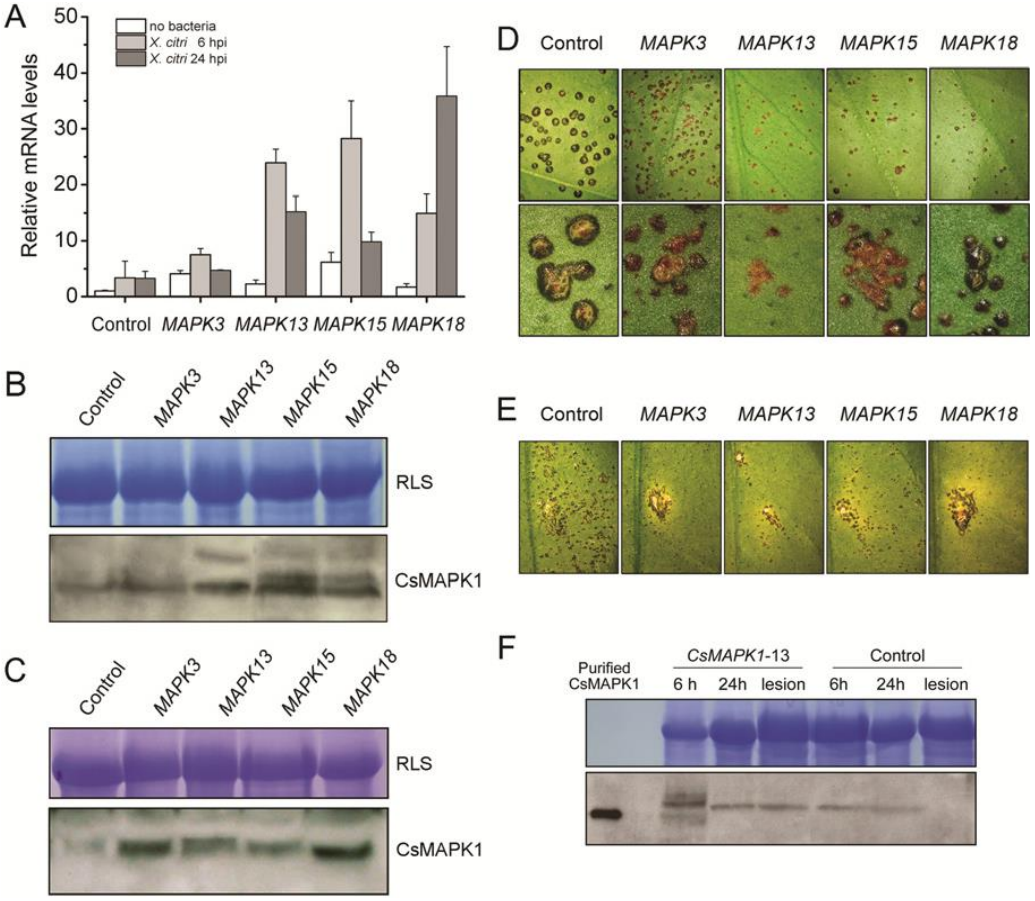

Fig. 3. Increased expression of CsMAPK1 correlates with increased resistance to *Xanthomonas citri*. **A,** Quantitative polymerase chain reaction analysis of CsMAPK1 expression in *CsMAPK1* transgenic plants challenged with *X. citri*. Four independent *CsMAPK1* transgenic plants (3, 13, 15, and 18) overexpress CsMAPK1 at 6 and 24 h after bacterial inoculation as compared with nontransformed plants (Control). Although the native CsMAPK1 promoter is induced by *X. citri* (Control), higher expression levels of the CsMAPK1 mRNA are driven by the *PR5* promoter in the transgenic plants at 6 and 24 h after bacterial inoculation. **B,** Western blot analysis of proteins extracted from leaves of control and transgenic plants 6 h after *X. citri* inoculation. The anti-CsMAPK1 serum detected increased levels of CsMAPK1 in the transgenic plants compared with control. Protein loads were controlled by Coomassie brilliant blue staining of the ribulose-1,5-bisphosphate carboxylase large subunit (RLS) bands (upper panel). **C,** Western blot analysis of control and transgenic plants 2 h after leaves had been wounded, showing higher levels of CsMAPK1 in the transgenic lines compared with control. Protein loads were controlled by Coomassie brilliant blue staining of the RLS bands (upper panel). **D,** Troyer leaves of control and transgenic plants that had been spray-inoculated with *X. citri* showing a reduction in canker symptoms in the transgenic lines (upper panel, 10× magnification; lower panel, 50× magnification). Pustules in the *CsMAPK1* lines were reduced in number and size and showed an unusual morphology and pigmentation. **E,** Leaves of control and transgenic plants that had been infiltrated with a *X. citri* suspension (approximately 10^3 cells), showing a yellowing of the infiltrated leaf sectors and a reduction in canker symptoms in the transgenic lines (10× magnification). **F,** Western blot analysis of leaves of *CsMAPK1*-13 and control plants inoculated with *X. citri* at different time intervals (6 and 24 h postinfection) and of leaves showing developing canker pustules (lesion). CsMAPK1 was expressed at higher levels 6 h postinfection in leaves of the *CsMAPK1*-13 line compared with the control. CsMAPK1 was also detected in leaves of the transgenic but not a control plant showing canker lesions. Protein loads were controlled by Coomassie brilliant blue staining of the RLS bands (upper panel).

To examine whether the CsMAPK1 overexpression was interfering with the pathogen growth, we determined the bacterial population in leaves of transgenic and control plants infiltrated with *X. citri* suspensions of different cell densities. We noticed that even with a high bacterial density (approximately 10^5 cells), which we had used to determine the exponential growth of *X. citri* in citrus plants (Cernadas et al. 2008), bacterial growth was significantly reduced in the transgenic relative to control plants from day 2 to day 14 postinoculation (Fig. 4A). In these experiments, bacterial populations in the transgenic leaves were, on average, 50 times lower than in the control leaves 14 days postinoculation (Fig. 4A). However, when we infiltrated a lower density of *X. citri* cells (approximately 10^3 cells), the average bacterial growth determined at 2 and 14 days postinoculation were 100 and 700 times lower in the transgenic relative to control plants, respectively (Fig. 4B).

Collectively, these results emphasize the role of CsMAPK1 as an important component of the *Citrus sinensis* defense response against *X. aurantifolii* and it can also be effective against *X. citri.*

CsMAPK1-mediated resistance against *Xanthomonas* correlates with ROS production.

Since multiple lines of evidence support the role of MAPK in ROS-mediated defense response against bacterial pathogens, we sought to investigate a link between CsMAPK1 and ROS production (Jammes et al. 2009; Pitzschke et al. 2009; Sinha et al. 2011; Yoshioka et al. 2009). Therefore, we examined the accumulation of hydrogen peroxide on wounded areas of *CsMAPK* transgenics lines using diaminobenzidine (DAB) staining (Thordal et al. 1997). We noticed an increased DAB activity in the tissues adjacent to the wounds in the transgenic plants at 2 and 6 h after the treatment relative to controls. In particular, stronger DAB stainings were detected in leaves of the *CsMAPK1*-13 line at 6 h after the wound (Fig. 5A).

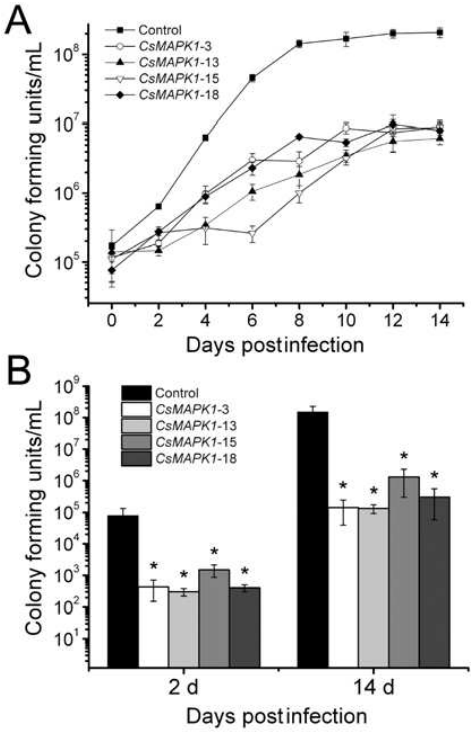

Fig. 4. Bacterial growth curves in leaves of control and transgenic Troyer plants expressing CsMAPK1. **A,** Leaves were infiltrated with approximately 0.1 ml of a high-density suspension of bacterial cells (approximately 10^6 cells per milliliter), and bacterial growth was followed daily by counting the number of bacterial cells retrieved from three independent infected leaves. **B,** Leaves of transgenic and control plants were infiltrated with approximately 0.1 ml of a 10^4 *Xanthomonas citri* cells-per-milliliter suspension, and the number of bacterial cells were determined at 2 and 14 days after inoculation. In both experiments, the growth of *X. citri* was significantly inhibited in the *CsMAPK1* transgenic plants relative to untransformed plants (control). Asterisks in B indicate that the differences between the control and transgenic means are statistically significant at the $P < 0.05$ level.

The pattern of DAB staining around the wounded sites in the *CsMAPK1* lines is reminiscent to that of GUS accumulation observed in the reporter plants (Fig. 2B), which indicates an overlapping between *CsMAPK1* expression and ROS production. To test whether CsMAPK1 is directly associated with a ROS-mediated defense response against *X. aurantifolii* in sweet orange leaves, we analyzed leaf tissues by DAB assays 24 h after bacterial infiltration. Consistently, the results revealed an increased DAB staining in the leaf sectors inoculated with *X. aurantifolii* relative to *X. citri*, which was only visible under high magnifications (Fig. 5B). In particular, DAB accumulation was more evident in the oil cells of tissues infiltrated with *X. aurantifolii* (Fig. 5B). These observations suggested to us that the ROS production of sweet orange 'Pera' in response to *X. aurantifolii* is a well-regulated stepwise process. This idea is partially supported by our microarray data and by the fact that the HR response to *X. aurantifolii* in this citrus variety is atypical, in the sense that cell death at the site of bacterial infiltration is not clearly visible (Cernadas et al. 2008). Thus, the higher accumulation of CsMAPK1 observed in the initial hours after *X. aurantifolii* infiltration (Fig. 1C) correlates with the local generation of hydrogen peroxide in response to this bacterium (Fig. 5B).

Since *X. citri* is able to suppress the host defense response (i.e., down-regulate the expression of defense-related genes) early after inoculation (Cernadas et al 2008), we asked whether *X. citri* have the ability to block the accumulation of hydrogen peroxide in the plants overexpressing *CsMAPK1*. We found that the leaf sectors of *CsMAPK1*-13 plants infiltrated with *X. citri* developed a stronger DAB staining compared with control plants (Fig. 5C), thereby supporting the role of CsMAPK1 during ROS production.

CsMAPK1 controls the expression of defense-related genes.

The relationship between CsMAPK1 overexpression and ROS production pointed us to test whether CsMAPK1 is regulating the expression of defense-related genes. Therefore, we analyzed the expression of five basal defense–related genes after wounding in *CsMAPK1*-13 plants. We selected genes encoding a PR1 protein and a WRKY factor induced by *X. aurantifolii* (Cernadas et al. 2008), a catalase similar to SPCAT1 (Chen et al. 2012) and a *S*-adenosyl-L-methionine–salicylic acid carboxyl methyltransferase (SAM-SACM) implicated in the synthesis of methyl salicylate (Negre et al. 2002). We used the CsCYP gene as a control because its expression is invariant during *X. citri* or *X. aurantifolii* infection (Fig. 1B). The results revealed that all five defense-related genes but not CsCYP were significantly induced by wounding in the *CsMAPK1*-13 line (Fig. 6A). In contrast, wounding treatment was not sufficient to induce significant expression changes of catalase, PR1, WRKY, or SAM-CM in plants used as controls. As expected, *CsMAPK1* was induced by wounding in both the control and *CsMAPK1*-13 plants. However, its expression was consistently higher in the transgenic line, as described before (Figs. 1D and 3C). The citrus *PR1* and *WRKY* factor genes were also much strongly induced by wounding in the *CsMAPK1*-13 line than in control plants (Fig. 6). However,

both the catalase and *SAM-SACM* genes were down-regulated in the control plants after wounding (Fig. 6A).

A similar pattern of defense gene activation, which is in accord with reported microarray data (Cernadas et al. 2008), was observed when control and *CsMAPK1*-13 plants were challenged with *X. citri* (Fig. 6B). Most notably, however, the expression of the catalase, PR1, and *SAM-SACM* genes, which were up-regulated by wounding, appeared to also be significantly induced by *X. citri* in the *CsMAPK1*-13 line, suggesting that CsMAPK1 might also be involved in SA metabolism (Fig. 6A).

Taken together, these results indicate that the ROS accumulation mediated by the CsMAPK1 is accompanied by a boost in the expression of basal defense response genes upon *Xanthomonas* infection.

DISCUSSION

Dissecting the citrus defense response against *Xanthomonas* pathogens.

Although many authors have reported the use of exogenous genes in transgenic citrus to increase disease resistance, more robust gene candidates are still lacking for canker resistance (Boscariol et al. 2006; Cardoso et al. 2009; Fu et al. 2011; Mendes et al. 2010; Yang et al. 2011; Zhang et al. 2010). For example, modulation of the citrus callose synthase (*CalS1*) and limonene synthase genes restrained the growth of *X. citri* in lemon and sweet orange plants, respectively. However, molecular mechanisms by which these genes provide partial resistance (or contribute to the resistance) against the bacterium were not described (Enrique et al. 2011; Rodríguez et al. 2011).

In this study, we present supporting evidences for the role of CsMAPK1 in the defense response against two citrus canker pathogens, *X. citri* and *X. aurantifolii*. The increased expression of *CsMAPK1* driven by the inducible *PR5* promoter in citrus leaves correlated with a decrease in canker development and pathogen growth (Figs. 3 and 4) as well as with the production of hydrogen peroxide and the transcriptional activation of defense-related genes (Figs. 5 and 6). As described above, we successfully used the *Xanthomonas*-induced *PR5* promoter to boost the *CsMAPK1* overexpression, which was presumably suppressed by *X. citri* between 6 and 48 h after infiltration (Cernadas et al. 2008). Experiments performed in transgenic Troyer plants revealed that the protein accumulation of CsMAPK1 (Fig. 3B) was concomitant with the upregulation of defense-related genes, catalase, WRKY, SAM-SACM, and PR1 (Fig. 6). We conceive that these genes are important components of the citrus defense response, since they were also strongly up-regulated in the HR-like response of sweet orange leaves infiltrated with *X. aurantifolii* (Cernadas et al. 2008).

Phylogenetic analyses clustered CsMAPK1 in Group A of MAPK (Fig. 1) along with WIPK and SIPK, which were suggested to regulate the tomato defense response against *Xanthomonas vesicatoria*, as well as the SA levels of tobacco after wounding, thereby indicating a potential crosstalk between these MAPK and SA-signaling (Seo et al. 2007). Moreover, transcriptional analyses of the *Arabidopsis* mutants *mkk1* and *mkk2* also support the interconnection between MAPK and SA accumulation, which also involves ROS production (Pitzschke et al. 2009). In particular, ROS synthesis appears to be an intrinsic mechanism of the *Citrus–Xanthomonas* defense response (Enrique et al. 2011). In agreement with this, we noticed increased hydrogen peroxide accumulations in the CsMAPK1 transgenic leaves challenged with *X. citri* (Fig. 5).

The nonhost defense response in *Arabidopsis thaliana* to *X. citri* is accompanied by the expression of defense genes, ROS generation, and synthesis of SA (An and Mou 2012). However, resistance appears to be compromised in the *sid2/npr1* double mutant, indicating a critical role of SA in the process (An and Mou 2012). Although we had found a link between CsMAPK1 signaling and ROS production, the only evidence for SA involvement was the strong induction of the citrus gene *SAM-CM* by *X. citri* in the plants overexpressing *CsMAPK1*, particularly in line 13 (Fig. 6). *SAM-CM* is a likely homolog of SA-carboxy-methyltransferase implicated in SA metabolism, reflecting the plausible relationship between *CsMAPK1* induction and SA (Negre et al. 2002).

Based on these observations, we conclude that continuous and prolonged gene induction of *CsMAPK1*, as observed in response to *X. aurantifolii* or in *PR5:CsMAPK1* transgenic plants infiltrated with *X. citri*, is an important signaling component of the citrus defense response involving defense genes induction, ROS synthesis, and plausible SA signaling, which needs further exploration.

MEK2 kinase: A putatively conserved signaling cascade triggered by *Xanthomonas* spp.

The tomato disease resistance against *X. vesicatoria* is mediated by a kinase cascade involving MEK2, which phosphorylates and activates WIPK and SIPK, resulting in the induction of defense genes and ROS production (Melech-Bonfil and Sessa 2010, 2011). We had identified the putative citrus MEK2 homolog (CsMEK2), which is also up-regulated in response to *X. aurantifolii* infiltration (Cernadas et al. 2008). This observation, in parallel with the larger levels of hydrogen peroxide accumulated in the CsMAPK1 transgenics, suggested to us that CsMAPK1 is targeted and activated by CsMEK2-mediated phosphorylation. Ongoing research is being addressed to test this hypothesis. However, and most interestingly, in some immunoblots, we detected extra bands of higher molecular weight at the early stages after bacterial infiltration, particularly in the transgenic lines (Fig. 3). We speculate that they may correspond with the phosphorylated forms of the CsMAPK1. Whether the CsMAPK1 requires activation via phosphorylation by CsMEK2 to initiate the defense response remains to be answered and will enlighten better strategies toward the generation of resistant citrus plants against *Xanthomonas* spp.

The role of radical burst in canker resistance.

The role of radical burst via MAPK signaling in plant immunity has been well documented (Asai and Yoshioka 2008; Yoshioka et al. 2009). In this work, we correlate the overexpression of CsMAPK1 with the increased resistance to *X. citri*, which appears to be mediated by the production of hydrogen peroxide and expression of defense-related genes. Particularly, we remark that the ROS toxicity to *X. citri* plays a fundamental role in defense and that *Xanthomonas* spp. are capable of tolerating the hydrogen peroxide generated by the host through the combined actions of xanthan gum and the expression of several antioxidant enzymes (Enrique et al. 2011; Kumar et al. 2011a and b; Tondo et al. 2010). This, in part, explains the low DAB staining observed in sweet orange leaves infiltrated with *X. citri* relative to *X. aurantifolii* (Fig. 5). Consistent with this, Fu and associates (2011) reported that the increased production of hydrogen peroxide in sweet orange overexpressing a spermidine synthase gene correlated with increased resistance to *X. citri.* In kumquat (*Fortunella* spp.), a citrus relative that is highly tolerant to citrus canker, the hydrogen peroxide turnover was suppressed during *X. citri* infection by the host expression of antioxidant enzymes (Kumar et al. 2011c and d). This is similar to what we observed in *X. aurantifolii*–infected sweet orange since *X. citri*–inoculated kumquat plants also overexpressed genes related to ROS scavenging, including superoxide dismutase, to preclude the oxidative damage over

the infected leaf areas (Khalaf et al. 2011). Accordingly, the upregulation of a citrus catalase gene in the *CsMAPK1*-13 line in response to wounding or *X. citri* infiltration could be reflecting the response to counteract the hydrogen peroxide accumulation observed upon wounding and *X. citri* infiltration (Figs. 5 and 6). These results are, therefore, in agreement with previous studies, which suggested that the resistance against *X. aurantifolii* in sweet orange is mediated by a MAPK signaling cascade associated with ROS production and that *X. citri*, on the other hand, is able to suppress the defense response in the early stages of infection (Cernadas et al. 2008).

We conclude that these findings establish a correlation between *CsMAPK1* expression, hydrogen peroxide accumulation, and defense-gene activation against *X. citri* in citrus plants. The modulation of ROS production in response to *X. citri* by using pathogen-induced promoters is a promising alternative to breed commercial citrus varieties resistant to the citrus canker disease.

MATERIALS AND METHODS

Gene cloning and promoter fusions.

The promoter of the *Citrus sinensis PR5* gene was cloned by PCR from a genomic DNA library. Total DNA extracted from sweet orange leaves was partially digested with *Sph*I, and fragments between 0.5 to 2 kb were gel-purified and subsequently ligated to adaptor A (TAATACGACTCACTATAGGGATCTG CACCAGAATTCCATG) containing the site for amplification with nested oligo A (GATCTGCACCAGAATTCCATG). Primers corresponding to the *PR5* gene (CGAAAGTGGCTGCGTT GACCC and AGCCCAGACCGTGTAGGGGC) were used in combination with adaptor and oligo A in nested PCR reactions to amplify sequences upstream of the start codon of the gene. A segment of approximately 400 bp upstream of the start codon of the *PR5* gene was amplified with oligos A and CCAT GGTGGCTATGTTTGGAGGGG and was ligated upstream of the initial ATG of the *CsMAPK1* gene (accession JQ678766).

The *CsMAPK1* gene was amplified by reverse transcription (RT)-PCR from total RNA extracted from sweet orange leaves (Cernadas et al. 2008), using oligos CCATGGCTGACGTGGC GCAGGTC and CTCGAGTTAAGCAAATCCCGGATTGAG TGCTAATG, and was cloned into the *Nco*I/*Sac*I sites of the pUC18 vector carrying the *PR5* promoter at the 5′ end. The *PR5*::*CSMAPK1* construct was subsequently subcloned into the binary vector pBI121 (*Hin*dIII/*Sac*I) for *Agrobacterium* transformation. The same *PR5* promoter was also cloned into the *Hin*dIII/*Bam*HI sites of pBI121 upstream of the *uidA* (GUS) gene to generate the control *PR5::uidA*. All constructs were verified by DNA sequencing and were transformed into the *Agrobacterium tumefaciens* EHA105 for plant transformation.

Multiple-sequence alignments and phylogenetic analysis.

Multiple sequence alignments of the deduced amino acid sequences of MAPK of citrus (CsMAPK1), *Nicotiana tabacum* (NtWIPK, Ntf4-2, and NtSIPK), and *Arabidopsis thaliana* (AtMAPK1-20) were generated, using the ClustalX program (version 2.0) (Larkin et al. 2007). The *Arabidopsis* and *N. tabacum* MAPK protein sequences were downloaded from The *Arabidopsis* Information Resource and National Center for Biotechnology Information, respectively. Phylogenetic trees

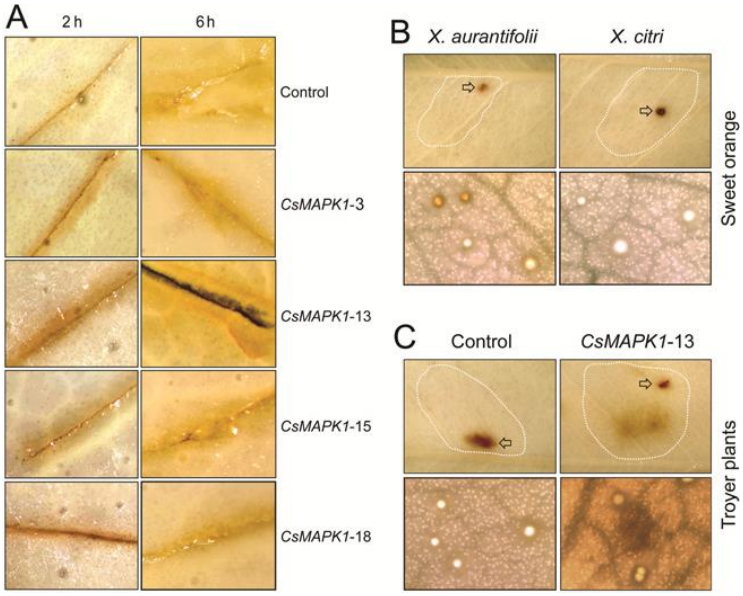

Fig. 5. *CsMAPK1* plants accumulate hydrogen peroxide upon wounding. **A,** Leaves of control and transgenic Troyer plants expressing CsMAPK1 were wounded and were subjected to diaminobenzidine (DAB) staining for the presence of hydrogen peroxide. The histological detection of hydrogen peroxide was performed at 2 and 6h after the wounding. Although control plants seem to accumulate hydrogen peroxide in response to wounding, the accumulation of hydrogen peroxide was more pronounced in the transgenic plants, particularly in the *CsMAPK1*-13 line, as judged by the intensity of the orange-brown pigmentation at the vicinity of the wounds. Increased DAB staining in response to wounding was observed in 10 of 10 transgenic leaves inspected. **B,** Histological detection of hydrogen peroxide (DAB staining) of sweet orange leaves infected with *Xanthomonas citri* or *X. aurantifolii* at 24 h postinoculation (dotted lines indicate the infiltrated leaf sectors). The upper panel, at 10× magnification, shows no significant differences between the two pathogens; however, at 50× magnification (lower panel), an orange-brownish color is primarily detected in the oil cells of tissues infiltrated with *X. aurantifolii*. **C,** Histological detection of hydrogen peroxide (DAB staining) in leaves of control and transgenic Troyer plants infected with *X. citri* during 24 h (dotted lines indicate the infiltrated leaf sectors). The upper panel, at 10× magnification, shows increased DAB staining in the infiltrated leaf sector of the transgenic plant compared with control. The increase in DAB staining in response to *X. citri* infection can be observed in more detail at 50× magnification (lower panel). Arrows in B and C indicate the site of pinprick inoculation. The pattern of differential DAB staining shown in B and C was observed in seven of 10 leaf sectors inspected outside the pinprick site.

were constructed using the MEGA 4.1 program (Tamura et al. 2007) with the neighbor-joining method (Saitou and Nei 1987) and bootstrap resampling analysis (1,000 replicates).

Plant transformation and bacteria infiltration.

Epicotyls of Troyer citrange plants were transformed with the *Agrobacterium* strains carrying the *PR5*::*CsMAPK1* or *PR5*::*uidA* constructs, as previously described (de Oliveira et al. 2009). The explants selected under kanamycin resistance were propagated in culture medium and, subsequently, were transplanted onto soil and maintained in a greenhouse under natural light regime with temperatures varying from 18 to 35°C and relative humidity ranging from 50 to 70%.

Plants were infiltrated with water suspensions of *X. citri* or *X. aurantifolii* pathotype C previously grown in LBON plates (Luria Bertani [LB] without NaCl), supplemented with ampicillin (100 mg per liter), for 48 h at 28°C (Cernadas et al. 2008). Approximately 0.1 ml of 10^5 or 10^6 cells per milliliter was infiltrated on each fully expanded leaf. Also, the lower side of the leaves was sprayed with a bacterial suspension of 10^6 cells per milliliter. Plants were monitored daily for the appearance of canker symptoms.

Histochemical GUS assays.

GUS activity in leaves of three independent two-year-old *PR5*::*uidA* reporter plants was detected by colorimetric assays at different time intervals after wounding or bacterial infiltration (Jefferson et al. 1987). Leaves detached from plants were immediately immersed into the GUS buffer (50 mM sodium phosphate, 10 mM EDTA, 0,1% sarkosyl, 0,1% Triton X-100, 10 mM 2-mercaptoethanol, 1 mM X-Gluc), were incubated at 37°C overnight in the dark, and were subsequently destained with 70% ethanol.

Bacterial growth assays.

The growth of *X. citri* in leaves of control and transgenic plants expressing CsMAPK1 were evaluated as previously described (Cernadas et al. 2008). Briefly, disks of leaf sectors that had been infiltrated with approximately 10^5 *X. citri* cells were removed daily and were ground in 1 ml of sterile water. Serial dilutions of the bacterial suspensions were plated on LBON with ampicillin at 100 mg per liter. Individual bacterial colonies or colony-forming units were counted from three independent leaf extractions.

Protein expression and antibody production.

The coding sequence of CsMAPK1 was subcloned into pET28a (*Nde*I/*Sac*I) vector using the oligos CATATGGCTGA CGTGGCGCAGGTC and CTCGAGTTAAGCAAATCCCGG ATTGAGTGCTAATG, and were subsequently transformed into *Escherichia coli* BL21 (DE3) cells for protein expression. Cells were grown at 37°C in LB supplemented with kanamycin (50 µg/ml) to an optical density at 600 nm = 0.6, followed by induction with 0.4 mM isopropyl-β-D-thiogalactoside for 3 h. Cells were harvested by centrifugation, were suspended in binding buffer (20 mM Tris-HCl, pH 8.0, 300 mM NaCl, 5 mM imidazole), and were incubated on ice with lysozyme (1.0 mg/ml) and sonicated. Clarified supernatants containing the 6xHis-CsMAPK1 fusion protein were loaded on a HiTrap chelating HP column (GE Healthcare, Piscataway, NJ. U.S.A.). Fractions were eluted with an imidazole gradient, and concentrated. purified CsMAPK1 (approximately 1 mg) was used to immunize rabbits for antiserum production.

CsMAPK1 detection in plant cell extracts.

Sweet orange and Troyer leaves of six- and 24-month-old plants, respectively, were infiltrated with a suspension of *X. citri* or *X. aurantifolii* (10^4 cells), and were collected for Western blot analysis at 6 and 24 h after bacterial inoculation. Sweet orange leaves were also wounded with a scalpel and were collected for analysis at 2 and 6 h after the wounding. Leaves were ground to powder in liquid nitrogen and were suspended in sodium dodecyl sulfate-polyacrylamide gel electrophoresis (SDS-PAGE) sample buffer. The suspension was heated for 5 min at 90°C, and cell debris and insoluble materials were separated by centrifugation at 14,000 × *g*, and the soluble fractions were analyzed in 8% SDS-PAGE gels and were subsequently transferred onto nylon membranes for Western blot detection. Blots were incubated with the anti-CsMAPK1 serum at 1:500 dilution and were developed by chemiluminescence.

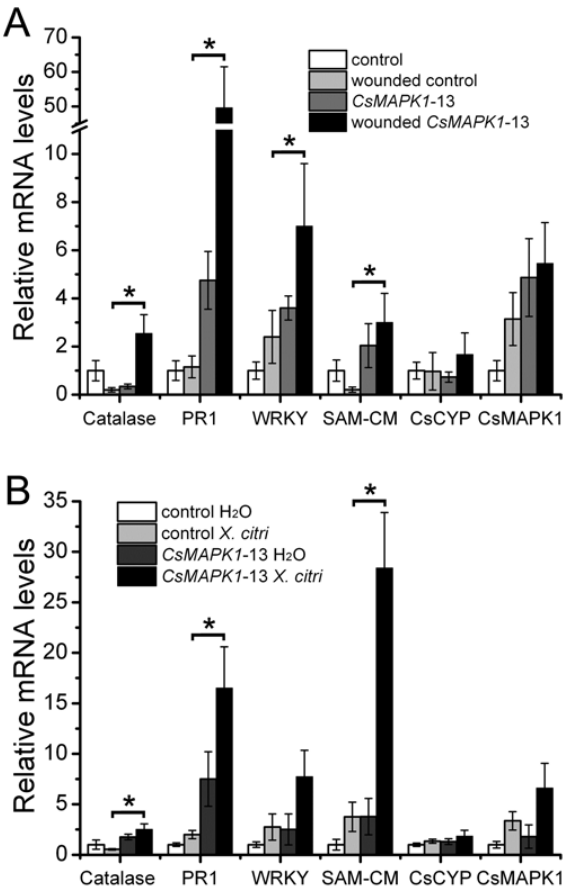

Fig. 6. *CsMAPK1*-13 plants show increased expression of defense- related genes. **A,** Relative fold-change expression levels by quantitative reverse-transcription polymerase chain reaction of *CsMAPK1* and four additional defense-related genes (*catalase*, *PR1*, *WRKY*, and *SAM- SACM*) in the *CsMAPK1*-13 transgenic and control plants, in response to wounding. The CsCYP gene, whose expression does not vary between the transgenic and control, was used as reference. Bars represent fold change of mRNA abundance in leaves of *CsMAPK1*-13 or control plants at 3 h after wounding. **B,** Relative fold change expression levels of cata- lase, *PR1*, *WRKY*, *SAM-SACM*, *CsCYP*, and CsMAPK1 genes in *CsMAPK1*-13 and control plants at 48 h after *X. citri* infiltration. Leaves were infiltrated with a suspension of 10^6 cells per milliliter or water as control. In panels A and B, the fold change values are normalized with 'control' and 'control H_2O' samples, respectively, and a malate translo- cator (accession CF834784) as internal control for equal cDNA inputs. Error bars denote standard deviations, and asterisks indicate statistically significant differences between control and transgenic leaves of at least three biological replicates ($P < 0.05$).

Hydrogen peroxide detection in plant tissues.

Hydrogen peroxide was detected in plant tissues using the DAB method (Thordal et al. 1997). Young leaves of Troyer plants were wounded with a scalpel, and after 2 and 6 h, leaves were vacuum-infiltrated for 10 min with a solution of 0.5 mg of DAB per milliliter in 20 mM sodium acetate, pH 3.8. Leaves were maintained in the DAB solution overnight at room temperature in the dark and were discolored with 100% ethanol for visualization.

Sweet orange and Troyer leaves infiltrated with a suspension of *X. citri* or *X. aurantifolii* (10^4 cells) were collected after 24 h and were placed in the DAB buffer, as described above. The orange brownish color observed in the examined tissues indicates the accumulation of hydrogen peroxide (Thordal et al. 1997).

Assays of semiquantitative and quantitative RT-PCR.

Total RNA was extracted from leaves of control and transformed Troyer citrange plants, using Trizol reagent (Invitrogen, Carlsbad, CA, U.S.A.) and treating with DNase I (Promega, Madison, WI, U.S.A.). Nearly 10 µg of total RNA was reverse-transcribed using the SuperScript synthesis system (Invitrogen), and cDNAs were used as templates in the semiquantitative and quantitative PCR analysis.

Semiquantitative PCR were performed, using standard amplification mixtures containing 1.5 mM $MgCl_2$, 200 µM each dNTP, 2.0 µl of cDNA, 2 U *Taq* DNA polymerase, and 0.25 µM primers in a 50 µl final volume. Amplification reactions were conducted in the following conditions:1 cycle at 94°C for 4 min, followed by 25 cycles of 1 min denaturation at 94°C for 1 min, 1.5 min annealing at 55°C for the *CsCYP* gene (accession ACX37092) or 57°C for the *CsMAPK*1 gene, and 1 min elongation at 72°C.

SYBR green real-time quantitative PCR was performed in 96-well reaction plates in an ABI Prism 7300 (Applied Biosystems, Foster City, CA, U.S.A.). Primer sequences corresponding to the *Citrus sinensis* genes *CsMAPK1*, *PR1* (accession CF653559), *WRKY* (Citrus Genome Database code orange1.1g019404m), *Catalase* (accession CX671534), and *SAM-SACM* (accession CN182915) were designed using the Primer Express 2.0 software (Applied Biosystems). Each 25-µl reaction mixture contained 12.5 µl of SYBR green 2× master mix (Applied Biosystems), 1 µl of forward and reverse primer mix (7.5 µM), 1 µl of cDNA, and 10.5 µl of diethyl pyrocarbonate–treated water. Amplifications were carried out for 2 min at 50°C and 10 min at 95°C, followed by 40 amplification cycles of 15 s at 95°C and 1 min at 60°C. The *Citrus sinensis* gene encoding a malate translocator (accession CF834784) was chosen as an internal control for normalization. Total RNA from three different leaves were used in the real-time PCR reactions as independent biological replicates.

ACKNOWLEDGMENTS

We thank financial support from Fundação de Amparo à Pesquisa do Estado de São Paulo (Fapesp) and Conselho Nacional de Desenvolvimento Científico e Tecnológico (CNPq). M. L. P. de Oliveira and C. E. Benedetti received fellowships from Fapesp and CNPq, respectively.

LITERATURE CITED

An C., and Mou Z. 2012. Non-host defense response in a novel Arabidopsis-*Xanthomonas citri* subsp. *citri* pathoystem. PLoS One 7:e31130. Published online.

Asai, S., and Yoshioka, H. 2008. The role of radical burst via MAPK signaling in plant immunity. Plant Signal Behav. 3:920-922.

Boscariol, R. L., Chabregas, S. M., Vieira, M. L. C., Pereira, L. F. P. P., Vieira, L. G. E., Bergamin Filho, A., Barbosa, J. M., Azevedo, F. A., Mourão-Filho, F. A. A., and Mendes, B. M. J. 2006. Attacin A gene from *Tricloplusia ni* reduces susceptibility to *Xanthomonas axonopodis* pv. *citri* in transgenic *Citrus sinensis* cv. Hamlin. J. Amer. Soc. Hort. Sci. 131:530-536.

Brunings, A. M., and Gabriel, D. W. 2003. *Xanthomonas citri*: Breaking the surface. Mol. Plant Pathol. 4:141-157.

Cardoso, S. C., Barbosa-Mendes, J. M., Boscariol-Camargo, R. L., Christiano, R. S. C., Bergamin Filho, A., Vieira, M. L. C., Mendes, B. M. J., and Mourão Filho, F. A. A. 2009. Transgenic sweet orange (*Citrus sinensis* L. Osbeck) expressing the attacin A gene for resistance to *Xanthomonas citri* subsp. *citri*. Plant Mol. Biol. Rep. 28:185-192.

Cernadas, R. A., and Benedetti, C.E. 2009. Role of auxin and gibberellin in citrus canker development and in the transcriptional control of cell- wall remodeling genes modulated by *Xanthomonas axonopodis* pv. *citri*. Plant Sci. 177:190-195.

Cernadas, R. A., Camillo, L. R., and Benedetti, C. E. 2008. Transcriptional analysis of the sweet orange interaction with the citrus canker patho- gens *Xanthomonas axonopodis* pv. *citri* and *Xanthomonas axonopodis* pv. *aurantifolii*. Mol. Plant Pathol. 9:609-631.

Chen, H. J., Wu, S. D., Huang, G. J., Shen, C. Y., Afiyanti, M., Li, W. J., and Lin, Y. H. 2012. Expression of a cloned sweet potato catalase SPCAT1 alleviates ethephon-mediated leaf senescence and H_2O_2 eleva- tion. J. Plant Physiol. 169:86-97.

Chisholm, S. T., Coaker, G., Day, B., and Staskawicz, B. J. 2006. Host-microbe interactions: Shaping the evolution of the plant immune response. Cell 124:803-814.

de Oliveira, M. L. P., Febres, V. J., Costa, M. G. C., Moore, G. A., and Otoni, W. C. 2009. High-efficiency Agrobacterium-mediated transfor- mation of citrus via sonication and vacuum infiltration. Plant Cell Rep. 28:387-395.

Enrique, R., Siciliano, F., Favaro, M. A., Gerhardt, N., Roeschlin, R., Rigano, L., Sendin, L., Castagnaro, A., Vojnov, A., and Marano, M. R. 2011. Novel demonstration of RNAi in citrus reveals importance of citrus callose synthase in defense against *Xanthomonas citri* subsp. *citri*. Plant Biotechnol. J. 9:394-407.

Fu, X-Z., Chen, C-W., Wand, Y., Liu, J-H., and Moriguchi, T. 2011. Ectopic expression of MdSPDS1 in sweet orange (*Citrus sinensis* OsbecK) reduces canker susceptibility: Involvement of H_2O_2 produc- tion and transcription alteration. BMC Plant Biol. 11:55.

Galletti, R., Ferrari, S., and De Lorenzo, G. 2011. Arabidopsis MPK3 and MPK6 play different roles in basal and oligogalacturonide- or flagellin-induced resistance against *Botrytis cinerea*. Plant Physiol. 157:804-14.

Huang, X. S., Luo, T., Fu, X. Z., Fan, Q. J., and Liu, J. H. 2011. Cloning and molecular characterization of a mitogen-activated protein kinase gene from *Poncirus trifoliata* whose ectopic expression confers dehydration/drought tolerance in transgenic tobacco. J Exp Bot. 62:5191-5206.

Ishihama, N., Yamada, R., Yoshioka, M., Katou, S., and Yoshioka, H. 2011. Phosphorylation of the *Nicotiana benthamiana* WRKY8 tran- scription factor by MAPK functions in the defense response. Plant Cell 23:1153-1170.

Jammes, F., Song, C., Shin, D., Munemasa, S., Takeda, K., Gu, D., Cho, D., Lee, S., Giordo, R., Sritubtim, S., Leonhardt, N., Ellis, B. E., Murata, Y., and Kwak, J. M. 2009. MAP kinases MPK9 and MPK12 are preferentially expressed in guard cells and positively regulate ROS-mediated ABA signaling. Proc. Natl. Acad. Sci. U.S.A. 106:20520-20525.

Jefferson, R. A., Kavanagh, N-H., and Bevan, M. W. 1987. GUS fusions: β-glucuronidase as a sensitive and versatile gene fusion marker in higher plants. EMBO (Eur. Mol. Biol. Organ.) J. 6:3901-3907.

Jonak, C., Kiegerl, S., Ligterink, W., Barker, P. J., Huskisson, N. S., and Hirt, H. 1996. Stress signaling in plants: A mitogen-activated protein kinase pathway is activated by cold and drought. Proc. Natl. Acad. Sci. U.S.A. 93:11274-11279.

Jones, J. D. G., and Dangl, J. L. 2006. The plant immune system. Nature 444:323-329.

Khalaf, A. A., Gmitter, F. G. Jr., Conesa, A., Dopazo, J., and Moore, G. A. 2011. *Fortunella margarita* transcriptional reprogramming triggered by *Xanthomonas citri* subsp. *citri*. BMC Plant Biol. 11:159.

Kumar, N., Ebel, R. C., and Roberts, P. D. 2011a. Antioxidant metabolism of grapefruit infected with *Xanthomonas axonopodis* pv. *citri*. Environ. Exp. Bot. 71:41-49.

Kumar, N., Ebel, R. C., and Roberts, P. D. 2011b. H_2O_2 metabolism during sweet orange (*Citrus sinensis* L. Osb.) "Hamlin" *Xanthomonas axonopodis* pv. *citri* interaction. Sci. Hort. 128:465-472.

Kumar, N., Ebel, R. C., and Roberts, P. D. 2011c. H_2O_2 is suppressed in kumquat leaves infected with *Xanthomonas axonopodis* pv. *citri*. Sci. Hort. 130:241-247.

Kumar, N., Ebel, R.C., and Roberts, P. D. 2011d. Superoxide dismutase activity in kumquat infected with *Xanthomonas axonopodis* pv. *citri*. J. Hort. Sci. Biotechnol. 86:62-68.

Larkin, M. A., Blackshields, G., Brown, N. P., Chenna, R., McGettigan, P.

A., McWilliam, H., Valentin, F., Wallace, I. M., Wilm, A., Lopez, R., Thompson, J. D., Gibson, T. J., and Higgins, D. G. 2007. Clustal W and Clustal X version 2.0. Bioinformatics 23:2947-2948.

Ligterink, W., Kroj, T., zur Nieden, U., Hirt, H., and Scheel, D. 1997. Receptor-mediated activation of a MAP kinase in pathogen defense of plants. Science 276:2054-2057.

Liu, X., Bai, X., Wang, X., and Chu, C. 2007a. OsWRKY71, a rice transcription factor, is involved in rice defense response. J. Plant Physiol. 164:969-979.

Liu, Y., Ren, D., Pike, S., Pallardy, S., Gassmann, W., and Zhang, S. 2007b. Chloroplast-generated reactive oxygen species are involved in hypersensitive response-like cell death mediated by a mitogen-activated protein kinase cascade. Plant J. 51:941-954.

MAPK Group. 2002. Mitogen-activated protein kinase cascades in plants: A new nomenclature. Trends Plant Sci. 7:301-308.

Melech-Bonfil, S., and Sessa, G. 2010. Tomato MAPKKKε is a positive regulator of cell-death signaling networks associated with plant immunity. Plant J. 64:379-391.

Melech-Bonfil, S., and Sessa, G. 2011. The SlMKK2 and SlMPK2 genes play a role in tomato disease resistance to *Xanthomonas campestris* pv. *vesicatoria*. Plant Signal Behav. 6:154-156.

Mendes, B. M. J., Cardoso, S. C., Boscariol-Camargo, R. L., Cruz, R. B., Mourão Filho, F. A. A., and Bergamin Filho, A. 2010. Reduction in susceptibility to *Xanthomonas axonopodis* pv. *citri* in transgenic *Citrus sinensis* expressing the rice *Xa21* gene. Plant Pathol. 59:68-75.

Mizoguchi, T., Irie, K., Hirayama, T., Hayashida, N., Yamaguchi-Shinozaki, K., Matsumoto, K., and Shinozaki, K. 1996. A gene encoding a mitogen-activated protein kinase kinase kinase is induced simultaneously with genes for a mitogen-activated protein kinase and an S6 ribosomal protein kinase by touch, cold, and water stress in *Arabidopsis thaliana*. Proc Natl Acad Sci U.S.A. 93:765-9.

Negre, F., Kolosova, N., Knoll, J., Kish, C. M., and Dudareva, N. 2002. Novel *S*-adenosyl-L-methionine: Salicylic acid carboxyl methyltransferase, an enzyme responsible for biosynthesis of methyl salicylate and methyl benzoate, is not involved in floral scent production in snapdragon flowers. Arch. Biochem. Biophys. 406:261-270.

Oh, S. K., Yi, S. Y., Yu, S. H., Moon, J. S., Park, J. M., and Choi, D. 2006. CaWRKY2, a chili pepper transcription factor, is rapidly induced by incompatible plant pathogens. Mol. Cells 22:58-64.

Pitzschke, A., Djamei, A., Bitton, F., and Hirt, H. 2009. A major role of the MEKK1-MKK1/2-MPK4 pathway in ROS signalling. Mol. Plant 2:120-137.

Ren, D., Yang, H., and Zhang, S. 2002. Cell death mediated by MAPK is associated with hydrogen peroxide production in Arabidopsis. J. Biol. Chem. 277:559-565.

Ren, D., Yang, K. Y., Li, G. J., Liu, Y., and Zhang, S. 2006. Activation of Ntf4, a tobacco mitogen-activated protein kinase, during plant defense response and its involvement in hypersensitive response-like cell death. Plant Physiol. 141:1482-1493.

Rodriguez, M. C. S., Petersen, M., and Mundy, J. 2010. Mitogen-activated protein kinase signaling in plants. Annu. Rev. Plant Biol.61:621–649.

Rodríguez, A., San Andrés, V., Cervera, M., Redondo, A., Alquézar, B., Shimada, T., Gadea, J., Rodrigo, M. J., Zacarías, L., Palou, L., López, M. M., Castañera, P., and Peña, L. 2011. Terpene down-regulation in orange reveals the role of fruit aromas in mediating interactions with insect herbivores and pathogens. Plant Physiol. 156:793-802.

Saitou, N., and Nei, M. 1987. The Neighbor-Joining method: A new method for reconstructing phylogenetic trees. Mol. Biol. Evol. 4:406- 425.

Seo, S., Okamoto, M., Seto, H., Ishizuka, K., Sano, H., and Ohashi, Y. 1995. Tobacco MAP kinase: A possible mediator in wound signal transduction pathways. Science 270:1988-1992.

Seo, S., Katou, S., Seto, H., Gomi, K., and Ohashi, Y. 2007. The mitogen-activated protein kinases WIPK and SIPK regulate the levels of jasmonic and salicylic acids in wounded tobacco plants. Plant J. 49:899-909.

Sinha, A. K., Jaggi, M., Raghuram, B., and Tuteja, N. 2011. Mitogen-activated protein kinase signaling in plants under abiotic stress. Plant Signal Behav. 6:196-203.

Takahashi, Y., Nasir, K. H., Ito, A., Kanzaki, H., Matsumura, H., Saitoh, H., Fujisawa, S., Kamoun, S., and Terauchi, R. 2007. A high-throughput screen of cell-death-inducing factors in *Nicotiana benthamiana* identifies a novel MAPKK that mediates INF1-induced cell death signaling and non-host resistance to *Pseudomonas cichorii*. Plant J. 49:1030- 1040.

Tamura, K., Dudley, J., Nei, M., and Kumar, S. 2007. MEGA4: Molecular evolutionary genetics analysis (MEGA) software version 4.0. Mol. Biol. Evol. 24:1596-1599.

Thordal Christensen, H., Zhang, Z. G., Wei, Y. D., and Collinge, D. B. 1997. Subcellular localization of H_2O_2 in plants. H_2O_2 accumulation in papillae and hypersensitive response during the barley-powdery mildew interaction. Plant J. 11:1187-1194

Tondo, M. L., Petrocelli, S., Ottado, J., and Orellano, E. G. 2010. The monofunctional catalase KatE of *Xanthomonas axonopodis* pv. *citri* is required for full virulence in citrus plants. PLoS One 5:e10803. Published online.

Vilela, B., Pagès, M., and Lumbreras, V. 2010. Regulation of MAPK signaling and cell death by MAPK phosphatase MKP2. Plant Signal Behav. 5:1497-1500.

Yang, L., Hu, C., Li, N., Zhang, J., Yan, J., and Deng, Z. 2011. Transformation of sweet orange [*Citrus sinensis* (L.) Osbeck] with *pthA*-nls for acquiring resistance to citrus canker disease. Plant Mol. Biol. 75:11-23.

Yoshioka, H., Asai, S., Yoshioka, M., and Kobayashi, M. 2009. Molecular mechanisms of generation for nitric oxide and reactive oxygen species, and role of the radical burst in plant immunity. Mol. Cells 28:321-329.

Zhang, X., Francis, M. I., Dawson, W. O., Graham, J. H., Orbović, V., Triplett, E. W., and Mou, Z. 2010. Over-expression of the Arabidopsis NPR1 gene in citrus increases resistance to citrus canker. Eur. J. Plant Pathol. 128:91-100.

AUTHOR-RECOMMENDED INTERNET RESOURCES

Arabidopsis Information Resourcewebsite: www.arabidopsis.org
National Centre for Biotechnology Information website: www.ncbi.nlm.nih.gov

UNICAMP
COORDENADORIA DE PÓS-GRADUAÇÃO
INSTITUTO DE BIOLOGIA
Universidade Estadual de Campinas
Caixa Postal 6109. 13083-970, Campinas, SP, Brasil
Fone (19) 3521-6378. email: cpgib@unicamp.br
IB

DECLARAÇÃO

Em observância ao **§5° do Artigo 1° da Informação CCPG-UNICAMP/001/15**, referente a Bioética e Biossegurança, declaro que o conteúdo de minha Tese de Doutorado, intitulada "***Análise funcional de efetores 'TAL' de Xanthomonas citri e Xanthomonas aurantifolii patotipo 'C' e estudo da ativação de seus genes alvos na planta hospedeira***", desenvolvida no Programa de Pós-Graduação em Genética e Biologia Molecular do Instituto de Biologia da Unicamp, não versa sobre pesquisa envolvendo seres humanos, animais ou temas afetos a Biossegurança.

Assinatura: Valeria Yukari Abe
Nome do(a) aluno(a): Valeria Yukari Abe

Assinatura: Celso Benedetti
Nome do(a) orientador(a): Celso Eduardo Benedetti

Data: 16/02/2016

Profa. Dra. Rachel Meneguello
Presidente
Comissão Central de Pós-Graduação
Declaração

As cópias de artigos de minha autoria ou de minha co-autoria, já publicados ou submetidos para publicação em revistas científicas ou anais de congressos sujeitos a arbitragem, que constam da minha Dissertação/Tese de Mestrado/Doutorado, intitulada **"Análise funcional de efetores 'TAL' de Xanthomonas citri e Xanthomonas aurantifolii patotipo 'C' e estudo da ativação de seus genes alvos na planta hospedeira"**, não infringem os dispositivos da Lei n.° 9.610/98, nem o direito autoral de qualquer editora.

Campinas, 16/02/2016

Assinatura : Valeria Yukari Abe
Nome do(a) autor(a): **Valeria Yukari Abe**
RG n.° 29.233.478-3

Assinatura : Celso Benedetti
Nome do(a) orientador(a): **Celso Eduardo Benedetti**
RG n.° 16.367.582